

Advanced Interference Suppression Techniques for Spread Spectrum Systems

This thesis is submitted in partial fulfilment of the requirements for
Doctor of Philosophy (Ph.D.)

Yunlong Cai
Communications Research Group
Department of Electronics
University of York

September 2009

Abstract

Code division multiple access (CDMA) techniques have been widely employed by different wireless systems with many advantages. However, the performance of these systems is limited by interference. A number of different interference suppression techniques have been proposed, including multiuser detection, beamforming, adaptive supervised and blind algorithms, and transmit processing techniques requiring a limited feedback channel. Recently, CDMA techniques have also been combined with multicarrier and multiantenna schemes to further increase the system capacity and performance. This thesis investigates the existing algorithms and structures and proposes novel interference suppression algorithms for spread spectrum systems.

Firstly we investigate blind constrained constant modulus (CCM) stochastic gradient (SG) receivers with a low-complexity variable step-size mechanism for downlink direct sequence CDMA (DS-CDMA) systems. This algorithm provides better performance than existing blind schemes in non-stationary scenarios. Convergence and tracking analyses of the proposed adaptation techniques are carried out for multipath channels.

Secondly, we propose a novel space-time adaptive minimum mean squared error (MMSE) decision feedback (DF) detection scheme for DS-CDMA systems with multiple receive antennas, which employs multiple-parallel feedback branches (MPF) for interference cancellation. The proposed scheme is further combined with multistage detectors to refine estimated symbols and provide uniform performance over all users. Simulation results show that the proposed space-time MPF-DF detector outperforms existing schemes.

Thirdly, we concentrate on transmit processing techniques. A novel switched interleaving algorithm is proposed to suppress interference for DS-CDMA systems, which requires the cooperation among the transmitter and the receiver, and a feedback channel sending the index of the interleaver to be used. The best interleaving pattern is chosen by the selection functions at the receiver from a codebook known to both the receiver and the transmitter and the codebook index is sent back using a limited number of bits. Symbol-based and block-based linear MMSE receivers are designed for detection.

Fourthly, the proposed switched interleaving technique is further extended to multiple antenna multicarrier code-division multiple-access (MC-CDMA) systems. A new hybrid transmit processing technique based on switched interleaving and chip-wise precoding is proposed for the downlink case, whereas a preprocessing technique is employed for the uplink. The simulation results show that the performance of the proposed scheme outperforms the existing chip-interleaving, conventional linear precoding and adaptive spreading techniques.

At last, we present a novel multistage receivers based on multiple parallel branches successive interference cancellation (MB-SIC) for the uplink of multiple-input multiple-output code-division multiple-access (MIMO-CDMA) systems. The proposed multistage receivers exploit a conventional ordered SIC for the first stage, followed by a grouping detection strategy and the novel MB-SIC scheme. Then, according to a selection rule, namely, the maximum likelihood (ML) or the MMSE, the MB-SIC selects the refined estimated vector with the best performance for the desired users antenna streams.

Contents

Acknowledgements	viii
Declaration	ix
Glossary	x
1 Introduction	1
1.1 Overview	1
1.2 Contributions	3
1.3 Thesis Outline	5
1.4 Notation	6
1.5 Publication List	6
2 Literature Review	9
2.1 Introduction	9
2.2 Multiuser Detection for DS-CDMA Systems	10
2.2.1 Direct-Sequence Spread Spectrum	10
2.2.2 Optimum Multiuser Detection	11

2.2.3	MMSE Linear Receiver	12
2.2.4	Decision Feedback Receivers	13
2.2.5	Interference Cancellation Receivers	14
2.3	Adaptive Receivers and Blind Linear Receivers	15
2.3.1	Stochastic Gradient Algorithm (SG)	16
2.3.2	Recursive Least Squares Algorithm (RLS)	16
2.3.3	Constrained Minimum Variance Algorithm	17
2.3.4	Constrained Constant Modulus Algorithm	17
2.4	Preprocessing Techniques for DS-CDMA Systems	18
2.4.1	Chip-Interleaving Algorithms	18
2.4.2	CDMA Precoding Techniques	20
2.4.3	Signature Optimization Techniques	21
2.5	Spread Spectrum with Multicarrier and Multiantenna Techniques	22
2.5.1	Spread Spectrum with Multicarrier Schemes and Transceiver Structure	23
2.5.2	Multiantenna CDMA Techniques	25
2.6	Limited Feedback Techniques	26
2.6.1	Feedback in Single-user Systems	27
2.6.2	Feedback in Multiuser Systems	29
2.7	Conclusions	30

3	Low-Complexity Blind Adaptive Interference Suppression	31
3.1	Introduction	31
3.2	DS-CDMA System Model	33
3.3	Blind Adaptive SG CCM Algorithms	35
3.3.1	Multipath Blind Adaptive SG CCM Algorithm	35
3.3.2	Blind CCM SG-AGSS in Multipath Channels	37
3.4	Blind Time Averaging Variable Step-size (TASS) Algorithm	37
3.4.1	TASS Mechanism	38
3.4.2	Computational Complexity	39
3.5	Analyses of the Proposed Algorithm	40
3.5.1	The Modification of the CCM Update Equation	40
3.5.2	The Range of Step-size Values for Convergence	41
3.5.3	Steady-State Analysis	42
3.5.4	Tracking Analysis	45
3.6	Simulation Results	47
3.7	Conclusions	52
4	Adaptive Decision Feedback Detectors for Space-Time CDMA Systems	54
4.1	Introduction	54
4.2	DS-CDMA System Model and Array Configurations	56
4.3	Space-time MPF Decision Feedback Receiver Structure	58

4.4	Multistage Space-time MPF-DF Detection	61
4.5	MMSE Design of Proposed Space-time Estimators	63
4.6	Analytical Results	64
4.6.1	On the MMSE with Perfect and Imperfect Feedback for Proposed Space-time MPF-DF Detectors	64
4.6.2	On the MMSE with Perfect and Imperfect Feedback for S-DF and P-DF with Antenna Arrays	65
4.7	Adaptive Estimation Algorithms	66
4.7.1	Stochastic Gradient Algorithm	66
4.7.2	Recursive Least Squares Algorithm	67
4.8	Simulation Results	70
4.9	Conclusions	77
5	Switched Interleaving Techniques for Interference Mitigation in DS-CDMA Systems	78
5.1	Introduction	78
5.2	Proposed System Models and MMSE Receivers	80
5.2.1	System Model	80
5.2.2	Proposed MMSE Receivers	82
	MMSE Symbol-based Receiver	83
	MMSE Block-based Receiver	83
5.3	System Optimization and Selection of Interleavers	84

5.3.1	Uplink	84
	Selection Rule for MMSE Block-based Receivers	84
	Selection Rules for Symbol-based Receivers	85
5.3.2	Downlink	86
5.3.3	Computational Complexity	86
5.3.4	Channel Estimation	87
5.4	Design of Codebooks and Low-rate Feedback Channels	87
5.4.1	Design of Codebooks	88
	Optimum Interleaving	88
	Random Interleaving	88
	Block Interleaving	89
	Frequently Selected Patterns Method (FSP)	90
5.4.2	Low-rate Feedback Schemes	91
5.5	Simulation Results	91
5.6	Conclusions	100
6	Transmit Processing Techniques for Multi-antenna MC-CDMA Systems	101
6.1	Introduction	101
6.2	Proposed system models	103
6.2.1	Downlink	104
6.2.2	Uplink	106

6.3	Design of Precoders and Receivers	106
6.3.1	Downlink	107
	Chip-wise Precoder	107
	Linear MMSE Receiver	107
6.3.2	Uplink	108
6.4	Selection of Parameters and Optimization	109
6.4.1	Downlink	109
6.4.2	Uplink	110
6.5	Design of Low-rate Feedback Frame Structures and Codebooks	110
6.5.1	Low-rate Feedback Frame Structures	111
6.5.2	Design of Codebooks for Channel Direction and Norm Quantization	112
6.5.3	Codebook of Interleavers	114
6.6	Simulation Results	115
6.7	Conclusions	121
7	Multistage MIMO Receivers Based on Multi-Branch Interference Cancellation for MIMO-CDMA Systems	123
7.1	Introduction	123
7.2	System Model	124
7.3	Detectors for MIMO-CDMA Systems	126
7.3.1	Linear MMSE Receiver	126

7.3.2	Parallel Interference Cancellation (PIC) Detection Schemes . . .	127
7.3.3	Successive Interference Cancellation (SIC) Detection Schemes . .	127
7.4	Multistage Multi-Branch SIC Detection	129
7.4.1	Proposed MB-SIC Scheme	129
7.4.2	Selection Criteria	130
	Maximum Likelihood	130
	Minimum Mean-Squared Error Criterion	131
7.5	Simulation Results	132
7.6	Conclusion	134
8	Conclusions and Future Work	135
8.1	Summary of the Work	135
8.2	Future Work	136
	Bibliography	137
	List of Figures	ix
	List of Tables	xiii

Acknowledgements

I would firstly like to thank my supervisor, Dr. Rodrigo C. de Lamare, for his advice, support and encouragement during the course of my Ph.D. study.

I would also like to thank all my dear colleagues in the Communications Research Group.

This thesis is dedicated to my parents.

Declaration

Some of the research presented in this thesis has resulted in some publications. These publications are listed at the end of Chapter 1.

All work presented in this thesis as original is so, to the best knowledge of the author. References and acknowledgements to other researchers have been given as appropriate.

Glossary

AGSS	Adaptive Gradient Step-size
AV	Averaging Method
AWGN	Additive White Gaussian Noise
BER	Bit Error Rate
BPSK	Binary Phase Shift Keying
BS	Base Station
C-CDMA	Conventional Code Division Multiple Access
CCM	Code-constrained Constant Modulus
CM	Constant Modulus
CMA	Constant Modulus Algorithm
CMV	Constrained Minimum Variance
CP	Cyclic Prefix
CSI	Channel State Information
DF	Decision Feedback
DOA	Direction of Arrival
DS-CDMA	Direct Sequence Code Division Multiple Access
EGC	Equal Gain Combining
EMSE	Excess Minimum Mean Squared Error
FDD	Frequency Division Duplexing
FFT	Fast Fourier Transform
FSP	Frequently Selected Patterns
FSS	Fixed Step-size
FIR	Finite impulse response
GMC	Generalized Multicarrier
IFFT	Inverse Fast Fourier Transform
ISI	Intersymbol interference
LMS	Least Mean Square
LS	Least Squares
MB-SIC	Multi-branch Successive Interference Cancellation
MC-CDMA	Multi-carrier Code Division Multiple Access
MC-DS-CDMA	Multicarrier Direct-sequence Code Division Multiple Access
ML	Maximum-likelihood
MIMO	Multiple Input Multiple Output
MISO	Multiple Input Single Output
MMSE	Minimum Mean Squared Error
MPF	Multiple Parallel Feedback
MRC	Maximum Ratio Combining

MS	Mobile Station
MSE	Mean Squared Error
MSMB-SIC	Multistage Multi-branch SIC
MUD	Multiuser Detection
MUI	Multiuser interference
MV	Minimum Variance
NLMS	Normalized LMS
P-DF	Parallel Decision Feedback
PIC	Parallel Interference Cancellation
PN	Pseudorandom noise
OFDM	Orthogonal Frequency Division Multiplexing
RLS	Recursive Least Squares
RVQ	Random Vector Quantization
SC	Single-carrier
SIDS-CDMA	Switched Interleaving Direct Sequence Code Division Multiple Access
SG	Stochastic Gradient
SIC	Successive Interference Cancellation
SINR	Signal-to-Interference-plus-Noise Ratio
SNR	Signal-to-Noise Ratio
S-DF	Successive Decision Feedback
S/P	Serial-to-parallel
TDD	Time Division Duplexing
TASS	Timing Averaging Variable Step-size

Chapter 1

Introduction

Contents

1.1 Overview	1
1.2 Contributions	3
1.3 Thesis Outline	5
1.4 Notation	6
1.5 Publication List	6

1.1 Overview

Code division multiple-access (CDMA) implemented with direct-sequence (DS) spread-spectrum signalling is among the most promising multiplexing technologies for current and future telecommunications services such as personal communications, third-generation cellular telephony, ad-hoc wireless communications, and sensor networks. The advantages of DS-CDMA include superior operation in multipath environments, flexibility in the allocation of channels, increased capacity in bursty and fading environments, and the ability to share bandwidth with narrowband communication systems without deterioration of either's systems performance [1–3].

The performance of CDMA systems is limited by different types of interference, namely, narrowband interference, intersymbol interference (ISI), multiuser interference (MUI) and the noise at the receiver. The major source of interference in most CDMA systems is MUI, which arises due to the fact that users communicate through the same

physical channel with non-orthogonal signals. A fair amount of techniques has been proposed for interference suppression in spread spectrum systems. One of them is multiuser detection (MUD) which has been proposed as a means to suppress MUI, increasing the capacity and the performance of CDMA systems [2], [1]. Among the main detectors are the decorrelating linear detector, the minimum mean squared error (MMSE) linear detector, the decision feedback (DF) detector and interference cancellation detectors.

The high complexity and the requirement of training sequences of the detectors have motivated the development of blind adaptive techniques. In [4] the adaptive supervised stochastic gradient (SG) and recursive least squares (RLS) algorithms are described, and an adaptive blind receiver has been introduced in [5]. The performance of adaptive SG receivers is strongly dependent on the choice of the step size. In non-stationary wireless environments, users frequently enter and exit the system, making it very difficult for the receiver to compute a pre-determined step size. Another interference mitigation technique for CDMA is based on transmit processing schemes, such as, chip-interleaving, signature adaptation, and CDMA precoding algorithms [6–9]. However, some of the preprocessing techniques need the channel state information (CSI) or other optimized parameter vectors at the transmitter, thus, limited feedback schemes are employed to meet the requirement of the transmitter by sending some quantized information from the receiver to the transmitter.

Recently, spread spectrum schemes have been considered in conjunction with multi-antenna and multicarrier techniques to increase the system capacity and the bit error rate (BER) performance. In multiple-input multiple-output CDMA (MIMO-CDMA) systems, vertical BLAST (V-BLAST) or successive interference cancellation (SIC) was proposed in [10, 11] for a single user MIMO system which can be easily extended to multiuser systems. Nordio et al. [12] proposed two types of linear MMSE receivers. The work in [13] proposed different space-time block spread CDMA systems. The signature and beamformer design problem was investigated in [14]. Multicarrier CDMA (MC-CDMA) has gained a great deal of attention lately, since it provides low-complexity detectors and robustness against intersymbol interference (ISI) and fading caused by multipath propagation [15, 16]. There are several variations of MC-CDMA, such as multicarrier DS-CDMA (MC-DS-CDMA) proposed by Zakharov and Kodanev [17] and multitone CDMA proposed by Vandendorpe [18].

In this thesis, we first investigate blind code-constrained constant modulus (CCM) SG receivers with variable step-size mechanisms for downlink DS-CDMA systems. We propose a novel variable step-size algorithm which provides better performance compared with existing blind schemes in non-stationary scenarios. Then, novel adaptive DF detectors for space-time uplink CDMA systems are proposed, which employ a novel in-

interference cancellation structure, namely, multiple-parallel feedback branches (MPF) in conjunction with multiple antennas at the receiver. To mitigate the large quantization error and the significant number of feedback bits in multiuser preprocessing systems with limited feedback [19], [20], we propose a novel switched interleaving scheme based on limited feedback for both downlink and uplink in DS-CDMA systems. A codebook of chip-interleavers is incorporated at the transmitter and receiver. Based on a selection function the receiver feeds back an index of the optimum interleaver in the codebook to the transmitter. Simulation results show that a significant gain can be achieved by using a few number of feedback bits. An extension work of the proposed preprocessing technique is further developed in multiantenna MC-CDMA systems. In particular, a new hybrid transmit processing technique based on switched interleaving and chip-wise precoding is proposed for the downlink transmission. At last, we propose novel multistage receivers based on multiple parallel branches successive interference cancellation (MB-SIC) for the uplink of MIMO-CDMA systems.

1.2 Contributions

The contributions of this thesis are summarized as following:

- The performance of blind CCM adaptive receivers for DS-CDMA systems that employ SG algorithms with variable step-size mechanisms is investigated. We propose a novel low-complexity variable step-size mechanism for blind CCM CDMA receivers. Convergence and tracking analyses of the proposed adaptation techniques are carried out for multipath channels. Finally, numerical experiments are presented for nonstationary environments, showing that the new mechanism achieves superior performance to previously reported methods at a reduced complexity.
- We propose a novel space-time MMSE DF detection scheme for DS-CDMA systems with multiple receive antennas, which employs MPF for interference cancellation. The proposed space-time receiver is then further combined with cascaded DF stages for mitigating the deleterious effects of error propagation for uncoded schemes. In order to adjust the parameters of the receiver, we also present modified adaptive SG and RLS algorithms that automatically switch to the best available interference cancellation feedback branch and jointly estimate the feedforward and feedback filters. The performance of the system with beamforming and diversity configurations is also considered.

- A novel switched-interleaving algorithm based on limited feedback is developed for both uplink and downlink DS-CDMA systems. The proposed switched chip-interleaving DS-CDMA scheme requires the cooperation among the transmitter and the receiver, and a feedback channel sending the index of the interleaver is used. The transmit chip-interleaver is chosen by the receiver from a codebook of interleaving matrices known to both the receiver and the transmitter and the codebook index is sent back using a limited number of bits. In order to design the codebook, we consider a number of different chip patterns by using random interleavers, block interleavers and a proposed frequently selected patterns method (FSP). The best interleaving patterns are chosen by the selection functions of the received signal to interference plus noise ratio (SINR) for both downlink and uplink systems. We present symbol-based and block-based linear MMSE receivers for interference suppression.
- Transmit processing techniques based on switched interleaving and limited feedback are investigated for both downlink and uplink MC-CDMA multiple antenna systems. We propose transceiver structures with switched interleaving, linear precoding and detectors for both uplink and downlink. In the novel schemes, a set of possible chip-interleavers are constructed and prestored at both the base station (BS) and mobile stations (MSs). For the downlink, a new hybrid transmit processing technique based on switched interleaving and chip-wise precoding is proposed to suppress the MUI. The BS and MSs are also equipped with another codebook of quantized downlink CSI. Each MS quantizes its own downlink CSI and feeds back the index to the BS by a low-rate feedback channel or link, then the selection function at the BS determines the optimum interleaver based on all users' quantized CSIs to transmit signals. Moreover, a transmit processing technique for the uplink of multiple antenna MC-CDMA systems requiring very low rate of feedback information is also proposed. A codebook design method for quantized CSI is also proposed.
- Novel multistage receivers based on MB-SIC are presented for the uplink of MIMO-CDMA systems. The proposed multistage receivers exploit a conventional ordered SIC for the first stage, followed by a grouping detection strategy and the novel MB-SIC scheme. The grouping detection strategy produces an estimate for the desired user, which consists of the user's antenna data streams, by using the detected information supplied from the first stage. The outputs of the second stage are processed by the proposed schemes using SICs which are equipped with different cancellation orders, so that the branches produce a group of estimated vectors for the desired user. Then, according to a selection rule the MB-SIC selects the refined estimated vector with the best performance for the desired user's antenna streams.

Two selection rules are considered, namely, the maximum likelihood (ML) and the MMSE criteria.

1.3 Thesis Outline

The structure of the thesis is as follows:

- In Chapter 2, a literature review is presented that describes existing multiuser detectors, interference suppression, adaptive blind receivers, preprocessing techniques and limited feedback techniques for DS-CDMA, MC-CDMA and multiantenna systems.
- In Chapter 3, the novel low-complexity variable step-size mechanism for blind CCM CDMA receivers is introduced. Convergence and tracking analyses are carried out, and simulations illustrate the performance of the proposed techniques against existing algorithms.
- In Chapter 4, we propose novel space-time decision feedback receivers based on the MPF scheme. Simulation results for an uplink scenario with uncoded systems show that the proposed space-time MPF-DF detector outperforms in terms of BER existing schemes, and achieves a substantial capacity increase in terms of the number of users over the existing schemes.
- In Chapter 5, switched interleaving techniques for interference mitigation in DS-CDMA systems is described. Simulation results show that our proposed algorithm achieves significantly better performance than the conventional DS-CDMA (C-CDMA) systems and the existing chip-interleaving, linear precoding and adaptive spreading techniques.
- In Chapter 6, we propose transmit processing techniques based on switched interleaving and limited feedback for both downlink and uplink MC-CDMA multiple antenna systems.
- In Chapter 7, we develop novel multistage receivers based on MB-SIC for the uplink of MIMO-CDMA systems.
- In Chapter 8, conclusions and a discussion on possibilities for future work are presented.

1.4 Notation

In this thesis, we use capital and small bold fonts to denote matrices and vectors, e.g., \mathbf{R} and \mathbf{r} , respectively. $(\cdot)^T$ and $(\cdot)^H$ denote transpose and Hermitian transpose, respectively, $E[\cdot]$ stands for expected value, $\Re(\cdot)$ selects the real part, and $\text{sgn}(\cdot)$ is the signum function. The variable i is used as a time index, i.e., $\mathbf{R}(i)$ is the matrix \mathbf{R} at time instant i , $\|\cdot\|$ and $|\cdot|$ denote the norm of a vector and a scalar, respectively, and the symbol j is an imaginary unit $j = \sqrt{-1}$. \otimes denotes the Kronecker product.

1.5 Publication List

Some of the research presented in this thesis has been published, submitted, or will be submitted to some publications at the time of submission of this thesis.

Journal Papers

1. Yunlong Cai and Rodrigo C. de Lamare, “Low-Complexity Variable Step-Size Mechanism for Code-Constrained Constant Modulus Stochastic Gradient Algorithms applied to CDMA Interference Suppression”, *IEEE Trans. on Signal Process.*, vol. 57, no. 1, pp. 313-323, Jan. 2009.
2. Lei Wang, Rodrigo C. de Lamare and Yunlong Cai “Low-Complexity Adaptive Step Size Constrained Constant Modulus SG-based Algorithms for Blind Adaptive Beamforming”, *Signal Processing, Elsevier*, vol. 89, no. 12, pp. 2503-2513, Dec. 2009.
3. Yunlong Cai and Rodrigo C. de Lamare, “Space-Time Adaptive MMSE Multiuser Decision Feedback Detectors with Multiple Feedback Interference Cancellation for CDMA Systems”, *IEEE Trans on Vehicular Technology*, vol. 58, no. 8, pp. 4129-4140, Oct. 2009.
4. Yunlong Cai, Rodrigo C. de Lamare and Rui Fa, “Switched Interleaving Techniques with Limited Feedback for Interference Mitigation in DS-CDMA Systems”, *IEEE Trans. on Commun.*, under review.
5. Yunlong Cai, Rodrigo C. de Lamare and Didier Le Ruyet, “Transmit Processing Techniques Based on Switched Interleaving and Limited Feedback for Interference

Mitigation in Multi-antenna MC-CDMA Systems”, *IEEE Trans. on Wireless Commun.*, under review.

6. Yunlong Cai, Rodrigo C. de Lamare, “Multistage MIMO Receivers Based on Multi-Branch Interference Cancellation for MIMO CDMA Systems”, *IET Commun.*, in preparation.

Conference Papers

1. Yunlong Cai and Rodrigo C. de Lamare, “Space-Time Adaptive MMSE Multiuser Decision Feedback Detectors with Multiple Feedback Interference Cancellation for CDMA Systems”, *IEEE International Symposium Wireless Communication Systems*, 2007 Trondheim, Norway.
2. Yunlong Cai and Rodrigo C. de Lamare, “Low-Complexity Variable Step-Size Mechanism for Code-Constrained Constant Modulus Stochastic Gradient Algorithms applied to CDMA Interference Suppression”, *Asilomar Conference on Signals, Systems, and Computers, Pacific Grove, CA, US*, 2007.
3. Lei Wang, Yunlong Cai and Rodrigo C. de Lamare, “Low-Complexity Adaptive Step Size Constrained Constant Modulus SG-based Algorithms for Blind Adaptive Beamforming”, *Proc. IEEE International Conference on Acoustics, Speech and Signal Processing*, 5, Las Vegas, USA, 2008
4. Yunlong Cai, Rodrigo C. de Lamare and Rui Fa, “Linear Interference Suppression for Spread Spectrum Systems with Switched Interleaving and Limited Feedback,” *Wireless Communications and Networking Conference*, Budapest, Hungary, Sep. 2009.
5. Yunlong Cai, Rodrigo C. de Lamare and Rui Fa, “Novel Switched Interleaving Techniques with Limited Feedback for DS-CDMA Systems,” *IEEE International Conference on Communications*, Dresden, Germany, 2009.
6. Yunlong Cai and Rodrigo C. de Lamare, “Multistage MIMO Receivers Based on Multi-Branch Interference Cancellation for MIMO CDMA Systems”, *IEEE International Symposium Wireless Communication Systems*, University of Siena, Italy, 2009.
7. Yunlong Cai, Rodrigo C. de Lamare, and Didier Le Ruyet, “Linear Precoding Based on Switched Interleaving and Limited Feedback for Interference Suppression in Downlink Multi-antenna MC-CDMA Systems”, *Proc. IEEE International Conference on Acoustics, Speech and Signal Processing*, Dallas, USA, 2010, submitted.

8. Yunlong Cai, Rodrigo C. de Lamare, and Didier Le Ruyet, “Interference Cancellation Using Switched Interleavers in Uplink Multi-Antenna MC-CDMA Systems”, *IEEE International Symposium on Circuits and Systems*, Paris, France, 2010, submitted.

Chapter 2

Literature Review

Contents

2.1 Introduction	9
2.2 Multiuser Detection for DS-CDMA Systems	10
2.3 Adaptive Receivers and Blind Linear Receivers	15
2.4 Preprocessing Techniques for DS-CDMA Systems	18
2.5 Spread Spectrum with Multicarrier and Multiantenna Techniques .	22
2.6 Limited Feedback Techniques	26
2.7 Conclusions	30

2.1 Introduction

This chapter presents the background of the techniques used to mitigate interference in CDMA systems. We first discuss the conventional MUD, and adaptive and blind detection algorithms for DS-CDMA systems. Secondly, we describe the existing transmit processing techniques including, chip-interleaving algorithms, precoding techniques and signature optimization schemes. Then, we introduce system models of the conventional CDMA combined with multicarrier and multiantenna schemes. At last, we mention the limited feedback techniques, which are employed in different systems.

The rest of this chapter is organized as follows. In Section 2.2, the optimum detector, the linear MMSE detector, the decision feedback detectors, and the interference cancellation receivers are introduced. Adaptive and blind algorithms are presented in Section 2.3.

A literature review on transmit preprocessing techniques and CDMA in conjunction with multicarrier and multiantenna schemes is presented in Sections 2.4 and 2.5, respectively. Limited feedback techniques are introduced in Section 2.6. Finally, conclusions are given in Section 2.7.

2.2 Multiuser Detection for DS-CDMA Systems

MUD deals with the demodulation of mutually interfering digital streams of information. Cellular telephony, satellite communications, multitrack magnetic recording are systems subject to multi-access interference. MUD exploits the structure of the MUI in order to increase the efficiency with which channel resources are employed. Multiuser communication channels have been investigated since 1965. However, it was not until the mid 1980s that MUD started developing as a cohesive body of analytical results taking into account the specific features of multiuser channels [1, 2].

2.2.1 Direct-Sequence Spread Spectrum

Developed initially for military antijamming communications in the mid-1950s, spread spectrum (SS) has been found a wide range of applications in commercial wireless systems [21]. The underlying idea of spread spectrum is to spread a signal over a large frequency band and transmit it with low power per unit bandwidth. Among many possible ways of spreading the bandwidth, the predominant type is DS spread-spectrum.

DS spread spectrum achieves band spreading by modulating the information symbol stream with a higher rate chip sequence. Assume that each symbol of duration T is spread into multiple chips of duration $T_c < T$. The bandwidth expansion factor $N = T/T_c$ determines the amount of redundancy injected during modulation. N is often called the spreading factor or the processing gain. In practice, pseudorandom noise (PN) chip sequences are often employed to make the spreading signal as random as possible. After spreading, the chip sequence is usually shaped by a chip pulse shaping filter, $p(t)$, to limit the bandwidth of the output. Mathematically, the spread spectrum modulated BPSK baseband signal of the k -th user can be expressed as:

$$x_k(t) = \sum_{i=-\infty}^{\infty} b_k(i) s_k^{(i)}(t - iT) \quad (2.1)$$

where

$$s_k^{(i)}(t) = \sum_{n=1}^N c_k^{(i)}(n)p(t - nT_c + T_c) \quad (2.2)$$

is the spreading waveform or signature waveform for the i -th symbol, where the binary code is $\{c_k^{(i)}(n) \in [-1, 1]\}$.

At the receiver side, a conventional single-user matched filter captures the desired signal from the one-dimensional subspace defined by the spreading waveform $s_k^{(i)}(t)$ and only those responses to the interference that lie in the direction of the signal. Here it should be mentioned that this thesis only considered synchronous CDMA models for both uplink and downlink. Assuming that the delay spread is not very large, a synchronous model captures well the features of an asynchronous model [2]. When the code period is the same as the symbol duration, the spreading waveform becomes "periodic", that is, the spreading waveform remains the same from symbol to symbol, in this case, the spreading waveform is called short code, namely, $s_k^{(i)}(t) = s_k(t)$. CDMA with short codes has been adapted for the third-generation high-performance personal communication services [3]. The spreading waveforms called long spreading codes are "aperiodic", that is, they vary from symbol to symbol.

2.2.2 Optimum Multiuser Detection

The optimum MUD was invented based on the principles of detection theory [22], and performs ML detection. The optimum receiver must know, in addition to the user signature waveforms, the received amplitudes of all users and the noise level. If the transmitted data are equiprobable and independent, in the AWGN channel the jointly optimum decisions are the ML decision [1]:

$$(\hat{b}_1(i), \hat{b}_2(i), \dots, \hat{b}_K(i)) = \min_{b_1(i), \dots, b_K(i) \in \{-1, +1\}} \left\{ \int_0^{T_s} [r(t) - \sum_{k=1}^K A_k b_k(i) s_k(t)]^2 dt \right\}, \quad (2.3)$$

where $r(t)$ is the received signal, A_k is the amplitude of the k -th user. In two-user scenario, $K = 2$, the optimum decisions are:

$$(\hat{b}_1(i), \hat{b}_2(i)) = \min_{b_1(i), b_2(i) \in \{-1, +1\}} \left\{ \int_0^{T_s} [r(t) - A_1 b_1(i) s_1(t) - A_2 b_2(i) s_2(t)]^2 dt \right\}. \quad (2.4)$$

In two-user scenario we need to consider four combinations of the transmitted data:

$$(\hat{b}_1(i), \hat{b}_2(i)) = \{(+1, +1); (+1, -1); (-1, +1); (-1, -1)\}, \quad (2.5)$$

then to calculate the integral four times (once for each combination) and take the minimum. We can rewrite (2.4) as

$$\begin{aligned} (\hat{b}_1(i), \hat{b}_2(i)) &= \max_{b_1(i), b_2(i) \in \{-1, +1\}} \{y_1 A_1 b_1(i) + y_2 A_2 b_2(i) - b_1(i) b_2(i) A_1 A_2 \rho\} \\ &= \max_{b_1(i), b_2(i) \in \{-1, +1\}} \{b_1(i) z_1 + b_2(i) z_2 - b_1(i) b_2(i) z_p\}, \end{aligned} \quad (2.6)$$

where $y_1 = \int_0^{T_s} r(t) s_1(t) dt$, $y_2 = \int_0^{T_s} r(t) s_2(t) dt$, $\rho = \int_0^{T_s} s_1(t) s_2(t) dt$, $z_1 = y_1 A_1$, $z_2 = y_2 A_2$, and $z_p = \rho A_1 A_2$. Thus, for $K = 2$, we obtain a simpler receiver, yet optimal [1].

However, for arbitrary K we have to analyse 2^K combinations. For example, if $K = 30$ we have $2^{30} \approx 1000,000,000$ combinations. This is too complicated for real-time implementation. And the optimum detector requires the knowledge of timing, amplitude and signature sequences. The large gaps in performance and complexity between the conventional single-user matched filter and the optimum multiuser detector encouraged the search for other multiuser detectors that exhibit good performance and complexity tradeoffs.

2.2.3 MMSE Linear Receiver

Linear multiuser detectors can be implemented in a decentralized fashion where only the user or users of interest need to be demodulated [1]. When the received amplitudes are completely unknown the decorrelating detector is a sensible choice. A common approach in estimation theory is the problem of estimating a random variable W on the basis of observations Z . This corresponds to choosing the function $\hat{W}(Z)$ that minimizes the mean-square error (MSE):

$$E[|W - \hat{W}(Z)|^2]. \quad (2.7)$$

We can turn the problem of linear multiuser detection into a problem of linear estimation, by requiring that the MSE between the i -th symbol of the k -th user $b_k(i)$ and the output of the k -th linear transformation $\mathbf{v}_k^H(i) \mathbf{r}(i)$ be minimized, where $\mathbf{r}(i) = \sum_{j=1}^K A_j b_j(i) \mathbf{s}_j + \mathbf{n}(i)$ denotes the $N \times 1$ received vector after sampling, \mathbf{s}_j and $\mathbf{n}(i)$ are the $N \times 1$ signature and noise vectors, respectively, the MMSE linear detector for the k -th user chooses the waveform $\mathbf{v}_k^H(i)$ of duration T that achieves

$$\min_{\mathbf{v}_k} E[|A_k b_k(i) - \mathbf{v}_k^H(i) \mathbf{r}(i)|^2] \quad (2.8)$$

where

$$E[|A_k b_k(i) - \mathbf{v}_k^H(i) \mathbf{r}(i)|^2] = E[(A_k b_k(i) - \mathbf{v}_k^H(i) \mathbf{r}(i))(A_k b_k(i) - \mathbf{v}_k^H(i) \mathbf{r}(i))^*], \quad (2.9)$$

and

$$\begin{aligned} E[(A_k b_k - \mathbf{v}_k^H \mathbf{r})(A_k b_k - \mathbf{v}_k^H \mathbf{r})^*] &= A_k^2 - A_k E[A_k b_k \mathbf{r}^H] \mathbf{v}_k - A_k \mathbf{v}_k^H E[\mathbf{r} A_k b_k^*] + \mathbf{v}_k^H \mathbf{R} \mathbf{v}_k \\ &= A_k^2 - A_k^2 \mathbf{s}_k^H \mathbf{v}_k - A_k^2 \mathbf{v}_k^H \mathbf{s}_k + \mathbf{v}_k^H \mathbf{R} \mathbf{v}_k, \end{aligned} \quad (2.10)$$

where, the index i is removed for simplicity, and \mathbf{R} is the correlation matrix of the received data. $\mathbf{R} = \sum_{j=1}^K A_j^2 \mathbf{s}_j \mathbf{s}_j^H + \sigma^2 \mathbf{I}$, where \mathbf{I} denotes an identity matrix. We take the gradient of the last expression with respect of \mathbf{v}_k^* , and we have the result

$$\mathbf{R} \mathbf{v}_k - A_k^2 \mathbf{s}_k, \quad (2.11)$$

setting it to zero, we have that the MMSE receiver for user k is given by

$$\begin{aligned} \mathbf{v}_k &= \mathbf{R}^{-1} A_k^2 \mathbf{s}_k \\ &= \left(\sum_{j=1}^K \frac{A_j^2}{A_k^2} \mathbf{s}_j \mathbf{s}_j^H + \frac{\sigma^2}{A_k^2} \mathbf{I} \right)^{-1} \mathbf{s}_k. \end{aligned} \quad (2.12)$$

The MMSE receiver also can be designed by using adaptive algorithms such as SG and RLS algorithms [1, 4, 5].

2.2.4 Decision Feedback Receivers

A number of works in MUD have proposed nonlinear receivers that use decisions on the bits of interfering users in the demodulation of the bit of interest. Some of those solutions use final decisions, while other proposed solutions employ tentative decisions used only internally by the demodulator. The successive and parallel interference cancellers are very popular approaches [1, 23].

Let us describe the design of general decision feedback receivers. As depicted in Fig 2.1, the input to the hard decision device corresponding to the i -th symbol is $\mathbf{z}(i) = \mathbf{W}^H(i) \mathbf{r}(i) - \mathbf{F}^H(i) \hat{\mathbf{b}}(i)$, where the input $\mathbf{z}(i) = [z_1(i) \dots z_K(i)]^T$, $\mathbf{W}(i) = [\mathbf{w}_1(i) \dots \mathbf{w}_K(i)]$ is the $N \times K$ feedforward matrix, $\hat{\mathbf{b}}(i) = [\hat{b}_1(i) \dots \hat{b}_K(i)]^T$ is the $K \times 1$ vector of estimated symbols, which are feedback through the $K \times K$ feedback matrix $\mathbf{F}(i) = [\mathbf{f}_1(i) \dots \mathbf{f}_K(i)]$. Specifically, the DF receiver design is equivalent to determining for user k a feedforward filter $\mathbf{w}_k(i)$ with N elements and a feedback one $\mathbf{f}_k(i)$ with K elements that provide an estimate of the desired symbol:

$$z_k(i) = \mathbf{w}_k^H(i) \mathbf{r}(i) - \mathbf{f}_k^H(i) \hat{\mathbf{b}}(i), \quad k = 1, 2, \dots, K \quad (2.13)$$

where $\hat{\mathbf{b}}(i) = \text{sgn}(\Re(\mathbf{W}^H \mathbf{r}^H(i)))$ is the vector with initial decisions provided by the linear detector, \mathbf{w}_k and \mathbf{f}_k are optimized by the MMSE criterion. The final detected symbol is:

$$\hat{b}_k^f(i) = \text{sgn}(\Re(z_k(i))) = \text{sgn}(\Re(\mathbf{w}_k^H(i) \mathbf{r}(i) - \mathbf{f}_k^H(i) \hat{\mathbf{b}}(i))). \quad (2.14)$$

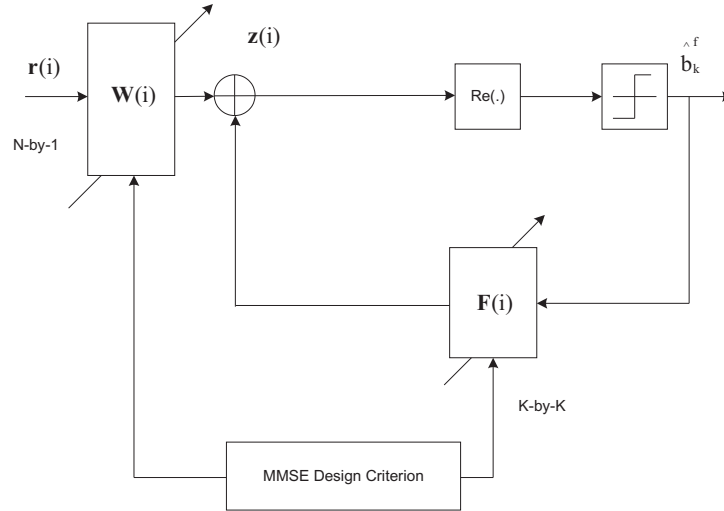


Figure 2.1: General DF receiver structure

2.2.5 Interference Cancellation Receivers

Here we consider that the estimates of interfering users' signals are the intermediate decisions for the receivers. We have two common used decision feedback receivers. The first one is named SIC [1]. Let us consider a two-user scenario, where the output of the matched filters are:

$$\begin{aligned} z_1(i) &= A_1 b_1(i) + \rho A_2 b_2(i) + n_1, \\ z_2(i) &= A_2 b_2(i) + \rho A_1 b_1(i) + n_2. \end{aligned} \quad (2.15)$$

The detected symbol for user k is

$$\hat{b}_k(i) = \text{sgn}(z_k(i)). \quad (2.16)$$

If user 1 is much stronger than user 2, the MUI term present in the signal of user 2 is very large. The SIC decision is made for the stronger user 1:

$$\hat{b}_1(i) = \text{sgn}(z_1(i)). \quad (2.17)$$

Then, we subtract the estimate of the MUI imposed by the first user from the signal of the second user:

$$\hat{b}_2(i) = \text{sgn}(z_2(i) - \rho A_1 \hat{b}_1(i)). \quad (2.18)$$

All MUI can be subtracted from user 2's signal provided that the initial data estimate of user 1 is correct. Hence, MUI is reduced. For the general case with K users, we should arrange the received signals and then detect them in order from the strongest one to the

weakest one to alleviate the error propagation. The k' -th detected signal is

$$\hat{b}_{k'}(i) = \text{sgn}(z_{k'}(i) - \sum_{j=1}^{k'-1} A_j \rho_{jk'} \hat{b}_j(i)), \quad (2.19)$$

where $\rho_{jk'} = \mathbf{s}_j^H \mathbf{s}_{k'}$. Another one is parallel interference cancellation (PIC) [1]. It has the similar structure but simultaneously subtracts off all of the users' signals from all of the others. This works better than the successive canceller when all of the users are received with equal strength for example under power control [1]. However, in the case of unequal power strength, SIC can be better than PIC in terms of the achievable BER performance.

$$\hat{b}_k(i) = \text{sgn}(z_k(i) - \sum_{j \neq k} A_k \rho_{jk} \hat{b}_j(i)) \quad (2.20)$$

Here, we treated feedforward and feedback receivers as matched filters, we also have other choices like decorrelating receivers or MMSE receivers and so on.

2.3 Adaptive Receivers and Blind Linear Receivers

Filtering is a signal processing operation whose objective is to process a signal in order to manipulate or extract the information contained in the signal [4]. For time-invariant filters the internal parameters and the structure of the filter are fixed. An adaptive filter is required when either the fixed specifications are unknown or the specifications cannot be satisfied by time-invariant filters. The adaptive filters are time-varying since their parameters are continually changing in order to meet a performance requirement. The adaptive algorithm is the procedure used to adjust the adaptive filter coefficients in order to minimize a prescribed criterion. We define the error signal as the difference between the output of an adaptive filter namely, recovered signal and the desired signal. The error signal is then used to form performance (or objective) function that is required by the adaptation algorithm in order to determine the appropriate updating of the filter coefficients. The minimization of the objective function implies that the adaptive filter output signal is matching the desired signal in some sense. Two common adaptive algorithms are introduced in the following sections.

In the multiuser detection literature, adaptive algorithms that operate without knowledge of the channel input are called blind. In this section, we show an adaptive linear detector that converges to the MMSE detector without requiring training sequences. The knowledge required by the detector is only the timing and the spreading code of the desired user.

2.3.1 Stochastic Gradient Algorithm (SG)

Assume that we have an error signal $e(i) = b(i) - \mathbf{w}^H(i)\mathbf{u}(i)$, where $b(i)$ is the desired signal, $\mathbf{w}(i)$ is the adaptive filter weight vector, and $\mathbf{u}(i)$ is the received data. The cost function $J(i)$ is the mean square error $J(i) = E[|e(i)|^2]$. In the steepest descent algorithm [4], we have the update equation

$$\mathbf{w}(i+1) = \mathbf{w}(i) - \mu \nabla J(i) \quad (2.21)$$

In the SG algorithm, we develop an estimate of the gradient vector $\nabla J(i)$, the most obvious strategy is to use instantaneous estimates that are based on sample values of the tap-input vector and the desired response. This is known as the least mean squares (LMS) algorithm [4], and at last we have the instantaneous estimate of the gradient vector given by

$$\hat{\nabla} J(i) = -\mathbf{u}(i)b^*(i) + \mathbf{u}(i)\mathbf{u}^H(i)\hat{\mathbf{w}}(i) \quad (2.22)$$

By substituting into the equation of (2.21) we have the update equation of the SG algorithm.

$$\mathbf{w}(i+1) = \mathbf{w}(i) + \mu \mathbf{u}(i)e^*(i) \quad (2.23)$$

where $e(i)$ is the error signal. To ensure the convergence of the SG algorithm, the step size μ should be chosen in the range [4]:

$$0 < \mu < \frac{2}{\lambda_{max}} \quad (2.24)$$

2.3.2 Recursive Least Squares Algorithm (RLS)

The RLS is an algorithm that exploits a recursive approach for implementing the method of least squares for the design of adaptive filters. By exploiting a relation in matrix algebra known as the matrix inversion lemma [4], we describe the RLS algorithm as:

Initialize the algorithm by setting $\mathbf{P}(0) = \delta^{-1}\mathbf{I}$, δ =small positive constant, $\hat{\mathbf{w}}(0) = \mathbf{0}$

For each instant of time, $i = 1, 2, \dots$, compute

$$\mathbf{k}(i) = \frac{\lambda^{-1}\mathbf{P}(i-1)\mathbf{u}(i)}{1 + \lambda^{-1}\mathbf{u}^H(i)\mathbf{P}(i-1)\mathbf{u}(i)} \quad (2.25)$$

$$\xi(i) = b(i) - \hat{\mathbf{w}}^H(i-1)\mathbf{u}(i) \quad (2.26)$$

$$\hat{\mathbf{w}}(i) = \hat{\mathbf{w}}(i-1) + \mathbf{k}(i)\xi^*(i) \quad (2.27)$$

$$\mathbf{P}(i) = \lambda^{-1}\mathbf{P}(i-1) - \lambda^{-1}\mathbf{k}(i)\mathbf{u}^H(i)\mathbf{P}(i-1), \quad (2.28)$$

where λ is exponential weighting factor or forgetting factor, it is a positive constant close to, but less than 1. The resulting rate of convergence is therefore typically an order of magnitude faster than the simple LMS algorithm [4]. This improvement in performance, however, is achieved at the expense of a large increase in computational complexity.

2.3.3 Constrained Minimum Variance Algorithm

The blind algorithm which is introduced here is named constrained minimum variance (CMV) algorithm. Consider the cost function $J = E[|\mathbf{w}_k^H(i)\mathbf{r}(i)|^2]$, where $\mathbf{w}_k(i)$ is the filter weight vector, $\mathbf{r}(i)$ is the received data, subject to the constraint given by $\mathbf{w}_k^H(i)\mathbf{s}_k = 1$. Thus, we derive an adaptive expression for the CMV linear receiver by solving an unconstrained optimization problem given in the form of a Lagrangian cost function [24, 25]:

$$\mathbf{J} = \mathbf{w}_k^H(i)\mathbf{r}(i)\mathbf{r}^H(i)\mathbf{w}_k(i) + \text{Re}[\lambda(\mathbf{w}_k^H(i)\mathbf{s}_k - 1)], \quad (2.29)$$

where λ is a Lagrange multiplier, by taking the gradient with respect to \mathbf{w}_k^* . We obtain the expression for the CMV-SG algorithm

$$\mathbf{w}_k(i+1) = \mathbf{w}_k(i) - \mu z^*(i)(\mathbf{r}(i) - z_{MF}(i)\mathbf{s}_k) \quad (2.30)$$

where $z(i) = \mathbf{w}_k^H(i)\mathbf{r}(i)$, $z_{MF}(i) = \mathbf{s}_k^H\mathbf{r}(i)$.

2.3.4 Constrained Constant Modulus Algorithm

Let us consider another cost function $J = E[e^2(i)]$, where $e(i) = |\mathbf{w}_k^H(i)\mathbf{r}(i)|^2 - 1$ subject to the constraint given by $\mathbf{w}_k^H(i)\mathbf{s}_k = 1$. We still can follow the same approach to get the update equation called CCM SG.

$$\mathbf{w}_k(i+1) = \mathbf{w}_k(i) - \mu e(i)z^*(i)(\mathbf{r}(i) - z_{MF}(i)\mathbf{s}_k) \quad (2.31)$$

In a number of papers, the CCM was found to outperform the CMV approach [26], [27]. In the following chapters, a low-complexity variable step-size mechanism for CCM SG algorithms is proposed. Here, the blind algorithms are introduced and considered in an AWGN channel. We will extend them to multipath fading channels later.

2.4 Preprocessing Techniques for DS-CDMA Systems

There has been increasing interest in preprocessing techniques for DS-CDMA systems, partly motivated by the possibility of shifting the bulk of processing from the mobile station to the base station on the downlink. In this section, we discuss some preprocessing techniques, including the chip-interleaving algorithms, CDMA precoding techniques and signature optimization techniques.

2.4.1 Chip-Interleaving Algorithms

Temporal variations in multipath fading channels restrict the performance of DS-CDMA systems. A typical fade in a wireless channel lasts over several bits duration and causes many burst errors. This is typically mitigated by bit interleaving [28]. Recently, a number of works have considered to employ chip-interleaving for CDMA systems.

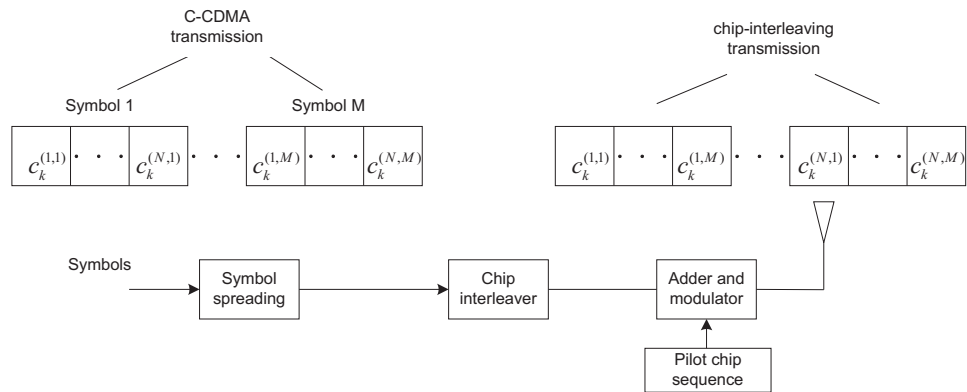


Figure 2.2: Pilot-aided chip-interleaving scheme

The work in [29] demonstrates that chip-interleaving overperforms bit-interleaving. This result is based on the assumption that the receiver has perfect channel state information. In [6] the authors proposed a pilot-aided chip-interleaving algorithm for the uplink of a CDMA system, and the proposed system is capable of outperforming the conventional CDMA (C-CDMA) one by using the estimated channel state information. Transmission of a pilot symbol along with the information symbol is a common practice for estimating fading-channel parameters. In the work of pilot-aided chip-interleaving algorithm, a continuous pilot signal is transmitted without chip-interleaving, and a simple matched filter receiver is employed to estimate time-varying multipath channel coefficients. After estimating the channel coefficients, the contribution of the pilot signals is subtracted

from the received signal prior to detection of the information symbols, and the Rake receiver is used to do the symbol recovery. Fig. 2.2 depicts the transmitter of user k in the chip-interleaving algorithm, where $c_k^{(1,\beta)} \dots c_k^{(N,\beta)}$ denotes the chip sequence of the β -th symbol, $\beta = 1 \dots M$, and M is the block length.

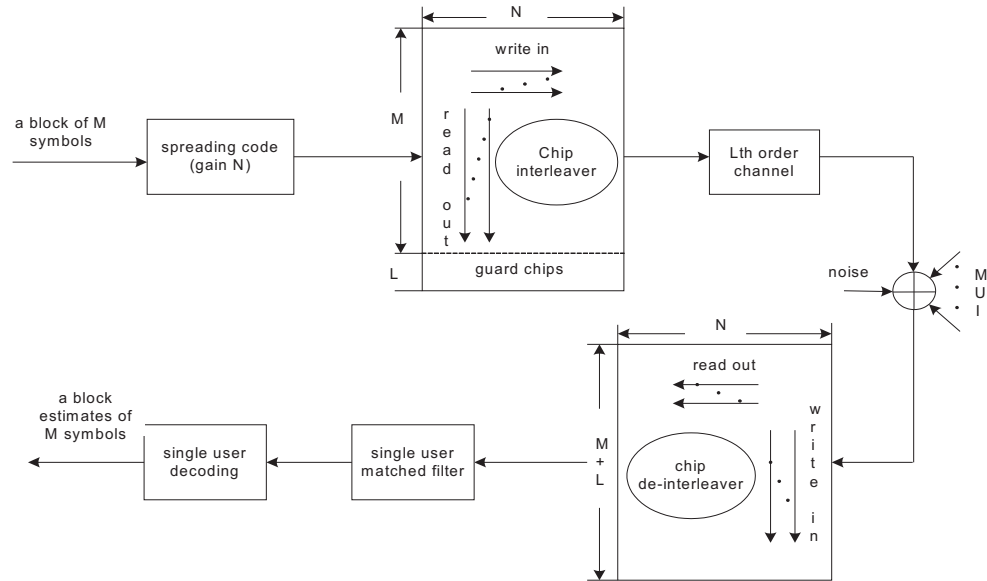


Figure 2.3: MUI-free transceiver for a single user.

The relevant work in [30] compared and analyzed two fade-resistant transmission systems, which are chip-interleaving and parallel transmission systems. It shows that the fade-resistant transmission CDMA systems exhibit identical performance when the system load is high. However, when the system load is light, the chip-interleaving system outperforms the system that transmits information symbols simultaneously due to higher self-interference in the latter. A CDMA system with partitioned chip-interleaving algorithm has been proposed by Schlegel in [31], where the signature sequences are partitioned into sections, which are interleaved before transmission, and processed at the receiver. Zhou et al. [7] proposed a MUI free transceiver for the frequency-selective multipath channels, which can be viewed as a block-spreading algorithm. Due to chip-interleaving and zero padding at the transmitter, mutual orthogonality between different users' codes is preserved even after multipath propagation, which enables deterministic multiuser separation through low-complexity matched filtering without loss of maximum likelihood optimality. Consequently, multiuser detection is successfully converted to a set of equivalent single-user equalization problem. The transceiver structure is shown in Fig. 2.3.

2.4.2 CDMA Precoding Techniques

Current MUD receivers offer attractive compromise between performance and complexity, but this has placed an ever increasing computational and cost burden on detectors, demodulators, decoders, etc. Nevertheless, the goal of maintaining low cost and complexity, especially at the mobile units, is as important as ever. As a result, research work has been recently introduced on new schemes that move toward that goal. In particular, a novel signal processing technique that has attracted a lot of attention in the last few years is transmitter-based multiuser interference mitigation at the base station. This is inspired by dirty-paper coding [32].

The critical assumption is that the base station has access to the CSI of all active mobile units. This is feasible if the CSI is obtained from receivers via feedback or can be estimated at the transmitter when a time-division duplex (TDD) mode is employed. Another important requirement is that the multipath channel is sufficiently slow, so that the length of the precoding block can be adjusted to match the channel dynamics. The practical applications of transmitter precoding can be found in wireless local loops, wireless LANs and indoor communications in general.

The simplest way to use this CSI at the transmitter in spread-spectrum modulation is to employ a pre-Rake [33]. In this technique, the channel matched filtering usually performed by a Rake receiver is transferred to the base station transmitter, such that just a simple one-finger receiver can be used at the mobile terminal. Even though the pre-Rake may increase the downlink capacity [34] under certain conditions, the signals from different users are precoded individually with this method and no attempt is made to combat the MUI.

When the signal is jointly optimized based on the knowledge of the data bits, spreading sequences and CSI of every user, MUI can be nevertheless reduced or even eliminated. This kind of transmitter precoding was originally proposed for additive white Gaussian noise (AWGN) channels in [8], [35] and independently for flat fading channels in [36]. The work in [35] proposed more complete treatments of transmitter precoding in both flat fading and multipath fading channels. Specifically, an optimum (in the MMSE sense) precoding transformation by means of unconstrained and constrained optimization is derived. In the former case, to maintain the transmit power the same as in the case without precoding, the powers of all signals are scaled by the factor corresponding to the power increase due to precoding. By means of precoding, the multiuser detection problem is reduced to decoupled single user detection problems.

Joint transmitter and receiver optimization in synchronous multiuser systems is proposed in [37]. In this work, joint optimization is represented by a linear transformation of the transmitted signals at the transmitter and a linear transformation of received signals at each receiving site that minimize the effect of MUI and multipath interference. The MMSE between the true bit value and its estimate at the output of the receiver is taken as the cost function. Another work in [38] proposed a nonlinear transmitter precoding scheme, where for each symbol period, an energy-constrained nonlinear transformation is applied at the transmitter output to minimize the MSE at the receiver, subject to a constraint on the peak transmitted energy. The proposed algorithm can be implemented with existing optimization techniques that solve the quadratic trust-region problem.

2.4.3 Signature Optimization Techniques

The use of short or repeat signature sequences in a DS-CDMA system enables the use of adaptive techniques for suppression of MUI [2]. In addition, short codes also enable the possibility of selecting a user signature sequence to avoid interference [37, 39–41]. Here, we describe the signature optimization techniques for uplink CDMA. In general, adaptation of a user signature sequence serves two purposes: pre-equalization of the channel and interference avoidance. Joint optimization of a user signature sequence with a linear adaptive receiver was presented in [9]. No multipath is assumed in that work, so that the transmitter signature sequence is matched to the receiver filter. It is shown that continuous adaptation achieves single-user performance for the loads considered. Selection of an ensemble of signature sequences that minimize total interference power with matched filter receivers is considered in [39] and [40]. The design of signature waveforms to optimize bandwidth efficiency is studied in [42].

A user-by-user optimization algorithm without multipath, based on individual updates, has been presented and analyzed in [43] where it is referred to as interference avoidance. In [44], a modified version of interference avoidance is presented which is guaranteed to converge to a solution which minimizes the sum MSE. In the presence of multipath, the work in [45] presented a "reduced-rank" transmitter adaptation scheme, in which each signature sequence is constrained to lie in a lower dimensional subspace, spanned by some orthogonal basis. The weights for the basis are then selected to optimize the performance criterion, namely output SINR. Fig. 2.4 shows a block diagram of a single user communications system with joint signature-receiver adaptation, where the dimension of each basis vector is $N \times 1$, the $N \times D$ basis matrix consists of the D basis vectors, the reduced-rank vector contains D amplitudes, which is alternatively updated at the receiver, the $N \times 1$ spreading code is equal to the basis matrix multiplied by the reduced-rank vector.

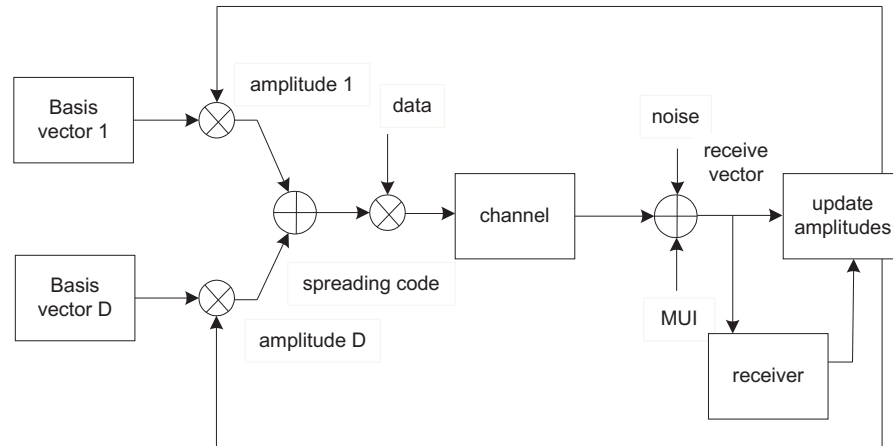


Figure 2.4: Discrete-time baseband model for joint signature-receiver adaptation

Different orthogonal bases are assigned to different users. The work distinguishes between individual and collective adaptation. Individual adaptation refers to the scenario in which each user adapts to optimize its own performance without regard to the performance of other users in the system. This is motivated by a peer-peer network where a receiver may not have access to parameters for other users. Collective adaptation refers to the scenario in which each user adapts to optimize an overall system objective function. This is more appropriate for the uplink of a cellular system.

2.5 Spread Spectrum with Multicarrier and Multi-antenna Techniques

Recently, code division and Orthogonal Frequency Division Multiplexing (OFDM) based multiple access schemes have drawn a lot of attention in the field of wireless personal and multimedia communications [46]. It is mainly because of the need to transmit high data rate in a mobile environment which makes a highly hostile radio channel [15]. A combination of CDMA and multiple antennas techniques has also been investigated, which further improved the system performance and capacity [13, 14, 47]. In this part, we review two types of multicarrier spread spectrum schemes and some extension works of CDMA interference suppression techniques in multiantenna systems.

2.5.1 Spread Spectrum with Multicarrier Schemes and Transceiver Structure

MC-CDMA and MC-DS-CDMA schemes are proposed by N. Yee et al. [48] and V. DaSilva et al. [17], respectively. These signals can be easily transmitted and received using the Fast Fourier Transform (FFT) device without increasing the transmitter and receiver complexities [15]. The MC-CDMA technique spreads the original data stream using a given spreading code, and then modulates a different subcarrier with each chip, in a sense, the spreading operation in the frequency domain [15, 48], and the MC-DS-CDMA technique spreads the serial-to-parallel (S/P) converted data streams using a given spreading code, and then modulates a different subcarrier with each data stream, where the spreading operation is in the time domain [15, 17].

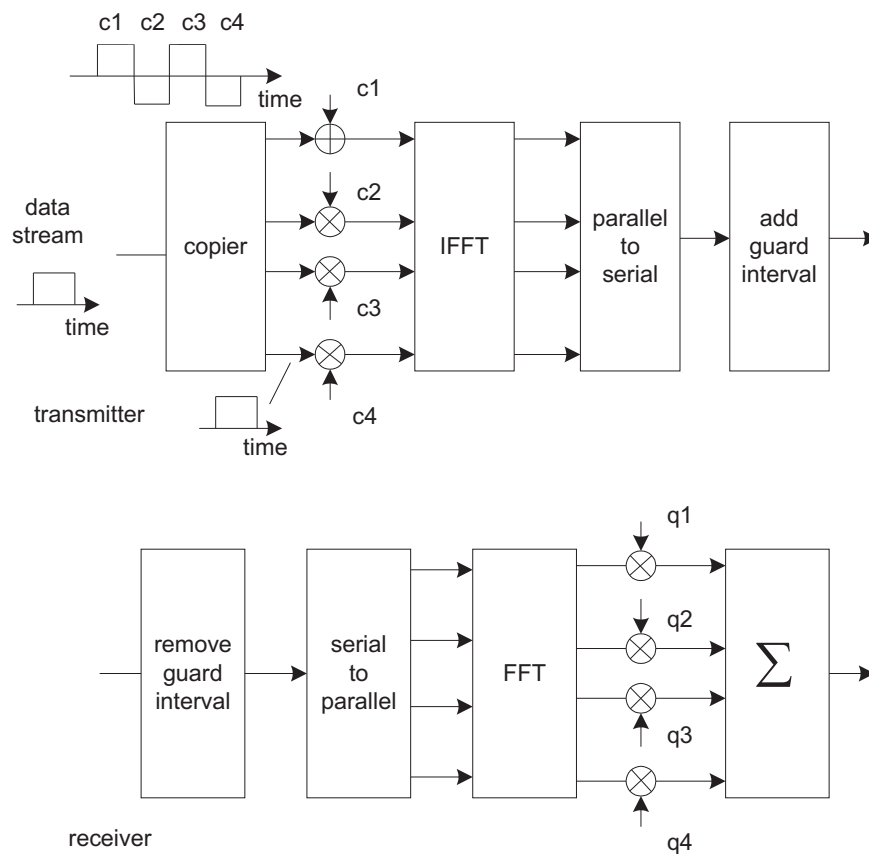


Figure 2.5: MC-CDMA scheme: transmitter and receiver

Fig. 2.5 shows the MC-CDMA transmitter and receiver for BPSK scheme, where the number of subcarriers $N_c = 4$ and the processing gain $N = 4$. The transmitted signal of

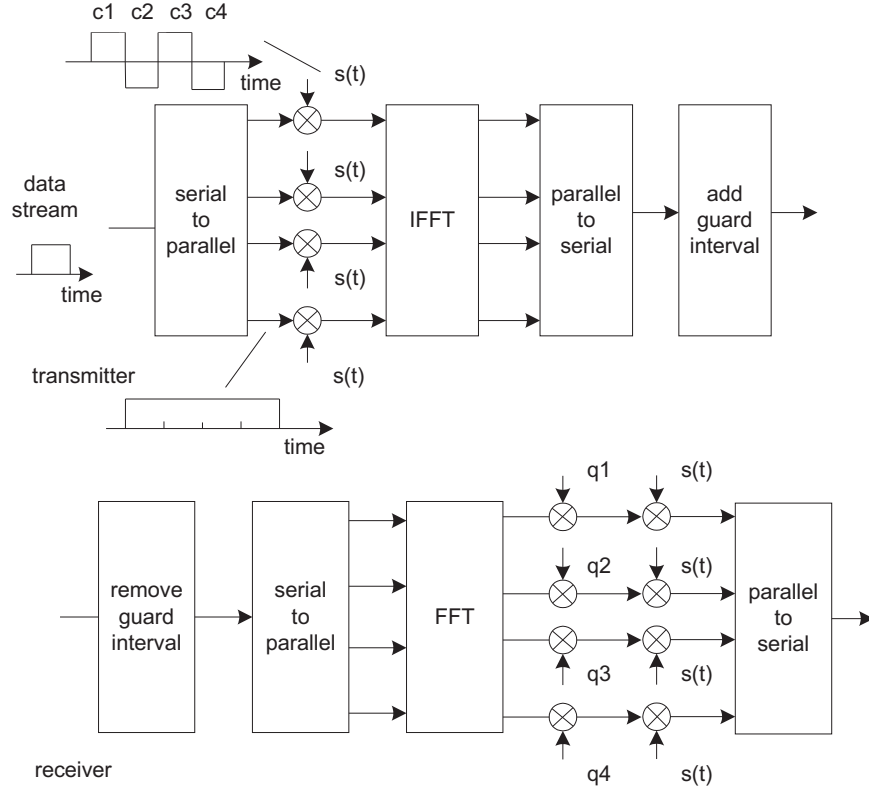


Figure 2.6: MC-DS-CDMA scheme: transmitter and receiver

the k -th user at the i symbol time is written as

$$x_v^k = \sum_{m=0}^{N_c-1} b_k(i) c_m^k e^{j2\pi m v \Delta f}, v = 0 \dots N_c - 1, \quad (2.32)$$

where $b_k(i)$ is the i -th symbol of the k -th user, Δf denotes the subcarrier separation, c_m^k is the m -th chip of the spreading code, $k = 1 \dots K$. At the receiver, after the serial-to-parallel conversion and FFT, the m -th subcarrier is multiplied by the gain q_m^k to combine the received signal in the frequency domain. The decision variable is given by

$$d_k = \sum_{m=0}^{N_c-1} q_m^k y_m, \quad (2.33)$$

$$y_m = \sum_{k=1}^K z_m^k b_k(i) c_m^k + n_m, \quad (2.34)$$

where y_m and n_m are the complex baseband component of the received signal after down-conversion with subcarrier frequency synchronization and the complex additive Gaussian noise at the m -th subcarrier, respectively, z_m^k is the channel realization of the m -th subcarrier regarding user k . We choose the gain q_m^k as $q_m^k = z_m^{k*} c_m^k / |z_m^k|^2$.

Fig. 2.6 shows the MC-DS-CDMA transmitter and receiver with the number of subcarriers $N'_c = 4$, block length $M = N'_c = 4$ symbols, and the processing gain $N = 4$. The transmitted signal of the k -th user regarding one block is given as

$$x'_{v,n} = \sum_{m=0}^{N'_c-1} b_k^m(i) c_n^k e^{j2\pi mv\Delta f'}, v = 0 \dots N'_c - 1, n = 0 \dots N - 1, \quad (2.35)$$

where $b_k^m(i)$ is the m -th symbol of this block regarding user k , c_n^k denotes the n -th chip of the k -th user's spreading code, $\Delta f'$ is the subcarrier separation, and the N'_c outputs $x'_{0,n}, \dots, x'_{N'_c-1,n}$ correspond to the n -th chip. The MC-DS-CDMA receiver is composed of N'_c normal coherent receivers in this example. Moreover, the receiver design for MC-DS-CDMA systems is discussed in [49], and the work in [50] investigated transmitter and receiver optimization in MC-CDMA systems.

2.5.2 Multiantenna CDMA Techniques

Considering the rapidly increasing demand for high data rate and reliable wireless communications, high-capacity multiuser transmission schemes are of great importance for next generation wireless systems. Recent studies indicate that using multiple antennas at the transmitter and receiver can dramatically increase the performance of wireless communication systems [51–53].

More recently, the use of multiple antennas for CDMA systems provides additional interference suppression capability by exploiting the spatial structure of the system [54,55]. Nordio et al. [12], proposed two types of linear MMSE receivers for MIMO-CDMA systems, which are the separate and joint receivers. V-BLAST or SIC was proposed in [10], [11] for a single user MIMO system, and can be easily extended to MIMO-CDMA systems. Due to the higher number of users and streams, interference cancellation in future MIMO-CDMA systems is more challenging and calls for novel methods with attractive performance and complexity trade-offs. In Chapter 7, we propose a novel interference cancellation algorithm for uplink MIMO-CDMA systems with spatial multiplexing techniques.

In addition, the chip-interleaving and other preprocessing algorithms can also be extended to the system with multiple antennas. The recent work in [13] studied two MIMO architectures for single-carrier CDMA system employing block spreading, namely layered space-time block spread CDMA and space-time coded block spread CDMA. In this work, the practical challenges facing MIMO block spread CDMA schemes were highlighted and discussed in detail and extensive simulation study was conducted to investi-

gate the performance of MIMO block spread CDMA under various mobile environments. The work in [56] dealt with the uplink of a wireless MIMO communication system based on MC-CDMA, and developed a novel low-complexity receiver that exploits the multiple antenna structure of the system and performs joint iterative multiuser detection and channel estimation. The receiver algorithms are based on the Krylov subspace method, which solves a linear system with low complexity, trading accuracy for efficiency.

According to the high system complexity of MIMO-CDMA systems, Serbetli and Yener investigated the signature and beamformer design problem in [14]. The work designed the appropriate transmit beamformers and signatures considering the sum capacity, and the system-wide MSE as the performance metric. The authors first investigate the unlimited reliable feedback case and construct iterative algorithms to find the optimum transmit beamformer and signature set. Next, motivated by the need to reduce the amount of feedback, a low-complexity sequential orthogonal temporal signature assignment algorithm is presented for given transmit beamformers. The approach is based on minimizing the difference between the performance of the MIMO-CDMA system and the described upper bounds at each signature assignment step. At last, they investigate the cases of various levels of available feedback resulting in different beamformer structures and present a joint orthogonal temporal signature assignment and beamforming algorithm. More description about the limited feedback techniques will be introduced in the following part.

2.6 Limited Feedback Techniques

Employing channel adaptive signaling in wireless communication systems can enable the transmitter to avoid interference and yield large improvements [19, 57]. Unfortunately, many kinds of channel adaptive techniques have been deemed impractical in the past because of the problem of obtaining CSI at the transmitter. Over the last few years, research has shown that allowing the receiver to send a small number of information bits about the channel conditions to the transmitter can allow near optimal channel adaptation [57–59]. The practical systems are referred to as limited or finite-rate feedback systems. In this section, we briefly review the work in single user and multiuser systems.

2.6.1 Feedback in Single-user Systems

The design of single-user wireless systems with limited feedback has a long history. In the case of narrowband single antenna systems, the capacity achieving power allocation frameworks [60] allows the receiver to utilize the reverse link as a feedback channel, send some channel information on this channel, and give the transmitter some kind of side information about the current channel realization. The work was later extended to the fast-fading case in [61] by adding the additional requirement of a cardinality constraint on the side information. The problem of properly designing the side information is shown to be one of scalar quantization that can be solved using the Lloyd algorithm. Extensive analysis of the narrowband single antenna system has been conducted in [62] when the transmitter is provided with a quantized version of the magnitude of the current channel. This quantized approach is taken by dividing up the non-negative part of the real line into quantization regions.

The application of limited feedback to multiple antennas wireless systems has received much attention in the recent years. The spatial degree-of-freedom and the potentially sizeable benefits available by adapting over it make limited feedback a very attractive option. When the transmitter and receiver both perfectly know the channel, the ergodic capacity expression is shown in [63]. The covariance of the transmitted signal could incorporate both the spatial power allocation as well as unitary precoding. The spatial power allocation is important especially for cases when the number of transmit antennas is greater than the number of receive antennas. Employing a codebook of possible covariance matrices that is known to both the transmitter and receiver, the receiver can determine a rate maximizing covariance and feed this index back to the transmitter. Designing a fixed covariance codebook to maximize the average rate is a challenging problem that depends on the stationary distribution of the channel [64], vector quantization approaches using the Lloyd algorithm have been shown to efficiently generate codebooks that achieve a large rate [64].

Much of the early limited feedback beamforming work focused on the multiple-input single-out (MISO) case when there is only a single receive antenna. In this case, the received signal can be formulated as

$$y(i) = \sqrt{\rho} \mathbf{h}^T(i) \mathbf{f}(i) b(i) + \mathbf{n}(i), \quad (2.36)$$

where ρ denotes the transmitter power constraint, $\mathbf{h}(i)$ and $\mathbf{n}(i)$ are the channel and noise vectors, $\mathbf{f}(i)$ is a channel dependent vector referred to as a beamforming vector and $b(i)$ is a single-dimensional complex symbol chosen independently of the instantaneous channel conditions. For MIMO beamforming and combining, a receive-side combining vector

$\mathbf{z}(i)$ is used so that after processing

$$y(i) = \sqrt{\rho} \mathbf{z}^*(i) \mathbf{H}(i) \mathbf{f}(i) b(i) + \mathbf{z}^* \mathbf{n}(i), \quad (2.37)$$

where $\mathbf{H}(i)$ denotes the MIMO channel matrix. The simplest form of this feedback is transmit antenna selection [65, 66]. In this scenario, the transmit beamforming vector is restricted such that only one entry is non-zero. With this kind of set-up in a MISO system, the optimal solution is to send data on the antenna that maximizes the receiver signal to noise ratio (SNR) meaning all data is sent on antenna $m_{opt}(i)$ where

$$m_{opt}(i) = \arg \max_{1 \leq m \leq M_t} |h_m(i)|^2 \quad (2.38)$$

where $|h_m(i)|^2$ denotes the m -th antenna entry of the channel vector $\mathbf{h}(i)$. Clearly, antenna selection is limited in terms of its benefits to the overall capacity as it does not allow for the full beamforming gain. The new approaches allow the receiver to directly design the beamforming vector and send this designed vector information back to the transmitter. The main idea is to restrict $\mathbf{f}(i)$ to lie in a codebook $F = \{\mathbf{f}_1, \dots, \mathbf{f}_{2^B}\}$, where B is the number of feedback bits. The receiver can use its channel knowledge to pick the optimal vector from this codebook. This kind of approach is demonstrated in Fig. 2.7.

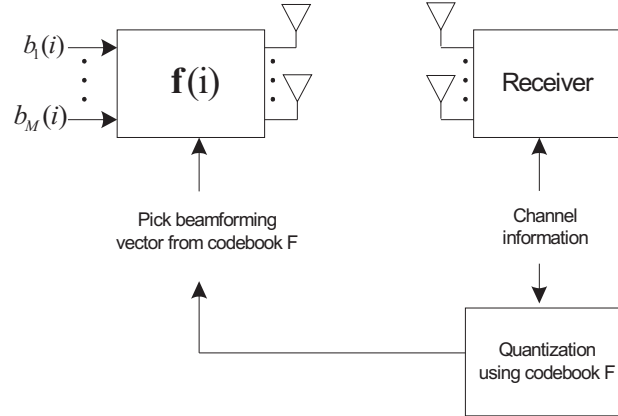


Figure 2.7: A block diagram of a limited feedback linear beamforming MIMO system

The problem of designing the codebook F is well known in applied mathematics as the Grassmannian line packing problem. Mathematically, this means that the set F is chosen to maximize its minimum distance defined as

$$d(F) = \sqrt{1 - \max_{1 \leq i < j \leq 2^B} |\mathbf{f}_i^* \mathbf{f}_j|^2} = \min_{1 \leq i < j \leq 2^B} \sin(\theta_{i,j}) \quad (2.39)$$

where $\theta_{i,j}$ is the angle between the lines generated by the column spaces of \mathbf{f}_i and \mathbf{f}_j . Another work is linear precoding based on limited feedback, which extends beamforming ideas to sending multiple data streams spatially [59, 67].

In the case of wideband single-user MIMO systems with limited feedback, the OFDM technology is employed. The systems often send feedback only for pilot subcarriers. One technique is based on interpolation, the idea of [68] was to weight and sum together the fed back beamforming vectors from the two nearest pilots to recreate all beamforming vectors based on the information and the channel correlation in the frequency domain. In [69], the precoder interpolation problem was formulated as a weighted least squares problem. The weights correspond to the distance from the different pilot precoders. More works on interpolation are available in [70, 71]. Instead of trying to interpolate a much simpler approach is clustering [72, 73], where a common precoder is chosen for several contiguous subcarriers.

2.6.2 Feedback in Multiuser Systems

Adapting the transmitter signal across multiple users is an additional degree-of-freedom that can be leveraged in most communication systems. In broadband systems with multiple access in frequency, users can be scheduled in various subchannels. Feedback and subcarrier allocation in orthogonal frequency division multiple access can be done using limited feedback [74]. When multiple access is done in the time domain, limited feedback can allow the system to map users to time slots and adapt coding and modulation [75]. Another interesting area is the signature optimization using limited feedback for CDMA systems. In fact, spreading code design using randomly generated codes formed the basis behind the development of random vector quantization (RVQ) ideas [76]. The performance of an RVQ signature codebook is analyzed in [77]. Reduced-rank signature optimization leads to further designs using subspace concepts [78]. Performance analysis of signature optimization with CDMA can be found in [79]. Limited feedback has also been applied to peer-to-peer MC-CDMA [80]. Other work on interference avoidance with limited feedback is available in [81]. In CDMA systems, power control is also critical. Feedback approaches to CDMA power control have been widely studied.

While single-user multiple antenna systems provide many benefits, multiuser multiple antennas systems can provide even larger total system rates when the spatial resources are spread among multiple users [57]. A downlink multiuser MIMO system with each user possessing a single receive antenna and normalized noise will give the k -th user an input-output relation

$$y_k(i) = \mathbf{h}_k^T(i)\mathbf{x}(i) + n_k(i) \quad (2.40)$$

where the transmitted signal is restricted such that $E[|\mathbf{x}(i)|^2] \leq \rho$. Various signaling approaches can be employed to divide the spatial resources. Most relate to using the form

of precoding [57]. In this case, $\mathbf{x}(i) = \mathbf{F}(i)\mathbf{b}(i)$. Here $\mathbf{F}(i)$ is the linear precoding matrix. The signal $\mathbf{b}(i)$ is an independently generated vector of symbols that correspond to different users. Most limited feedback multiuser MIMO schemes let users quantize some function of $\mathbf{h}_k(i)$ and send this channel information to the base station. The problem is that the purpose of $\mathbf{F}(i)$ is to orthogonalize the various user signals. When the channel is quantized, the user signals can not be perfectly orthogonalized due to inherent quantization error [20]. This leads to a sum rate ceiling as the SNR increases. Improving this sum rate ceiling is a difficult problem. When the number of users increases, scheduling users with channels that satisfy near orthogonality conditions provides many improvements [82, 83].

When users have multiple receive antennas, performance of multiuser MIMO systems can be improved by leveraging the added degrees-of-freedom at the receiver [57]. With enough receive antennas even simple per antenna scheduling without precoding can provide good performance [84]. It was shown in [85] that combining the signals received at the multiple receive antennas provides substantial sum rate benefit because the negative effect of channel quantization error is reduced. Block diagonalized multiuser transmission with limited feedback is discussed in [86], which takes into account that each receive antenna should not be treated as a separate user when the antennas are co-located. Limited feedback can also be employed with regularized block diagonalization [87]. A vector quantization framework combined with improved scheduling is discussed in [62].

2.7 Conclusions

In this chapter we presented reviews on the existing interference suppression techniques for CDMA systems. Firstly, we introduced the conventional multiuser detection techniques including the linear and nonlinear detectors and the adaptive and blind algorithms. The following chapter describes the existing CDMA transmit processing techniques, namely, chip-interleaving, precoding, and signature optimization algorithms. Then, we reviewed some variation of the conventional CDMA, which are MC-CDMA, MC-DS-CDMA, and multiantenna CDMA systems. At last, the limited feedback techniques for single-user and multiuser systems are introduced. In the following chapters, we will concentrate on the proposed interference suppression techniques.

Chapter 3

Low-Complexity Blind Adaptive Interference Suppression

Contents

3.1	Introduction	31
3.2	DS-CDMA System Model	33
3.3	Blind Adaptive SG CCM Algorithms	35
3.4	Blind Time Averaging Variable Step-size (TASS) Algorithm	37
3.5	Analyses of the Proposed Algorithm	40
3.6	Simulation Results	47
3.7	Conclusions	52

3.1 Introduction

The constant modulus algorithm (CMA) is based on a criterion that penalizes deviations of the modulus of the received signal away from a fixed value determined by the source alphabet [88], the original work on the CMA has been done independently by Godard [89] and by Treichler and Agee [90]. The code-constrained constant modulus (CCM) algorithm is based on the CM criterion and is forced to satisfy one or a set of linear constraints. Then, this approach has been considered for detection in flat fading channels [24], [25] and multipath environment [91], [92]. The CCM algorithm has been studied and implemented in many wireless communication applications including blind multiuser detection, blind equalization, source separation, interference suppression, and

antenna beamforming. A linear receiver equipped with the CCM algorithm is a very effective blind approach for ISI and MUI suppression when a communication channel is frequency-selective [26], [27], [93]. The CCM design approach has proven to be highly suitable to certain communications technologies such as spread spectrum systems. In particular, DS-CDMA spread spectrum signalling has become a highly popular multiple access technique which is widely used for personal communications, third-generation mobile telephony, and indoor wireless communications. The advantages of DS-CDMA include superior operation in multipath environments, flexibility in the allocation of channels, increased capacity in bursty and fading environments, and the ability to share bandwidth with narrowband communication systems without significant deterioration of either's systems performance [2], [5].

Detecting a desired user in a DS-CDMA system requires processing the received signal in order to mitigate different types of interference, namely, MUI, ISI, and the noise at the receiver. The major source of interference in most CDMA systems is MUI, which arises due to the fact that users communicate through the same physical channel with nonorthogonal signals. Multiuser detection has been proposed as a means to suppress MUI, increase the capacity and the performance of CDMA systems [1, 2]. The optimal multiuser detector proposed by Verdu [94] suffers from exponential complexity and requires: the knowledge of timing, amplitude and signature sequences. This fact has motivated the development of various sub-optimal strategies with affordable complexity. The linear MMSE receiver implemented with an adaptive filter is one of the most prominent schemes for use in the downlink because it only requires the timing of the desired user and a training sequence [4]. A blind adaptive linear receiver has been developed in [5], and operates without knowledge of the channel input. In [95] Yang has shown that the minimum variance distortionless response (MVDR) criterion, the minimum power distortionless response (MPDR) criterion and the minimum variance (MV) criterion lead to a solution identical to that obtained from the minimization of the MSE. A disadvantage of the original MV detector is that it suffers from the problem of signature mismatch and thus has to be modified for multipath environments [96].

When designing an adaptive receiver for a DS-CDMA system, we need to consider what kind of algorithm should be used. Despite the fast convergence of RLS algorithms, however, it is preferable to implement adaptive receivers with SG algorithms (e.g., LMS) due to complexity and cost issues. For this reason the improvement of blind SG techniques is an important research and development topic. In this regard, the works in [27] and [5] employ standard SG algorithms with fixed step-size (FSS) that are not efficient with respect to the convergence and steady-state performance. Indeed, the performance of adaptive SG receivers is strongly dependent on the choice of the step-size [4]. In non-stationary

wireless environments, users frequently enter and exit the system, making it very difficult for the receiver to compute a pre-determined step-size. This suggests the deployment of mechanisms to automatically adjust the step-size of an SG algorithm in order to ensure good tracking of the interference and the channel. Previous works have shown significant gains in performance due to the use of averaging methods (AV) [97], [98] or adaptive gradient step-size (AGSS) mechanisms [99], [100], where one SG algorithm adapts the parameter vector and another SG recursion adapts the step-size. The works in [97] and [98] have borrowed the idea of averaging originally developed by Polyak [101] and applied it to CDMA receivers with the MV criterion. The AGSS algorithms in [99], [100] can be considered MV and CCM extensions of the papers [102–104]. All these methods require an additional number of operations (i.e., additions and multiplications) proportional to the processing gain N and to the number of multipath components L_p .

Furthermore, there are very few works employing variable step-size mechanisms with blind techniques using the constant modulus criterion. In this chapter, we propose a novel low-complexity variable step-size mechanism for blind CDMA receivers in multipath channels that are used for MUI and ISI suppression based on an SG algorithm and the CCM approach. The additional number of operations of the proposed techniques does not depend on the processing gain N and the number of paths of the channel L_p . Convergence and tracking analyses of the proposed adaptation techniques are carried out for a multipath scenario, and analytical results are derived for the computation of the excess MSE. We also generalize the CCM SG-AGSS in [100] for multipath scenarios. In addition, simulation experiments are presented for nonstationary environments, showing that the new mechanisms are superior to previously reported methods and require a reduced complexity.

This chapter is structured as follows. Section 3.2 briefly describes the DS-CDMA system model. The adaptive blind SG CCM receiver design and CCM SG-AGSS algorithm extension for multipath channel are described in Section 3.3. Section 3.4 is devoted to the novel variable step-size mechanism. Convergence and tracking analyses of the resulting algorithm are developed in Section 3.5. Section 3.6 presents and discusses the simulation results. Section 3.7 draws the conclusions.

3.2 DS-CDMA System Model

Let us consider the downlink of an uncoded synchronous binary phase shift keying (BPSK) DS-CDMA system with K users, N chips per symbol and L_p propagation paths.

The signal broadcasted by the base station intended for user k has a baseband representation given by

$$x_k(t) = A_k \sum_{i=-\infty}^{\infty} b_k(i) s_k(t - iT) \quad (3.1)$$

where $b_k(i) \in \{\pm 1\}$ denotes the i -th symbol for user k , the real valued spreading waveform and the amplitude associated with user k are $s_k(t)$ and A_k , respectively. The spreading waveforms are expressed by $s_k(t) = \sum_{i=0}^{N-1} a_k(i) \phi(t - iT_c)$, where $a_k(i) \in \{\pm 1/\sqrt{N}\}$, $\phi(t)$ is the chip waveform, T_c is the chip duration and $N = T/T_c$ is the processing gain. Assuming that the channel is constant during each symbol and the receiver is synchronized with the main path, the received signal is

$$r(t) = \sum_{k=1}^K \sum_{l=0}^{L_p-1} h_l(t) x_k(t - \tau_l) + n(t), \quad (3.2)$$

where $h_l(t)$ and τ_l are, respectively, the channel coefficient and the delay associated with the l -th path. Assuming that the delays are multiples of the chip rate, the spreading codes are repeated from symbol to symbol and the received signal $r(t)$ after filtering by a chip-pulse matched filter and sampled at chip rate yields the M -dimensional received vector

$$\begin{aligned} \mathbf{r}(i) &= \sum_{k=1}^K (A_k b_k(i) \mathbf{C}_k \mathbf{h}(i) + \boldsymbol{\eta}_k(i)) + \mathbf{n}(i) \\ &= \sum_{k=1}^K (A_k b_k(i) \mathbf{p}_k(i) + \boldsymbol{\eta}_k(i)) + \mathbf{n}(i), \end{aligned} \quad (3.3)$$

where $M = N + L_p - 1$, $\mathbf{n}(i) = [n_1(i) \dots n_M(i)]^T$ is the complex Gaussian noise vector, and $E[\mathbf{n}(i)\mathbf{n}^H(i)] = \sigma^2 \mathbf{I}$. The channel vector is $\mathbf{h}(i) = [h_0(i) \dots h_{L_p-1}(i)]^T$ with $h_l(i) = h_l(iT_c)$ for $l = 0, \dots, L_p - 1$, $\boldsymbol{\eta}_k(i)$ is the ISI, and it is assumed that the channel order is not greater than N , i.e. $L_p - 1 \leq N$, $\mathbf{s}_k = [a_k(1) \dots a_k(N)]^T$ is the signature sequence for user k and $\mathbf{p}_k(i) = \mathbf{C}_k \mathbf{h}(i)$ is the effective signature sequence for user k , the $M \times L_p$ convolution matrix \mathbf{C}_k contains one-chip shifted versions of \mathbf{s}_k .

$$\mathbf{C}_k = \begin{pmatrix} a_k(1) & 0 & \dots & 0 \\ \vdots & a_k(1) & \ddots & \vdots \\ a_k(N) & \vdots & \ddots & 0 \\ 0 & a_k(N) & \ddots & a_k(1) \\ \vdots & \vdots & \ddots & \vdots \\ 0 & 0 & \ddots & a_k(N) \end{pmatrix}.$$

3.3 Blind Adaptive SG CCM Algorithms

The linear receiver design is equivalent to determining a finite impulse response (FIR) filter $\mathbf{w}_k(i)$ with M coefficients that provides an estimate of the desired symbol, as illustrated in Fig. 3.1 and given by

$$\hat{b}_k(i) = \text{sgn}(\Re(\mathbf{w}_k^H(i)\mathbf{r}(i))), \quad (3.4)$$

where the receiver parameter vector \mathbf{w}_k is optimized according to the CM cost function subject to appropriate constraints.

In this section, we describe the multipath blind adaptive SG CCM algorithm for estimating the parameters of the linear receiver first, and then we generalize the blind CCM-AGSS [100] for multipath scenarios.

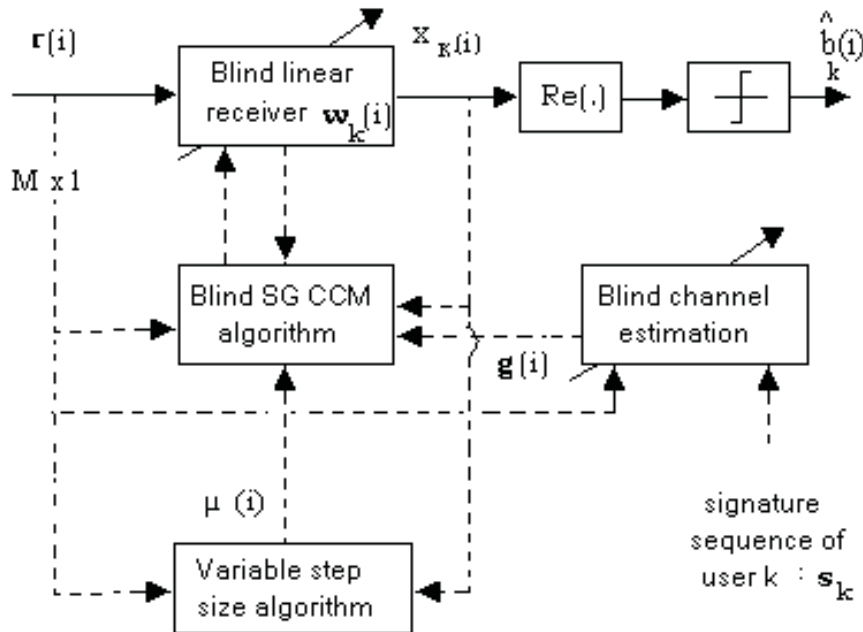


Figure 3.1: Block diagram of the blind adaptive CCM receiver with variable step-size mechanisms.

3.3.1 Multipath Blind Adaptive SG CCM Algorithm

Firstly, let us describe the design of the blind adaptive SG CCM algorithm in multipath channel. Consider the cost function, $J = E[e^2(i)]$, where $e(i) = |\mathbf{w}_k^H(i)\mathbf{r}(i)|^2 - 1$ subject to the multipath constraint given by $\mathbf{C}_k^H \mathbf{w}_k(i) = \mathbf{g}(i)$, where the matrix \mathbf{C}_k was

introduced in section 3.2, and $\mathbf{g}(i)$ is the $L_p \times 1$ constraint channel vector to be determined. The blind channel estimation in [105] is employed in these algorithms. Thus, in order to derive an adaptive expression for the SG CCM linear receiver let us consider the unconstrained optimization problem given in the form of a Lagrangian cost function:

$$\mathcal{L} = (\mathbf{w}_k^H(i)\mathbf{r}(i)\mathbf{r}^H(i)\mathbf{w}_k(i) - 1)^2 + \boldsymbol{\lambda}^H(\mathbf{C}_k^H\mathbf{w}_k(i) - \mathbf{g}(i)) + (\mathbf{w}_k^H(i)\mathbf{C}_k - \mathbf{g}^H(i))\boldsymbol{\lambda}, \quad (3.5)$$

where $\boldsymbol{\lambda}$ is a vector of Lagrange multipliers, we consider the following gradient search procedure:

$$\mathbf{w}_k(i+1) = \mathbf{w}_k(i) - \mu \nabla_{\mathbf{w}_k^*} \mathcal{L} \quad (3.6)$$

where μ is the SG algorithm step-size. The recursion in (3.6) may be obtained from (3.5). By taking the gradient with respect to \mathbf{w}_k^* . We obtain $\nabla_{\mathbf{w}_k^*} \mathcal{L} = e(i)\mathbf{r}(i)\mathbf{r}^H(i)\mathbf{w}_k(i) + \mathbf{C}_k\boldsymbol{\lambda}$. Then, (3.6) becomes

$$\mathbf{w}_k(i+1) = \mathbf{w}_k(i) - \mu(e(i)\mathbf{r}(i)\mathbf{r}^H(i)\mathbf{w}_k(i) + \mathbf{C}_k\boldsymbol{\lambda}), \quad (3.7)$$

where $\boldsymbol{\lambda}$ also needs to be determined. By using (3.6) and enforcing the constraints on \mathbf{w}_k as $\mathbf{C}_k^H\mathbf{w}_k(i+1) = \mathbf{g}(i)$, $\boldsymbol{\lambda}$ can be solved

$$\boldsymbol{\lambda} = \frac{1}{\mu}(\mathbf{C}_k^H\mathbf{C}_k)^{-1}(\mathbf{C}_k^H\mathbf{w}_k(i) - \mu\mathbf{C}_k^H e(i)\mathbf{r}(i)\mathbf{r}^H(i)\mathbf{w}_k(i) - \mathbf{g}(i)). \quad (3.8)$$

Substituting (3.8) in (3.7), we arrive at the update rule for the adaptive filter weight vector \mathbf{w}_k

$$\mathbf{w}_k(i+1) = \prod_{\mathbf{C}}[\mathbf{w}_k(i) - \mu e(i)\mathbf{r}(i)\mathbf{r}^H(i)\mathbf{w}_k(i)] + \mathbf{C}_k(\mathbf{C}_k^H\mathbf{C}_k)^{-1}\mathbf{g}(i), \quad (3.9)$$

where $\prod_{\mathbf{C}} = \mathbf{I} - \mathbf{C}_k(\mathbf{C}_k^H\mathbf{C}_k)^{-1}\mathbf{C}_k^H$ as reported in [106], and $\mathbf{g}(i)$ is the blind channel estimation vector which has been proposed in [105]

$$\mathbf{g}(i) = \frac{(\mathbf{I} - \alpha(i)\mathbf{Y}_k(i))\mathbf{g}(i-1)}{\|(\mathbf{I} - \alpha(i)\mathbf{Y}_k(i))\mathbf{g}(i-1)\|} \quad (3.10)$$

where $\alpha(i) = 1/\text{tr}\{\mathbf{Y}_k(i)\}$. To generate estimates for $\mathbf{Y}_k(i)$ consists of writing

$$\mathbf{Y}_k(i) = \mathbf{C}_k^H\mathbf{V}_k(i) \quad (3.11)$$

where

$$\mathbf{V}_k(i) = \lambda_L\mathbf{V}_k(i-1) + \mu(\mathbf{C}_k - \mathbf{r}(i)\mathbf{r}^H(i)\mathbf{V}_k(i-1)) \quad (3.12)$$

where $\mathbf{V}_k(0) = \mathbf{C}_k$, $0 < \lambda_L < 1$ is a leakage factor.

3.3.2 Blind CCM SG-AGSS in Multipath Channels

The CCM SG-AGSS algorithm in single path channel has been proposed by Yuvapoositanon and Chambers in [100]. In this part we extend the algorithm to multipath channels.

We treat \mathbf{w}_k as a function of μ , the step-size variation can change the filter weights, and define $\mathbf{y}_k(i) = \frac{\partial \mathbf{w}_k(i)}{\partial \mu}$. We consider the gradient search procedures of variable step-size as follows

$$\mu(i+1) = \mu(i) - \alpha \nabla_{\mu} J, \quad (3.13)$$

where α denotes the adaptation rate of the step-size $\mu(i)$ with $\alpha > 0$. By taking the gradient of the cost function $J = E[e^2(i)]$ with respect to the step-size μ we have

$$\nabla_{\mu} J = e(i)(\mathbf{y}_k^H(i)\mathbf{r}(i)z_k^*(i) + \mathbf{r}^H(i)\mathbf{y}_k(i)z_k(i)) \quad (3.14)$$

Based on (3.13) and (3.14), we can have another SG update equation which is

$$\mu(i+1) = [\mu(i) - \alpha e(i) \text{Re}(\mathbf{y}_k^H(i)\mathbf{r}(i)z_k^*(i))]_{\mu^-}^{\mu^+}, \quad (3.15)$$

where $z_k(i) = \mathbf{w}_k^H(i)\mathbf{r}(i)$, and $[\cdot]_{\mu^-}^{\mu^+}$ denotes the truncation to the limits of the range $[\mu^-, \mu^+]$, From equation (3.9) we can derive the update equation of $\mathbf{y}_k(i)$

$$\begin{aligned} \mathbf{y}_k(i+1) = \prod_{\mathbf{C}} \{ & \mathbf{y}_k(i) - \mu(i)\mathbf{r}(i)\mathbf{r}^H(i)[\mathbf{y}_k(i)e(i) \\ & + \mathbf{w}_k(i)(\mathbf{y}_k^H(i)\mathbf{r}(i)z_k^*(i) + \mathbf{r}^H(i)\mathbf{y}_k(i)z_k(i))] \}. \end{aligned} \quad (3.16)$$

By combining equations (3.9), (3.15), and (3.16) we obtain the multipath blind CCM SG-AGSS algorithm.

3.4 Blind Time Averaging Variable Step-size (TASS) Algorithm

This section describes the proposed low-complexity TASS mechanism for CDMA receivers that adjust the step-size μ of the update equation of the receiver. A convergence analysis of the mechanism is carried out and approximate expressions relating to the mean convergence factor $E[\mu(i)]$, the mean square convergence factor $E[\mu^2(i)]$ and the minimum variance are derived. It is worth noting that in the mechanism, $\mu(i)$ is truncated between $\{\mu^-, \mu^+\}$. In addition, the computational complexity of the novel mechanism is presented in terms of additions and multiplications and compared to the CCM-AGSS one.

3.4.1 TASS Mechanism

The proposed TASS mechanism employs the instantaneous cost function $e^2(i) = (|\mathbf{w}_k^H(i)\mathbf{r}(i)|^2 - 1)^2$ and uses the update rule

$$\mu(i+1) = a\mu(i) + b(|\mathbf{w}_k^H(i)\mathbf{r}(i)|^2 - 1)^2, \quad (3.17)$$

where $0 < a < 1$, $b > 0$ and \mathbf{w}_k is the parameter vector of the receiver. In the proposed TASS algorithm the step-size adjustment is controlled by the instantaneous constant modulus cost function. The motivation is that a large prediction error will cause the step-size to increase and provide faster tracking while a small prediction error will result in a decrease in the step-size to yield smaller misadjustment [107]. The step-size $\mu(i)$ is always positive and is controlled by the size of the prediction error and the parameters a and b . Furthermore, it is worth pointing out that other rules have been experimented and the TASS is a result of several attempts to devise a simple and yet effective mechanism. Indeed, the mechanism is simple to implement and a detailed analysis of the algorithm is possible under a few assumptions.

Assumption 1: Let us consider that for the algorithms in (3.17) when $i \rightarrow \infty$

$$E[\mu(i)e^2(i)] = E[\mu(i)]E[e^2(i)]$$

This assumption holds if μ is a constant, and we claim that it is approximately true if b is small and also because a should be close to one (as will be shown in the simulations), because $\mu(i)$ will vary slowly around its mean value. By writing

$$E[\mu(i)e^2(i)] = E[\mu(i)]E[e^2(i)] + E[(\mu(i) - E\{\mu(i)\})e^2(i)], \quad (3.18)$$

we note that for b sufficiently small, the second term on the right-hand side of (3.18) will be small compared to the first one. Assumption 1 helps us to proceed with the analysis.

Let us define the first- $(E[\mu(i)])$ and second-order $(E[\mu^2(i)])$ statistics of the proposed TASS mechanism,

$$E[\mu(i+1)] = aE[\mu(i)] + bE[e^2(i)]. \quad (3.19)$$

By computing the square of $\mu(i+1)$, we obtain $\mu^2(i+1) = a^2\mu^2(i) + 2ab\mu(i)e^2(i) + b^2e^4(i)$. Since b^4 is small, the last term of the previous equation is negligible as compared to the other terms, thus, with the help of Assumption 1 we assume that the expected value of $E[\mu^2(i+1)]$ is approximately

$$E[\mu^2(i+1)] \approx a^2E[\mu^2(i)] + 2abE[\mu(i)]E[e^2(i)]. \quad (3.20)$$

If we consider the steady-state values of $E[\mu(i+1)]$ and $E[\mu^2(i+1)]$ by making $\lim_{i \rightarrow \infty} E[\mu(i+1)] = \lim_{i \rightarrow \infty} E[\mu(i)] = E[\mu(\infty)]$ and $\lim_{i \rightarrow \infty} E[\mu^2(i+1)] = \lim_{i \rightarrow \infty} E[\mu^2(i)] = E[\mu^2(\infty)]$, and using $\lim_{i \rightarrow \infty} E[(|\mathbf{w}_k^H(i)\mathbf{r}(i)|^2 - 1)^2] = \xi_{min} + \xi_{ex}(\infty)$ [5], [4] we have the following:

$$E[\mu(\infty)] \approx \frac{b(\xi_{min} + \xi_{ex}(\infty))}{1-a}, \quad (3.21)$$

$$E[\mu^2(\infty)] \approx \frac{2ab^2(\xi_{min} + \xi_{ex}(\infty))^2}{(1-a)^2(1+a)}, \quad (3.22)$$

where the steady-state minimum value ξ_{min} is provided by [108], $\xi_{min} \approx 1 - \bar{\mathbf{s}}_k^H \mathbf{R}^{-1} \bar{\mathbf{s}}_k$, where $\bar{\mathbf{s}}_k = \mathbf{C}_k \mathbf{g}(i)$, and $\mathbf{R} = (\mathbf{P}\mathbf{P}^H + \sigma_n^2 \mathbf{I})$, $\mathbf{P} = [\bar{\mathbf{s}}_1, \dots, \bar{\mathbf{s}}_K]$, the σ_n^2 here is the additive noise power in the receiver. The blind CCM receiver is assuming convergence to the MMSE receiver. The quantity ξ_{ex} is the steady-state excess error of the CM cost function. To further simplify those expressions, let us consider another assumption.

Assumption 2: Let us consider that for (3.21) and (3.22), $(\xi_{min} + \xi_{ex}(\infty)) \approx \xi_{min}$ and $(\xi_{min} + \xi_{ex}(\infty))^2 \approx \xi_{min}^2$, respectively.

This assumption holds if $\xi_{min} \gg \xi_{ex}(\infty)$ and we claim that it is approximately true when the SG adaptive algorithm is close to the optimum solution and $\xi_{ex}(\infty)$ is a small fraction of ξ_{min} .

By using Assumption 2 we have the following:

$$E[\mu(\infty)] \approx \frac{b\xi_{min}}{1-a}, \quad (3.23)$$

$$E[\mu^2(\infty)] \approx \frac{2ab^2\xi_{min}^2}{(1-a)^2(1+a)}. \quad (3.24)$$

Note that (3.23) and (3.24) will be used for the computational of the excess MSE of the algorithm. Our studies reveal that (3.23) and (3.24) have proven to be valid and useful for predicting the steady-state performance of the TASS mechanism.

3.4.2 Computational Complexity

In this section, we detail the additional computational complexity of the proposed TASS algorithm and AGSS algorithm. We compute the number of additions and multiplications to compare the different parts of those two variable step-size mechanisms. In Table I, we show the additional computational complexity of the algorithms for multipath channels.

An important advantage of the proposed adaptation rule is that it requires only a few fixed number of operations while the other existing technique has additional complexity proportional to the processing gain N and to the number of propagation paths L_p . Note that we computed the number of arithmetic operations by taking into account the number of complex additions and multiplications required by the mechanisms.

Table 3.1: Additional computational complexity in multipath channels.

Mechanism	Number of operations per symbol	
	Additions	Multiplications
AGSS	$2M^2 + 3M$	$3M^2 + 7M + 5$
TASS	1	3

3.5 Analyses of the Proposed Algorithm

In this section, we investigate the convergence behavior and tracking analysis of our algorithm when used in the CCM-based algorithm in terms of the steady-state excess MSE (EMSE). The CCM blind algorithms are inherently nonlinear and time-variant. The nonlinearities in the update equations of these receivers usually lead to significant difficulties in the study of their performance. A very efficient approach named energy conservation principle has been proposed by Sayed and Rupp in [109] and [110], and it was extended by Mai and Sayed in [111] and Yousef and Sayed in [112] to the steady-state and tracking analyses of CMA that bypasses many of these difficulties. This approach has been proposed with CCM algorithms for analyzing adaptive multiuser receivers by Whitehead and Takawira in [113]. The work of this section makes two contributions, the first of which is the derivation of the steady-state and tracking performance of the blind CCM receiver in multipath channels. The second contribution is that we focus on the analysis of the novel variable step-size mechanism and incorporate them in the derived expressions.

3.5.1 The Modification of the CCM Update Equation

In order to use the energy conservation principle to do the steady-state and tracking analyses, we write the multipath channel CCM filter weights update equation in another way.

We consider an equivalent Lagrangian cost function:

$$\mathcal{L} = (|\mathbf{w}_k^H(i)\mathbf{r}(i)|^2 - 1)^2 + 2\text{Re}[\lambda^*(\mathbf{w}_k^H(i)\bar{\mathbf{s}}_k(i) - 1)], \quad (3.25)$$

where $\bar{\mathbf{s}}_k(i)$ is the effective signature waveform of user k , $\bar{\mathbf{s}}_k(i) = \mathbf{C}_k \mathbf{g}(i)$. By taking the gradient with respect to $\mathbf{w}_k^*(i)$, we get the new filter weight vector update equation

$$\mathbf{w}_k(i+1) = \mathbf{w}_k(i) - \mu(i)e(i)z_k^*(i)\left(\mathbf{I} - \frac{\bar{\mathbf{s}}_k(i)\bar{\mathbf{s}}_k^H(i)}{\|\bar{\mathbf{s}}_k(i)\|^2}\right)\mathbf{r}(i), \quad (3.26)$$

where $e(i) = |\mathbf{w}_k^H(i)\mathbf{r}(i)|^2 - 1$, $z_k(i) = \mathbf{w}_k^H(i)\mathbf{r}(i)$. These two equations (3.9) and (3.26) are equivalent with different forms. We will drop the index k for notation simplicity in what follows.

3.5.2 The Range of Step-size Values for Convergence

Before the convergence analysis of the proposed variable step-size algorithm, we discuss the range of the step-size for convergence. Here, let us consider the blind CCM filter weight update equation:

$$\begin{aligned} \mathbf{w}(i+1) &= \mathbf{w}(i) - \mu(i)e(i)z^*(i)\left(\mathbf{I} - \frac{\bar{\mathbf{s}}(i)\bar{\mathbf{s}}^H(i)}{\|\bar{\mathbf{s}}(i)\|^2}\right)\mathbf{r}(i) \\ &= \mathbf{w}(i) - \mu(i)e(i)\mathbf{r}^H(i)\mathbf{w}(i)\left(\mathbf{I} - \frac{\bar{\mathbf{s}}(i)\bar{\mathbf{s}}^H(i)}{\|\bar{\mathbf{s}}(i)\|^2}\right)\mathbf{r}(i) \\ &= [\mathbf{I} - \mu(i)e(i)\mathbf{v}(i)\mathbf{r}^H(i)]\mathbf{w}(i), \end{aligned} \quad (3.27)$$

$$\begin{aligned} \tilde{\mathbf{w}}(i+1) &= \mathbf{w}_{opt} - \mathbf{w}(i+1) \\ &= (\mathbf{I} - \mu(i)e(i)\mathbf{v}(i)\mathbf{r}^H(i))\tilde{\mathbf{w}}(i) + \mu(i)e(i)\mathbf{v}(i)\mathbf{r}^H(i)\mathbf{w}_{opt}, \end{aligned} \quad (3.28)$$

where $\mathbf{v}(i) = \left(\mathbf{I} - \frac{\bar{\mathbf{s}}(i)\bar{\mathbf{s}}^H(i)}{\|\bar{\mathbf{s}}(i)\|^2}\right)\mathbf{r}(i)$. By taking expectations on both sides of (3.28) and using Assumption 1 we have

$$E[\tilde{\mathbf{w}}(i+1)] = (\mathbf{I} - E[\mu(i)]\mathbf{R}_{vr}(i))E[\tilde{\mathbf{w}}(i)], \quad (3.29)$$

where $\mathbf{R}_{vr}(i) = E[e(i)\mathbf{v}(i)\mathbf{r}^H(i)]$ and $\mathbf{R}_{vr}(i)\mathbf{w}_{opt} = \mathbf{0}$ [5]. Therefore, it can be concluded that \mathbf{w} converges to \mathbf{w}_{opt} and (3.29) is stable if and only if $\prod_{i=0}^{\infty} (\mathbf{I} - E[\mu(i)]\mathbf{R}_{vr}(i)) \rightarrow \mathbf{0}$, which is a necessary and sufficient condition for $\lim_{i \rightarrow \infty} E[\tilde{\mathbf{w}}(i)] = \mathbf{0}$ and $E[\mathbf{w}(i)] \rightarrow \mathbf{w}_{opt}$. For stability, a sufficient condition for (3.29) to hold implies that [4]

$$0 \leq E[\mu(\infty)] < \min_k \frac{2}{|\lambda_k^{vr}|}. \quad (3.30)$$

where λ_k^{vr} is the k th eigenvalue of $\mathbf{R}_{vr}(i)$ that is not real since $\mathbf{R}_{vr}(i)$ is not symmetric.

3.5.3 Steady-State Analysis

The EMSE arises and depends on the presence of MUI, ISI, AWGN in multipath channels and the nature of the SG algorithm. It is related to the error in the filter coefficients $\tilde{\mathbf{w}}(i)$ via the a priori estimation error, which is defined as

$$e_a(i) \triangleq \tilde{\mathbf{w}}^H(i)\mathbf{r}(i), \quad (3.31)$$

where $\tilde{\mathbf{w}}(i) = \mathbf{w}_{opt} - \mathbf{w}(i)$, and \mathbf{w}_{opt} is the optimum filter in terms of the blind algorithm. Let us define the MSE at time i using the fact that $\tilde{\mathbf{w}}(i)$

$$\begin{aligned} \epsilon(i) &= E[|b(i) - \mathbf{w}^H(i)\mathbf{r}(i)|^2] \\ &= \epsilon_{min} + E[|e_a(i)|^2] + \bar{\mathbf{s}}^H(i)E[\tilde{\mathbf{w}}(i)] + E[\tilde{\mathbf{w}}^H(i)]\bar{\mathbf{s}}(i) \\ &\quad - E[\mathbf{w}_{opt}^H\mathbf{r}(i)\mathbf{r}^H(i)\tilde{\mathbf{w}}(i)] - E[\tilde{\mathbf{w}}^H(i)\mathbf{r}(i)\mathbf{r}^H(i)\mathbf{w}_{opt}], \end{aligned} \quad (3.32)$$

where

$$\epsilon_{min} = E[|b(i) - \mathbf{w}_{opt}^H\mathbf{r}(i)|^2]. \quad (3.33)$$

When $i \rightarrow \infty$, since $\mathbf{w}(i) \rightarrow \mathbf{w}_{opt}$ and $E[\tilde{\mathbf{w}}(i)] \rightarrow 0$ we have the steady-state MSE

$$\lim_{i \rightarrow \infty} \epsilon(i) = \epsilon_{min} + \lim_{i \rightarrow \infty} E[|e_a(i)|^2]. \quad (3.34)$$

The steady-state EMSE is then defined as [111]

$$\zeta \triangleq \lim_{i \rightarrow \infty} E[|e_a(i)|^2]. \quad (3.35)$$

The approach for performance analysis was derived in [111], [112] and [114] and based on the energy conservation principle. By following the idea of Sayed [111], we provide a unified approach to quantifying the EMSE of our adaptive blind receiver that can be made to fit the general class of adaptive SG algorithms given by

$$\mathbf{w}(i+1) = \mathbf{w}(i) + \mu\mathbf{u}(i)F_e(i), \quad (3.36)$$

where $F_e(i)$ is a generic scalar function determined by the adaptive algorithm. The major result of the feedback approach is the energy-preserving equation which relates the a priori estimation error to the error function $F_e(i)$ and the vector \mathbf{u} in (3.36) once the algorithm has reached the steady state. In our case $\mathbf{u}(i) = (\mathbf{I} - \frac{\bar{\mathbf{s}}(i)\bar{\mathbf{s}}^H(i)}{\|\bar{\mathbf{s}}(i)\|^2})\mathbf{r}(i)$, and $F_e(i) = -e(i)z^*(i)$.

Subtracting both sides of (3.36) from some vector \mathbf{w}_{opt} we get the weight error equation

$$\tilde{\mathbf{w}}(i+1) = \tilde{\mathbf{w}}(i) - \mu\mathbf{u}(i)F_e(i), \quad (3.37)$$

where $\tilde{\mathbf{w}}(i) = \mathbf{w}_{opt} - \mathbf{w}(i)$. Define a priori and a posteriori estimation errors $e_a(i) = \tilde{\mathbf{w}}^H(i)\mathbf{r}(i)$ and $e_p(i) = \tilde{\mathbf{w}}^H(i+1)\mathbf{r}(i)$. We now show how to rewrite (3.37) in terms of

the error measures $[\tilde{\mathbf{w}}(i), \tilde{\mathbf{w}}(i+1), e_a(i), e_p(i)]$ alone. For this purpose, we note that if we multiply the Hermitian of (3.37) by $\mathbf{r}(i)$ from the right, we obtain

$$\begin{aligned} e_a(i) &= e_p(i) + \mu \mathbf{u}^H(i) \mathbf{r}(i) F_e^*(i) \\ &= e_p(i) + \mu \mathbf{r}^H(i) \left(\mathbf{I} - \frac{\bar{\mathbf{s}}(i) \bar{\mathbf{s}}^H(i)}{\|\bar{\mathbf{s}}(i)\|^2} \right) \mathbf{r}(i) F_e^*(i). \end{aligned} \quad (3.38)$$

Since $\mathbf{r}^H(i) \left(\mathbf{I} - \frac{\bar{\mathbf{s}}(i) \bar{\mathbf{s}}^H(i)}{\|\bar{\mathbf{s}}(i)\|^2} \right) \mathbf{r}(i) = \|\mathbf{u}(i)\|^2$, we can obtain

$$e_p(i) = e_a(i) - \mu \|\mathbf{u}(i)\|^2 F_e^*(i). \quad (3.39)$$

Solving for $F_e^*(i)$ gives

$$F_e^*(i) = \frac{e_a(i) - e_p(i)}{\mu \|\mathbf{u}(i)\|^2}, \quad (3.40)$$

so that we can rewrite (3.37) as

$$\tilde{\mathbf{w}}(i+1) = \tilde{\mathbf{w}}(i) - \frac{\mathbf{u}(i)}{\|\mathbf{u}(i)\|^2} [e_a^*(i) - e_p^*(i)]. \quad (3.41)$$

Rearranging (3.41) leads to

$$\tilde{\mathbf{w}}(i) + \frac{\mathbf{u}(i)}{\|\mathbf{u}(i)\|^2} e_p^*(i) = \tilde{\mathbf{w}}(i+1) + \frac{\mathbf{u}(i)}{\|\mathbf{u}(i)\|^2} e_a^*(i). \quad (3.42)$$

If we define

$$\bar{\mu}(i) = 1 / \|\mathbf{u}(i)\|^2, \quad (3.43)$$

then by squaring (3.42), we observe that the following energy relation is obtained:

$$\begin{aligned} \|\tilde{\mathbf{w}}(i)\|^2 + \bar{\mu}(i) |e_p(i)|^2 + \bar{\mu}(i) \mathbf{u}^H(i) \tilde{\mathbf{w}}(i) e_p(i) + \bar{\mu}(i) \tilde{\mathbf{w}}^H(i) \mathbf{u}(i) e_p^*(i) \\ = \|\tilde{\mathbf{w}}(i+1)\|^2 + \bar{\mu}(i) |e_a(i)|^2 + \bar{\mu}(i) \mathbf{u}^H(i) \tilde{\mathbf{w}}(i+1) e_a(i) \\ + \bar{\mu}(i) \tilde{\mathbf{w}}^H(i+1) \mathbf{u}(i) e_a^*(i). \end{aligned} \quad (3.44)$$

By taking expectations of both sides of (3.44), when the filter operation is in steady state, namely $i \rightarrow \infty$, we can obtain

$$E[\|\tilde{\mathbf{w}}(i)\|^2] + E[\bar{\mu}(i) |e_p(i)|^2] = E[\|\tilde{\mathbf{w}}(i+1)\|^2] + E[\bar{\mu}(i) |e_a(i)|^2]. \quad (3.45)$$

When the filter operation is in steady state for $i \rightarrow \infty$, we also can write

$$E[\|\tilde{\mathbf{w}}(i)\|^2] = E[\|\tilde{\mathbf{w}}(i+1)\|^2]. \quad (3.46)$$

Now, with (3.36), the effect of the weight error vector is canceled out from (3.45), and we are reduced to studying only the equality $E[\bar{\mu}(i)|e_a(i)|^2] = E[\bar{\mu}(i)|e_p(i)|^2]$. Substituting (3.39) into the equation we can have the energy preserving equation.

The energy preserving equation in the steady state is used to solve for the EMSE and is given as

$$E[\bar{\mu}(i)|e_a(i)|^2] = E[\bar{\mu}(i)|e_a(i) - \frac{\mu(i)}{\bar{\mu}(i)}F_e^*(i)|^2], \quad (3.47)$$

where $F_e(i) = -e(i)z^*(i) = (1 - |y(i)|^2)y^*(i)$, and $y(i) = (\mathbf{w}_{opt} - \tilde{\mathbf{w}}(i))^H \mathbf{r}(i) = \mathbf{w}_{opt}^H \mathbf{r}(i) - e_a(i) = Ab(i) + M(i) + \eta(i) + v(i) - e_a(i)$, where $Ab(i)$ is the desired user's signal, M is the residual MUI as the output of the optimum filter, η is the filtered ISI, v is the filtered AWGN.

By expanding the right-hand side of (3.47) the equation can be simplified to $D = F$, where $D = E[\mu(i)]E[e_a^*y(i)(1 - |y(i)|^2)] + E[\mu(i)]E[e_ay^*(i)(1 - |y(i)|^2)]$ and $F = E[\mu^2(i)]E[\|\mathbf{u}\|^2 |y(i)|^2(1 - |y(i)|^2)^2]$. Based on the analytical results in [112] and [113], we can make several assumptions.

Assumption 3: In the steady state, $\|\mathbf{u}\|^2$ and $|F_e|^2$ are uncorrelated.

Assumption 4: The quantities $\{b, M, \eta, v, e_a\}$ are zero-mean random variables, and are mutually independent.

Assumption 5: We also have $E[b_k^{2m}] = 1$ for any positive integer m . The user's power A_k is equal to 1.

Assumption 6: The residual MUI and ISI are Gaussian random variables.

By using these assumptions above and substituting $y(i)$ into equation $D = F$, we have

$$\begin{aligned} & E[\mu^2]E[\|\mathbf{u}\|^2]G_1E[|e_a|^2] + 3E[\mu^2]E[\|\mathbf{u}\|^2]E[M^2]E[|e_a|^4] \\ & + 3E[\mu^2]E[\|\mathbf{u}\|^2]E[v^2]E[|e_a|^4] + E[\mu^2]E[\|\mathbf{u}\|^2](3E[\eta^2] + 1)E[|e_a|^4] \\ & + E[\mu^2]E[\|\mathbf{u}\|^2]G_2 + E[\mu^2]E[\|\mathbf{u}\|^2]E[|e_a|^6] \\ & = 2E[\mu](E[M^2]E[|e_a|^2] + E[v^2]E[|e_a|^2] + E[\eta^2]E[|e_a|^2] + E[|e_a|^4]). \end{aligned} \quad (3.48)$$

$$G_1 = 3 + 3\sigma_M^4 + 6\sigma_M^2\sigma_v^2 + 6\sigma_M^2\sigma_\eta^2 + 3\sigma_v^4 + 6\sigma_v^2\sigma_\eta^2 + 3\sigma_\eta^4. \quad (3.49)$$

$$\begin{aligned}
G_2 = & \sigma_\eta^6 + 3\sigma_v^2\sigma_\eta^4 + 3\sigma_v^4\sigma_\eta^2 + 3\sigma_M^2\sigma_\eta^4 + \sigma_v^6 \\
& + 6\sigma_v^2\sigma_\eta^2\sigma_M^2 + 3\sigma_M^2\sigma_v^4 + 3\sigma_M^4\sigma_\eta^2 + 3\sigma_M^4\sigma_v^2 + \sigma_M^6 \\
& + \sigma_\eta^4 + 2\sigma_v^2\sigma_\eta^2 + \sigma_v^4 + 2\sigma_M^2\sigma_\eta^2 + 2\sigma_M^2\sigma_v^2 \\
& + \sigma_M^4 + 4\sigma_v^2 + 2\sigma_\eta^2 + 2\sigma_M^2 + 2.
\end{aligned} \tag{3.50}$$

It is the convergence state $i \rightarrow \infty$, so we can assume $E[M^{2m}] = (E[M^2])^m = \sigma_M^{2m}$, $E[\eta^{2m}] = (E[\eta^2])^m = \sigma_\eta^{2m}$, and $E[v^{2m}] = (E[v^2])^m = \sigma_v^{2m}$, where σ_M , σ_η and σ_v are the variances of the Gaussian distribution.

In this circumstance, the high power terms $E[|e_a|^4]$ and $E[|e_a|^6]$ may be neglected. So we obtain the EMSE,

$$\begin{aligned}
\zeta = & E[|e_a|^2] \\
= & \frac{E[\mu^2(\infty)]E[\|\mathbf{u}\|^2]G_2}{2E[\mu(\infty)](\sigma_M^2 + \sigma_v^2 + \sigma_\eta^2) - E[\mu^2(\infty)]E[\|\mathbf{u}\|^2]G_1},
\end{aligned} \tag{3.51}$$

where, $E[\mu(\infty)] \approx \frac{b\xi_{min}}{1-a}$, $E[\mu^2(\infty)] \approx \frac{2ab^2\xi_{min}^2}{(1-a)^2(1+a)}$ and, the details of G_1 and G_2 are given by (3.49) and (3.50), respectively.

Assumption 7: The residual MUI and ISI powers σ_M^2 and σ_η^2 at the output of the optimum filter are significantly lower than the output noise power σ_v^2 , namely, $\sigma_v^2 \gg \sigma_M^2$ and $\sigma_v^2 \gg \sigma_\eta^2$.

Thus, a simplified expression can be derived if all the terms that contain M and η are removed. The simplified expression is then given by

$$\zeta = E[|e_a|^2] \approx \frac{ab\xi_{min}E[\|\mathbf{u}\|^2](\sigma_v^6 + \sigma_v^4 + 4\sigma_v^2 + 2)}{(1+a)(1-a)\sigma_v^2 - ab\xi_{min}E[\|\mathbf{u}\|^2](3 + 3\sigma_v^4)}. \tag{3.52}$$

3.5.4 Tracking Analysis

In this part we examine the operation of these novel step-size algorithms in a nonstationary environment, for which the optimum solution takes on a time-varying form. The minimum point of the error-performance surface is no longer fixed. Consequently, the adaptive blind algorithm now has the added task of tracking the minimum point of the error-performance surface. In other words, the algorithm is required to continuously track the statistical variations of the input, the occurrence of which is assumed to be “slow” enough for the tracking to be feasible. We shall continue to rely on the energy-conservation framework [112] and use it to derive expressions for the excess mean-square

error of an adaptive filter when the input signal properties vary with time. The presentation will reveal that there are actually minor differences between mean-square analysis and tracking analysis.

EMSE expressions for the tracking performance of the CCM algorithm were published in [112]. The derivation of tracking performance EMSE for the blind MUD was proposed in [113]. Here we focus on the analysis of the novel variable step-size mechanism incorporated in the parameter estimation of the CCM-SG algorithm.

In the time-varying channel, the optimum filter coefficients are assumed to vary according to the model $\mathbf{w}_{opt}(i+1) = \mathbf{w}_{opt}(i) + \mathbf{q}(i)$, where $\mathbf{q}(i)$ denotes a random perturbation. This is typical in the context of tracking analyses of adaptive filters [4], [115] and [116]. Based on these works, we make an assumption.

Assumption 8: The sequence $\mathbf{q}(i)$ is a stationary sequence of independent zero-mean vectors and positive definite autocorrelation matrix $\mathbf{Q} = E(\mathbf{q}(i)\mathbf{q}^H(i))$, which is mutually independent of the sequences $\{\mathbf{u}(i)\}$, $\{v(i)\}$, $\{M(i)\}$ and $\{\eta(i)\}$.

Now, we first redefine the weight error vector as $\tilde{\mathbf{w}}(i) = \mathbf{w}_{opt}(i) - \mathbf{w}(i)$ and then, $\tilde{\mathbf{w}}(i)$ satisfies

$$\tilde{\mathbf{w}}(i+1) = \tilde{\mathbf{w}}(i) - \mu \mathbf{u}(i)F_e(i) + \mathbf{q}(i). \quad (3.53)$$

We define $e_a(i) = (\mathbf{w}_{opt}(i) - \mathbf{w}(i))^H \mathbf{r}(i)$ and $e_p(i) = (\mathbf{w}_{opt}(i) - \mathbf{w}(i+1))^H \mathbf{r}(i)$, so from (3.36) we have

$$e_a(i) = e_p(i) + \mu \|\mathbf{u}(i)\|^2 F_e^*(i). \quad (3.54)$$

We conclude that (3.39) and (3.41) still hold for the nonstationary case, and from (3.53) and (3.54) we obtain

$$\tilde{\mathbf{w}}(i+1) + \bar{\mu}(i)\mathbf{u}(i)e_a^*(i) = \tilde{\mathbf{w}}(i) + \mathbf{q}(i) + \bar{\mu}(i)\mathbf{u}(i)e_p^*(i). \quad (3.55)$$

As we discussed before, by squaring (3.55) and taking the expected value, when the filter is operating in steady state we have

$$E[\|\tilde{\mathbf{w}}(i+1)\|^2] + E[\bar{\mu}(i)|e_a(i)|^2] = E[\|\tilde{\mathbf{w}}(i) + \mathbf{q}(i)\|^2] + E[\bar{\mu}(i)|e_p(i)|^2]. \quad (3.56)$$

$$\begin{aligned} E[\|\tilde{\mathbf{w}}(i) + \mathbf{q}(i)\|^2] &= E[(\tilde{\mathbf{w}}^H(i) + \mathbf{q}^H(i))(\tilde{\mathbf{w}}(i) + \mathbf{q}(i))] \\ &= E[\|\tilde{\mathbf{w}}(i)\|^2] + E[\tilde{\mathbf{w}}^H(i)\mathbf{q}(i)] + E[\mathbf{q}^H(i)\tilde{\mathbf{w}}(i)] + E[\mathbf{q}^H(i)\mathbf{q}(i)], \end{aligned} \quad (3.57)$$

by using Assumption 5, we have $E[\tilde{\mathbf{w}}^H(i)\mathbf{q}(i)] = E[\mathbf{q}^H(i)\tilde{\mathbf{w}}(i)] = 0$.

When $i \rightarrow \infty$, $E[|\tilde{\mathbf{w}}(i+1)|^2] = E[|\tilde{\mathbf{w}}(i)|^2]$, so based on Assumption 5 the energy preserving equation of the tracking performance is given as

$$E[\bar{\mu}(i)|e_a(i)|^2] = \text{Tr}(\mathbf{Q}) + E[\bar{\mu}(i)|e_a(i) - \frac{\mu}{\bar{\mu}(i)}F_e^*(i)|^2]. \quad (3.58)$$

Expanding the equation, it can be simplified to

$$D = \text{Tr}(\mathbf{Q}) + F \quad (3.59)$$

where D and F were described before, $\text{Tr}(\mathbf{Q}) = E(\mathbf{q}^H(i)\mathbf{q}(i))$. By using the previous assumptions, the high power terms $E[|e_a|^4]$ and $E[|e_a|^6]$ may be neglected. Finally, we obtain

$$\begin{aligned} \zeta &= E[|e_a|^2] \\ &= \frac{E[\mu^2(\infty)]E[\|\mathbf{u}\|^2]G_2 + \text{Tr}(\mathbf{Q})}{2E[\mu(\infty)](\sigma_M^2 + \sigma_v^2 + \sigma_\eta^2) - E[\mu^2(\infty)]E[\|\mathbf{u}\|^2]G_1}, \end{aligned} \quad (3.60)$$

where $E[\mu(\infty)] \approx \frac{b\xi_{min}}{1-a}$, $E[\mu^2(\infty)] \approx \frac{2ab^2\xi_{min}^2}{(1-a)^2(1+a)}$.

By using assumption 4, a simplified expression can be derived if all the terms that contain M and η are removed. The simplified solution is given by

$$\zeta = E[|e_a|^2] \approx \frac{ab\xi_{min}^2 E[\|\mathbf{u}\|^2](\sigma_v^6 + \sigma_v^4 + 4\sigma_v^2 + 2) + (1-a)^2(1+a)\text{Tr}(\mathbf{Q})}{(1+a)(1-a)\xi_{min}\sigma_v^2 - ab\xi_{min}^2 E[\|\mathbf{u}\|^2](3 + 3\sigma_v^4)}. \quad (3.61)$$

3.6 Simulation Results

In this section, we evaluate the performance of the proposed variable step-size mechanism and compare it to the existing algorithms. Firstly, the MSE performance of a non-stationary scenario is compared in an AWGN single-path channel to evaluate the mechanisms, and then we carry out simulations to assess SINR performance of the algorithms in non-stationary environments for multipath time-varying channels. The BER performance is also taken into account, and at last we focus on the convergence and tracking performances to compare the results of simulations and analytical expressions. The DS-CDMA system employs spreading codes with spreading gain $N = 31$. Our simulation results are based on the downlink of an uncoded system.

The first experiment studies the performance of the proposed CCM SG-TASS algorithm, the existing CCM SG-AGSS and the CCM SG fixed step-size algorithms in an

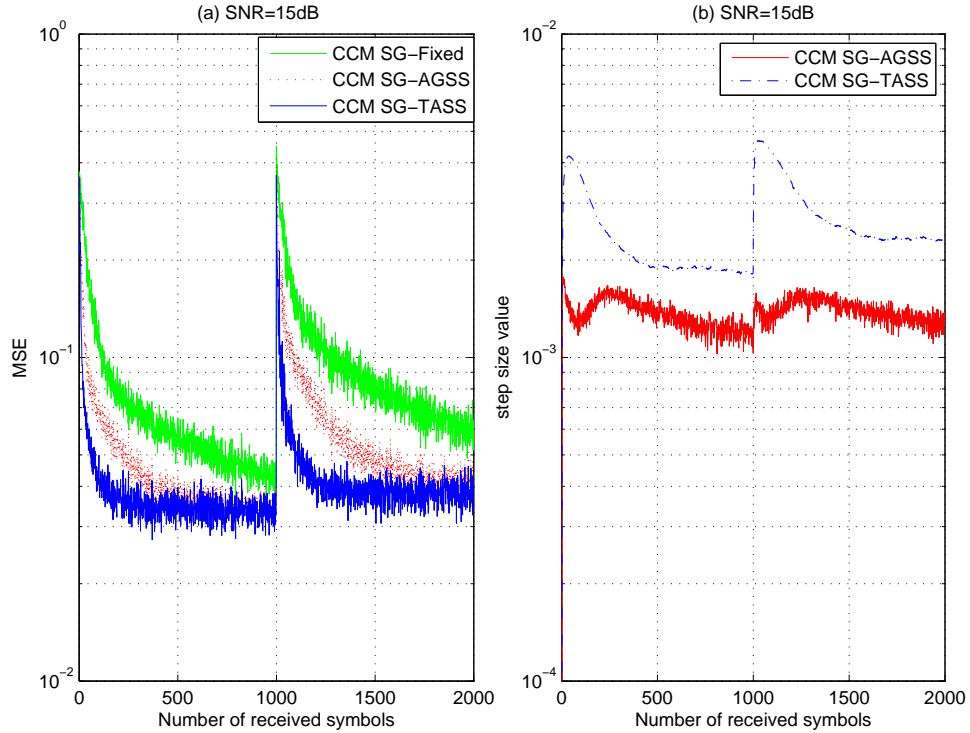


Figure 3.2: (a) MSE performance in a non-stationary environment with an AWGN channel, where the system starts with 4 users including a 5dB high power level interferer. After 1000 received symbols 4 new users including a 5dB high power level interferer enter the system. (b) Step-size variation in the same non-stationary environment.

AWGN channel. The DS-CDMA system employs binary random sequences as the spreading codes. Fig.3.2 (a) shows the MSE performance of the algorithms in a non-stationary environment with an AWGN channel, the SNR is 15dB, where the SNR is defined as the received desired user's signal to noise power ratio. We show the convergence of the receivers in terms of MSE. For the non-stationary case the system starts with 4 users including 1 high power level interferer with 5dB and after 1000 symbols, 4 new users including a 5dB high power level user enter the system. These results in Fig.3.2 (a) indicate that the convergence of the proposed CCM SG-TASS outperforms the convergence of the CCM SG-AGSS and the fixed step-size algorithms in an AWGN non-stationary environment. Fig.3.2 (b) shows the variation of the step-size values in the non-stationary environment. In this experiment, the parameters of the TASS mechanism have been optimized with $\mu_- = 10^{-6}$, $\mu_+ = 5 \times 10^{-3}$, $\mu_0 = 10^{-4}$, $a = 0.98$, and $b = 5 \times 10^{-4}$. The optimized parameters of the AGSS mechanism are $\mu_- = 10^{-6}$, $\mu_+ = 2 \times 10^{-3}$, $\mu_0 = 10^{-4}$, $\alpha = 0.0003$, and fixed step-size is 5×10^{-4} . The optimized parameters are chosen based on simulations results, to make the system work in a stable way and obtain good performance.

The second phase considers the algorithms in multipath time-varying channels. In order to avoid the ambiguity, we only considered real channel models. Thus, the algorithm deals with the amplitude variation of the channel. The channel has a profile with 3 paths, and it is normalized. The channel parameters for these experiments are $p_0 = 0.8367$, $p_1 = 0.4472$, $p_2 = 0.3162$. The sequence of channel coefficients is $h_l(i) = \sqrt{p_l}\alpha_l(i)$ ($l = 0, 1, 2$), where $\alpha_l(i)$ is computed according to the Jakes' model. We optimized the limits of the parameters of the variable step-size mechanisms with $\mu_+ = 10^{-3}$, $\mu_- = 10^{-5}$, and $\mu_0 = 10^{-4}$, 2000 symbols are transmitted. The channel estimation algorithm in [105] is employed in the simulation.

Firstly we assess the SINR performance of the proposed TASS mechanism, the AGSS and FSS mechanisms, all based on the SG CCM blind algorithm. In this case, the random sequence is employed for the spreading code. Fig.3.3 (a) shows the convergence of the receivers in terms of SINR, in a scenario where the power levels of 3 interferers are 5dB above the desired user, whilst the remaining interferers work at the same power level of the desired signal. In order to test the non-stationary scenario, the system starts with 5 users and 3 new users enter after 1000 symbols. We optimized the parameters of the mechanisms with $a = 0.98$, $b = 6 \times 10^{-5}$ for the TASS and $\alpha = 0.06$ for the AGSS. These results indicate that the proposed TASS mechanism converges to a higher SINR than the other methods. Fig.3.3 (b) shows the variation of the step-size values. Finally, we can see that the novel variable step-size algorithm can work very well in the non-stationary environment of the multipath time-varying channel.

The BER performance is studied next. In particular we show the BER performance versus the received desired user's signal to noise power ratio and number of users (K) for the analyzed algorithms. Here, we use Gold sequences with $N = 31$, and assume every user's power is equal to 1, the fading rate $f_d T$ is 1×10^{-3} , and 2000 symbols are transmitted. The results in Fig.3.4(a) indicate that the best performance is achieved with the proposed CCM SG-TASS algorithm, followed by the CCM SG-AGSS and the CCM SG fixed step-size algorithms. Fig.3.4(b) shows us that with an increase in the number of users in the system, our proposed algorithm still has the best performance. Specifically, CCM SG-TASS algorithm can save up to 4dB and support up to 3 more users in comparison with the CCM SG-AGSS algorithm for the same performance.

In the third experiment, we consider the convergence and tracking analyses. The multipath channel model is the same as before. In order to simplify the simulations we employ the normalized fixed vector $[p_0, p_1, p_2]^T$ as the vector \mathbf{g} to calculate the effective signature waveform $\bar{\mathbf{s}}_k$, where p_0, p_1 and p_2 are the values in the second experiment. The steady-state MSE between the desired and the estimated symbol obtained through sim-

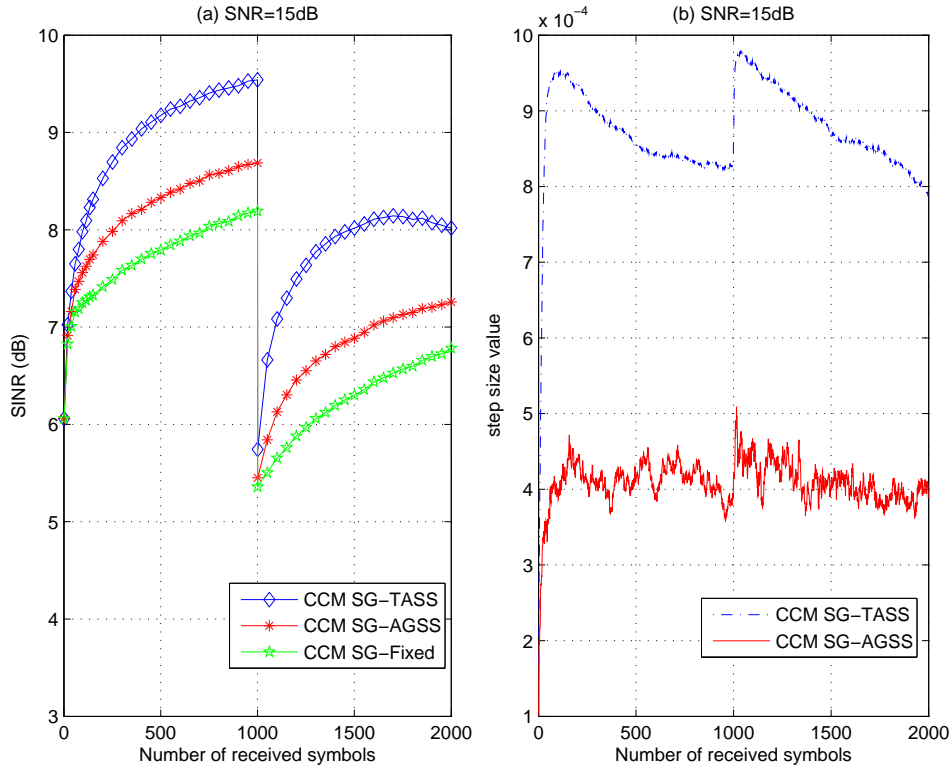


Figure 3.3: (a) SINR performance in non-stationary environment of multipath time-varying channel, (b) Step-size values for the variable step-size mechanisms in the non-stationary environment, SNR=15dB, $f_d T = 5 \times 10^{-6}$, FSS is 10^{-4} .

ulation is compared with the steady-state MSE computed via the expressions derived in Section 3.5. Before using (3.52) and (3.61) we have to calculate several values. From the conclusion in [108], we know that the optimal CCM minimum ξ_{min} roughly corresponds to the minimum mean square error. The residual noise power σ_v^2 in (3.52) is equal to $\mathbf{w}_{opt}^H \sigma_n^2 \mathbf{w}_{opt}$, where $\mathbf{w}_{opt} = \mathbf{R}^{-1} \bar{\mathbf{s}}_k$. $E[\|\mathbf{u}\|^2] = (M-1)\sigma_n^2 + \sum_{k=2}^K A_k^2 \rho_{kk} - \sum_{k=2}^K A_k^2 \rho_{k1}^2 / \rho_{11}$, where $\rho_{ij} = \bar{\mathbf{s}}_i^H \bar{\mathbf{s}}_j$. The results can be derived by using a similar approach to [113].

Firstly let us verify that the results (3.23), (3.24), and (3.52) of the section on convergence analysis of the mechanism can provide a means of estimating the excess MSE. In this simulation of convergence analysis, we employ random sequences of length $N = 31$, and assume that 4 users operate in the system and they have the same power level. The time-invariant multipath scenario with AWGN is considered. The results are shown in Fig.3.5(a), for the multipath case. By comparing the curves, it can be seen that as the number of received symbols increases and the simulated MSE converges to the analytical result, showing the usefulness of our analysis and assumptions, where $a = 0.98$,

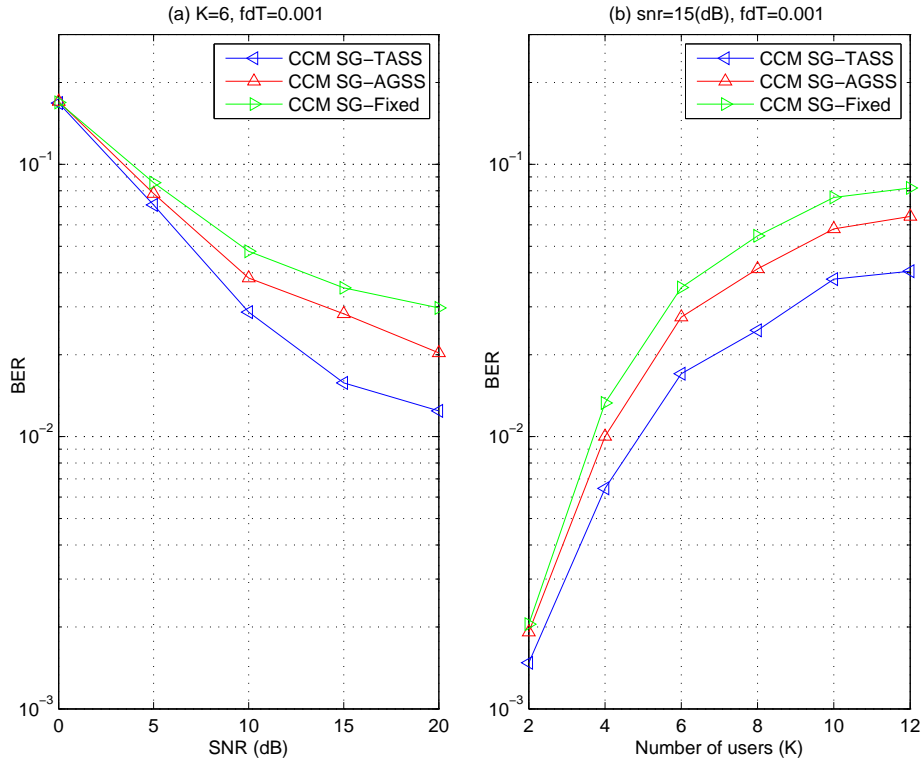


Figure 3.4: (a) BER versus the SNR with multipath channels and (b) BER versus number of users with multipath channels. $f_d T = 1 \times 10^{-3}$, FSS is 10^{-4} .

$b = 0.00005$. The Fig.3.5(b) shows the effect that the desired user's signal to noise power ratio has on the MSE, and a comparison between the steady-state analysis and simulation results. The results confirm that the MSE decreases monotonically with SNR. For each input SNR we can find suitable values of parameters a and b to let the simulation and analysis results agree well with each other.

The tracking analysis of the CCM SG-TASS algorithm in a fading channel has been discussed in 3.5. In this part we verify that the results (3.23), (3.24), and (3.61) of the section on tracking analysis of the mechanism can provide a means of estimating the MSE. The tracking analysis has been evaluated by using random sequences with spreading gain 31, and we assume that 6 users operate with the same power level in the system. A time-varying multipath channel has been taken into account, the 5×10^{-5} fading rate Jakes' model is employed. The value of $\text{Tr}(\mathbf{Q})$ was computed with the aid of $J_0(2\pi f_d T)$ [117], which is the autocorrelation function of the Jakes' model, where J_0 is the zero-order Bessel function of the first kind, f_d is the maximum Doppler shift, and T is the symbol interval [118]. $\text{Tr}(\mathbf{Q})$ is equal to 1.6×10^{-6} . Fig. 3.6 indicates that as the number of received symbols increases, the simulated MSE converges to the analytical result, showing

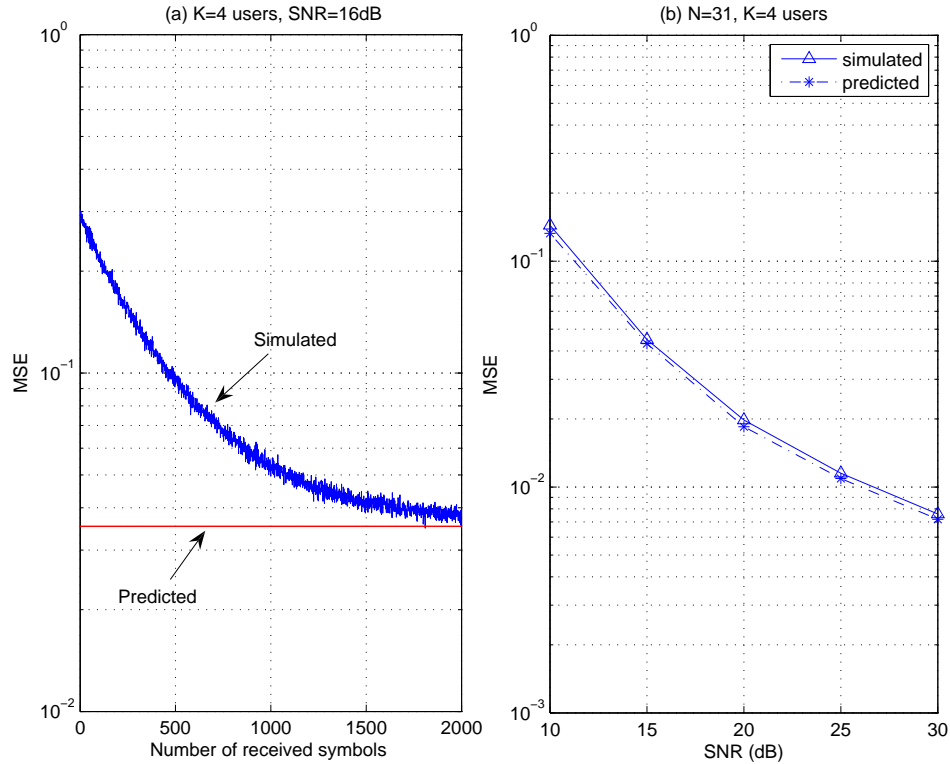


Figure 3.5: MSE analytical versus simulated performance for the proposed TASS mechanism convergence analysis. (a) Number of users is 4, the SNR is 16 dB. (b) Number of users is 4.

the usefulness of our analysis and assumptions, where $a = 0.98$, $b = 0.00016$.

3.7 Conclusions

In this chapter, we have investigated blind adaptive CCM receivers for DS-CDMA systems that employ SG algorithms with variable step-size mechanisms. A low-complexity variable step-size mechanism has been proposed and analyzed for estimating the parameters of linear CDMA receiver that operate with SG algorithms in multipath channels. We compared the computational complexity of the new algorithm with the existent methods and further investigated the characteristics of the new mechanism via derived analytical expressions using the energy-preserving approach to predict the EMSE for convergence and tracking analyses. Simulation experiments were conducted to verify the analytical results and illustrate that the new blind adaptation mechanism significantly outperforms the conventional variable step-size mechanism for blind CCM receivers at a lower complexity in both stationary and nonstationary scenarios.

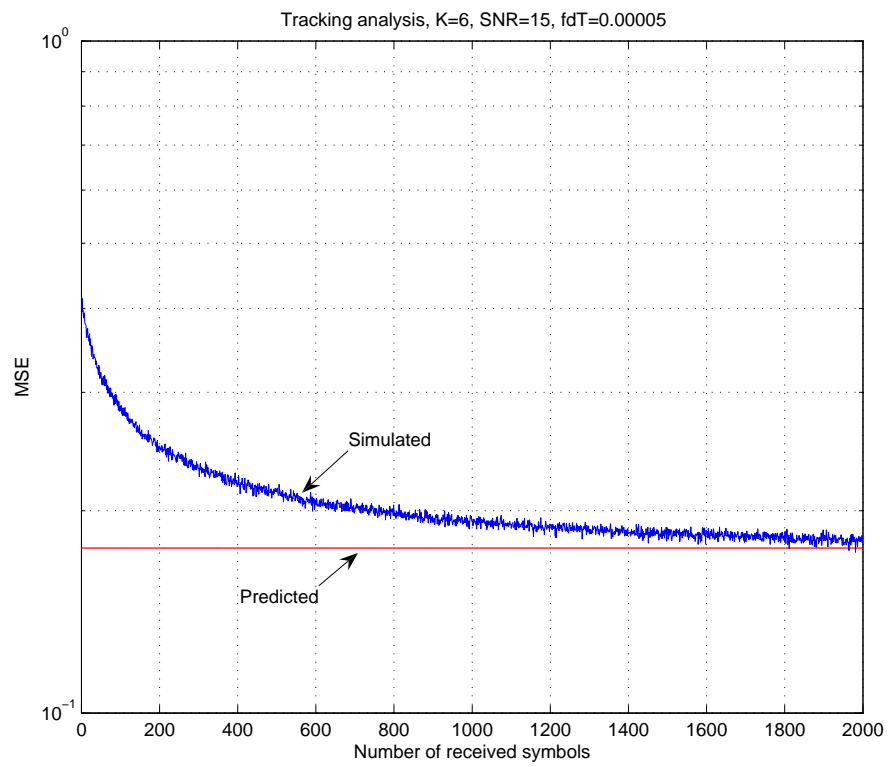


Figure 3.6: MSE analytical versus simulated performance for the proposed TASS mechanism tracking analysis. Number of users is 6, the SNR is 15 dB, $f_d T = 5 \times 10^{-5}$.

Chapter 4

Adaptive Decision Feedback Detectors for Space-Time CDMA Systems

Contents

4.1	Introduction	54
4.2	DS-CDMA System Model and Array Configurations	56
4.3	Space-time MPF Decision Feedback Receiver Structure	58
4.4	Multistage Space-time MPF-DF Detection	61
4.5	MMSE Design of Proposed Space-time Estimators	63
4.6	Analytical Results	64
4.7	Adaptive Estimation Algorithms	66
4.8	Simulation Results	70
4.9	Conclusions	77

4.1 Introduction

In DS-CDMA systems, substantial work has been devoted to the design of schemes for interference mitigation. The exponential complexity of the optimal multiuser detector proposed by Verdu [94] has motivated the development of various sub-optimal strategies with affordable complexity: the linear [119] and DF [120] receivers, the successive interference canceller [121] and the multistage detector [122]. For uplink scenarios, some works [23], [123] have shown that DF structures, which are relatively simple and perform

linear interference suppression followed by interference cancellation, provide substantial gains over linear detection.

Among these schemes, the MMSE multiuser decision feedback detectors have emerged as highly effective solutions for the uplink as they provide effective MUI suppression, significant capacity increase and excellent performance as compared to related detectors [123–129], at a relatively modest complexity. In particular, when using short or repeated spreading sequences the MMSE design criterion leads to adaptive versions which only require a training sequence for estimating the receiver parameters. The work of Honig and Woodward [125] has shown that the design of adaptive decision feedback receivers based on the MMSE criterion using the successive DF (S-DF) and the parallel DF (P-DF) schemes which can provide substantial gains over linear schemes. The P-DF scheme, which is more sensitive to error propagation than the S-DF, provides relatively better performance. Another technique that can substantially increase the capacity of CDMA systems is the use of smart antennas. Indeed, detectors equipped with antenna arrays can process signals in both temporal and spatial domains, increase the reliability of the links via diversity and separate interferers via beamforming [130]. The literature on the combined use of antenna arrays and decision feedback structures is relatively unexplored. The works in [124], [125] however, did not consider the incorporation of antenna arrays. Adaptive space-time decision feedback detectors were proposed by Smee and Schwartz in [126], although the work was limited to the use of adaptive algorithms for only the feedforward filter with S-DF structures.

In this chapter, we propose a novel space-time MMSE decision feedback detection scheme for uplink DS-CDMA systems with antenna arrays, which employs multiple parallel feedback (MPF) for interference cancellation. The basic idea is to improve the conventional S-DF structure by using different orders of cancellation and then select the most likely estimate. For each user, the proposed detection structure is equipped with several parallel branches which employ different ordering patterns, namely, each branch produces a symbol estimate by exploiting a certain ordering pattern. Thus, there is a group of symbol estimates at the end of the MPF branches structure. The criterion of Euclidean distance is used as selection rule to select the branch with best performance. The novel structure for detection exploits different patterns and orderings for the modification of the original S-DF architecture and achieves higher detection diversity by selecting the branch which yields the estimates with the best performance. A near-optimal user ordering algorithm which employs several particular cancellation orders is described for the proposed space-time MPF-DF structure due to the high complexity of the optimal ordering algorithm which employs all the possible cancellation orders. Furthermore, the proposed DF receiver structure is combined with cascaded DF stages to mitigate the deleterious effects

of error propagation and refine the symbol estimates of the users. We present modified adaptive algorithms for both feedforward and feedback filters using SG and RLS algorithms. Basically, we use a switching rule amongst different ordering branches, for each iteration we select the optimum branch based on all the feedback results, and adapt the filters using the selected branch of data. The performance of the system with antenna arrays in a beamforming environment and a diversity environment is considered. We derive the MMSE expressions achieved by the considered DF structures with imperfect and perfect feedback. The main contributions of this chapter are: *I)* Novel space-time MMSE DF receivers with MPF are introduced for interference suppression in uplink DS-CDMA systems with antenna arrays, where beamforming and diversity configurations are considered. *II)* The proposed space-time MPF-DF receiver is combined with multistage detection. *III)* The modified adaptive algorithms are developed for both feedforward and feedback filters. *IV)* Analytical works are carried out for the proposed space-time MPF-DF. Our proposed space-time adaptive DF scheme and algorithms can be used in other scenarios, including MIMO and MC-CDMA systems.

This chapter is structured as follows. Section 4.2 briefly describes the DS-CDMA system model and array configurations. The proposed space-time MPF-DF scheme is described in Section 4.3. Section 4.4 is devoted to the proposed scheme combined with cascaded DF stages. The proposed MMSE space-time estimators are derived in section 4.5, and some analytical works are carried out in section 4.6. Section 4.7 discusses the adaptive estimation algorithms for feedforward and feedback receivers. Section 4.8 presents and discusses the simulation results. Section 4.9 draws the conclusions.

4.2 DS-CDMA System Model and Array Configurations

Let us consider the uplink of an uncoded synchronous BPSK DS-CDMA system with K users, N chips per symbol and L_p propagation paths. It should be remarked that a synchronous model is assumed for simplicity, although it captures most of the features of more realistic asynchronous models with small to moderate delay spreads [3]. The baseband signal transmitted by the k -th active user to the base station is given by

$$x_k(t) = A_k \sum_{i=-\infty}^{\infty} b_k(i) s_k(t - iT) \quad (4.1)$$

where $b_k(i) \in \{\pm 1\}$ denotes the i -th symbol for user k , the real valued spreading waveform and the amplitude associated with user k are $s_k(t)$ and A_k , respectively. The

spreading waveforms are expressed by $s_k(t) = \sum_{i=0}^{N-1} a_k(i)\phi(t - iT_c)$, where $a_k(i) \in \{\pm 1/\sqrt{N}\}$, $\phi(t)$ is the chip waveform, T_c is the chip duration and $N = T/T_c$ is the processing gain. Assuming that the channel modelled as a parameter vector \mathbf{h} is constant during each symbol and the base station receiver with a J -element linear antenna-array is synchronized with the main path, the received signal at the j -th antenna element is

$$r_j(t) = \sum_{k=1}^K \sum_{l=0}^{L_p-1} h_{j,k,l}(t)x_k(t - \tau_{j,k,l}) + n_j(t), \quad (4.2)$$

where $h_{j,k,l}$ and $\tau_{j,k,l}$ are, respectively, the channel coefficient and the delay associated with the l -th path and the k -th user of the j -th antenna element, $j = 1, 2, \dots, J$. Assuming that the delays $\tau_{j,k,l}$ are multiples of the chip rate, the received signal at each antenna $r_j(t)$ after filtering by a chip-pulse matched filter and sampled at chip rate yields the M -dimensional received vector for each antenna element

$$\begin{aligned} \mathbf{r}_j(i) &= \sum_{k=1}^K (A_k b_k(i) \mathbf{C}_k \mathbf{h}_{j,k}(i) + \boldsymbol{\eta}_{j,k}(i)) + \mathbf{n}_j(i) \\ &= \sum_{k=1}^K (A_k b_k(i) \tilde{\mathbf{p}}_{k,j}(i) + \boldsymbol{\eta}_{j,k}(i)) + \mathbf{n}_j(i), \end{aligned} \quad (4.3)$$

where $M = N + L_p - 1$, $\mathbf{n}_j(i) = [n_{j,1}(i) \dots n_{j,M}(i)]^T$ is the complex Gaussian noise vector. The user k channel vector of the j -th antenna element is $\mathbf{h}_{j,k}(i) = [h_{j,k,0}(i) \dots h_{j,k,L_p-1}(i)]^T$ with $h_{j,k,l}(i) = h_{j,k,l}(iT_c)$ for $l = 0, \dots, L_p - 1$, $\boldsymbol{\eta}_{j,k}(i)$ is the ISI, and assumes that the channel order is not greater than N , i.e. $L_p - 1 \leq N$, $\mathbf{s}_k = [a_k(1) \dots a_k(N)]^T$ is the signature sequence for user k and $\tilde{\mathbf{p}}_{k,j}(i) = \mathbf{C}_k \mathbf{h}_{j,k}(i)$ is the effective signature sequence for user k at the j -th antenna element, the $M \times L_p$ convolution matrix \mathbf{C}_k contains one-chip shifted versions of \mathbf{s}_k .

$$\mathbf{C}_k = \begin{pmatrix} a_k(1) & & \mathbf{0} \\ \vdots & \ddots & a_k(1) \\ a_k(N) & & \vdots \\ \mathbf{0} & \ddots & a_k(N) \end{pmatrix}.$$

We stack the samples of the received data of the J antenna elements in a $JM \times 1$ vector, so that the coherently demodulated composite received signal of the antenna-array

system is

$$\mathbf{r}(i) = \begin{pmatrix} \mathbf{r}_1(i) \\ \mathbf{r}_2(i) \\ \vdots \\ \mathbf{r}_J(i) \end{pmatrix} = \sum_{k=1}^K \tilde{\mathbf{x}}_k(i) + \mathbf{n}(i), \quad (4.4)$$

where $\tilde{\mathbf{x}}_k(i)$ is a JM -dimensional vector, it is a stack of vectors $A_k b_k(i) \tilde{\mathbf{p}}_{k,j}(i) + \boldsymbol{\eta}_{j,k}(i)$, $j = 1, \dots, J$ for user k , $\mathbf{n}(i) = [\mathbf{n}_1^T(i), \dots, \mathbf{n}_J^T(i)]^T$, and $E[\mathbf{n}(i)\mathbf{n}^H(i)] = \sigma^2 \mathbf{I}_{JM}$, where \mathbf{I}_{JM} denotes a square identity matrix with dimension JM . For the diversity configuration we space the antenna elements in order to make the channel coefficients between every two antenna elements independent. In the beamforming case the spacing between antenna elements is half wavelength, and the following relation holds for the k -th user channel coefficients relevant to antenna elements $j - 1$ and j [130]:

$$h_{j,k,l}(i) = h_{j-1,k,l}(i) e^{-j\phi_l}, \quad (4.5)$$

where $h_{j,k,l}$ is the l -th path channel coefficient of the j -th antenna element regarding user k , $\phi_l = \pi \sin \theta_l$ and θ_l is the direction of arrival (DOA) of the l -th path.

For beamforming or diversity configuration we can design a $JM \times 1$ feedforward filter for each user, which combines the signals from different antennas together. Specifically, regarding diversity, in order to reduce the length of the feedforward filter we can use a group of $M \times 1$ filters $\boldsymbol{\omega}_{k,j}$, $j = 1 \dots J$, which correspond to different antennas to handle the received vectors separately instead of using a long filter [131] and then combine the output signals from each filter by the maximum ratio combining (MRC) or equal-gain combining (EGC) methods. The output signal is

$$z_k(i) = \sum_{j=1}^J c_{k,j} \boldsymbol{\omega}_{k,j}^H(i) \mathbf{r}_j(i), \quad (4.6)$$

where $c_{k,j}$ is the combining weight and $\mathbf{r}_j(i)$ is the $M \times 1$ received data from antenna element j . In the following parts we design the novel DF receiver based on the long feedforward filter structure, even though we remark that for a diversity configuration a designer can resort to the approach outlined above.

4.3 Space-time MPF Decision Feedback Receiver Structure

In this section, we present the principles and structures of the proposed space-time MMSE decision feedback detector with MPF-DF for interference cancellation. The proposed al-

gorithm employs different orders of cancellation to produce a group of estimated candidates, and on the basis of the Euclidean distance, our approach selects the most likely estimate.

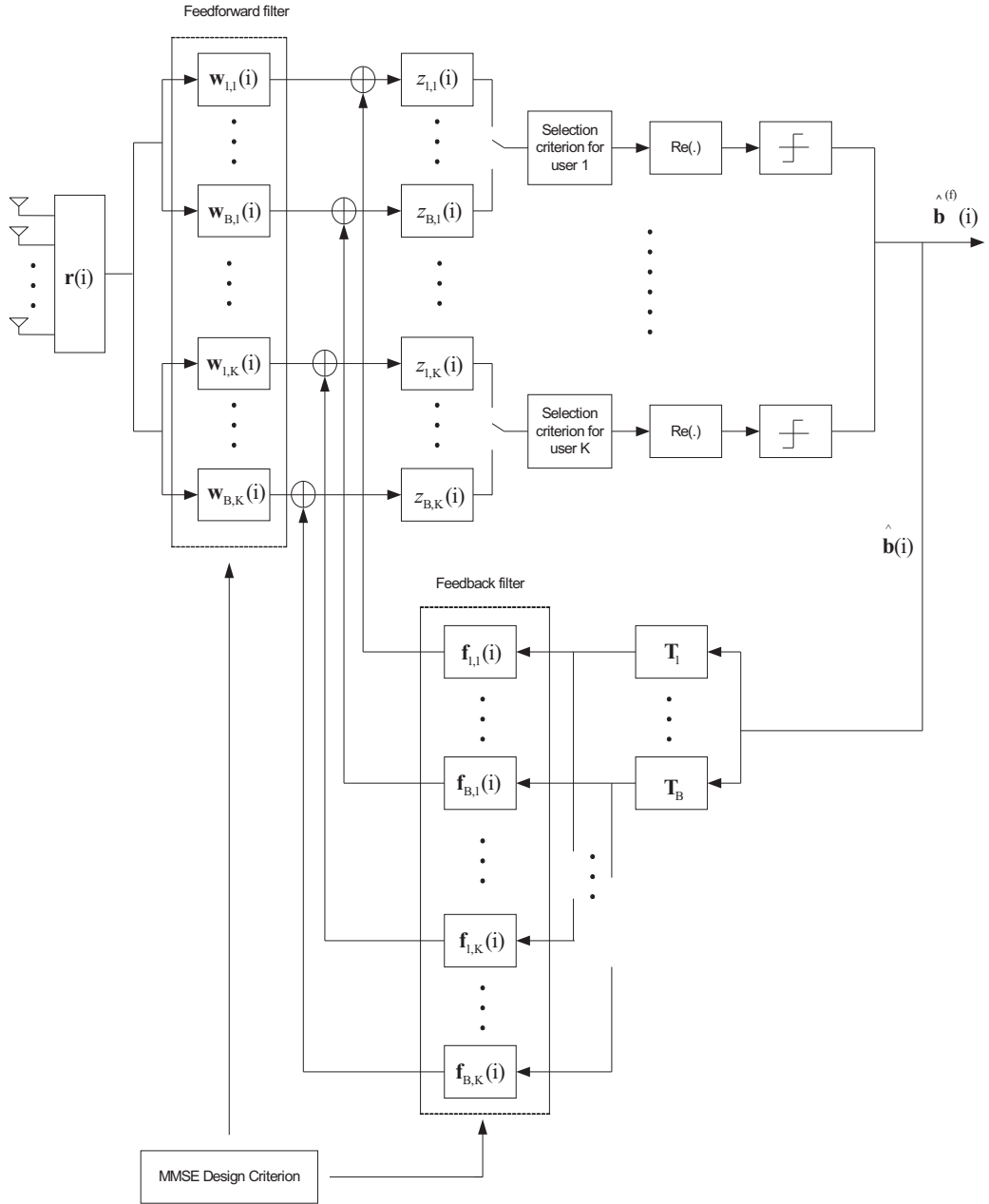


Figure 4.1: Proposed multi-antenna MPF-DF receiver structure

The space-time or multi-antenna MPF-DF structure is presented in Fig 4.1. The proposed receiver employs B parallel branches of SIC with different orders of feedback for the k -th user, where $k = 1 \dots K$, and K is the number of users. We equip the β -th branch of the k -th user with a pair of feedforward and feedback filters, namely, $JM \times 1$ vector $\mathbf{w}_{\beta,k}(i)$ and $K \times 1$ vector $\mathbf{f}_{\beta,k}(i)$, where $\beta = 1 \dots B$. According to those branches, each user obtains a group of different multiuser interference estimates which are subtracted

from the soft outputs of the feedforward filters respectively. The output of the β -th branch for k -th user is

$$z_{\beta,k}(i) = \mathbf{w}_{\beta,k}^H(i)\mathbf{r}(i) - \mathbf{f}_{\beta,k}^H(i)[\mathbf{T}_\beta^H \hat{\mathbf{b}}(i)], \quad (4.7)$$

where the $JM \times 1$ received vector $\mathbf{r}(i)$ is the input to a nonlinear structure, $\hat{\mathbf{b}}(i)$ is the $K \times 1$ feedback vector, namely, the tentative decision vector of preceding iteration at time i . In this work the DF receiver only employs 1 iteration, and the value of the feedback vector is computed by $\hat{\mathbf{b}}(i) = \text{sgn}(\Re(\mathbf{W}_{\text{lin}}^H(i)\mathbf{r}(i)))$, where \mathbf{W}_{lin} is a $JM \times K$ linear filtering matrix designed by MMSE criterion. The matrices \mathbf{T}_β are permuted square identity \mathbf{I}_K matrices with dimension K whose structures for an $B=4$ -branch MPF-DF scheme are given by:

$$\begin{aligned} \mathbf{T}_1 &= \mathbf{I}_K, \mathbf{T}_2 = \begin{pmatrix} \mathbf{0}_{K/4,3K/4} & \mathbf{I}_{3K/4} \\ \mathbf{I}_{K/4} & \mathbf{0}_{K/4,3K/4} \end{pmatrix}, \\ \mathbf{T}_3 &= \begin{pmatrix} \mathbf{0}_{K/2} & \mathbf{I}_{K/2} \\ \mathbf{I}_{K/2} & \mathbf{0}_{K/2} \end{pmatrix}, \mathbf{T}_4 = \begin{pmatrix} 0 & \dots & 1 \\ \vdots & \ddots & \vdots \\ 1 & \dots & 0 \end{pmatrix}, \end{aligned} \quad (4.8)$$

where $\mathbf{0}_{m,n}$ denotes an $m \times n$ -dimensional matrix full of zeros and the structures of the permutation matrices \mathbf{T}_β correspond to phase shifts regarding the cancellation order of the users. The purpose of the matrices in (4.8) is to change the order of cancellation. Specifically, the above matrices perform the cancellation with the following order with respect to user powers: \mathbf{T}_1 with indices $1, \dots, K$; \mathbf{T}_2 with indices $K/4, K/4 + 1, \dots, K, 1, \dots, K/4 - 1$; \mathbf{T}_3 with indices $K/2, K/2 + 1, \dots, K, 1, \dots, K/2 - 1$; \mathbf{T}_4 with $K, \dots, 1$ (reverse order). The quantity $\mathbf{T}_\beta^H \hat{\mathbf{b}}(i)$ is the feedback vector corresponding to the β -th branch. For more branches, additional phase shifts are applied with respect to user cancellation ordering. Note that different update orders were tested although they did not result in performance improvement.

The feedback filter $\mathbf{f}_{\beta,k}(i)$ which is designed based on SIC controls the permuted feedback vector $\mathbf{T}_\beta^H \hat{\mathbf{b}}(i)$. The structure of the feedback filter is given by $\mathbf{f}_{\beta,k}(i) = [f_{\beta,k,1}(i), f_{\beta,k,2}(i), \dots, f_{\beta,k,K}(i)]^T$, where the elements $f_{\beta,k,\gamma}(i) = 0$, when $k \leq \gamma \leq K$, $\gamma = 1 \dots K$. The non-zero elements of the filter $\mathbf{f}_{\beta,k}(i)$ correspond to the number of used feedback connections and to the users to be cancelled.

The number of parallel branches B that yield detection candidates is a parameter that must be chosen by the designer. The number of candidates of the optimal ordering algorithm is $B = K!$ and is clearly very complex for practical systems. The goal of the proposed scheme is to improve performance using parallel searches and to select the most likely symbol estimate. The final output $\hat{b}_k^{(f)}(i)$ for the k -th user of the space-time MPF-DF detector chooses the best estimate of the B candidates based on the criterion of Eu-

clidean distance for each symbol interval i as described by:

$$\beta_{opt,k} = \arg \min_{\beta \in \{1, \dots, B\}} e_{\beta,k}(i), \quad (4.9)$$

$$\hat{b}_k^{(f)}(i) = \text{sgn}(\Re(z_{\beta_{opt,k}}(i))), \quad (4.10)$$

where $e_{\beta,k}(i) = |b_k(i) - z_{\beta,k}(i)|$, and $\hat{b}_k^{(f)}(i)$ forms the vector of final decisions $\hat{\mathbf{b}}_k^{(f)}(i) = [\hat{b}_1^{(f)}(i) \dots \hat{b}_K^{(f)}(i)]^T$. Our studies indicate that the $B = 4$ near-optimal user ordering algorithm achieves most of the gains of the proposed structure and offers a good trade-off between performance and complexity.

4.4 Multistage Space-time MPF-DF Detection

In this section, the proposed receiver structure is considered in conjunction with cascaded DF stages [124], [125], which are of great interest for uplink scenarios due to the capability of providing uniform performance over the users.

In [124], Woodward et al. presented a multistage detector with an S-DF in the first stage and P-DF or S-DF structures, with users being demodulated in reverse order, in the second stage. Firstly, let us describe the multistage receiver with only the S-DF or P-DF detector. For the first stage $m = 1$ we have the output defined by:

$$\hat{\mathbf{b}}^{(m-1)}(i) = \text{sgn}(\Re(\mathbf{W}_{\text{lin}}^H(i)\mathbf{r}(i))). \quad (4.11)$$

$$\mathbf{z}^{(m)}(i) = \mathbf{W}^{(m)H}(i)\mathbf{r}(i) - \mathbf{F}^{(m)H}(i)\hat{\mathbf{b}}^{(m-1)}(i). \quad (4.12)$$

For the stages $m \geq 2$, we obtain

$$\hat{\mathbf{b}}^{(m-1)}(i) = \text{sgn}(\Re(\mathbf{z}^{(m-1)}(i))), \quad (4.13)$$

$$\mathbf{z}^{(m)}(i) = [\mathbf{W}^{(m)}(i)\mathbf{M}]^H \mathbf{r}(i) - [\mathbf{M}\mathbf{F}^{(m)}(i)]^H \hat{\mathbf{b}}^{(m-1)}(i), \quad (4.14)$$

where the number of stages m depends on the application. More stages can be added and the order of the users is reversed from stage to stage, the $JM \times K$ filtering matrix $\mathbf{W}^{(m)}$ is given by $\mathbf{W}^{(m)}(i) = [\mathbf{w}_1^{(m)}(i), \dots, \mathbf{w}_K^{(m)}(i)]$, and the $K \times K$ matrix $\mathbf{F}^{(m)}$ is given by $\mathbf{F}^{(m)}(i) = [\mathbf{f}_1^{(m)}(i), \dots, \mathbf{f}_K^{(m)}(i)]$, where $\mathbf{w}_k^{(m)}(i)$ and $\mathbf{f}_k^{(m)}(i)$ are the $JM \times 1$ and $K \times 1$ filtering vectors corresponding to the k -th user, $k = 1 \dots K$, and $\hat{\mathbf{b}}^{(m-1)}(i)$ is the $K \times 1$ vector of the $(m - 1)$ -th stage tentative decisions, \mathbf{M} is a $K \times K$ square permutation

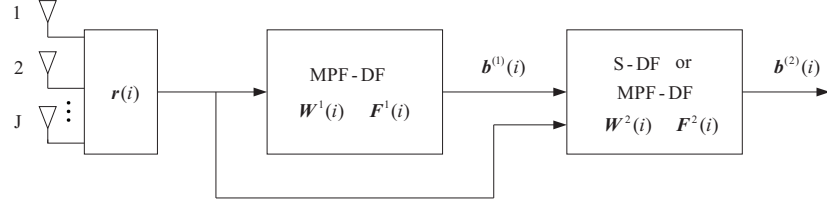


Figure 4.2: The two-stage DF receiver with space-time MPF-DF scheme in the first stage

matrix with ones along the reverse diagonal and zeros elsewhere (similar to \mathbf{T}_4 in (4.8)). The $K \times 1$ decision vector of the m -th stage $\mathbf{z}^{(m)}(i) = [z_1^{(m)}(i), \dots, z_K^{(m)}(i)]^T$.

Let us now focus on the proposed algorithm and combine the space-time MPF-DF structure with multistage detection. To equalize the performance over the user population, we consider a two-stage structure, namely $m = 2$ as shown in Fig. 4.2, the first stage is an MPF-DF scheme, and an S-DF or an MPF-DF are considered in the second stage. The multistage receiver system is denoted IMPFS-DF when an S-DF is employed in the second stage. The outputs of the first stage enter the second stage, which are treated as the estimates of the interference. The proposed multistage scheme is denoted by IMPFMPF-DF and corresponds to an MPF-DF architecture employed in both stages. The j -th component of the soft output vector $\mathbf{z}_{\beta}^{(2)}(i)$ corresponding to the β -th branch of its second stage is:

$$z_{\beta,j}^{(2)}(i) = [\mathbf{W}_{\beta}^{(2)}(i)\mathbf{M}]_j^H \mathbf{r}(i) - [\mathbf{T}_{\beta}\mathbf{F}_{\beta}^{(2)}(i)]_j^H \hat{\mathbf{b}}^{(1)}(i), \quad (4.15)$$

where $[\cdot]_j$ denotes the j -th column of the argument (a matrix), and the second stage MPF-DF filtering matrices corresponding to the β -th branch are given by $\mathbf{W}_{\beta}^{(2)}(i) = [\mathbf{w}_{\beta,1}^{(2)}(i), \dots, \mathbf{w}_{\beta,K}^{(2)}(i)]$, $\mathbf{F}_{\beta}^{(2)}(i) = [\mathbf{f}_{\beta,1}^{(2)}(i), \dots, \mathbf{f}_{\beta,K}^{(2)}(i)]$, where $\mathbf{w}_{\beta,k}^{(2)}(i)$ and $\mathbf{f}_{\beta,k}^{(2)}(i)$ are the $JM \times 1$ and $K \times 1$ filtering vectors corresponding to the β -th branch of the k -th user, $k = 1 \dots K$. The final decision is:

$$\beta_{opt,j} = \arg \min_{\beta \in \{1, \dots, B\}} e_{\beta,j}^{(2)}(i), \quad (4.16)$$

$$\hat{b}_j^{(2)}(i) = \text{sgn}(\Re(z_{\beta_{opt,j}}^{(2)}(i))), \quad (4.17)$$

where $e_{\beta,j}^{(2)}(i) = |b_k(i) - z_{\beta,j}^{(2)}(i)|$. The role of reversing the cancellation order in successive stages is to equalize the performance of the users over the population or at least reduce the performance disparities.

4.5 MMSE Design of Proposed Space-time Estimators

Let us describe in this section the design of the proposed space-time MMSE decision feedback detectors. A general case where each branch has a pair of feedforward and feedback filters is considered. Firstly, let us consider the cost function for the branch β of user k :

$$\begin{aligned}
 J_{MSE} &= E[|b_k(i) - \mathbf{w}_{\beta,k}^H(i)\mathbf{r}(i) + \mathbf{f}_{\beta,k}^H(i)\hat{\mathbf{b}}_{\beta}(i)|^2] \\
 &= \sigma_b^2 - \mathbf{w}_{\beta,k}^H(i)\mathbf{p}_k - \mathbf{p}_k^H\mathbf{w}_{\beta,k}(i) + \mathbf{w}_{\beta,k}^H(i)\mathbf{R}\mathbf{w}_{\beta,k}(i) + \mathbf{f}_{\beta,k}^H(i)E[\hat{\mathbf{b}}_{\beta}(i)\hat{\mathbf{b}}_{\beta}^H(i)]\mathbf{f}_{\beta,k}(i) \\
 &\quad - \mathbf{w}_{\beta,k}^H(i)\mathbf{B}\mathbf{f}_{\beta,k}(i) - \mathbf{f}_{\beta,k}^H(i)\mathbf{B}^H\mathbf{w}_{\beta,k}(i)
 \end{aligned} \tag{4.18}$$

where $\hat{\mathbf{b}}_{\beta}(i) = \mathbf{T}_{\beta}^H\hat{\mathbf{b}}(i)$ is the feedback vector of the branch β , \mathbf{T}_{β} is the permutation matrix, which is used to change the order of cancellation, $\mathbf{w}_{\beta,k}(i)$ and $\mathbf{f}_{\beta,k}(i)$ have been described in Section 4.3. The associated covariance matrix is $\mathbf{R} = E[\mathbf{r}(i)\mathbf{r}^H(i)] = \mathbf{P}\mathbf{P}^H + \sigma_b^2\mathbf{I}$, $\sigma_b^2 = E[|b_k(i)|^2]$, and $\mathbf{B} = E[\mathbf{r}(i)\hat{\mathbf{b}}_{\beta}^H(i)]$. Here we define the matrices of effective spreading sequences $\mathbf{P} = [\mathbf{p}_1, \dots, \mathbf{p}_K]$, $\mathbf{p}_k = [\tilde{\mathbf{p}}_{k,1}^T, \dots, \tilde{\mathbf{p}}_{k,J}^T]^T$, and $\tilde{\mathbf{p}}_{k,j} = \mathbf{C}_k\mathbf{h}_{j,k}(i)$ is the $M \times 1$ effective spreading sequence of user k regarding the j -th antenna, $k = 1, \dots, K$, $j = 1, \dots, J$. To minimize the cost function in (4.18), we first take the gradient with respect to the filter $\mathbf{w}_{\beta,k}(i)$ and $\mathbf{f}_{\beta,k}(i)$, which yields:

$$\nabla J_{\mathbf{w}_{\beta,k}^*(i)} = \mathbf{R}\mathbf{w}_{\beta,k}(i) - \mathbf{p}_k - \mathbf{B}\mathbf{f}_{\beta,k}(i) \tag{4.19}$$

$$\nabla J_{\mathbf{f}_{\beta,k}^*(i)} = (E[\hat{\mathbf{b}}_{\beta}(i)\hat{\mathbf{b}}_{\beta}^H(i)])\mathbf{f}_{\beta,k}(i) - \mathbf{B}^H\mathbf{w}_{\beta,k}(i). \tag{4.20}$$

Thus, the solution can be obtained by setting the gradient terms equal to zero

$$\mathbf{w}_{\beta,k}(i) = \mathbf{R}^{-1}(\mathbf{p}_k + \mathbf{B}\mathbf{f}_{\beta,k}(i-1)) \tag{4.21}$$

$$\mathbf{f}_{\beta,k}(i) = (E[\hat{\mathbf{b}}_{\beta}(i)\hat{\mathbf{b}}_{\beta}^H(i)])^{-1}\mathbf{B}^H\mathbf{w}_{\beta,k}(i) \approx \mathbf{B}^H\mathbf{w}_{\beta,k}(i). \tag{4.22}$$

If we assume imperfect feedback, then $E[\hat{\mathbf{b}}_{\beta}(i)\hat{\mathbf{b}}_{\beta}^H(i)] = E[\mathbf{T}_{\beta}^H\hat{\mathbf{b}}(i)\hat{\mathbf{b}}^H(i)\mathbf{T}_{\beta}] \approx \mathbf{I}_K$ for small error rates. The complexity of (4.21) and (4.22) are $O((JM)^3)$ and $O(K^3)$ due to the matrix inversion.

4.6 Analytical Results

In this section, we mathematically study the associated MMSE for the general space-time DF receivers (S-DF and P-DF with antenna arrays) and the proposed space-time MPF-DF scheme with imperfect and perfect feedback.

4.6.1 On the MMSE with Perfect and Imperfect Feedback for Proposed Space-time MPF-DF Detectors

The proposed space-time MPF-DF employs multiple branches in parallel and chooses the best estimate among these parallel branches. Firstly, let us consider the imperfect feedback case. As we discussed in Section 4.5, the feedforward and feedback filters for the branch β of user k are

$$\mathbf{w}_{\beta,k} = \mathbf{R}^{-1}(\mathbf{p}_k + \mathbf{B}\mathbf{f}_{\beta,k}) \quad (4.23)$$

$$\mathbf{f}_{\beta,k} = (E[\hat{\mathbf{b}}_{\beta}\hat{\mathbf{b}}_{\beta}^H])^{-1}\mathbf{B}^H\mathbf{w}_{\beta,k} \approx \mathbf{B}^H\mathbf{w}_{\beta,k} \quad (4.24)$$

Substituting (4.23) and (4.24) into (4.18), we obtain the associated MMSE corresponding to the branch β :

$$\begin{aligned} J_{MMSE,\beta} &\approx \sigma_b^2 - (\mathbf{p}_k + \mathbf{B}\mathbf{f}_{\beta,k})^H\mathbf{R}^{-1}\mathbf{p}_k - \mathbf{p}_k^H\mathbf{R}^{-1}(\mathbf{p}_k + \mathbf{B}\mathbf{f}_{\beta,k}) \\ &\quad + (\mathbf{p}_k + \mathbf{B}\mathbf{f}_{\beta,k})^H\mathbf{R}^{-1}(\mathbf{p}_k + \mathbf{B}\mathbf{f}_{\beta,k}) - (\mathbf{p}_k + \mathbf{B}\mathbf{f}_{\beta,k})^H\mathbf{R}^H\mathbf{B}\mathbf{f}_{\beta,k} \\ &\approx \sigma_b^2 - \mathbf{p}_k^H\mathbf{R}^{-1}\mathbf{p}_k - \mathbf{p}_k^H\mathbf{R}^{-1}\mathbf{B}\mathbf{f}_{\beta,k} \end{aligned} \quad (4.25)$$

where $\beta = 1, 2, \dots, B$, B is the number of branches. Therefore, the MMSE of the proposed MPF-DF for user k is approximately given by:

$$J'_{MMSE} \approx \min_{\{\beta \in 1, \dots, B\}} (\sigma_b^2 - \mathbf{p}_k^H\mathbf{R}^{-1}\mathbf{p}_k - \mathbf{p}_k^H\mathbf{R}^{-1}\mathbf{B}\mathbf{f}_{\beta,k}) \quad (4.26)$$

Regarding the case of perfect feedback, let us divide the users into two sets, similarly to [124]

$$D = \{j : \hat{b}_j \text{ is fed back}\} \quad (4.27)$$

$$U = \{j : j \notin D\} \quad (4.28)$$

where the two sets D and U correspond to detected and undetected users, respectively. Here we define the matrices $\mathbf{P}_D = [\mathbf{p}_1, \dots, \mathbf{p}_D]$ and $\mathbf{P}_U = [\mathbf{p}_1, \dots, \mathbf{p}_U]$, $\mathbf{R}_U = \mathbf{P}_U \mathbf{P}_U^H + \sigma^2 \mathbf{I} = \mathbf{R} - \mathbf{P}_D \mathbf{P}_D^H$, the covariance matrices \mathbf{R}_D and \mathbf{R}_U change with different branches. Let us consider perfect feedback case, that is $\hat{\mathbf{b}}_\beta(i) = \mathbf{b}_\beta(i)$. Note that the DF receivers based on the imperfect feedback depend on the matrix $\mathbf{B} = E[\mathbf{r}(i) \hat{\mathbf{b}}_\beta^H(i)]$, that under perfect feedback equals $\mathbf{P}_{D\beta}$. Following the same approach we have the feedforward and feedback filters as:

$$\mathbf{w}_{\beta,k} = \mathbf{R}_{U\beta}^{-1} \mathbf{p}_k \quad (4.29)$$

$$\mathbf{f}_{\beta,k} = \mathbf{P}_{D\beta}^H \mathbf{w}_{\beta,k} \quad (4.30)$$

substituting (4.29) and (4.30) into (4.18) we obtain the associated MMSE corresponding to the branch β :

$$J_{MMSE,\beta} = \sigma_b^2 - \mathbf{p}_k^H \mathbf{R}_{U\beta}^{-1} \mathbf{p}_k \quad (4.31)$$

where the covariance matrix $\mathbf{R}_{U\beta}$ corresponds to the set of undetected users and changes with different branches. Similarly, we obtain the MMSE for MPF-DF detectors in perfect feedback case:

$$J'_{MMSE} \approx \min_{\{\beta \in 1, \dots, B\}} (\sigma_b^2 - \mathbf{p}_k^H \mathbf{R}_{U\beta}^{-1} \mathbf{p}_k) \quad (4.32)$$

4.6.2 On the MMSE with Perfect and Imperfect Feedback for S-DF and P-DF with Antenna Arrays

The conventional S-DF detector with antenna arrays can be treated as a special case of the proposed space-time MPF-DF detector (with $B = 1$). We have quite similar equations of feedforward and feedback filters as we discussed before, here we focus on perfect feedback case for simplicity. The MMSE of the multi-antenna S-DF detector is:

$$J_{MMSE} = \sigma_b^2 - \mathbf{p}_k^H \mathbf{R}_U^{-1} \mathbf{p}_k \quad (4.33)$$

where \mathbf{p}_k is a stack of the effective spreading sequence regarding different antennas.

Specifically, for the P-DF detector with antenna arrays, we have,

$$D = \{1, \dots, k-1, k+1, \dots, K\}, U = \{k\} \quad (4.34)$$

since D is a single cell so the MMSE associated with the space-time P-DF can be simplified by substituting $\mathbf{R}_U = \mathbf{p}_k \mathbf{p}_k^H + \sigma^2 \mathbf{I}$ into (4.33), which yields:

$$J_{MMSE} = \sigma_b^2 - \mathbf{p}_k^H (\mathbf{p}_k \mathbf{p}_k^H + \sigma^2 \mathbf{I})^{-1} \mathbf{p}_k \quad (4.35)$$

4.7 Adaptive Estimation Algorithms

In this section we present modified SG and RLS algorithms to estimate the feedforward and feedback filters of the proposed multi-antenna MPF-DF receiver using MMSE criteria. In order to reduce the complexity, we employ a pair of feedforward and feedback adaptive filters for all B branches instead of assigning each branch a pair of feedforward and feedback adaptive filters. Note that multiple filters have been considered in our studies, however, they did not yield better results than the single-filter approach adopted here. We show these results in the simulation section. In the proposed algorithms, for each iteration we select the optimum branch based on all the feedback results, and adapt the filters using the branch of data with lowest metric.

4.7.1 Stochastic Gradient Algorithm

Let us discuss SG algorithms first, and consider the cost function based on the MSE criterion:

$$J_{MSE} = E[|b_k(i) - \mathbf{w}_k^H(i)\mathbf{r}(i) + [\mathbf{T}_\beta \mathbf{f}_k(i)]^H \hat{\mathbf{b}}(i)|^2], \quad (4.36)$$

where \mathbf{T}_β are the permutation matrices which are employed to change the cancellation order of the users. For each iteration, we select the most likely branch before adapting $\mathbf{w}_k(i)$ and $\mathbf{f}_k(i)$.

$$\beta_{opt,k} = \arg \min_{\beta \in \{1, \dots, B\}} e_{\beta,k}(i), \quad (4.37)$$

$$e_{\beta,k}(i) = |b_k(i) - z_{\beta,k}(i)|. \quad (4.38)$$

The best branch $\beta_{opt,k}$ is selected to minimize the Euclidean distance. The final output $\hat{\mathbf{b}}_k^{(f)}(i)$ chooses the best estimate from the B candidates for each symbol interval i . The SG solution to (4.36) can be devised by using instantaneous estimates and taking the gradient terms with respect to $\mathbf{w}_k^*(i)$ and $\mathbf{f}_k^*(i)$ which should adaptively minimize J_{MSE} . Using the selected branch $\beta_{opt,k}$, we obtain the expressions of the gradients as

$$\nabla J_{\mathbf{w}_k^*(i)} = -(b_k^*(i) - \mathbf{r}^H(i)\mathbf{w}_k(i) + \hat{\mathbf{b}}^H(i)\mathbf{T}_{\beta_{opt,k}}\mathbf{f}_k(i))\mathbf{r}(i), \quad (4.39)$$

$$\nabla J_{\mathbf{f}_k^*(i)} = (b_k^*(i) - \mathbf{r}^H(i)\mathbf{w}_k(i) + \hat{\mathbf{b}}^H(i)\mathbf{T}_{\beta_{opt,k}}\mathbf{f}_k(i))\mathbf{T}_{\beta_{opt,k}}^H \hat{\mathbf{b}}(i). \quad (4.40)$$

According to the SG or LMS filter theory in [4] we have the following update equations:

$$\mathbf{w}_k(i+1) = \mathbf{w}_k(i) - \mu_w \nabla J_{\mathbf{w}_k^*(i)}, \quad (4.41)$$

$$\mathbf{f}_k(i+1) = \mathbf{f}_k(i) - \mu_f \nabla J_{\mathbf{f}_k^*(i)}, \quad (4.42)$$

where μ_w and μ_f are the values of step size. Substituting (4.39) and (4.40) into (4.41) and (4.42), respectively, we arrive at the update equations for the estimation of $\mathbf{w}_k(i)$ and $\mathbf{f}_k(i)$ based on the SG algorithms

$$\mathbf{w}_k(i+1) = \mathbf{w}_k(i) + \mu_w \epsilon^*(i) \mathbf{r}(i), \quad (4.43)$$

$$\mathbf{f}_k(i+1) = \mathbf{f}_k(i) - \mu_f \epsilon^*(i) \mathbf{T}_{\beta_{opt,k}}^H \hat{\mathbf{b}}(i), \quad (4.44)$$

where $\epsilon(i) = b_k(i) - (\mathbf{w}_k^H(i) \mathbf{r}(i) - \mathbf{f}_k^H(i) \mathbf{T}_{\beta_{opt,k}}^H \hat{\mathbf{b}}(i))$. The steps of the algorithm are summarized in table 4.1. Thanks to the fact that most elements of the permutation matrices are zeros, our SG algorithm can be implemented with low complexity.

It is worth noting that, for stability and to facilitate tuning of parameters, it is useful to employ normalized step sizes when operating in a changing environment. The normalized version of this algorithm is described by $\mu'_w = \mu_w / (\mathbf{r}^H(i) \mathbf{r}(i))$ and $\mu'_f = \mu_f / (\hat{\mathbf{b}}^H(i) \mathbf{T}_{\beta_{opt,k}} \mathbf{T}_{\beta_{opt,k}}^H \hat{\mathbf{b}}(i))$.

Table 4.1: Proposed adaptive estimation algorithm: SG.

Step 1:	Choose initial values for \mathbf{w}_k and \mathbf{f}_k , and appropriate step sizes μ_w, μ_f .
Step 2:	For $i=0, 1, 2, \dots$
	(1) Compute the feedback vectors $\mathbf{T}_{\beta}^H \hat{\mathbf{b}}(i)$ and the outputs for different branches of the proposed space-time MPF-DF detector.
	(2) Select the most likely branch $\beta_{opt,k} = \arg \min_{\beta \in \{1, \dots, B\}} e_{\beta,k}(i)$.
	(3) Update $\mathbf{w}_k(i+1) = \mathbf{w}_k(i) + \mu_w \epsilon^*(i) \mathbf{r}(i)$.
	(4) Update $\mathbf{f}_k(i+1) = \mathbf{f}_k(i) - \mu_f \epsilon^*(i) \mathbf{T}_{\beta_{opt,k}}^H \hat{\mathbf{b}}(i)$.

4.7.2 Recursive Least Squares Algorithm

Let us consider the RLS algorithm for feedforward and feedback filters. According to the RLS theory in [4], we express the cost function to be minimized as $\xi(i)$, where i is the length of the observable data. Also, it is customary to introduce a forgetting factor λ into the definition of the cost function $\xi(i)$. We thus write

$$\xi(i) = \sum_{n=1}^i \lambda^{i-n} |b_k(n) - \mathbf{w}_k^H(i) \mathbf{r}(n) + [\mathbf{T}_{\beta} \mathbf{f}_k(i)]^H \hat{\mathbf{b}}(n)|^2. \quad (4.45)$$

For each iteration, we select the most likely branch corresponding to the minimum Euclidean distance

$$\beta_{opt,k} = \arg \min_{\beta \in \{1, \dots, B\}} e_{\beta,k}(i) \quad (4.46)$$

$$e_{\beta,k}(i) = |b_k(i) - z_{\beta,k}(i)|. \quad (4.47)$$

The RLS solution to (4.45) can be obtained by taking the gradient of (4.45) with respect to $\mathbf{w}_k^*(i)$. Using the selected branch $\beta_{opt,k}$ yields:

$$\nabla \xi_{\mathbf{w}_k^*(i)} = - \sum_{n=1}^i \lambda_{\mathbf{w}}^{i-n} \mathbf{r}(n) b_k(n) + \sum_{n=1}^i \lambda_{\mathbf{w}}^{i-n} \mathbf{r}(n) \mathbf{r}^H(n) \mathbf{w}_k(i) - \sum_{n=1}^i \lambda_{\mathbf{w}}^{i-n} \mathbf{r}(n) \hat{\mathbf{b}}^H(n) \mathbf{T}_{\beta_{opt,k}} \mathbf{f}_k(i). \quad (4.48)$$

Let us further define

$$\mathbf{a}_k(i) = - \sum_{n=1}^i \lambda_{\mathbf{w}}^{i-n} \mathbf{r}(n) b_k(n), \quad (4.49)$$

$$\mathbf{R}(i) = \sum_{n=1}^i \lambda_{\mathbf{w}}^{i-n} \mathbf{r}(n) \mathbf{r}^H(n) \quad (4.50)$$

$$\mathbf{B}_k(i) = \sum_{n=1}^i \lambda_{\mathbf{w}}^{i-n} \mathbf{r}(n) \hat{\mathbf{b}}^H(n) \mathbf{T}_{\beta_{opt,k}}. \quad (4.51)$$

Then, by setting $\nabla \xi_{\mathbf{w}_k^*(i)} = 0$, we obtain

$$\mathbf{w}_k(i) = \mathbf{R}^{-1}(i) [\mathbf{B}_k(i) \mathbf{f}_k(i) + \mathbf{a}_k(i)]. \quad (4.52)$$

Because $\mathbf{R}(i) = \lambda_{\mathbf{w}} \mathbf{R}(i-1) + \mathbf{r}(i) \mathbf{r}^H(i)$, and based on the matrix inversion lemma in [4], the update equation for $\mathbf{R}^{-1}(i)$ is given by:

$$\mathbf{R}^{-1}(i) = \lambda_{\mathbf{w}}^{-1} \mathbf{R}^{-1}(i-1) - \lambda_{\mathbf{w}}^{-1} \mathbf{q}_1(i) \mathbf{r}^H(i) \mathbf{R}^{-1}(i-1) \quad (4.53)$$

where $\mathbf{q}_1(i) = \frac{\mathbf{u}_1(i)}{\lambda_{\mathbf{w}} + \mathbf{r}^H(i) \mathbf{u}_1(i)}$, and $\mathbf{u}_1(i) = \mathbf{R}^{-1}(i-1) \mathbf{r}(i)$. We also have the following two equations:

$$\mathbf{a}_k(i) = \lambda_{\mathbf{w}} \mathbf{a}_k(i-1) + \mathbf{r}(i) b_k(i) \quad (4.54)$$

$$\mathbf{B}_k(i) = \lambda_{\mathbf{w}} \mathbf{B}_k(i-1) + \mathbf{r}(i) \hat{\mathbf{b}}^H(i) \mathbf{T}_{\beta_{opt,k}}. \quad (4.55)$$

By combining equation (4.52), (4.53), (4.54) and (4.55), we obtain the RLS algorithm to update the feedforward filter $\mathbf{w}_k(i)$.

By following the similar approach to take the gradient of (4.45) with respect to $\mathbf{f}_k^*(i)$ yields:

$$\begin{aligned} \nabla \xi_{\mathbf{f}_k^*(i)} &= \sum_{n=1}^i \lambda_{\mathbf{f}}^{i-n} \mathbf{T}_{\beta_{opt,k}}^H \hat{\mathbf{b}}(n) b_k(n) - \sum_{n=1}^i \lambda_{\mathbf{f}}^{i-n} \mathbf{T}_{\beta_{opt,k}}^H \hat{\mathbf{b}}(n) \mathbf{r}^H(n) \mathbf{w}_k(i) \\ &+ \sum_{n=1}^i \lambda_{\mathbf{f}}^{i-n} \mathbf{T}_{\beta_{opt,k}}^H \hat{\mathbf{b}}(n) \hat{\mathbf{b}}^H(n) \mathbf{T}_{\beta_{opt,k}} \mathbf{f}_k(i). \end{aligned} \quad (4.56)$$

Let us define

$$\mathbf{c}_k(i) = \sum_{n=1}^i \lambda_{\mathbf{f}}^{i-n} \mathbf{T}_{\beta_{opt,k}}^H \hat{\mathbf{b}}(n) b_k(n), \quad (4.57)$$

Table 4.2: Proposed adaptive estimation algorithm: RLS.

-
- Step 1: Choose initial values for \mathbf{a}_k , \mathbf{B}_k , \mathbf{R}_k^{-1} , \mathbf{c}_k , \mathbf{D}_k and \mathbf{S}_k^{-1} , and appropriate forgetting factors λ_w , λ_f .
- Step 2: For $i=0, 1, 2, \dots$
- (1) Compute the feedback vectors $\mathbf{T}_{\beta}^H \hat{\mathbf{b}}(i)$ and the outputs for different branches of the proposed space-time MPF-DF detector.
 - (2) Select the most likely branch $\beta_{opt,k} = \arg \min_{\beta \in \{1, \dots, B\}} e_{\beta,k}(i)$.
 - (3) Update $\mathbf{a}_k(i) = \lambda_w \mathbf{a}_k(i-1) + \mathbf{r}(i)b_k(i)$.
 - (4) Update $\mathbf{B}_k(i) = \lambda_w \mathbf{B}_k(i-1) + \mathbf{r}(i)\hat{\mathbf{b}}^H(i)\mathbf{T}_{\beta_{opt,k}}$.
 - (5) $\mathbf{R}^{-1}(i) = \lambda_w^{-1}\mathbf{R}^{-1}(i-1) - \lambda_w^{-1}\mathbf{q}_1(i)\mathbf{r}^H(i)\mathbf{R}^{-1}(i-1)$.
 - (6) Update $\mathbf{w}_k(i) = \mathbf{R}^{-1}(i)[\mathbf{B}_k(i)\mathbf{f}_k(i) + \mathbf{a}_k(i)]$.
 - (7) Update $\mathbf{c}_k(i) = \lambda_f \mathbf{c}_k(i-1) + \mathbf{T}_{\beta_{opt,k}}^H \hat{\mathbf{b}}(i)b_k(i)$.
 - (8) Update $\mathbf{D}_k(i) = \lambda_f \mathbf{D}_k(i-1) + \mathbf{T}_{\beta_{opt,k}}^H \hat{\mathbf{b}}(i)\mathbf{r}^H(i)$.
 - (9) $\mathbf{S}_k^{-1}(i) = \lambda_f^{-1}(\mathbf{S}_k^{-1}(i-1) - \mathbf{q}_2(i)\hat{\mathbf{b}}^H(i)\mathbf{T}_{\beta_{opt,k}}\mathbf{S}_k^{-1}(i-1))$.
 - (10) Update $\mathbf{f}_k(i) = \mathbf{S}_k^{-1}(i)[\mathbf{D}_k(i)\mathbf{w}_k(i) - \mathbf{c}_k(i)]$.
-

$$\mathbf{D}_k(i) = \sum_{n=1}^i \lambda_f^{i-n} \mathbf{T}_{\beta_{opt,k}}^H \hat{\mathbf{b}}(n) \mathbf{r}^H(n) \quad (4.58)$$

$$\mathbf{S}_k(i) = \sum_{n=1}^i \lambda_f^{i-n} \mathbf{T}_{\beta_{opt,k}}^H \hat{\mathbf{b}}(n) \hat{\mathbf{b}}^H(n) \mathbf{T}_{\beta_{opt,k}} \quad (4.59)$$

By setting $\nabla \xi_{\mathbf{f}_k^*(i)} = 0$, we have

$$\mathbf{f}_k(i) = \mathbf{S}_k^{-1}(i)[\mathbf{D}_k(i)\mathbf{w}_k(i) - \mathbf{c}_k(i)] \quad (4.60)$$

and also the following equations:

$$\mathbf{c}_k(i) = \lambda_f \mathbf{c}_k(i-1) + \mathbf{T}_{\beta_{opt,k}}^H \hat{\mathbf{b}}(i)b_k(i) \quad (4.61)$$

$$\mathbf{D}_k(i) = \lambda_f \mathbf{D}_k(i-1) + \mathbf{T}_{\beta_{opt,k}}^H \hat{\mathbf{b}}(i)\mathbf{r}^H(i). \quad (4.62)$$

Since $\mathbf{S}_k(i) = \lambda_f \mathbf{S}_k(i-1) + \mathbf{T}_{\beta_{opt,k}}^H \hat{\mathbf{b}}(i)\hat{\mathbf{b}}^H(i)\mathbf{T}_{\beta_{opt,k}}$, and by using the matrix inversion lemma [4], we obtain the update equation for $\mathbf{S}_k^{-1}(i)$, given by:

$$\mathbf{S}_k^{-1}(i) = \lambda_f^{-1}\mathbf{S}_k^{-1}(i-1) - \lambda_f^{-1}\mathbf{q}_2(i)\hat{\mathbf{b}}^H(i)\mathbf{T}_{\beta_{opt,k}}\mathbf{S}_k^{-1}(i-1), \quad (4.63)$$

where $\mathbf{q}_2(i) = \frac{\mathbf{u}_2(i)}{\lambda_f + \hat{\mathbf{b}}^H(i)\mathbf{T}_{\beta_{opt,k}}\mathbf{u}_2(i)}$, and $\mathbf{u}_2(i) = \mathbf{S}_k^{-1}(i-1)\mathbf{T}_{\beta_{opt,k}}^H \hat{\mathbf{b}}(i)$. By combining equation (4.60), (4.61), (4.62) and (4.63) we obtain the RLS algorithm for feedback filter $\mathbf{f}_k(i)$.

In order to implement the RLS algorithms, firstly let us set the initial values for \mathbf{a}_k , \mathbf{B}_k , \mathbf{R}^{-1} , \mathbf{c}_k , \mathbf{D}_k , and \mathbf{S}_k^{-1} at $i = 0$, and choose forgetting factors λ_w , λ_f . Secondly,

calculate the feedback vectors $\mathbf{T}_\beta^H \hat{\mathbf{b}}(i)$ and the outputs for all branches regarding user k , and select the most likely branch at iteration i . Thirdly, update the feedforward filter $\mathbf{w}_k(i)$ by following equations (4.54), (4.55), (4.53) and (4.52), and update the feedback filter $\mathbf{f}_k(i)$ by following equations (4.61), (4.62), (4.63) and (4.60). Then, we set $i = i + 1$, and go back to the second step. The final output $\hat{\mathbf{b}}_k^{(f)}(i)$ chooses the best estimate from the B candidates for each symbol interval i . The steps of the algorithm are summarized in Table 4.2.

The superior performance of the RLS algorithm compared to the SG algorithm is attained at the expense of a large increase in computational complexity. The complexity is evaluated by the number of multiplications. The RLS algorithm requires a total of $O((JM)^2) + O(K^2)$ multiplications, which increase as the square of JM and K , where J is the number of antenna elements, M is the gain of effective spreading sequence and K is the number of users. On the other hand, the SG algorithm requires $O(JM) + O(K)$ multiplications, increasing linearly with JM and K . Note, however, that the operations required to compute $\mathbf{R}^{-1}(i)$ are common to all K users and can be used for saving computations.

4.8 Simulation Results

In this section, we evaluate the performance of the novel space-time MPF-DF schemes and compare them to other existing structures. We adopt a simulation approach and conduct several experiments in order to verify the effectiveness of the proposed techniques. We carried out simulations to assess the BER performance of the DF receivers for different loads, channel fading rates, number of antenna elements and signal to noise ratios. The users in the system are assumed to have a power distribution given by log-normal random variables with associated standard deviation 0.5. Our simulation results are based on an uncoded system and the receivers have access to pilot channels for estimating the filters. We calculate the average BER by taking the average performance over the users. All channels have a profile with 3 paths whose powers are $p_0 = 0$ dB, $p_1 = -7$ dB and $p_2 = -10$ dB, which are normalized. The sequence of channel coefficients $h_l(i) = p_l \psi_l(i)$ ($l = 0, 1, 2$), where $\psi_l(i)$, is computed according to Jakes' model. We optimized the parameters of the normalized step size SG algorithms with step sizes $\mu_w = 0.1$, $\mu_f = 0.1$, and of the RLS algorithms with forgetting factors $\lambda_w = 0.998$, $\lambda_f = 0.998$. We consider packets with 1000 symbols. The DOAs are uniformly distributed in $(0, 2\pi)$. It is indicated the receiver structure (linear or DF), the type of DF scheme, and multi-antenna configurations namely:

- S-DF: the successive DF detector of [123], [127].
- P-DF: the parallel DF detector of [124].
- MPF-DF: the proposed multiple-parallel feedback branches DF detector.
- ISS-DF: the iterative system of Woodward et al. [124] with S-DF in the first and second stages.
- IMPFS-DF: the proposed iterative detector with the novel MPF-DF in the first stage and the S-DF in the second stage.
- IMPFMPF-DF: the proposed iterative receiver with the MPF-DF in the first and second stages.
- (D): antenna-array system using diversity configuration.
- (B): antenna-array system using beamforming configuration.

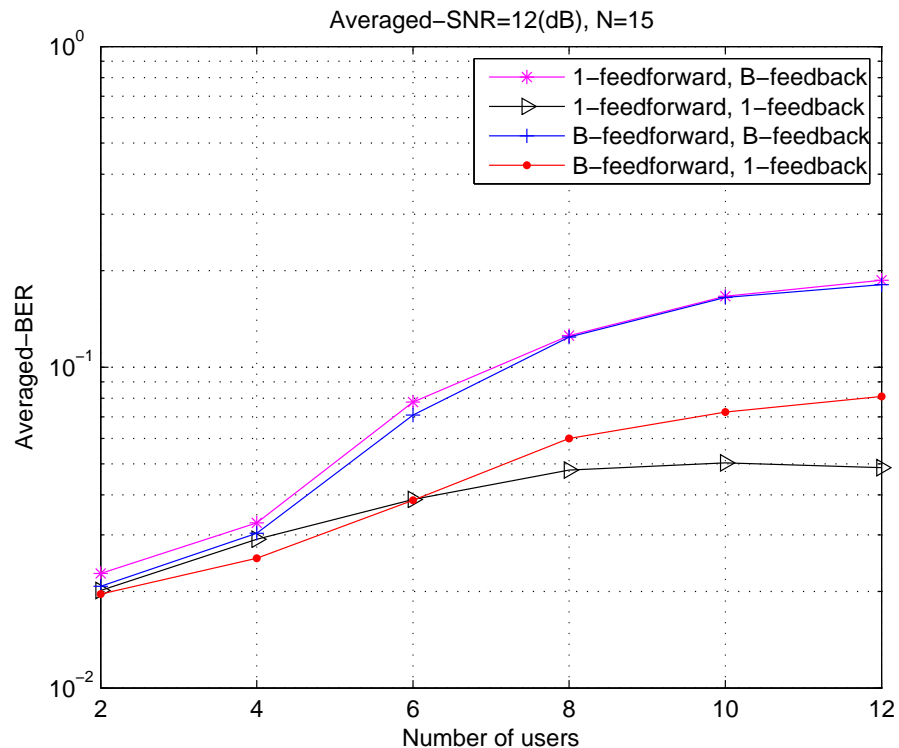


Figure 4.3: Four adaptive schemes for MPF-DF structure

Initially, we study the performance of four different adaptive structures of the proposed MPF-DF, namely, the multiple feedforward multiple feedback, the multiple feedforward

single feedback, the single feedforward multiple feedback, and the single feedforward single feedback structures. Fig 4.3 shows that the performance of the averaged-BER versus number of users over the four different adaptive schemes in the uplink DS-CDMA system with $N = 15$ Gold sequences. We can notice that the single feedforward and single feedback adaptive receiver is the best choice, since it can support more users than the other structures and has the lowest complexity. In our studies, this was verified for a wide range of scenarios.

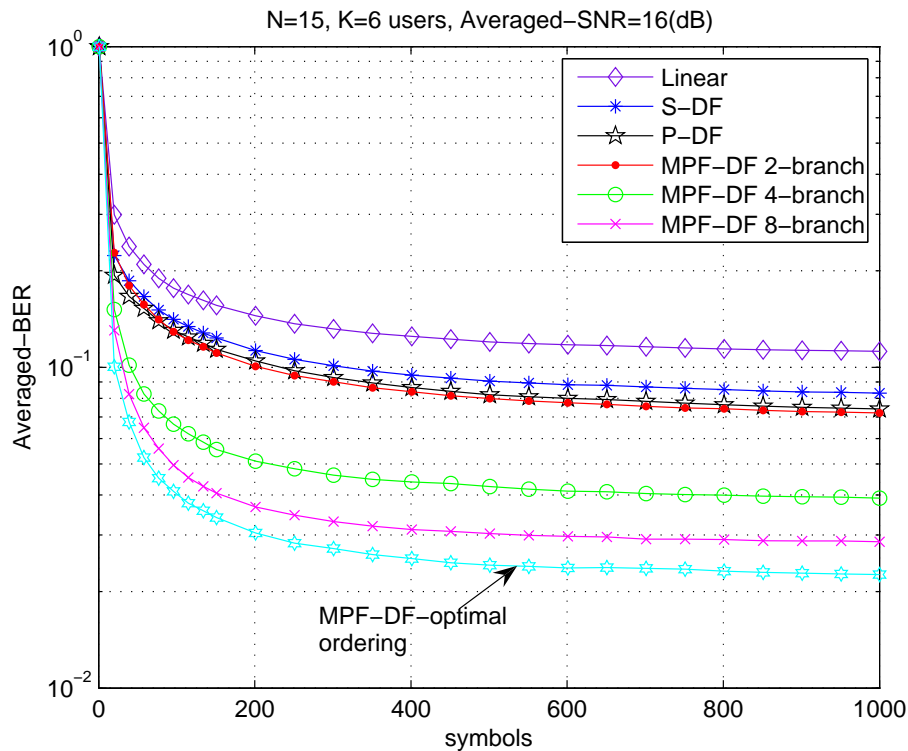


Figure 4.4: BER performance versus number of symbols, normalized SG algorithms, $N = 15$, $K=6$ users, $f_d T = 5 \times 10^{-5}$, 1-antenna configuration.

In the second experiment, we study the impact of the number of branches on the MPF-DF performance. The DS-CDMA system employs Gold sequences with $N = 15$ as the spreading codes. The normalized step size SG algorithms are employed to update feedforward and feedback filters. We designed the novel DF receivers with $B = 2, 4, 8$ parallel branches and compared their BER performance versus number of symbols with the existing S-DF and P-DF structures, as depicted in Fig. 4.4. The results show that the low-complexity ordering algorithm achieves a performance close to the optimal ordering where $B = K!$, whilst keeping the complexity reasonably low for practical utilization. Furthermore, the performance of the new MPF-DF scheme with $B = 2, 4, 8$ outperforms the S-DF and the P-DF detector. It can be noted from the curves that the performance of the new MPF-DF improves as the number of parallel branches increases. In this re-

gard, we also notice that the gains of performance obtained through additional branches decrease as B is increased. Thus, we adopt $B = 4$ for the remaining experiments because it presents a very attractive trade-off between performance and complexity. The fading rate is ($f_d T = 5 \times 10^{-5}$) in this experiment.

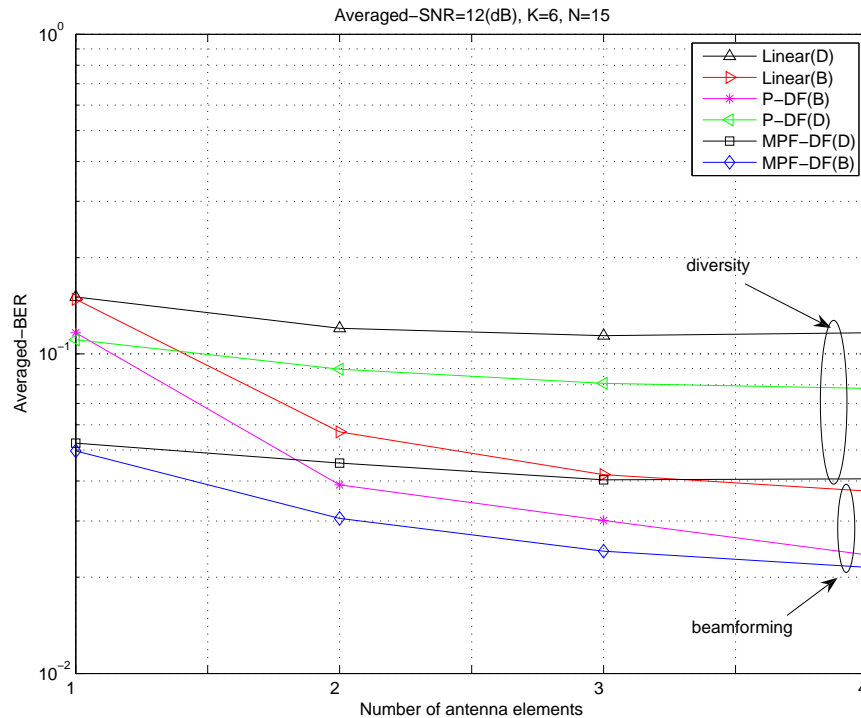


Figure 4.5: BER performance versus number of antennas, normalized SG algorithms, $N = 15$, $K=6$ users, $f_d T = 1 \times 10^{-3}$

We compare the beamforming and diversity configurations in Fig. 4.5 with the considered receiver structures. We can see that the performance of those two multi-antenna configurations improves as we increase the number of antennas, and beamforming outperforms diversity. Note that the gain of performance obtained decreases as the number of antenna elements increases. It is better to use 2-antenna for this array system due to a reasonable trade-off between performance and complexity. This experiment is based on a channel with fading rate $f_d T = 1 \times 10^{-3}$.

In Fig. 4.6, we illustrate the performance of the following algorithms: linear, P-DF, MPF-DF combining diversity and beamforming configurations, respectively, as the fading rate of the channel varies. Firstly, we can see that as the fading rate increases, the performance gets worse and our proposed space-time MPF-DF receivers outperform the existing schemes. Moreover, we observe that beamforming is better than diversity. Secondly, Fig. 4.6 shows the ability of the novel adaptive MPF-DF to deal with error propagation and

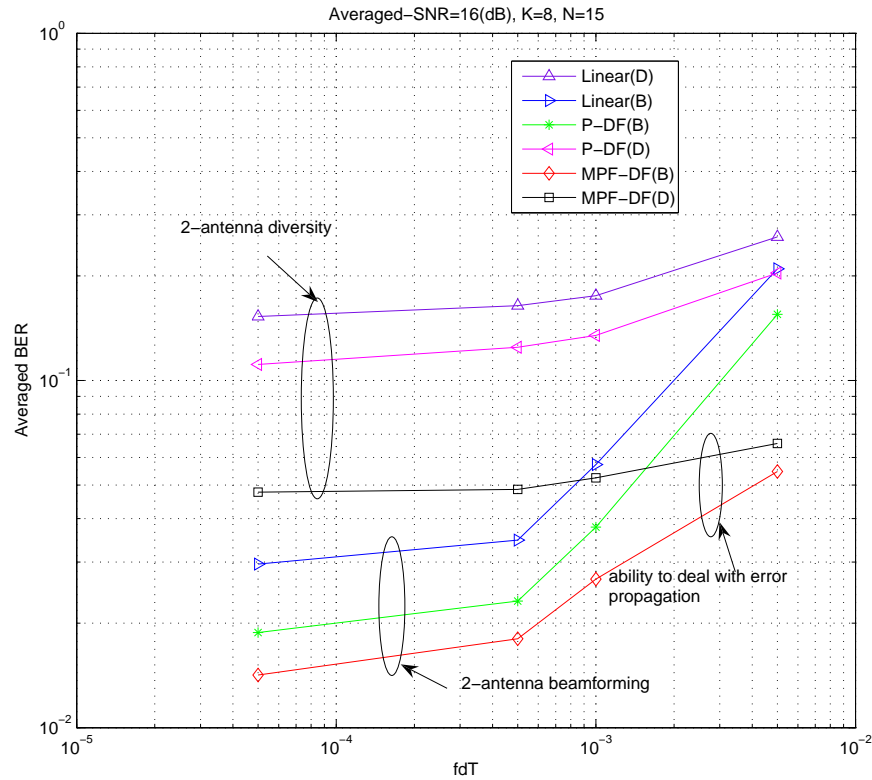


Figure 4.6: BER performance versus channel fading rate, normalized SG algorithms, $N = 15$, $K=8$ users, 2-antenna for both diversity and beamforming configurations.

channel uncertainties. The novel MPF-DF structure using beamforming has the best performance. The experiments of Fig. 4.5 and Fig. 4.6 employ the Gold sequences with $N = 15$ as the spreading codes.

The next scenario, shown in Fig. 4.7, considers the comparison in terms of BER of the proposed DF structures, namely MPF-DF and MPF-DF combining beamforming technique with existing detectors for uncoded systems. Here we use Gold sequences with $N = 15$ as spreading codes, and the normalized SG algorithms are employed to update the feedforward and feedback filters. In particular, we show averaged BER performance curves versus averaged SNR and number of users (K) for the analyzed receivers. The results in Fig. 4.7 indicate that the best performance is achieved with the novel MPF-DF with beamforming technique, followed by the P-DF receiver with beamforming, the linear with beamforming, the MPF-DF, the P-DF, the linear receiver with a single antenna. Specifically, the MPF-DF with beamforming receiver can save up to 2 dB or support up to 3 more users in comparison with the P-DF with beamforming for the same performance. It can substantially increase the system capacity. In this experiment, the channel fading rate $f_d T$ is equal to 5×10^{-5} .

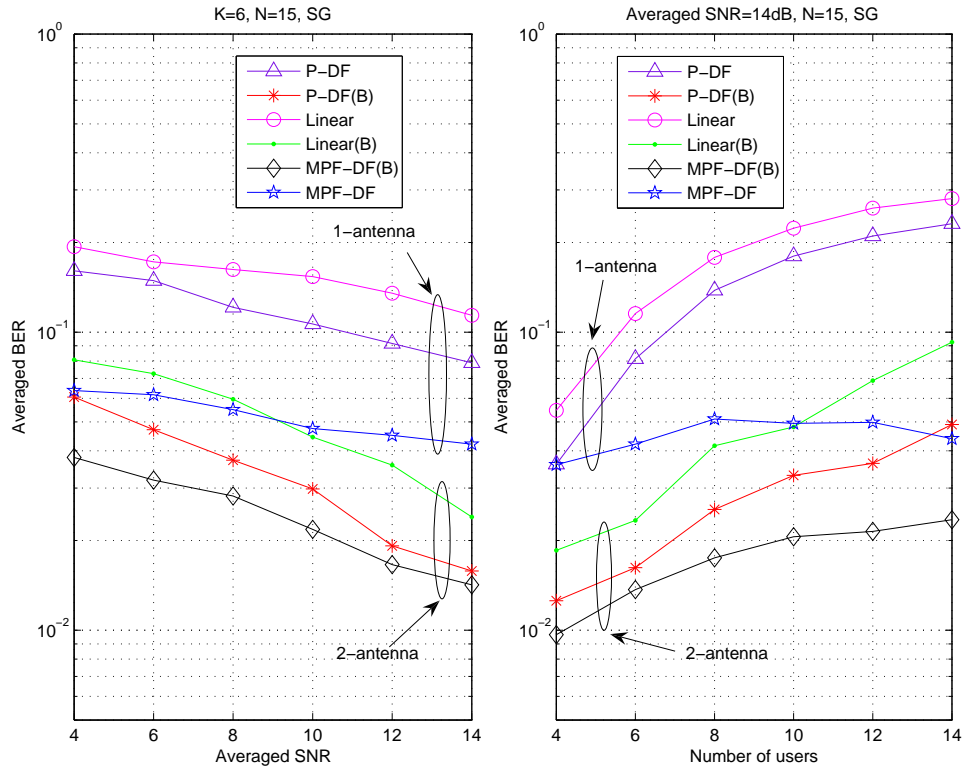


Figure 4.7: BER performance versus (a) Averaged-SNR and (b) number of users (K). Normalized SG algorithms, $N = 15$, $f_d T = 5 \times 10^{-5}$, 2-antenna for beamforming configurations.

The system employs RLS algorithms to estimate the values of feedforward and feedback filters, we use random sequences as the spreading codes. The results for a system with $N = 16$ are illustrated in Fig. 4.8. In particular, the same BER performance hierarchy is observed for the detection schemes, namely MPF-DF, MPF-DF with beamforming, P-DF, P-DF with beamforming, linear receiver, and linear receiver with beamforming. Comparing the curves obtained with the normalized SG algorithms in Fig. 4.7, we notice that the detection schemes with RLS algorithms outperform those with normalized SG algorithms, and also there are some additional gains in performance for the proposed schemes over the existing techniques. Specifically, the MPF-DF detector can save up to 8 dB or support up to 10 additional users in comparison with the P-DF for the same BER performance based on RLS algorithms. Regarding the 2-antenna combined beamforming configurations, the MPF-DF with beamforming scheme can save up to 5 dB or support up to 6 users in comparison with the P-DF with beamforming for the same BER performance based on RLS algorithms. In the experiment the channel fading rate is $f_d T = 5 \times 10^{-5}$.

The last scenario, shown in Fig. 4.9, considers the experiments of our proposed space-

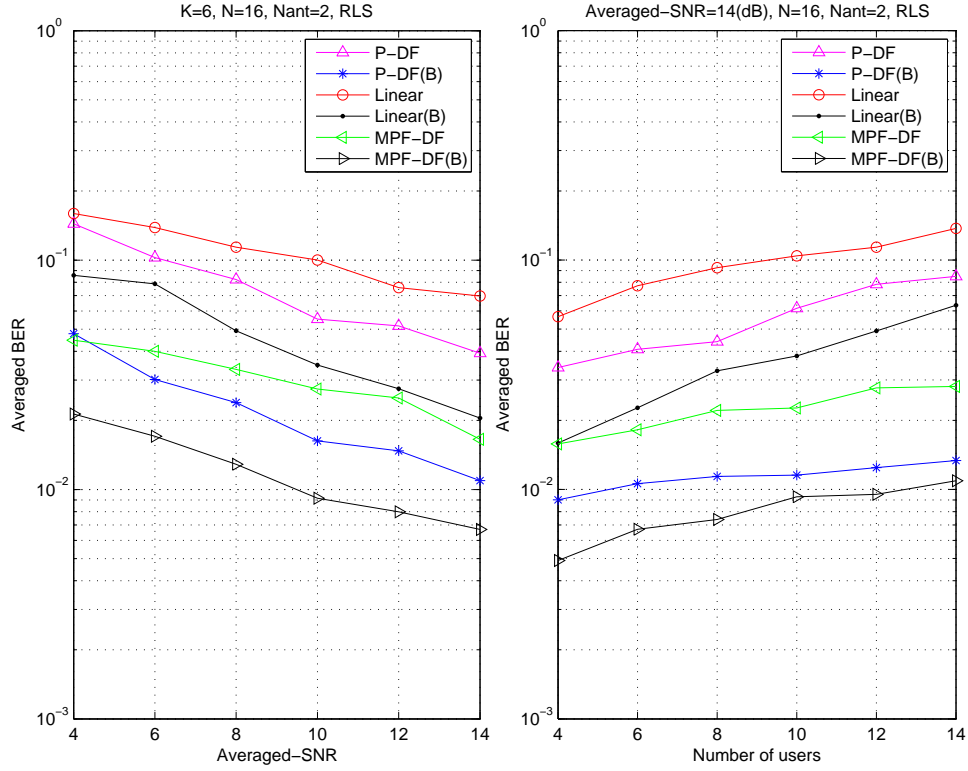


Figure 4.8: BER performance versus (a) Avergaed-SNR and (b) number of users (K). RLS algorithms, $N = 16$, $f_d T = 5 \times 10^{-5}$, 2-antenna ($N_{ant} = 2$) for beamforming configurations.

time MPF-DF receiver structure equipped with 2-antenna diversity and beamforming configurations combined with iterative cascaded DF stages. We compare the performance in terms of BER of the proposed DF structures, namely MPF-DF, IMPFS-DF, IMPFMPF-DF employing diversity and beamforming techniques with existing iterative and conventional DF for uncoded systems. In particular, we show BER performance curves versus averaged SNR and number of users (K) for the analyzed receivers. The systems use $N = 32$ random sequences as the spreading codes, and we employ the RLS algorithms to estimate the values of the feedforward and feedback filters for the 1st and 2nd stage, the channel fading rate is $f_d T = 5 \times 10^{-5}$. The results depicted in Fig. 4.9 indicate that the best performance is achieved by the novel IMPFMPF-DF with beamforming, followed by the new IMPFMPF-DF with diversity, the IMPFS-DF with beamforming, the MPF-DF with beamforming, the IMPFS-DF with diversity, the MPF-DF with diversity, the existing ISS-DF with beamforming, the S-DF with beamforming, the ISS-DF with diversity, and the S-DF with diversity. Specifically, the IMPFMPF-DF detector with beamforming can save up to more than 10 dB or support up to 20 more users in comparison with the existing ISS-DF with beamforming for the same BER performance. The IMPFS-DF with beamforming scheme can save up to 8 dB or support up to 16 more users in comparison

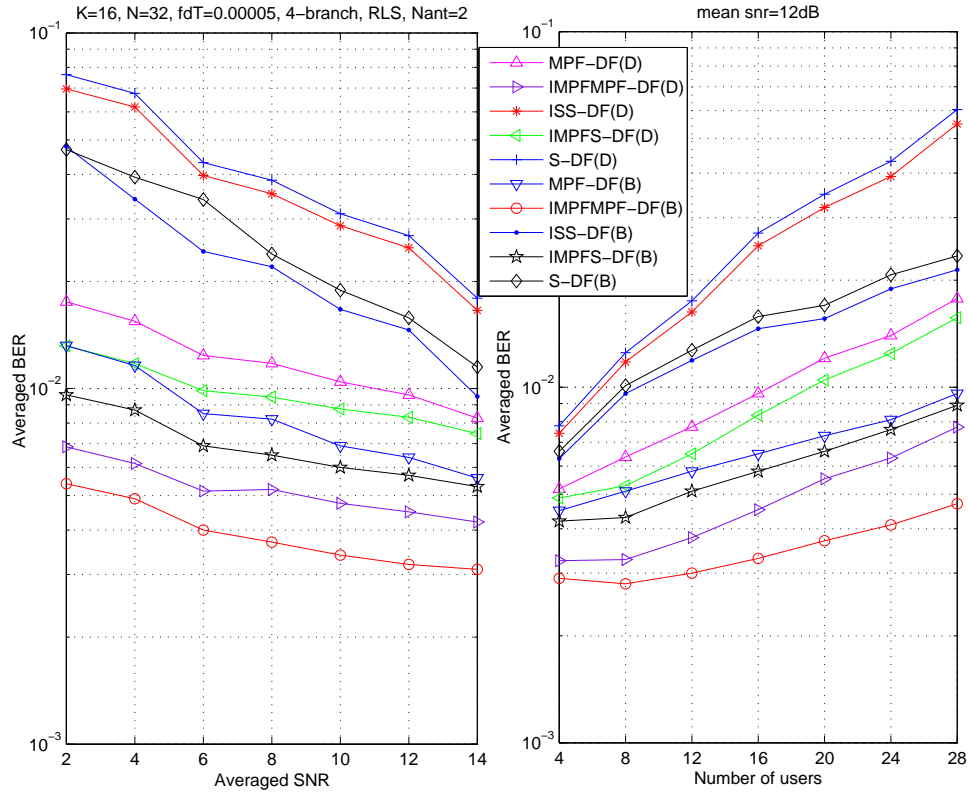


Figure 4.9: BER performance versus (a) Averaged-SNR and (b) number of users (K). RLS algorithms, $N = 32$, $f_d T = 5 \times 10^{-5}$, 2-antenna ($N_{ant} = 2$) for diversity and beamforming configurations.

with the ISS-DF with beamforming scheme for the same BER performance. Moreover, the performance advantages of the IMPFMPF-DF and IMPFS-DF using diversity and beamforming techniques are substantially superior to the other existing approaches.

4.9 Conclusions

In this chapter, we discussed the low-complexity near-optimal ordering algorithms and compared the results of diversity and beamforming configurations for array systems. A novel MPF-DF receiver with diversity and beamforming techniques for DS-CDMA systems and two adaptive algorithms were proposed. The proposed schemes were also combined with the iterative cascaded DF stages. It was shown that the new detection schemes significantly outperform existing DF and linear receivers, support systems with higher loads and mitigate the phenomenon of error propagation.

Chapter 5

Switched Interleaving Techniques for Interference Mitigation in DS-CDMA Systems

Contents

5.1	Introduction	78
5.2	Proposed System Models and MMSE Receivers	80
5.3	System Optimization and Selection of Interleavers	84
5.4	Design of Codebooks and Low-rate Feedback Channels	87
5.5	Simulation Results	91
5.6	Conclusions	100

5.1 Introduction

Channel adaptive techniques [39, 132–135] are expected to be exploited in the next generation of wireless communications systems. These signaling approaches allow the transmitter to adapt to the propagation conditions [57]. This implies that the transmitter requires some form of knowledge of the channel state information at the transmitter. While it is sometimes possible to use the uplink channel estimate for the downlink in TDD systems, a problem arises when it is implemented with frequency division duplexing (FDD) systems, which lack downlink and uplink channel reciprocity. Alternatively, the transmitter can obtain the channel knowledge by allowing the receiver to send a small number

of feedback bits. Then, it can use the feedback information to modify the transmit signal prior to transmission over the channel. Limited feedback approaches have been widely investigated in MIMO systems [19, 20, 58, 59, 67, 136–138]. In particular, the works in [136] and [58] introduced feedback information corresponding to beamforming, and limited feedback precoding was proposed in [67] and [59]. However, prior work [19, 20, 137, 138] has focused on the quantization of the channel information, which may cause problems in time-varying fading and requires a significant amount of bits for satisfactory performance. A number of works on adaptive spreading techniques for DS-CDMA systems have been discussed in [39, 43–45, 76]. An optimization algorithm for single path channels, based on individual updates, has been presented and analyzed in [39, 43, 44]. In [45], joint transmitter-receiver adaptation is studied for the uplink of a system with short signature sequences, two alternating update algorithms are derived for estimating the transmitter coefficients in the presence of multipath. The work in [76] studied the performance of the signature optimization with limited feedback using the RVQ scheme.

In this chapter, we investigate a novel chip-interleaving algorithm based on limited feedback. A set of possible chip-interleavers are constructed and pre-stored at both the transmitter and receiver. During the transmission, the optimum interleaver is chosen by the selection function at the receiver, which then relays the index of the interleaver to the transmitter by a low-rate feedback channel or link. The transmitter will send data by using the interleaver corresponding to the index sent from the receiver in this particular channel situation. It is worth to note that the optimum interleaver may change per transmission block. In order to design the codebook, we consider a number of different chip patterns by using random interleavers, block interleavers [6] and a proposed FSP. The symbol-based and block-based MMSE receivers for the proposed scheme are investigated. The proposed scheme shows substantial performance gains, has much lower requirements for feedback bits than most channel-based feedback schemes, and also has increased robustness against channel variations. The simulations show that our proposed algorithm achieves better performance than the conventional CDMA (C-CDMA) systems and the existing chip-interleaving, linear precoding and adaptive spreading schemes. The main contributions of this chapter are: *I*) Novel limited-feedback techniques combined with chip-interleaving algorithms are introduced for interference suppression in uplink and downlink DS-CDMA systems. *II*) We develop symbol-by-symbol and block linear MMSE receivers for the proposed scheme. *III*) We design the selection functions based on the different MMSE receivers. *IV*) Several chip-interleaving codebook design methods are proposed.

The chapter is structured as follows. Section 5.2 briefly describes the proposed switched interleaving DS-CDMA (SIDS-CDMA) scheme and system model. The proposed MMSE receivers are introduced in Section 5.2.2. Section 5.3 presents the selection

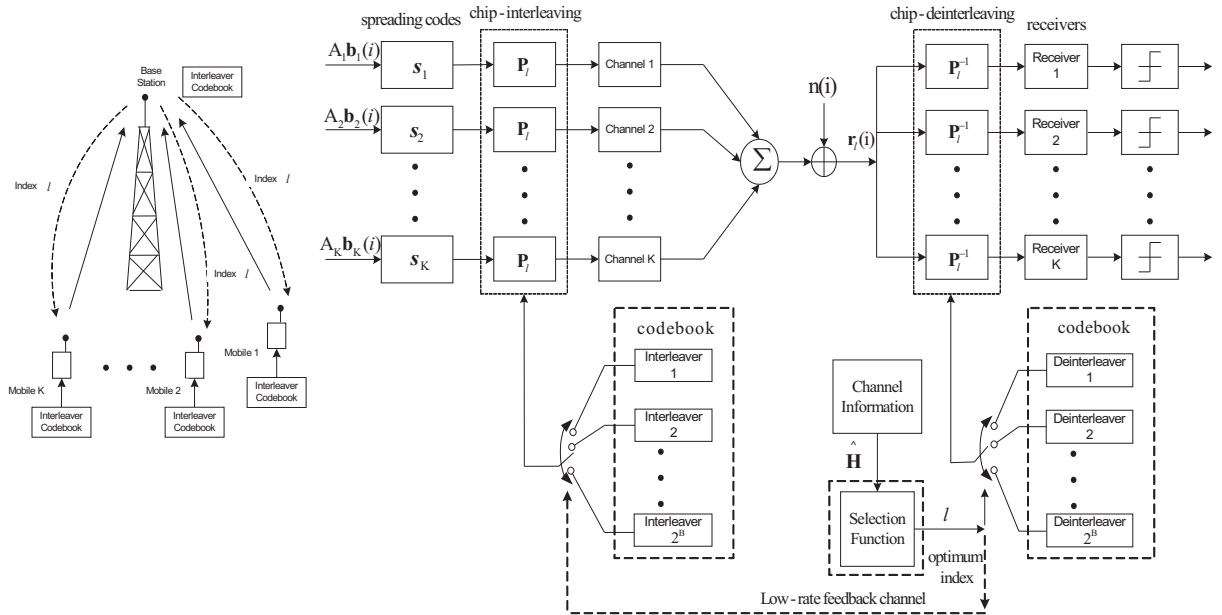


Figure 5.1: Proposed uplink limited feedback-based SIDS-CDMA model and transceiver structure

functions for both downlink and uplink. Techniques to design chip-interleaver codebooks are described in Section 5.4. The simulation results are presented in Section 5.5. Section 5.6 draws the conclusions.

5.2 Proposed System Models and MMSE Receivers

In this section, we focus on the description of the proposed system models and linear MMSE receivers. We first consider an uplink scenario and describe the proposed SIDS-CDMA system model, where the channel coefficients vary per symbol. Then we explain how the uplink scenario can be extended to the case of downlink. Subsequently, we introduce the design of the relevant linear block and symbol-based MMSE receivers.

5.2.1 System Model

The proposed uplink limited feedback-based SIDS-CDMA model and transceiver structure is presented in Fig. 5.1. All the mobile stations and the base station are equipped with the same codebook of chip-interleavers. We assume that the channel varies per symbol duration, and the base station predicts the future uplink channel coefficients with one

block length for each user [139]- [140]. Based on the interleaving index patterns and the predicted channel information, the selection function at the receiver selects an index from the codebook, which corresponds to the optimum interleaver, the index is updated per block. With the aid of a low-rate feedback channel, the base station relays the index to each mobile station. The signal is transmitted after preprocessing by a chip-interleaver which is chosen from the codebook available at the transmitter. The received vector is first processed by a relevant chip-deinterleaver and then handled by linear receivers.

Let us consider the uplink of an uncoded synchronous BPSK DS-CDMA system with K users, N chips per symbol and M symbols per block. We assume that the proposed algorithm is employed in the multipath fading channels with L_p propagation paths, the delays are multiples of the chip duration and the receiver is synchronized with the main path. The channel vector of the β -th symbol in the i -th block for the k -th user is defined as $\mathbf{h}_k^{(\beta)}(i) = [h_0^{(\beta)}(i), \dots, h_{L_p-1}^{(\beta)}(i)]^T$, where $\beta = 1 \dots M$, and $(\cdot)^T$ denotes transpose. The MN -dimensional received vector of the i -th block is given by

$$\mathbf{r}_l(i) = \sum_{k=1}^K A_k \mathbf{P}_l^{-1} \check{\mathbf{H}}_k(i) \mathbf{P}_l \mathbf{S}_k \mathbf{b}_k(i) + \mathbf{n}(i), \quad (5.1)$$

where $\mathbf{b}_k(i) = [b_1^{(k)}(i), b_2^{(k)}(i), \dots, b_M^{(k)}(i)]^T$, denotes the i -th block of symbols for user k , $b_m^{(k)}(i) \in \{\pm 1\}$, $m = 1 \dots M$. The quantity A_k is the amplitude associated with user k . \mathbf{P}_l and \mathbf{P}_l^{-1} denote the l -th $MN \times MN$ interleaving and relevant deinterleaving matrices, respectively, which are designed by the interleaving patterns of the codebook, where $l = 1 \dots 2^B$, B is the number of feedback bits, the number 2^B denotes the length of the interleaving codebook. The function of this interleaving matrix is to permute the orders of these chips per block. The quantity $\mathbf{S}_k = \mathbf{s}_k \otimes \mathbf{I}_M$ is the $MN \times M$ spreading code matrix, where we define $\mathbf{s}_k = [a_{k,1}, \dots, a_{k,N}]^T$ as the $N \times 1$ signature sequence vector for user k , which is repeated from symbol to symbol, and $a_{k,\gamma} \in \{\pm 1/\sqrt{N}\}$, $\gamma = 1 \dots N$. \mathbf{I}_M represents an $M \times M$ identity matrix. The $MN \times MN$ matrix $\check{\mathbf{H}}_k(i)$ is generated by discarding the last $L_p - 1$ rows of the matrix $\mathbf{H}_k(i)$, which represents the $(MN + L_p - 1) \times MN$ Toeplitz channel matrix of the k -th user, with the structure shown

in (5.2),

$$\left(\begin{array}{cccccccc} h_0^{(1)}(i) & & & & & & & \\ \vdots & \cdots & h_0^{(1)}(i) & & & & & \\ h_{L_p-1}^{(1)}(i) & & \vdots & h_0^{(2)}(i) & & & & \\ & \cdots & h_{L_p-1}^{(1)}(i) & \vdots & \cdots & h_0^{(2)}(i) & & \\ & & & h_{L_p-1}^{(2)}(i) & & \vdots & \cdots & \\ & & & & \cdots & h_{L_p-1}^{(2)}(i) & & \cdots \\ & & & & & & \cdots & h_0^{(M)}(i) \\ & & & & & & & \vdots & \cdots & h_0^{(M)}(i) \\ & & & & & & & h_{L_p-1}^{(M)}(i) & & \vdots \\ & & & & & & & & \cdots & h_{L_p-1}^{(M)}(i) \end{array} \right), \quad (5.2)$$

whose columns are shifted by one position versions of the M channel vectors $\mathbf{h}_k^{(\beta)}(i)$ in the i -th block. The vector $\mathbf{n}(i) = [n_1(i), \dots, n_{MN}(i)]^T$ is the complex Gaussian noise vector, $E[\mathbf{n}(i)\mathbf{n}^H(i)] = \sigma^2\mathbf{I}_{MN}$, the quantity σ^2 denotes the noise variance. $(\cdot)^H$ denotes Hermitian transpose. $E[\cdot]$ stands for ensemble average.

We note that the proposed downlink scheme has the same system model, but the channel matrix only corresponds to the desired user since the composite signals broadcasted from the base station to the particular user experience the same propagation conditions. In this case, the base station broadcasts signals by employing the interleaver entry corresponding to the feedback index of the user of interest, and each user is deinterleaved using the same entry in the codebook. The proposed downlink system provides the best performance for the user of interest among the codebook entries. Note that the index selected in the downlink is the optimum index for the desired user. In the following section, the proposed linear MMSE receivers are described.

5.2.2 Proposed MMSE Receivers

In this part, we present the design of the linear receivers of our proposed scheme based on the MMSE criterion [1], which are symbol-based and block-based receivers.

MMSE Symbol-based Receiver

The symbol-based MMSE detector is designed as a parameter vector which operates with a symbol-length received data. Let us recall the proposed system model in (5.1) with the $MN \times 1$ received vector $\mathbf{r}_l(i)$. We assume that the vector $\mathbf{r}_l(i) = [\mathbf{r}'_{l,1}(i), \mathbf{r}'_{l,2}(i), \dots, \mathbf{r}'_{l,M}(i)]^T$, $\mathbf{n}(i) = [\check{\mathbf{n}}_1^T(i), \check{\mathbf{n}}_2^T(i), \dots, \check{\mathbf{n}}_M^T(i)]^T$, where $\mathbf{r}'_{l,j}(i)$ and $\check{\mathbf{n}}_j(i)$ are $N \times 1$ vectors, and define the matrix $\Theta_l^{(k)} = \mathbf{P}_l^{-1} \check{\mathbf{H}}_k(i) \mathbf{P}_l$, which is partitioned into $N \times N$ submatrices as $\mathbf{T}_{j,m}^{(k,l)} = \Theta_l^{(k)}((j-1)N+1 : jN, (m-1)N+1 : mN)$, where $j = 1 \dots M$ and $m = 1 \dots M$, the operation generates a submatrix by taking row $(j-1)N+1$ to row jN and column $(m-1)N+1$ to mN from the matrix $\Theta_l^{(k)}$. Thus, we obtain the j -th received symbol per block of user k

$$\mathbf{r}'_{l,j}(i) = \sum_{k=1}^K \sum_{m=1}^M A_k \bar{\mathbf{s}}_{l,j,m}^{(k)}(i) b_m^{(k)}(i) + \check{\mathbf{n}}_j(i), \quad (5.3)$$

where $N \times 1$ vector $\bar{\mathbf{s}}_{l,j,m}^{(k)}(i) = \mathbf{T}_{j,m}^{(k,l)} \mathbf{s}_k$. The received symbol vector $\mathbf{r}'_{l,j}(i)$ consists of MK different signals corresponding to the different users and symbols per block. Thus, we can design a group of symbol-based receivers $\mathbf{w}_{l,j,m}^{(k)}(i)$ according to the MK different signals, where $k = 1 \dots K$. Let us consider the MSE cost function of the j -th received symbol per block for user k of the branch l :

$$J_{MSE} = E[|A_k b_j^{(k)}(i) - \mathbf{w}_{l,j,m}^{(k)H}(i) \mathbf{r}'_{l,j}(i)|^2], \quad (5.4)$$

We minimize the cost function (5.4) with respect to $\mathbf{w}_{l,j,m}^{(k)*}(i)$ and set the gradient terms equal to zero. After further mathematical manipulations [1], we have the symbol-based MMSE receivers for the j -th received symbol per block of user k

$$\mathbf{w}_{l,j,m}^{(k)}(i) = \left(\sum_{k=1}^K \sum_{m=1}^M A_k^2 \bar{\mathbf{s}}_{l,j,m}^{(k)}(i) \bar{\mathbf{s}}_{l,j,m}^{(k)H}(i) + \sigma^2 \mathbf{I}_N \right)^{-1} A_k^2 \bar{\mathbf{s}}_{l,j,m}^{(k)}(i), \quad (5.5)$$

where $m = 1 \dots M$. Since the desired signal is the j -th symbol within this block, we should choose $m = j$ as the detector of the received data $\mathbf{r}'_{l,j}(i)$.

MMSE Block-based Receiver

The block-based MMSE detector is designed as a matrix to deal with a block-length received data per time. Generally, let us consider an index l ($l = 1 \dots 2^B$) in the interleaver codebook, the cost function for the branch l of user k at the i -th block is given by

$$J_{MSE} = E[||A_k \mathbf{b}_k(i) - \mathbf{W}_{k,l}^H(i) \mathbf{r}_l(i)||^2], \quad (5.6)$$

where the $MN \times M$ matrix $\mathbf{W}_{k,l}(i)$ is the block-based MMSE detector for user k corresponding to the branch l . By minimizing (5.6) with respect to $\mathbf{W}_{k,l}$ we obtain the MMSE block-based receiver

$$\mathbf{W}_{k,l} = \left(\sum_{k=1}^K A_k^2 \hat{\mathbf{S}}_{k,l}(i) \hat{\mathbf{S}}_{k,l}^H(i) + \sigma^2 \mathbf{I}_{MN} \right)^{-1} A_k^2 \hat{\mathbf{S}}_{k,l}(i), \quad (5.7)$$

where $\hat{\mathbf{S}}_{k,l}(i) = \mathbf{P}_l^{-1} \check{\mathbf{H}}_k(i) \mathbf{P}_l \mathbf{S}_k$ denotes the effective spreading matrix after deinterleaving process.

5.3 System Optimization and Selection of Interleavers

In this section, the selection functions of the two proposed MMSE receivers for both downlink and uplink scenarios are introduced. Our proposed selection functions select the best available indices based on the channel coefficients, interleaving patterns and the spreading sequences. Then, the computational complexity of the proposed and conventional schemes is discussed.

5.3.1 Uplink

The system performance that we consider for the proposed uplink scheme is the sum received SINR. In this case, each user's uplink channel information is employed to compute the effective spreading sequence. The function selects the optimum index corresponding to the maximum sum received SINR over all the users in this codebook in order to feed it back to the transmitter.

Selection Rule for MMSE Block-based Receivers

The selection function at the base station contains all the information of chip-interleavers in this codebook, the mobile users' channels and also the MMSE receivers. The selection function uses this information to compute the received SINR of each branch for each user, and selects the optimum index to feed back to the transmitters. The received SINR of the l -th branch for the k -th user is computed as the ratio between the signals energy of user k

per block and the energy of interference plus noise in the same block:

$$\begin{aligned} SINR_l^{(k)} &= \frac{E[Tr(\mathbf{W}_{k,l}^H(i)\hat{\mathbf{S}}_{k,l}A_k^2\mathbf{b}_k(i)\mathbf{b}_k^H(i)\hat{\mathbf{S}}_{k,l}^H\mathbf{W}_{k,l}(i))] }{E[Tr(\mathbf{W}_{k,l}^H(i)\mathbf{F}_l(i)\mathbf{F}_l^H(i)\mathbf{W}_{k,l}(i))] } \\ &= \frac{Tr[\mathbf{W}_{k,l}^H(i)\mathbf{R}_s^{(l)}\mathbf{W}_{k,l}(i)]}{Tr[\mathbf{W}_{k,l}^H(i)\mathbf{R}_I^{(l)}\mathbf{W}_{k,l}(i)]}, \end{aligned} \quad (5.8)$$

where $Tr[\cdot]$ denotes the matrix trace calculation, the interference plus noise component $\mathbf{F}_l(i) = \mathbf{r}_l(i) - \hat{\mathbf{S}}_{k,l}\mathbf{b}_k(i)$, and $MN \times MN$ matrices $\mathbf{R}_s^{(l)} = A_k^2\hat{\mathbf{S}}_{k,l}\hat{\mathbf{S}}_{k,l}^H$, $\mathbf{R}_I^{(l)} = \mathbf{U}_{I,l}\mathbf{U}_{I,l}^H + \sigma^2\mathbf{I}$, $\mathbf{U}_{I,l} = [A_1\hat{\mathbf{S}}_{1,l}, \dots, A_{k-1}\hat{\mathbf{S}}_{k-1,l}, A_{k+1}\hat{\mathbf{S}}_{k+1,l}, \dots, A_K\hat{\mathbf{S}}_{K,l}]$, and $l = 1 \dots 2^B$, $k = 1 \dots K$. The optimum index l_{opt} for the uplink system maximizes the summation of the SINRs which is given by

$$l_{opt} = arg \max_{l=1 \dots 2^B} \left\{ \sum_{k=1}^K SINR_l^{(k)} \right\}, \quad (5.9)$$

the final output $\hat{\mathbf{b}}_k^{(f)}(i)$ is given by

$$\hat{\mathbf{b}}_k^{(f)}(i) = \text{sgn}(\Re(\mathbf{W}_{k,l_{opt}}^H(i)\mathbf{r}_{l_{opt}}(i))), \quad (5.10)$$

where $\hat{\mathbf{b}}_k^{(f)}(i)$ is the $M \times 1$ estimation vector for the i -th block symbols of user k .

Selection Rules for Symbol-based Receivers

When the symbol-based receivers are employed, we assume that the M symbol-based MMSE receivers $\mathbf{w}_{l,j}^{(k)}$ within a block for each user regarding the l -th branch are available for the selection function. Similarly, The received SINR within the i -th block is given by

$$SINR_l^{(k)} = \frac{\sum_{j=1}^M \mathbf{w}_{l,j}^{(k)H}(i)\mathbf{R}_s^{(l,k,j)}\mathbf{w}_{l,j}^{(k)}(i)}{\sum_{j=1}^M \mathbf{w}_{l,j}^{(k)H}(i)\mathbf{R}_I^{(l,k,j)}\mathbf{w}_{l,j}^{(k)}(i)}, \quad (5.11)$$

where the $N \times N$ matrices $\mathbf{R}_s^{(l,k,j)} = A_k^2\bar{\mathbf{s}}_{l,j}^{(k)}\bar{\mathbf{s}}_{l,j}^{(k)H}$, $\mathbf{R}_I^{(l,k,j)} = \mathbf{U}_{I,l,k,j}\mathbf{U}_{I,l,k,j}^H + \sigma^2\mathbf{I}$, $\mathbf{U}_{I,l,k,j} = [A_1\bar{\mathbf{s}}_{l,j,1}^{(1)} \dots A_1\bar{\mathbf{s}}_{l,j,M}^{(1)}, \dots, A_k\bar{\mathbf{s}}_{l,j,1}^{(k)} \dots A_k\bar{\mathbf{s}}_{l,j,j-1}^{(k)} \dots A_k\bar{\mathbf{s}}_{l,j,j+1}^{(k)} \dots A_k\bar{\mathbf{s}}_{l,j,M}^{(k)}, \dots, A_K\bar{\mathbf{s}}_{l,j,1}^{(K)} \dots A_K\bar{\mathbf{s}}_{l,j,M}^{(K)}]$ denote the interference component, namely, exclude the component $A_k\bar{\mathbf{s}}_{l,j}^{(k)}$.

The selection function chooses the optimum index l_{opt} corresponding to the maximum sum received SINR, the expression is equivalent to (5.9). The final output of the j -th symbol of the i -th block of the k -th user $\hat{b}_k^{(f)}(i)$ is given by

$$\hat{b}_k^{(f)}(i) = \text{sgn}(\Re(\mathbf{w}_{l_{opt},j}^{(k)H}(i)\mathbf{r}'_{l_{opt},j}(i))). \quad (5.12)$$

Table 5.1: Computational complexity

Complexity	C-CDMA	SIDS-CDMA	
Receivers (Block)	$O((MN)^3)$	$O((MN)^3)$	
Receivers (Symbol)	$O(MN^3)$	$O(MN^3 + M^2KN^2)$	
		Additions	Multiplications
$\Theta_l^{(k)}$ (Downlink)	–	$2(MN - 1)(MN)^2$	$2(MN)^3$
$\Theta_l^{(k)}$ (Uplink)	–	$2(MN - 1)(MN)^2K$	$2(MN)^3K$
$\hat{\mathbf{S}}_{k,l}$ (Block)	–	$M^2N(N - 1)K$	$(MN)^2K$
$\bar{\mathbf{s}}_{l,j,m}^{(k)}$ (Symbol)	–	$M^2N(N - 1)K$	$(MN)^2K$
SINR expression (Block)	–	$O(M^3NK)$	$O(M^3NK)$
SINR expression (Symbol)	–	$O(M^2NK)$	$O(M^2NK)$

5.3.2 Downlink

For the downlink, the received SINR of the user of interest is considered as the selection function, we make an assumption that the desired user knows the other users' spreading sequences, in order to obtain the theoretical received SINR expressions. Note however that the downlink SINR also can be measured and derived without the knowledge of the other spreading sequences [141] for practical use. The selection function chooses the optimum interleaver corresponding to the maximum received SINR of the desired user. The expressions (5.8) and (5.11) can be employed for the downlink. In this case, the desired user's downlink channel information is employed to compute the effective spreading sequences instead of using all the uplink channels. For the desired user, the selection function contains the information of the interleaving codebook, the desired user's channel and the MMSE receiver.

5.3.3 Computational Complexity

In this part, we focus on the computational complexity of the proposed SIDS-CDMA and conventional CDMA schemes. The complexity of the matrix inversion for the block-based and symbol-based MMSE receivers are $(MN)^3$ and MN^3 respectively for the whole block [1]. In Table 5.1, we show the complexity of the block-based and symbol-based receivers for both conventional CDMA and SIDS-CDMA systems, and the complexity of the quantities for the selection mechanisms of the proposed schemes per interleaving branch. We compute the number of additions and multiplications to compare the complexity of the equivalent channel matrix $\Theta_l^{(k)}$, the effective spreading matrix $\hat{\mathbf{S}}_{k,l}$ of the block-based receiver and the effective spreading vector $\bar{\mathbf{s}}_{l,j,m}^{(k)}$ of the symbol-based

receiver, and the received SINR expressions.

5.3.4 Channel Estimation

In this work, we employ the least squares (LS) channel estimation algorithm [142]. In the LS algorithm, the interested channel estimation must minimize the cost function whose expression at the time instant i is defined based on a weighted average of error squares as

$$\xi(i) = \sum_{k=1}^i \lambda^{i-k} \|\mathbf{r}(k) - \mathbf{V}(k)\hat{\mathbf{h}}(i)\|^2 \quad (5.13)$$

where $\mathbf{r}(k)$ is the $N' \times 1$ received data vector, and $\mathbf{V}(k)$ represents the $N' \times L_p$ observation matrix:

$$\begin{pmatrix} v(k) & v(k-1) & \dots & v(k-L_p+1) \\ v(k+1) & v(k) & \dots & v(k-L_p+2) \\ \dots & \dots & \dots & \dots \\ v(k+N'-1) & v(k+N'-2) & \dots & v(k+N'-L_p) \end{pmatrix}$$

where N' is the observation window length, λ is the forgetting factor, $\hat{\mathbf{h}}(i)$ is the channel estimate in the time instant i , $v(i)$ is the pilot signal.

To minimize the cost function, the gradient of the cost function with regard to channel matrix estimate can be given by

$$\nabla_{\hat{\mathbf{h}}(i)} \xi(i) = \sum_{k=1}^i \lambda^{i-k} \mathbf{V}^H(k) (\mathbf{r}(k) - \mathbf{V}(k)\hat{\mathbf{h}}(i)) = \mathbf{0}_{L_p,1}, \quad (5.14)$$

where $\mathbf{0}_{L_p,1}$ denotes an $L_p \times 1$ zero vector. By solving (5.14), we may obtain the LS estimation of channel matrix as

$$\hat{\mathbf{h}}(i) = \left(\sum_{k=1}^i \lambda^{i-k} \mathbf{V}^H(k) \mathbf{V}(k) \right)^{-1} \left(\sum_{k=1}^i \lambda^{i-k} \mathbf{V}^H(k) \mathbf{r}(k) \right). \quad (5.15)$$

5.4 Design of Codebooks and Low-rate Feedback Channels

In this section, we introduce techniques to design the codebook based on the interleaving algorithms. The optimum interleaving is described first, whose high complexity motivates several suboptimum methods, namely, the random and block interleaving methods, and

the proposed FSP algorithm. Then, low-rate feedback channels are described, we mention that our proposed algorithms also can be applied in block fading channels.

5.4.1 Design of Codebooks

The codebook design schemes like the Lloyd and Grassmannian algorithms have been widely employed in MIMO systems for beamforming and precoding techniques [132] [136]. However, they are not suitable for the interleaver-oriented limited feedback system, because the entries of the codebook are based on the permutation orders of one block chips. In this work, we design a number of interleavers for the codebook by using a random method and the block interleaving method [6]. We also propose a method based on selecting the most frequently used patterns for codebook design.

Optimum Interleaving

In order to obtain the optimum interleaving order we have to test $(MN)!$ possibilities, where $!$ represents the factorial operator, and the number of entries of the optimum codebook is equal to $(MN)!$. For instance, a system with spreading gain $N = 16$ transmits a block data with $M = 10$ symbols and the optimum codebook contains $160!$ entries, which is clearly impractical for any system. Therefore, we need to select a subset of entries from the optimum codebook to build a practical suboptimum codebook with good performance.

Random Interleaving

The general way to interleave the chips is to change the locations of the MN chips within one block randomly, and deinterleave then at the receiver. We create the codebook by generating 2^B random interleaving patterns. In section 5.2 we have introduced the i -th block signal transmitted by each user. Here, let us concentrate on the permutation matrix \mathbf{P}_l structure. The matrix is filled with 0s and 1s, which is related to the locations of the interleaving chips. Assume that the sequence $f_1^{(l)}, f_2^{(l)}, \dots, f_{MN}^{(l)}$ is the l -th interleaving order in the codebook, which is a random permutation of the sequence $1, 2, \dots, MN$. The l -th permutation matrix is generated as follows. Firstly, the matrix \mathbf{P}_l is initialized, we generate an $MN \times MN$ zero matrix for it. Secondly, for the γ -th row of matrix \mathbf{P}_l , the element in the $f_\gamma^{(l)}$ -th location is changed to 1. Thirdly, we move to the $(\gamma + 1)$ -th

row and repeat the same approach until the element in the last row is changed, where $\gamma = 1 \dots MN$. The structure of the permutation matrix \mathbf{P}_l is given by

$$\mathbf{P}_l = [\mathbf{v}_{1,l}^T, \mathbf{v}_{2,l}^T, \dots, \mathbf{v}_{MN,l}^T]^T, \quad (5.16)$$

where $\mathbf{v}_{\gamma,l}$ denotes the $1 \times MN$ vector, $\gamma = 1 \dots MN$,

$$\mathbf{v}_{\gamma,l} = [0, \dots, 0, 1, 0, \dots, 0]. \quad (5.17)$$

$\underbrace{\hspace{10em}}_{j_{\gamma}^{(l)}-1}$

For instance, assume $MN = 6$ and the l -th interleaving order is 5, 2, 4, 3, 6, 1, therefore the permutation matrix is given by

$$\mathbf{P}_l = \begin{pmatrix} 0 & 0 & 0 & 0 & 1 & 0 \\ 0 & 1 & 0 & 0 & 0 & 0 \\ 0 & 0 & 0 & 1 & 0 & 0 \\ 0 & 0 & 1 & 0 & 0 & 0 \\ 0 & 0 & 0 & 0 & 0 & 1 \\ 1 & 0 & 0 & 0 & 0 & 0 \end{pmatrix}. \quad (5.18)$$

Block Interleaving

An alternative way to interleave chips is the block interleaving method [6], which is described by (5.19),

$$\mathbf{\Lambda} = \begin{pmatrix} c_1 & c_{d+1} & c_{2d+1} & \cdots & c_{(t-1)d+1} \\ c_2 & c_{d+2} & c_{2d+2} & \cdots & c_{(t-1)d+2} \\ \vdots & \vdots & \vdots & \vdots & \vdots \\ c_d & c_{2d} & c_{3d} & \cdots & c_{td} \end{pmatrix}, \quad (5.19)$$

assuming that the dimension of the block interleaving matrix $\mathbf{\Lambda}$ is d by t , and $td = MN$, which is the number of chips within one block. A block of chips c_1, c_2, \dots, c_{td} comes into the matrix $\mathbf{\Lambda}$ column-wise, and goes out row-wise. Note that, when $d = 1$, it simply reverts to a conventional DS-CDMA system, when the duration $d = N$, it will become the algorithm in [6]. The deinterleaving algorithm is the reverse process. It corresponds to entering the entries row-wise, while it outputs the deinterleaved entries column-wise. By varying t and d we can obtain different interleaving patterns. In (5.19) the input chips are taken from the sequence $c_1 c_2 \dots c_{td}$, and the interleaved chips are $c_1, \dots, c_{(t-1)d+1}, c_2, \dots, c_{(t-1)d+2}, \dots, c_d, \dots, c_{td}$. In our experiments, for simplicity, we select the integer factors of MN as the candidates of t and d , and shift the input chips, in

order to generate different interleaving patterns for the codebook. For the l -th interleaver, we set $t = t^{(l)}$ and $d = d^{(l)}$, and the permutation matrix \mathbf{P}_l is given by

$$\mathbf{P}_l = \begin{pmatrix} \mathbf{u}_{1,l} \otimes \mathbf{I}_{t^{(l)}} \\ \mathbf{u}_{2,l} \otimes \mathbf{I}_{t^{(l)}} \\ \vdots \\ \mathbf{u}_{d^{(l)},l} \otimes \mathbf{I}_{t^{(l)}} \end{pmatrix}, \quad (5.20)$$

where $\mathbf{I}_{t^{(l)}}$ represents a $t^{(l)} \times t^{(l)}$ identity matrix, and the $1 \times d^{(l)}$ vector $\mathbf{u}_{\gamma,l}$ is given for $\gamma = 1 \dots d^{(l)}$ by

$$\mathbf{u}_{\gamma,l} = [0, \dots, 0, 1, 0, \dots, 0]. \quad (5.21)$$

$\underbrace{\hspace{1.5cm}}_{\gamma-1}$

For instance, assume $MN = 6$, and for the l -th interleaving pattern we set $d = 2$ and $t = 3$, based on (5.19) the l -th interleaving order is given by 1, 3, 5, 2, 4, 6, and vector $\mathbf{u}_{1,l} = [1, 0]$, $\mathbf{u}_{2,l} = [0, 1]$, so the permutation matrix is written as

$$\mathbf{P}_l = \begin{pmatrix} 1 & 0 & 0 & 0 & 0 & 0 \\ 0 & 0 & 1 & 0 & 0 & 0 \\ 0 & 0 & 0 & 0 & 1 & 0 \\ 0 & 1 & 0 & 0 & 0 & 0 \\ 0 & 0 & 0 & 1 & 0 & 0 \\ 0 & 0 & 0 & 0 & 0 & 1 \end{pmatrix}. \quad (5.22)$$

Frequently Selected Patterns Method (FSP)

The basic principle of the proposed FSP algorithm is to build a codebook which contains the interleaving patterns for the most likely selected branches. In order to build the codebook, we need to do thousands of experiments and count the frequency of the indices of the selected patterns. Finally, we create the codebook based on the statistics and choose the 2^B patterns, which are selected most frequently, as the entries of the codebook. The algorithm is summarized in Table 5.2, where \mathbf{d}_{SINR} denotes the vector of SINR for β possible patterns, due to the number of all possible patterns $(MN)!$ is dramatically large, so we generate β interleaving orders randomly, namely choose β patterns from the optimum codebook, where β should be a large integer and practical for the experiment. N_e denotes the total number of experiments, \mathbf{L}_{idx} is defined for the storage of the selected patterns for every experiment and \mathbf{L}_0 is the codebook for the β interleaving patterns generated by $\text{ordering}(\beta)$, which provides the list containing all permutations of the β elements. We highlight that in each run, after we measure the SINR for all patterns, the pattern which brings the maximum SINR is stored in \mathbf{L}_{idx} at step 9. Finally, the FSP codebook \mathbf{L}_{FSP} is

created by selecting the most frequently selected 2^B patterns according to the histogram of L_{idx} . Note that the algorithm is described based on downlink channels. An extension scheme for the uplink is straightforward.

5.4.2 Low-rate Feedback Schemes

For every block prior to payload transmission, there is a preamble transmission for this block channel prediction [139], [143]. The optimum index is chosen by the selection function based on the predicted one block channel information, and fed back to the transmitter before payload transmission. Note that the predicted channel information is only employed by the selection function, more accurate channel information is available for the MMSE receivers. The feedback rate of the optimum index is once per transmission block. In particular, when the channel coefficients can be treated as constants over several blocks, we can follow the same approach to feed back the index, where the constant channel is estimated from the preamble at the receiver. The index will be only updated when the channel changes. Furthermore, error-free transmission of feedback information is not possible if the feedback channel is noisy. In the next section, we will show the performance of the novel feedback schemes based on feedback channels with errors, and the performance of the novel feedback schemes based on both fading varying per symbol channels and block fading channels.

5.5 Simulation Results

In this section, we evaluate the performance of the novel switched interleaving schemes and compare them to other existing chip-interleaving, linear precoding and adaptive spreading algorithms. We adopt a simulation approach and conduct several experiments in order to verify the effectiveness of the proposed techniques. We carried out simulations to assess the bit error rate (BER) performance of the interleaving algorithms for different loads, signal-to-noise ratios (SNR), number of patterns and feedback errors. The users in the system are assumed to have perfect power control. All channels have a profile with 3 paths whose powers are $p_0 = 0$ dB, $p_1 = -7$ dB and $p_2 = -10$ dB, which are normalized, and the spacing between paths is 1 chip. The sequence of channel coefficients $h_l(i) = \sqrt{p_l}\alpha_l(i)$ ($l = 0, 1, 2$), where $\alpha_l(i)$ are zero-mean circularly symmetric complex Gaussian random variables with unit variance. We transmit 3000 blocks per frame, and a transmission block contains 10 symbols. The spreading gain $N = 16$ is used for the sim-

Table 5.2: Frequently Selected Patterns (FSP) Scheme

1:	Initialize the vector \mathbf{d}_{SINR} , matrices \mathbf{L}_{idx} and \mathbf{L}_{FSP} , generate null vector and matrices for them. $\mathbf{d}_{SINR} \leftarrow \mathbf{0}, \mathbf{L}_{idx} \leftarrow \mathbf{0}, \mathbf{L}_{FSP} \leftarrow \mathbf{0}$. Decide the number of experiments N_e and the length of the codebook 2^B .
2:	Choose an appropriate value for β , and give it to L . $L \leftarrow \beta$.
3:	Generate β random interleaving patterns, give the list of the interleavers to the matrix \mathbf{L}_0 . $\mathbf{L}_0 \leftarrow \text{ordering}(\beta)$.
4:	for $n_e = 1$ to N_e do
5:	for $l = 1$ to L do
6:	Generate the l -th permutation matrix corresponding to the l -th entry in the interleaver list \mathbf{L}_0 . $\mathbf{P}_l \leftarrow \mathbf{L}_0(l)$
7:	The SINR of the l -th interleaver entry is computed based on the permutation matrix \mathbf{P}_l , channel matrix \mathbf{H}_k , and spreading sequences \mathbf{s}_k , give it to the l -th element of the vector \mathbf{d}_{SINR} . $\mathbf{d}_{SINR}(l) \leftarrow \text{SINR}[\mathbf{P}_l, \mathbf{H}_k, \mathbf{s}_k]$.
8:	end
9:	Select the interleaver entry corresponding to the maximum SINR from the matrix \mathbf{L}_0 in the n_e -th experiment, give it to the n_e -th row of the matrix \mathbf{L}_{idx} . $\mathbf{L}_{idx}(n_e) \leftarrow \text{MAXIndex}(\mathbf{d}_{SINR})$.
10:	end
11:	Based on the matrix \mathbf{L}_{idx} , a histogram $\text{HIST}(\mathbf{L}_{idx})$ is generated. The codebook \mathbf{L}_{FSP} is created by selecting the most frequently selected 2^B patterns according to $\text{HIST}(\mathbf{L}_{idx})$. $\mathbf{L}_{FSP} = \text{SELECT}(\text{HIST}(\mathbf{L}_{idx}))$.

ulations. Among the different chip-interleaving algorithms and detectors, we consider:

- C-CDMA: the conventional DS-CDMA system with MMSE detector.
- G-CI-block: the general chip-interleaved algorithm of [6] exploiting the MMSE block based receiver.
- Block-CDMA: the general MMSE block-based receiver without chip-interleaving.
- MUI-free: the MUI-free algorithm proposed by Zhou et al. [7].
- MMSE-symbol: the proposed limited feedback SIDS-CDMA symbol-based MMSE receiver.
- MMSE-block: the proposed limited feedback SIDS-CDMA block-based MMSE receiver.
- B -bit: the limited feedback schemes employ B bits, namely 2^B is the codebook size.
- precoder: the constrained transmitter precoding algorithm proposed by Vojcic and Jang. [144]
- Rake: Rake receiver.
- CSI: channel state information.
- individual: the alternating update individual signature optimization algorithm [45].
- collective: the alternating update collective signature optimization algorithm [45].

In the first experiment, we compare the codebooks of the interleavers which are created by the three methods, namely the random interleaving, the block interleaving and the FSP algorithms. In particular, we show BER performance curves versus number of feedback bits. For the FSP algorithm we set the number of simulation $N_e = 10000$ and the number of candidates $\beta = 1000$, and one block of symbols is transmitted per simulation. In the experiment which determines the FSP codebook, all the interleavers generated by the block interleaving method are employed as a part of the 1000 candidates and the rest are random interleavers. The system employs the random sequences as the spreading codes. The channel coefficients vary per symbol, which are generated independently. The perfectly predicted channel information with one block length is provided at the desired

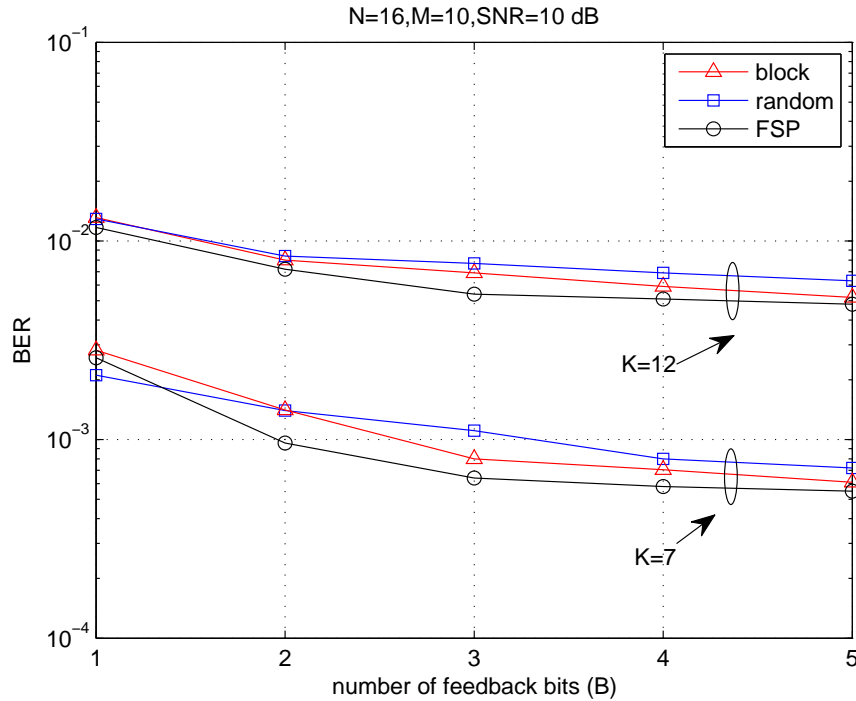


Figure 5.2: BER performance versus number of feedback bits. $N = 16$. Downlink system and independent multipath fading channels. $N_e = 10000$. $\beta = 1000$.

user, and the MMSE block-based receivers are used. The results for a downlink system in the scenario of multipath fading channels are illustrated in Fig. 5.2, we can see that the best performance is achieved with the FSP algorithm, followed by the block interleaving method and the random interleaving method. The BER decreases as the number of feedback bits increases, furthermore, the performance of the low-loaded system changes faster than the performance of the high-loaded system.

The second experiment, shown in Fig. 5.3, considers the comparison in terms of BER of the proposed SIDS-CDMA block-based and symbol-based MMSE receivers with the existing chip-interleaving techniques for uncoded systems in the case of downlink block fading channels. Here we use orthogonal (Walsh) codes as spreading codes, and the codebook is designed by the block interleaving approach. The channel coefficients vary every 10 blocks. For the sake of simplicity, the receivers employ perfect CSI in this experiment. Note that the performance hierarchy does not change with imperfect channel estimates and the performance degradation shifts the BER curves. The channel fading $\alpha_l(i)$ is generated independently between fading blocks. In particular, we show BER performance curves versus SNR and total number of users over processing gain (K/N) for the analyzed receivers. The results in Fig. 5.3 indicate that the best performance is achieved with the novel SIDS-CDMA MMSE block-based receivers with 3 bits feedback (8 interleaving patterns), followed by the novel SIDS-CDMA MMSE symbol-based receivers

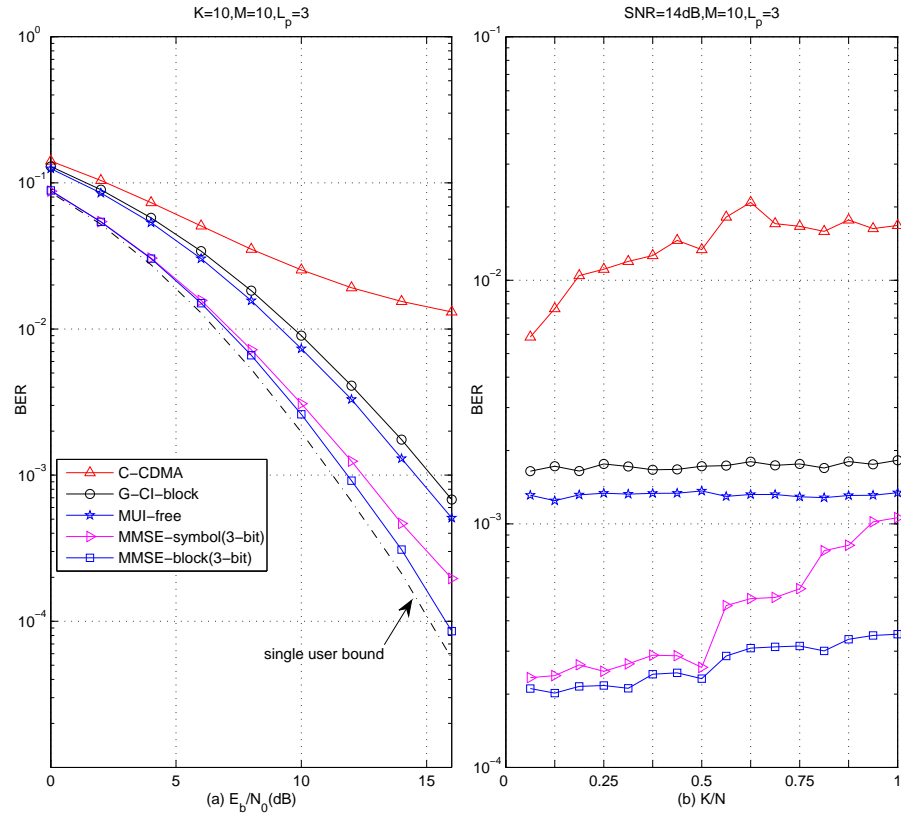


Figure 5.3: BER performance versus (a) SNR and (b) K/N for the proposed SIDS-CDMA schemes, existing chip-interleaving algorithms and the conventional CDMA with MMSE receiver. Downlink block fading channels, Walsh codes and the codebook of block interleavers.

with 3 bits feedback, the MUI-free algorithm proposed by Zhou et al. in [7], the general chip-interleaving algorithm [6] with block-based MMSE receiver, the C-CDMA MMSE receiver. Specifically, the proposed block-based MMSE receiver with 3 bits feedback can save up to almost 4 dB in comparison with the general chip-interleaving algorithm with block-based MMSE receiver, and can save up to over 2 dB in comparison with the MUI-free algorithm, at the BER level of 10⁻³.

In the next scenario, we compare the performance in terms of BER of the proposed SIDS-CDMA symbol-based receivers with Rake receiver and the CDMA precoders [144] employing channel quantization techniques for downlink uncoded systems in the case of block fading channels. The systems also use Walsh codes as the spreading codes, and the channel model is the same as the one in the second experiment. The bit-wise constrained transmitter precoding algorithm proposed by Vojcic and Jang [144] is considered and combined with channel quantization techniques, which works by mapping a complex

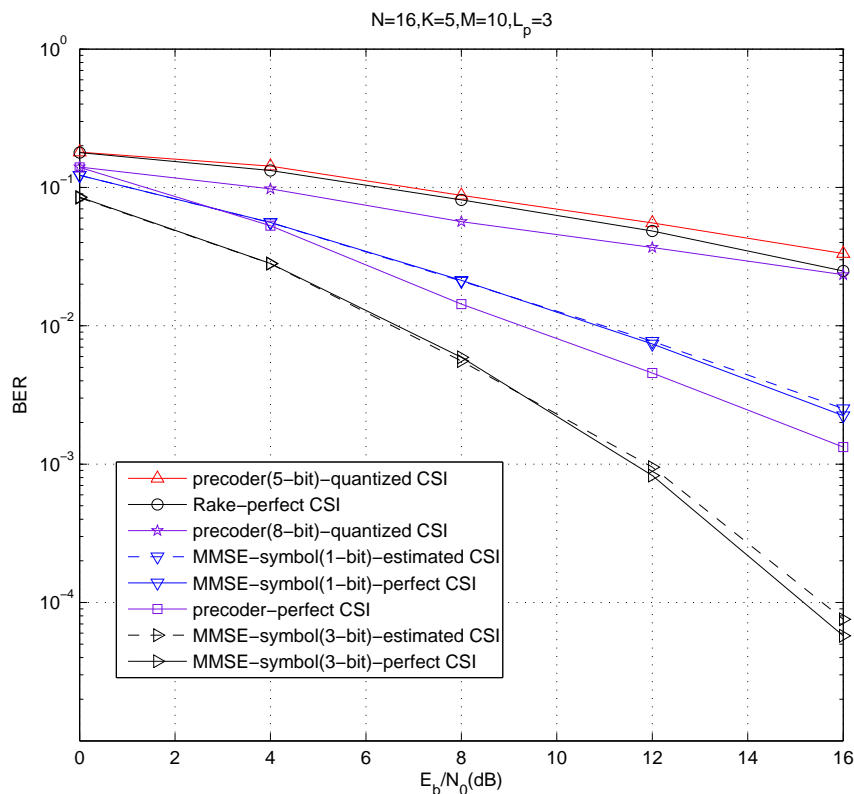


Figure 5.4: BER performance versus SNR for the proposed SIDS-CDMA schemes and the conventional DS-CDMA precoders with channel quantization. Downlink block fading channels. Walsh codes and the codebook of block interleavers.

valued channel vector into one of a finite number of vector realizations. The mapping is designed to minimize the distance between the input vector and the quantized vector. The codebook of the channel quantizer is designed by Grassmannian line packing algorithm [136]. From the curves in Fig. 5.4 we can see the proposed symbol-based receiver based on estimated CSI approaches to a performance of that with perfect CSI, which indicates our proposed scheme works well in a more realistic situation, where the LS channel estimation algorithm is employed at the receiver. The proposed switched interleaving schemes with 3 bits feedback provide the best performance. In particular, the proposed algorithm with 3 feedback bits based on estimated CSI can save up to 4 dB in comparison with the constrained precoder with perfect CSI at the transmitter, near the BER level of 10^{-3} . The channel quantization technique with a relatively small number of feedback bits can not provide a good performance, due to the large quantization error and the lack of reliable CSI at the transmitter. Therefore, a significant amount of feedback bits are needed to get close to the performance of the precoder with perfect CSI [19]. The proposed scheme shows substantial performance gains with much lower requirements for feedback bits than the channel-based feedback schemes.

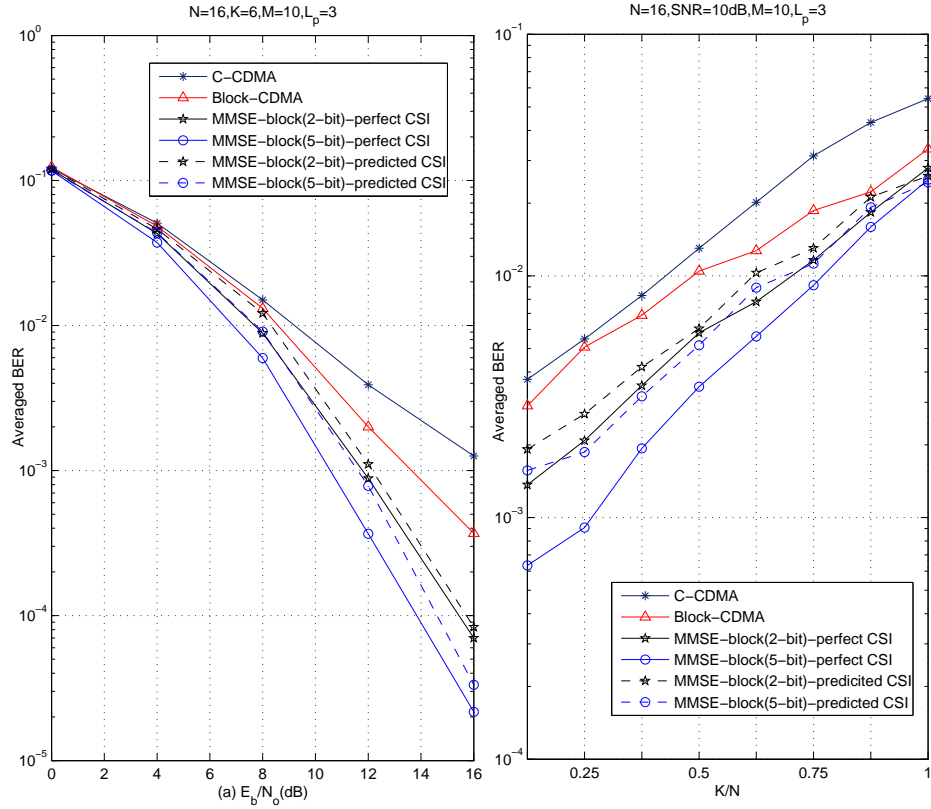


Figure 5.5: Averaged BER performance versus (a) SNR and (b) K/N for the proposed SIDS-CDMA schemes, the block-based MMSE receiver and the conventional DS-CDMA with MMSE receiver. Random spreading sequence and the codebook designed by the FSP algorithm are employed. Uplink multipath fading channels with $f_d T = 0.05$.

The results in Fig. 5.5 show the averaged BER performance of our proposed uplink SIDS-CDMA structure with perfect and predicted CSI versus SNR and K/N . We compare the proposed limited feedback structures with MMSE block-based receivers, the block-based MMSE receivers without feedback and the C-CDMA system with MMSE receivers for uncoded uplink multipath fading systems. The channel prediction algorithm based on autoregressive model is used [139]. Note that the predicted CSI is only used by the selection function to determine the optimum interleaver for one block, more accurate CSI is employed by the receivers for symbol recovery. The systems use random sequences as the spreading codes. The channel coefficients vary per symbol in this experiment, and the channel coefficients $\alpha_l(i)$ are computed according to Jakes' model [145], the channel fading rate is $f_d T = 5 \times 10^{-2}$. As we increase the number of feedback bits the effect of choosing a wrong index as the optimum one becomes larger due to the prediction error, the proposed algorithm using 5 feedback bits with predicted CSI loses 1 dB compared with that with perfect CSI. Specifically, when 16 processing gain is employed, the SIDS-

CDMA using 5 bits with predicted CSI can save up to more than 4 dB, near the BER level of 10^{-3} , or support up to 4 more users, at the BER level of 4×10^{-3} , in comparison with the C-CDMA system with MMSE receiver. Moreover, the performance advantages of the proposed limited feedback SIDS-CDMA techniques are substantially superior to the other existing approaches.

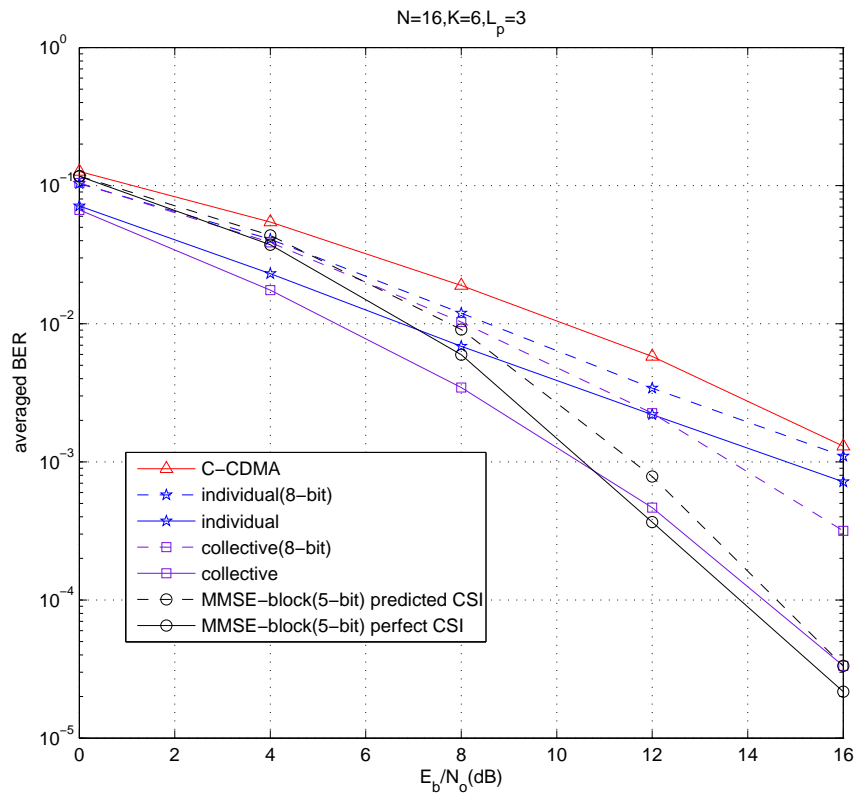


Figure 5.6: Averaged BER performance versus SNR for the proposed SIDS-CDMA schemes and the adaptive spreading schemes.

Fig. 5.6 shows the results of the proposed uplink scheme with the MMSE block based receiver in comparison with the results of the existing adaptive spreading techniques. In particular, we use the alternating update signature optimization algorithms proposed in [45], and combine them with the limited feedback technique. The same uplink channel scenario is used here, and the Lloyed algorithm [132] is employed to generate the codebook of the quantized optimized signatures, which is isotropically distributed in N -dimension hypersphere of unit radius. From Fig. 5.6 we can see that both the individual and collective optimization algorithms are significantly better than the conventional CDMA in the case of 6 users, assuming that the optimized signature vectors are available at the transmitter. However, due to the quantization error the gains lose too much. The proposed uplink scheme with predicted CSI using 5 feedback bits can save up to 4 dB compared with the individual signature optimization algorithm using 8 feedback bits and 2 dB compared with the collective signature optimization algorithm using 8 feedback bits,

at the BER level of 10^{-3} .

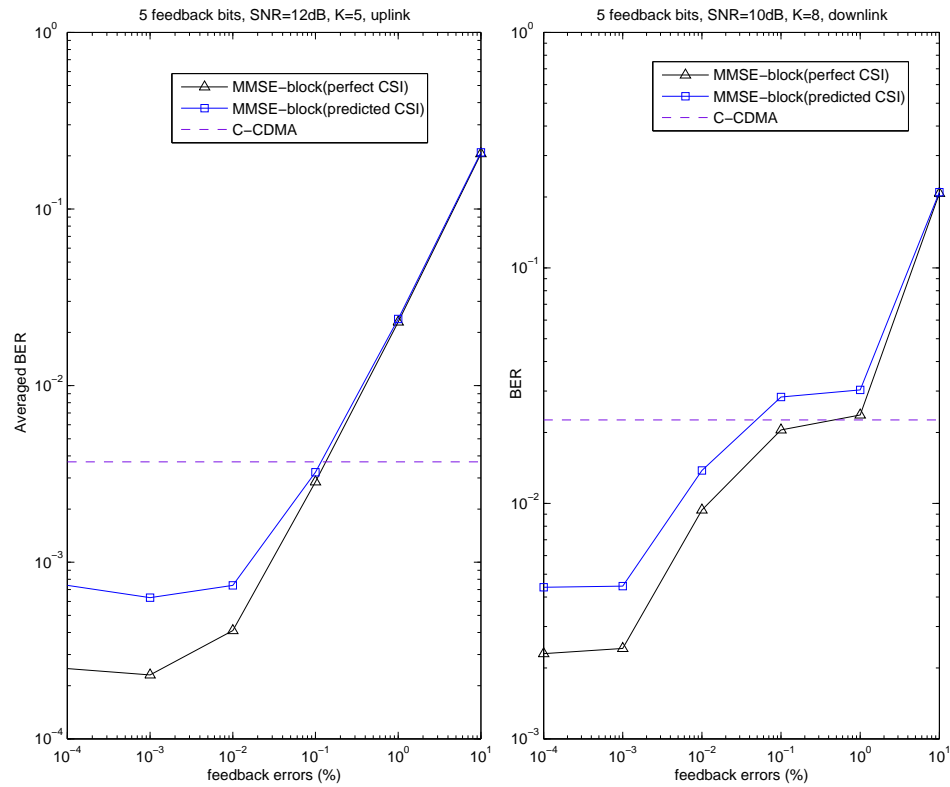


Figure 5.7: BER performance versus the percentage of feedback errors for the proposed uplink and downlink schemes. The block-based MMSE receivers, random spreading sequence and the codebook designed by the FSP algorithm are employed.

The last two results, shown in Fig. 5.7 illustrate the averaged BER performance versus the percentage of each user’s feedback errors for the uplink and the desired user’s BER versus the percentage of the desired user’s feedback errors for the downlink. The percentage is computed within one frame, and the feedback errors are generated randomly. In particular, we consider to use $SNR = 12\text{dB}$ and 5 users for the uplink and $SNR = 10\text{dB}$ and 8 users for the downlink. The same fading varying per symbol channel model is employed here, and we consider to use 5 feedback bits. The random spreading sequences are employed for both the uplink and downlink. As we increase the feedback errors, the performance of the proposed limited feedback schemes decreases, since the interleaver is not in accordance with the deinterleaver due to the feedback errors. The performance of the uplink decreases fast after 0.01%, and compared with the C-CDMA, the proposed scheme with predicted CSI starts to lose around 0.1% and 0.04% for the uplink and downlink, respectively. To ensure the errors are controlled, the coding techniques should be employed for the feedback channels with errors.

5.6 Conclusions

In this chapter, we proposed a novel switched interleaving technique with limited feedback for DS-CDMA system and discussed two kinds of MMSE receivers with selection functions. Three codebooks were designed by using the random interleaving, block interleaving and FSP methods for the block-based and symbol-based receivers. The results showed that the proposed interleaving and detection schemes significantly outperform existing chip-interleaving algorithms and support systems with higher loads. We remark that our proposed algorithms also can be extended to take into account coded systems, MIMO systems, OFDM systems and other types of communications systems.

Chapter 6

Transmit Processing Techniques for Multi-antenna MC-CDMA Systems

Contents

6.1	Introduction	101
6.2	Proposed system models	103
6.3	Design of Precoders and Receivers	106
6.4	Selection of Parameters and Optimization	109
6.5	Design of Low-rate Feedback Frame Structures and Codebooks . .	110
6.6	Simulation Results	115
6.7	Conclusions	121

6.1 Introduction

Future generations of broadband wireless systems are expected to support a wide range of services and bit rates by employing a variety of techniques capable of achieving the highest possible spectrum efficiency [146]. MC-CDMA, which is a combination of OFDM and CDMA, has been attracting much attention [15]. The benefits of MC-CDMA include high spectral efficiency, easy adaptation to severe channel conditions without complex detection, and robustness against ISI and fading caused by multipath propagation [16]. There are several variations of MC-CDMA, such as MC-DS-CDMA proposed by DaSilva and Sousa [17] and multitone CDMA proposed by Vandendorpe [18]. These signals

can be easily transmitted and received using the FFT without increasing the transmitter and receiver complexities, and have the attractive feature of high spectral efficiency due to minimally densely subcarrier spacing [15]. Giannakis et al. proposed the generalized multicarrier (GMC) CDMA system, and afforded an all-digital unifying framework, which encompasses single-carrier (SC) and several MC-CDMA systems [147].

Moreover, transmitter processing techniques implemented at the BS with multiple antennas have received wide attention [148], [149], since they require a simple receiver at the MS. This leaves the BS with the task of precoding the signals in view of suppressing the MUI and adapting to the propagation channels. The essential premise of using transmitter processing techniques is the knowledge of the CSI at the transmitter. In TDD systems, CSI can be obtained at the BS by exploiting reciprocity between the forward and reverse links. In FDD systems, reciprocity is usually not available, but the BS can obtain knowledge of the downlink user channels by allowing the users to send a small number of feedback bits on the uplink. The limited feedback approach has been widely investigated in MIMO systems [20, 82, 135, 137, 150–154]. In particular, the works in [151] and [20] let users quantize some function of downlink CSI and send this information to the BS. When the channel is quantized, the user signals can not be perfectly orthogonalized due to inherent quantization error. The works in [82, 152, 153] provide many improvements. Another limited feedback category for MIMO broadcast channels is a multiuser version of the opportunistic beamforming approach in [135, 150, 154].

In this chapter, we investigate and propose novel transmit processing techniques based on a switched interleaving algorithm for both downlink and uplink MC-CDMA multiple antenna systems. We propose transceiver structures with switched interleaving, linear precoding and detectors for both downlink and uplink. In the novel schemes, a set of chip-interleavers are constructed and prestored at both the BS and MSs. During the transmission, the optimum interleaver is chosen by the selection function at the BS. For the downlink, a new hybrid transmit processing technique based on switched interleaving and chip-wise precoding techniques requiring all users' feedback quantized CSIs is proposed to suppress the MUI, and the relevant linear MMSE receiver is designed for symbol recovery at the MS. It is worth to note that the preprocessing application to uplink transmission is relatively unheeded due to the limitation of MS. We also propose a transmit processing technique for the uplink of multiple antenna MC-CDMA systems requiring very low rate of feedback information. For the uplink, instead of sending the quantized CSI, the BS feeds back the index corresponding to the optimum interleaver to the MSs. The users will send data by using the interleaver corresponding to the index sent from the BS in this particular channel situation. In particular, we will show that the proposed uplink scheme is very efficient and simple to design. The main contributions of this chapter are: *I*)

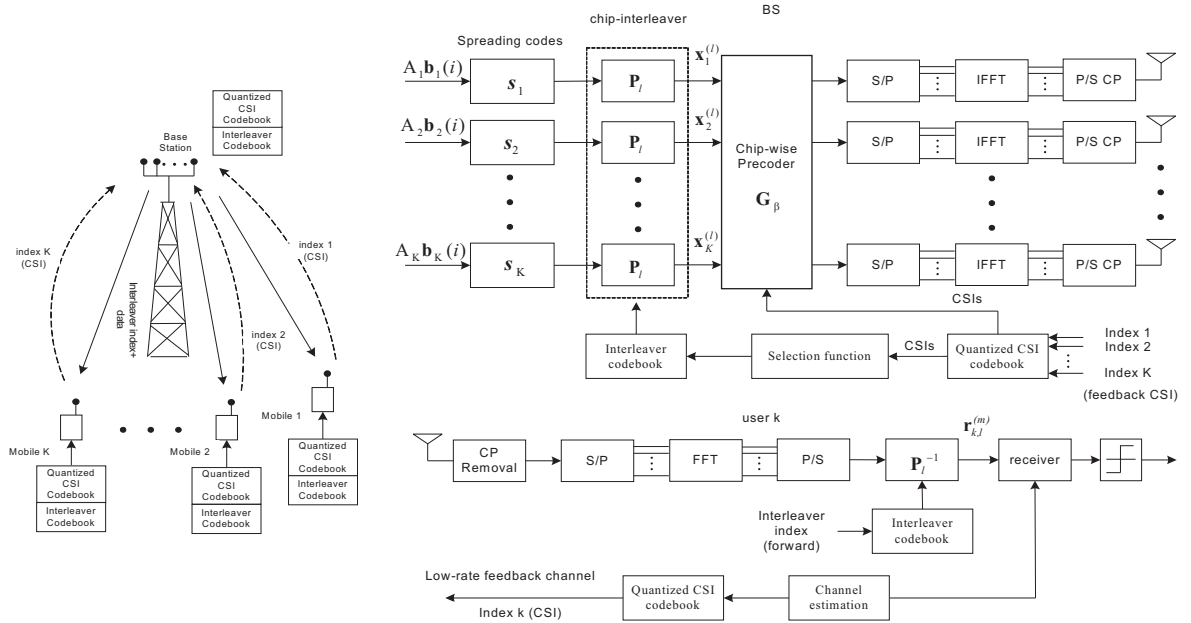


Figure 6.1: Proposed downlink limited feedback-based multiple antenna MC-CDMA model and transceiver structure

The precoding technique is combined with the novel switched interleaving scheme in the downlink. *II*) For the uplink, a preprocessing technique with low rate feedback information is proposed. *III*) We design the selection functions and the MMSE receivers for both downlink and uplink. *IV*) Chip-interleaving codebook design methods are proposed. The simulations show that the performance of the proposed techniques is significantly better than prior art.

This chapter is structured as follows. Section 6.2 briefly describes the proposed multiple antenna switched interleaving based MC-CDMA schemes and system models. The proposed precoders and MMSE receivers are introduced in Section 6.3. Section 6.4 presents the selection functions for both downlink and uplink. Limited feedback timing structures and techniques to design codebooks are described in Section 6.5. The simulation results are presented in Section 6.6. Section 6.7 draws the conclusions.

6.2 Proposed system models

In this section, we will introduce the proposed system models for both downlink and uplink schemes. The system has control channels and feedback channels that can provide the required indices. In practice, most standards have such channels [155–157]. For simplicity, we consider that the BS is equipped with multiple antennas and the MS is

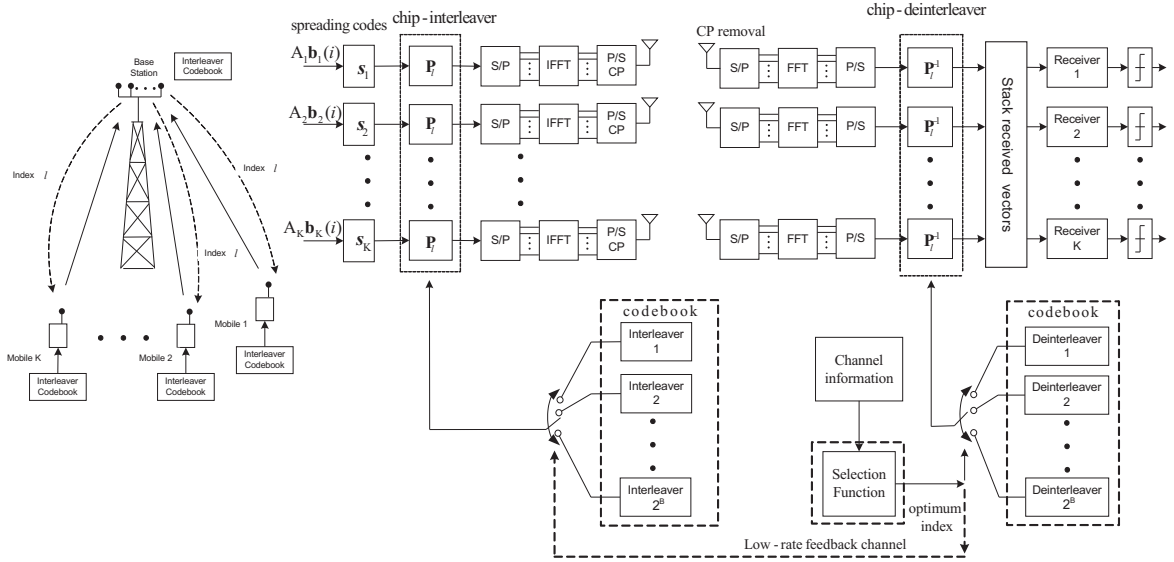


Figure 6.2: Proposed uplink limited feedback-based multiple antenna MC-CDMA model and transceiver structure

equipped with a single antenna. Specifically, for the downlink, the chip-wise precoding technique is combined with the proposed interleaving scheme.

6.2.1 Downlink

The proposed downlink limited feedback based MC-CDMA multi-antenna model is presented in Fig. 6.1 (left hand side), where the solid line represents the transmission link and the dashed line represents the limited feedback link, all the MSs and the BS are equipped with the codebook of quantized CSI and the same codebook of chip-interleavers. Each user selects an index from the codebook of quantized CSI based on the downlink channel estimation and relays it to the BS by a limited feedback channel. The feedback quantized CSIs are employed by the selection function at the BS to calculate and choose the index of the optimum interleaver from the codebook of interleavers. The downlink data is operated by the optimum interleaver, the BS broadcasts the index of the optimum interleaver to all the MSs before data transmission.

The downlink transceiver structure of the proposed scheme is presented in Fig. 6.1 (right hand side), we consider an uncoded synchronous BPSK MC-CDMA system with K users, N chips per symbol and N_t transmit antennas, where the $N \times 1$ vectors $\mathbf{s}_1 \dots \mathbf{s}_K$ denote the spreading codes. We assume that each block contains M symbols, and $\mathbf{b}_k(i) = [b_1^{(k)}(i), \dots, b_M^{(k)}(i)]^T$ denotes the i -th block data for user k , $b_m^{(k)}(i) \in \{\pm 1\}$, $m = 1 \dots M$, $k = 1 \dots K$. Here we dropped the index i for notation simplicity. For each user, the

chip-interleaver permutes one block of chips per time. The permuted chips of user k before the precoding procedure are given by

$$\mathbf{x}_k^{(l)} = A_k \mathbf{P}_l \mathbf{S}_k \mathbf{b}_k, \quad (6.1)$$

where the quantity A_k is the amplitude associated with user k . The matrix \mathbf{P}_l denotes the l -th $MN \times MN$ interleaving matrix designed by the interleaving patterns of the codebook, where $l = 1 \dots 2^B$, B is the number of bits to represent the index of the interleaver, the number 2^B is the length of the interleaver codebook. The quantity $\mathbf{S}_k = \mathbf{s}_k \otimes \mathbf{I}_M$ is the $MN \times M$ spreading code matrix, \mathbf{I}_M represents an $M \times M$ identity matrix. We define the $K \times MN$ matrix $\mathbf{X}^{(l)} = [\mathbf{x}_1^{(l)}, \dots, \mathbf{x}_K^{(l)}]^T$, which consists of a block of permuted chips of all the users, \mathbf{G}_β is the $N_t \times K$ precoding matrix of the β -th chip, and we assume

$$\mathbf{G}_\beta = [\mathbf{g}_1^{(\beta)}, \dots, \mathbf{g}_K^{(\beta)}], \quad (6.2)$$

where $\beta = 1 \dots MN$, and $\mathbf{g}_k^{(\beta)}$ is the $N_t \times 1$ precoding vector for the k -th user. With the aid of the MN -point FFT and IFFT and a cyclic prefix, the multipath fading channel can be divided into MN narrowband channels in frequency domain [158], where we define a $K \times N_t$ matrix \mathbf{D}_β as the equivalent channel matrix of the β -th chip or subcarrier. The $K \times 1$ received vector $\mathbf{c}_{\beta,l}$ consisting of the β -th received chips of all the users before the deinterleaving process denotes

$$\mathbf{c}_{\beta,l} = \mathbf{D}_\beta \mathbf{G}_\beta \mathbf{X}^{(l)}(:, \beta) + \tilde{\mathbf{n}}_\beta, \quad (6.3)$$

where the operation $(:, y)$ is taking the y -th column of a matrix, the $K \times 1$ noise vector $\tilde{\mathbf{n}}_\beta = [\tilde{n}_{1,\beta}, \dots, \tilde{n}_{K,\beta}]^T$, and the $K \times MN$ matrix $\mathbf{C}_l = [\mathbf{c}_{1,l}, \dots, \mathbf{c}_{MN,l}]$ collects the received chips regarding all the subcarriers within one block. The received vector corresponding to the m -th symbol after deinterleaving for the desired user k_0 is given by

$$\mathbf{r}_{k_0,l}^{(m)} = \mathbf{C}_l^r((m-1)N+1 : mN), k_0) = \sum_{k=1}^K A_k \tilde{\mathbf{s}}_{k,k_0,l}^{(m)} b_m^{(k)} + \bar{\mathbf{n}}_m, \quad (6.4)$$

where the matrix $\mathbf{C}_l^r = \mathbf{P}_l^{-1} \mathbf{C}_l^T$, \mathbf{P}_l^{-1} denotes the deinterleaving matrix, define the operation $(x : y)$ as the one that generates a new vector by taking the elements from the x -th to the y -th entries of a vector, and the operation $(x, :)$ is taking the x -th row of a matrix, the $N \times 1$ vector $\tilde{\mathbf{s}}_{k,k_0,l}^{(m)} = \tilde{\mathbf{s}}_{k,k_0,l}((m-1)N+1 : mN)$ denotes the effective spreading code of the k -th user corresponding to the k_0 user's channel for the m -th symbol, $k_0 = 1 \dots K$, and the final $MN \times 1$ effective spreading code of the l -th interleaver

$$\tilde{\mathbf{s}}_{k,k_0,l} = \mathbf{P}_l^{-1} \hat{\mathbf{s}}_{k,k_0,l}, \quad (6.5)$$

where $\hat{\mathbf{s}}_{k,k_0,l}$ denotes the $MN \times 1$ effective spreading code of the k -th user

$$\hat{\mathbf{s}}_{k,k_0,l} = [\mathbf{D}_1(k_0, :) \mathbf{g}_k^{(1)}(\mathbf{p}_{k,l})_1, \dots, \mathbf{D}_{MN}(k_0, :) \mathbf{g}_k^{(MN)}(\mathbf{p}_{k,l})_{MN}]^T, \quad (6.6)$$

where $\mathbf{p}_{k,l} = \mathbf{P}_l \bar{\mathbf{s}}_k$, the operation $(x, :)$ and $(\cdot)_x$ are taking the x -th row of a matrix and the x -th element of a vector, respectively, and the $MN \times 1$ vector $\bar{\mathbf{s}}_k$ is generated by stacking M copies of the k -th user's spreading code vector on top of each other, the vector $\bar{\mathbf{n}}_m$ is the $N \times 1$ deinterleaved noise vector with $E[\bar{\mathbf{n}}_m \bar{\mathbf{n}}_m^H] = \sigma^2 \mathbf{I}_N$. The design of the chip-wise precoder \mathbf{G}_β , the receiver of the desired user and the selection function for the proposed downlink will be introduced in the following section.

6.2.2 Uplink

The proposed uplink scheme and transceiver structure are presented in Fig. 6.2. Similar to the downlink, the BS with N_r receive antennas and each MS are equipped with the same codebook of chip-interleavers, based on the estimated uplink CSI of each user, the BS feeds back an index corresponding to the best available codebook entry to all the MSs, which select the same chip-interleaver corresponding to the feedback index to transmit signals. Spatial processing techniques can be employed at the BS receiver to detect users' symbols [159]. The $MN \times 1$ received vector of the l -th interleaver for the n_r -th receive antenna after deinterleaving is given by

$$\bar{\mathbf{r}}_{n_r,l} = \sum_{k=1}^K \mathbf{P}_l^{-1} \Lambda_{k,n_r} A_k \mathbf{P}_l \mathbf{S}_k \mathbf{b}_k + \mathbf{n}_{n_r}, \quad (6.7)$$

where $n_r = 1 \dots N_r$, the quantity \mathbf{n}_{n_r} is the $MN \times 1$ complex Gaussian noise vector of the n_r -th receive antenna and the matrix Λ_{k,n_r} denotes an $MN \times MN$ diagonal matrix, which is the equivalent frequency domain uplink channel matrix between the k -th user and the n_r -th received antenna,

6.3 Design of Precoders and Receivers

In this section, the design of the chip-wise precoding technique and the relevant MMSE detector are presented for the proposed downlink multi-antenna MC-CDMA system. Then an MMSE receiver based on a spatial-temporal processing technique for the uplink is proposed.

6.3.1 Downlink

In the downlink, the proposed interleaving scheme is combined with the chip-wise precoder in order to separate the chips based on the frequency domain multiple antenna channel. At the receiver, the relevant MMSE detector is designed to recover the symbols.

Chip-wise Precoder

Numerous criteria have been proposed for designing the downlink preprocessing matrix [148], [149]. In this work, the preprocessing matrix \mathbf{G}_β is chosen based on the MMSE criterion. Let us consider the MSE cost function of the β -th received chips of the l -th interleaver for all the users, $\beta = 1 \dots MN$,

$$\xi_{MSE} = E[||\mathbf{c}_{\beta,l} - \mathbf{X}^{(l)}(:, \beta)||^2]. \quad (6.8)$$

Minimizing the cost function (6.8) by substituting (6.3) and taking the gradient with respect to \mathbf{G}_β^* yields

$$\nabla \xi_{\mathbf{G}_\beta^*} = (\mathbf{D}_\beta^H \mathbf{D}_\beta \mathbf{G}_\beta - \mathbf{D}_\beta^H) E[\mathbf{X}^{(l)}(:, \beta) \mathbf{X}^{(l)H}(:, \beta)]. \quad (6.9)$$

Setting (6.9) to zero, finally, we arrive at a zero forcing solution

$$\mathbf{G}_\beta = (\mathbf{D}_\beta^H \mathbf{D}_\beta)^{-1} \mathbf{D}_\beta^H. \quad (6.10)$$

The normalized preprocessing matrix \mathbf{G}'_β has to be used instead of \mathbf{G}_β for the sake of satisfying the constraint

$$E[||\mathbf{G}'_\beta \mathbf{X}^{(l)}(:, \beta)||^2] = E[||\mathbf{X}^{(l)}(:, \beta)||^2] = U. \quad (6.11)$$

We allocate the total BS transmitter power to all the users employing the same normalized coefficient γ for all the users, yielding

$$\mathbf{G}'_\beta = \gamma \mathbf{G}_\beta. \quad (6.12)$$

where $\gamma = \sqrt{\frac{U}{\text{Tr}(\mathbf{G}_\beta \mathbf{G}_\beta^H)}}$.

Linear MMSE Receiver

To minimize the MSE cost function

$$J_{MSE} = E[||A_{k_0} b_m^{(k_0)} - \mathbf{w}_{m,k_0,l}^H \mathbf{r}_{k_0,l}^{(m)}||^2], \quad (6.13)$$

we take the gradient with respect to the filter $\mathbf{w}_{m,k_0,l}^*$ which yields

$$\nabla J_{\mathbf{w}_{m,k_0,l}^*} = E[\mathbf{r}_{k_0,l}^{(m)} \mathbf{r}_{k_0,l}^{(m)H}] \mathbf{w}_{m,k_0,l} - E[\mathbf{r}_{k_0,l}^{(m)} A_{k_0} b_m^{(k_0)}] \quad (6.14)$$

Setting (6.14) to zero, after further mathematical manipulations, we obtain the desired user's MMSE receiver of the l -th interleaver for m -th symbol is given by

$$\mathbf{w}_{m,k_0,l} = \left(\sum_{k=1}^K \tilde{\mathbf{s}}_{k,k_0,l}^{(m)} \tilde{\mathbf{s}}_{k,k_0,l}^{(m)H} + \sigma^2 \mathbf{I}_N \right)^{-1} \tilde{\mathbf{s}}_{k_0,k_0,l}^{(m)}. \quad (6.15)$$

The complexity of the downlink chip-wise precoder and the MMSE receiver is $O(N_t^3)$ and $O(N^3)$, respectively, due to the matrix inversion.

6.3.2 Uplink

In the case of the proposed uplink scheme, due to the multiple antennas at the BS, we propose an MMSE receiver based on the spatial-temporal processing techniques. To reuse the space dimension, we stack the $N \times 1$ deinterleaved vectors $\bar{\mathbf{r}}_{n_r,l}((m-1)N+1 : mN)$ from all the receive antenna elements on top of each other, thus, we obtain an $N_r N \times 1$ vector regarding the m -th symbol,

$$\bar{\mathbf{r}}_{m,l}^s = [\bar{\mathbf{r}}_{1,l}^{(m)T}, \bar{\mathbf{r}}_{2,l}^{(m)T}, \dots, \bar{\mathbf{r}}_{N_r,l}^{(m)T}]^T, \quad (6.16)$$

where the vector $\bar{\mathbf{r}}_{n_r,l}^{(m)} = \bar{\mathbf{r}}_{n_r,l}((m-1)N+1 : mN)$. The final $MN \times 1$ effective spreading code vector of the l -th interleaver for the k -th user regarding the n_r -th receive antenna is given by:

$$\tilde{\mathbf{p}}_{k,n_r,l} = \mathbf{P}_l^{-1} \mathbf{\Lambda}_{k,n_r} \mathbf{p}_{k,l}. \quad (6.17)$$

If we define the vector $\tilde{\mathbf{p}}_{k,n_r,l}^{(m)} = \tilde{\mathbf{p}}_{k,n_r,l}((m-1)N+1 : mN)$, then the stacked received vector regarding the m -th symbol can be written as

$$\bar{\mathbf{r}}_{m,l}^s = \sum_{k=1}^K \tilde{\mathbf{p}}_{m,k,l}^s A_k b_m^{(k)} + \bar{\mathbf{n}}_m^s, \quad (6.18)$$

where the $N_r N \times 1$ vector $\tilde{\mathbf{p}}_{m,k,l}^s = [\tilde{\mathbf{p}}_{k,1,l}^{(m)T}, \dots, \tilde{\mathbf{p}}_{k,N_r,l}^{(m)T}]^T$, and $\bar{\mathbf{n}}_m^s$ is the $N_r N$ stacked noise vector, $E[\bar{\mathbf{n}}_m^s \bar{\mathbf{n}}_m^{sH}] = \sigma^2 \mathbf{I}_{N_r N}$. By following the same approach of the previous subsection we obtain the uplink MMSE receiver expression of the l -th interleaver for the k_0 -th user corresponding to the m -th symbol,

$$\bar{\mathbf{w}}_{m,k_0,l} = \left(\sum_{k=1}^K A_k^2 \tilde{\mathbf{p}}_{m,k,l}^s \tilde{\mathbf{p}}_{m,k,l}^{sH} + \sigma^2 \mathbf{I}_{N_r N} \right)^{-1} A_{k_0}^2 \tilde{\mathbf{p}}_{m,k_0,l}^s. \quad (6.19)$$

The complexity of the uplink MMSE receiver is $O((N_r N)^3)$.

6.4 Selection of Parameters and Optimization

In this section, the selection functions of the proposed MMSE receivers and the precoder for both downlink and uplink scenarios are introduced. Our proposed selection functions select the best available indices based on the channel coefficients, interleaving patterns and the spreading sequences.

6.4.1 Downlink

Using the different interleaving patterns, we generate 2^B groups of effective spreading sequences with different cross-correlation, which cause different levels of MUI. The BS transmitter is equipped with the selection function. With the aid of the feedback quantized CSIs of all the users, the optimum interleaver index is chosen corresponding to the maximum sum received SINR over all the users in this codebook. The received SINR of the l -th branch for the k_0 -th user is given in (6.20), which is computed as the ratio between the signals energy of user k_0 per block and the energy of interference plus noise in the same block,

$$\begin{aligned} \text{SINR}_l^{(k_0)} &= \frac{\sum_{m=1}^M E[\mathbf{w}_{m,k_0,l}^H A_{k_0}^2 \tilde{\mathbf{s}}_{k_0,k_0,l}^{(m)} b_m^{(k_0)} b_m^{*(k_0)} \tilde{\mathbf{s}}_{k_0,k_0,l}^{(m)H} \mathbf{w}_{m,k_0,l}]}{\sum_{m=1}^M E[\mathbf{w}_{m,k_0,l}^H \mathbf{F}_{l,k_0} \mathbf{F}_{l,k_0}^H \mathbf{w}_{m,k_0,l}]} \\ &= \frac{\sum_{m=1}^M [\mathbf{w}_{m,k_0,l}^H \mathbf{R}_{s,k_0}^{(l)} \mathbf{w}_{m,k_0,l}]}{\sum_{m=1}^M [\mathbf{w}_{m,k_0,l}^H \mathbf{R}_{I,k_0}^{(l)} \mathbf{w}_{m,k_0,l}]} \end{aligned} \quad (6.20)$$

where the interference plus noise component $\mathbf{F}_{l,k_0} = \mathbf{r}_{k_0,l}^{(m)} - A_{k_0} \tilde{\mathbf{s}}_{k_0,k_0,l}^{(m)} b_m^{(k_0)}$, and the matrix $\mathbf{R}_{s,k_0}^{(l)} = A_{k_0}^2 \tilde{\mathbf{s}}_{k_0,k_0,l}^{(m)} \tilde{\mathbf{s}}_{k_0,k_0,l}^{(m)H}$, $\mathbf{R}_{I,k_0}^{(l)} = \mathbf{U}_{I,k_0}^{(l)} \mathbf{U}_{I,k_0}^{(l)H} + \sigma^2 \mathbf{I}$, and $\mathbf{U}_{I,k_0}^{(l)} = [A_1 \tilde{\mathbf{s}}_{1,k_0,l}^{(m)}, \dots, A_{k_0-1} \tilde{\mathbf{s}}_{k_0-1,k_0,l}^{(m)}, A_{k_0+1} \tilde{\mathbf{s}}_{k_0+1,k_0,l}^{(m)}, \dots, A_K \tilde{\mathbf{s}}_{K,k_0,l}^{(m)}]$, for $l = 1 \dots 2^B$, $k_0 = 1 \dots K$. The optimum index l_{opt} for the downlink system maximizes the sum received SINR, as given by

$$l_{opt} = \arg \max_{l=1 \dots 2^B} \left\{ \sum_{k_0=1}^K \text{SINR}_l^{(k_0)} \right\}. \quad (6.21)$$

The final output is given by

$$\hat{b}_{k_0}^{(f)} = \text{sgn}(\Re(\mathbf{w}_{m,k_0,l_{opt}}^H \mathbf{r}_{k_0,l_{opt}}^{(m)})), \quad (6.22)$$

where $\hat{b}_{k_0}^{(f)}$ is the m -th estimation symbol within a block for the k_0 -th user.

The MMSE receiver $\mathbf{w}_{m,k_0,l}$ in (6.20) can be replaced by the effective spreading sequence $\tilde{\mathbf{s}}_{k_0,k_0,l}^{(m)}$ to reduce the complexity of the selection function, thus (6.20) turns to

(6.23),

$$\begin{aligned}
 SINR_i^{(k_0)} &= \frac{\sum_{m=1}^M [\tilde{\mathbf{s}}_{k_0, k_0, l}^{(m)H} \mathbf{R}_{s, k_0}^{(l)} \tilde{\mathbf{s}}_{k_0, k_0, l}^{(m)}]}{\sum_{m=1}^M [\tilde{\mathbf{s}}_{k_0, k_0, l}^{(m)H} \mathbf{R}_{I, k_0}^{(l)} \tilde{\mathbf{s}}_{k_0, k_0, l}^{(m)}]} \\
 &= \frac{\sum_{m=1}^M A_{k_0}^2 \|\tilde{\mathbf{s}}_{k_0, k_0, l}^{(m)}\|^4}{\sum_{m=1}^M \sum_{k \neq k_0} A_k^2 |\rho_{k, k_0, l}^{(m)}|^2 + \sigma^2 \sum_{m=1}^M \|\tilde{\mathbf{s}}_{k_0, k_0, l}^{(m)}\|^2},
 \end{aligned} \tag{6.23}$$

where the cross-correlation of the m -th symbol is denoted by $\rho_{k, k_0, l}^{(m)} = \mathbf{s}_{k, k_0, l}^{(m)H} \mathbf{s}_{k_0, k_0, l}^{(m)}$. We know that the $MN \times 1$ effective spreading sequences of the l -th interleaver within a block is $\tilde{\mathbf{s}}_{k, k_0, l} = [\tilde{\mathbf{s}}_{k, k_0, l}^{(1)T}, \dots, \tilde{\mathbf{s}}_{k, k_0, l}^{(M)T}]^T$, where $k = 1 \dots K$, and it is not hard to see that (6.23) can be written as

$$SINR_i^{(k_0)} = \frac{A_{k_0}^2 \|\tilde{\mathbf{s}}_{k_0, k_0, l}\|^4}{\sum_{k \neq k_0} A_k^2 \tilde{\mathbf{s}}_{k_0, k_0, l}^H \tilde{\mathbf{s}}_{k, k_0, l} + \sigma^2 \|\tilde{\mathbf{s}}_{k_0, k_0, l}\|^2}, \tag{6.24}$$

where the value of $\|\tilde{\mathbf{s}}_{k_0, k_0, l}\|^2$ is the same for all the interleavers, thus, in order to improve the received SINR of the k_0 -th user, we try to reduce the value of the quantity $\sum_{k \neq k_0} A_k^2 \tilde{\mathbf{s}}_{k_0, k_0, l}^H \tilde{\mathbf{s}}_{k, k_0, l}$, which corresponds to the cross-correlation building on the l -th interleaver within one block.

6.4.2 Uplink

For the uplink, the selection function is also equipped at the BS, which contains all the information of chip-interleavers in this codebook, the estimated MSSs' uplink channels and also the MMSE receivers. Similar to the downlink case, the received SINR expression for the l -th interleaving pattern of the k -th user has the same form as (6.20), where the vectors $\mathbf{w}_{m, k_0, l}$ and $\tilde{\mathbf{s}}_{k, k_0, l}^{(m)}$ are replaced by the uplink $N_t N \times 1$ MMSE receiver and the stacked effective spreading code $\tilde{\mathbf{p}}_{m, k, l}^s$. The expression of the uplink optimum index is equivalent to (6.21), and the final output for the k_0 -th user of the m -th symbol is given by,

$$\hat{b}_{k_0}^{(f)} = \text{sgn}(\Re(\bar{\mathbf{w}}_{m, k_0, l_{opt}}^H \bar{\mathbf{r}}_{m, l_{opt}}^s)). \tag{6.25}$$

6.5 Design of Low-rate Feedback Frame Structures and Codebooks

In this section, the frame structures of the proposed downlink and uplink low-rate feedback schemes are introduced. Note that three methods for the interleaving codebook

design have been introduced in section 5.4, we employ the same algorithms to obtain the codebook of interleavers in this chapter. Moreover, we concentrate on the algorithm to design the codebook of quantized CSI.

6.5.1 Low-rate Feedback Frame Structures

For both uplink and downlink schemes, preamble transmission and limited feedback are prior to payload transmission within each fading block, the CSI is estimated from the preamble at the receiver. Fig. 6.3 shows the frame structure of the proposed downlink feedback scheme. Each MS quantizes its own CSI and feeds back the index of the quantized CSI to the BS, which selects the optimum interleaver to preprocess the data. Payload transmission starts after the limited feedback, the first B bits which are broadcasted are used to inform each MS the relevant optimum deinterleaver, the rest of the payload is the preprocessed data. In this work, we assume the deinterleaver index is known accurately by the MSs. Since we consider the channel is a block fading channel, namely, the channel coefficients can be treated as constants over one fading block, the feedback rate of the optimum index is once per fading block.

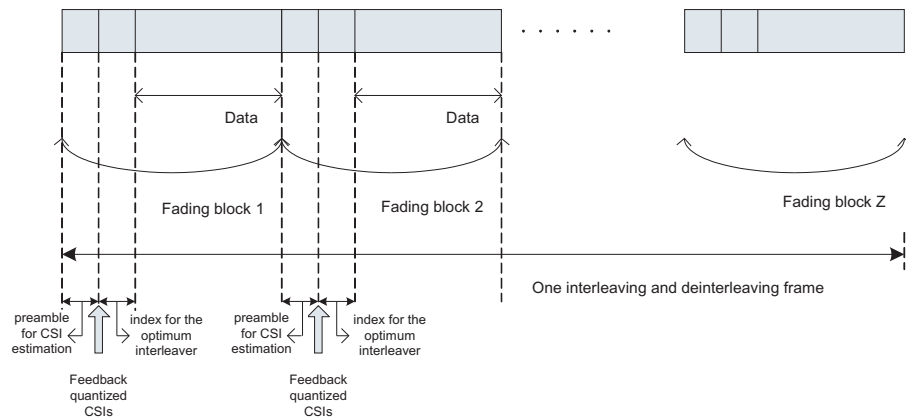


Figure 6.3: The frame structure of the proposed downlink feedback scheme

The proposed uplink scheme has a similar frame structure as the downlink. However, the BS feeds back the index of the optimum interleaver to each MS, thus, the uplink payload contains the preprocessed data only. In this chapter, we assume the CSI is estimated perfectly at the receiver. Furthermore, error-free transmission of feedback information is not possible if the feedback channel is noisy. In the next section, we will show the performance of the novel feedback schemes based on feedback channels with errors.

6.5.2 Design of Codebooks for Channel Direction and Norm Quantization

In order to use a relatively small number of feedback bits, we focus on the time domain CSI, and quantize the channel direction and channel norm separately. Then, we calculate the frequency domain CSI based on the time domain CSI. Note that the frequency domain reduced feedback quantization scheme in [72], [68] can also be employed. In this chapter, we use two methods to quantize the CSI for the multi-antenna multipath fading channel. For each user, one way is that we quantize the vector across the transmit antennas for each channel path, where the number of feedback bits for each user is $(\delta_1 + \delta_2)L_p$. L_p is the number of channel paths and the other way is that we quantize the vector across the channel paths for each transmit antenna. In this case, the number of feedback bits per user is $(\delta_1 + \delta_2)N_t$, where 2^{δ_1} and 2^{δ_2} are the direction codebook vector size and the norm codebook size, and δ_1 and δ_2 are the number of feedback bits for the channel direction part and the channel norm part, respectively. In the following, we introduce the codebook design based on the former, the method is straightforward for the latter.

The quantization of the channel direction information has been introduced by Narula et al.'s work in [132] where the Lloyd algorithm was suggested for the design of the beamforming vector codebook. [136] and [58] showed that the codebook should be constructed by minimizing the maximum inner product between any two beamforming vectors in the codebook. We define the normalized channel vector, namely, the channel direction:

$$\vec{\mathbf{h}} = \frac{\mathbf{h}}{\|\mathbf{h}\|}, \quad (6.26)$$

where \mathbf{h} denotes the $N_t \times 1$ channel vector across the transmit antennas per path, $\|\mathbf{h}\|$ is the channel norm, and $\vec{\mathbf{h}}$ is isotropically distributed in N_t -dimension hypersphere of unit radius. The receiver chooses the best quantized channel direction vector from a common codebook $\mathcal{T} = \{\vec{\mathbf{h}}_1^q, \dots, \vec{\mathbf{h}}_{2^{\delta_1}}^q\}$ in the maximum instantaneous correlation sense:

$$\vec{\mathbf{h}}_{opt}^q = \arg \max_{\vec{\mathbf{h}}_i^q \in \mathcal{T}} |\vec{\mathbf{h}}^H \vec{\mathbf{h}}_i^q|^2, \quad (6.27)$$

where $i = 1 \dots 2^{\delta_1}$.

An appropriate direction codebook is the one which is designed in order to maximize

the minimum distance [136].

$$\mathcal{T}_{opt} = \max_{\mathcal{T} \in \mathcal{C}^{N_t \times 2^{\delta_1}}} \min_{1 \leq i < j \leq 2^{\delta_1}} d(\vec{\mathbf{h}}_i^q, \vec{\mathbf{h}}_j^q), \quad (6.28)$$

where

$$d(\vec{\mathbf{h}}_i^q, \vec{\mathbf{h}}_j^q) = \sqrt{1 - |\vec{\mathbf{h}}_i^{qH} \vec{\mathbf{h}}_j^q|^2}, \quad (6.29)$$

and $\mathcal{C}^{N_t \times 2^{\delta_1}}$ denotes the $N_t \times 2^{\delta_1}$ complex matrix space. The Lloyd algorithm is described in the following:

1. *Step1: Initialization phase*

- Generate a training sequence consisting of source vectors \mathbf{h} with coefficients which are independently and identically distributed (i.i.d.) with a complex Gaussian distribution with zero mean and unit variance.

2. *Step2: Set $t = 1$.*

3. *Step3: nearest neighbor rule*

- All input vectors \mathbf{h} closer to the codeword $\vec{\mathbf{h}}_{i,t-1}^q$ than any other codeword, should be assigned to the neighborhood of $\vec{\mathbf{h}}_{i,t-1}^q$ or region Ω_i .
- $\mathbf{h} \in \Omega_i$ if and only if $d(\mathbf{h}, \vec{\mathbf{h}}_{i,t-1}^q) \leq d(\mathbf{h}, \vec{\mathbf{h}}_{j,t-1}^q), \quad \forall i, j = 1 \dots 2^{\delta_1}$.

4. *Step4: centroid condition*

- Take the i -th region Ω_i for example, whose local correlation matrix $\Sigma_i := E[\mathbf{h}\mathbf{h}^H | \mathbf{h} \in \Omega_i]$. According to the centroid condition, the optimal vector $\vec{\mathbf{h}}_{i,t}^q$ should maximize $\omega_i^H \Sigma_i \omega_i$ subject to the unit norm constraint.

$$\vec{\mathbf{h}}_{i,t}^q = \arg \max_{\omega_i^H \omega_i = 1} \omega_i^H \Sigma_i \omega_i = \mathbf{u}_i, \quad (6.30)$$

where \mathbf{u}_i is the eigenvector corresponding to the largest eigenvalue of Σ_i .

5. *loop back to Step3 until convergence*

To avoid the sum rate degradation we propose to use different direction codebooks for each user, and each user rotates the common codebook by a random unitary matrix in order to generate its own codebook [20]. Concerning the channel norm (scalar information), the algorithm is much simpler and we use a nonuniform scalar quantizer.

6.5.3 Codebook of Interleavers

We propose another method for the interleaving codebook design. The basic principle is to build a codebook which contains the interleaving patterns with the maximum sum SINR (MASS). In order to implement the method, we need to conduct an extensive set of experiments and compute the sum SINRs for the indices of the random candidate patterns. The codebook is generated based on the statistics by choosing 2^B patterns with maximum average sum SINR, as the entries of the codebook. We define an $N_i \times N_e$ matrix \mathbf{V}_{SINR} as the storage of the sum SINRs for N_i possible interleavers over N_e testing channels, where N_i should be a large integer and practical for the experiment, N_e as the total number of experiments, and \mathbf{V}_0 as the list containing all N_i interleaving patterns. The algorithm is summarized in the following.

1. *Step1: Initialization phase*

- Initialize N_e and 2^B , and choose an appropriate value for N_i . Set the vector \mathbf{v}_{idx} , and matrices \mathbf{V}_{SINR} and \mathbf{V}_{MASS} to null.
- Generate N_i random interleaving patterns, give the list of the interleavers to the matrix \mathbf{V}_0 .

2. *Step2: Set $n_e = 1$*

3. *Step3: Set $l = 1$*

4. *Step4: Sum SINR calculation*

- Generate the l -th permutation matrix corresponding to the l -th entry in the interleaver list \mathbf{V}_0 .
- The sum SINR of the l -th interleaver entry is computed based on the permutation matrix \mathbf{P}_l , the n_e -th testing channel matrix, and spreading sequences \mathbf{s}_k , give it to the l -th element of the column vector $\mathbf{V}_{SINR}(:, n_e)$.

5. *Step5: $l \leftarrow l + 1$, loop back to Step4 until $l > N_i$*

6. *Step6: $n_e \leftarrow n_e + 1$, loop back to Step3 until $n_e > N_e$*

7. *Step7: Compute the average sum SINR*

- Based on the matrix \mathbf{V}_{SINR} , by averaging the sum SINRs over the N_e testing channels, an $N_i \times 1$ vector \mathbf{v}_{idx} is generated.

8. *Step8: Generate codebook*

- The final codebook \mathbf{V}_{MASS} is generated by selecting 2^B patterns from \mathbf{V}_0 with maximum average sum SINR according to \mathbf{v}_{idx} .

6.6 Simulation Results

In this section, we evaluate the performance of the proposed linear processing schemes with switched interleaving and compare them to other existing ones. We adopt a simulation approach and conduct several experiments in order to verify the effectiveness of the proposed techniques. We carried out simulations to assess average bit error rate (BER) performance of the interleaving algorithms for different loads, signal-to-noise ratios (SNR), number of antennas and number of interleaving patterns. In this work, our simulation results are based on an uncoded system with perfect channel information at the receiver. The length of the data block is set to $M = 8$ symbols, and 128 subcarriers are used for each block, the random spreading code with a spreading gain $N = 16$ is generated for the simulations, and the length of the CP is enough to eliminate interblock interference. All channels have a profile with 3 taps whose powers are $p_0 = 0$ dB, $p_1 = -7$ dB and $p_2 = -10$ dB, which are normalized, and the spacing between paths is $1/(MN)$ symbol duration. The sequence of channel coefficients $h_l(i) = \sqrt{p_l}\alpha_l(i)$ ($l = 0, 1, 2$), where $\alpha_l(i)$ are zero-mean circularly symmetric complex Gaussian random variables with unit variance. We have studied the proposed schemes with other channel profiles, however, we have opted for this in order to make the results easily reproducible. Among the different schemes and quantization algorithms, we consider:

- C-MC-CDMA: the conventional MC-CDMA system with the MMSE detector.
- P-MC-CDMA-prec-SI: the proposed preprocessing MC-CDMA system with switched interleaving and chip-wise precoding schemes for the downlink.
- P-MC-CDMA-SI: the proposed preprocessing MC-CDMA system with switched interleaving scheme for the uplink.
- MC-CDMA-prec: the conventional MC-CDMA system employing the chip-wise precoding scheme for the downlink.
- perfect CSI: perfect channel state information at the transmitter.
- quan-ant: vector quantization for the CSI across the channel paths per transmit an-

tenna.

- quan-tap: vector quantization for the CSI across the transmit antennas per channel path.
- B -bit: the proposed system employs B bits for the switched interleaving scheme.

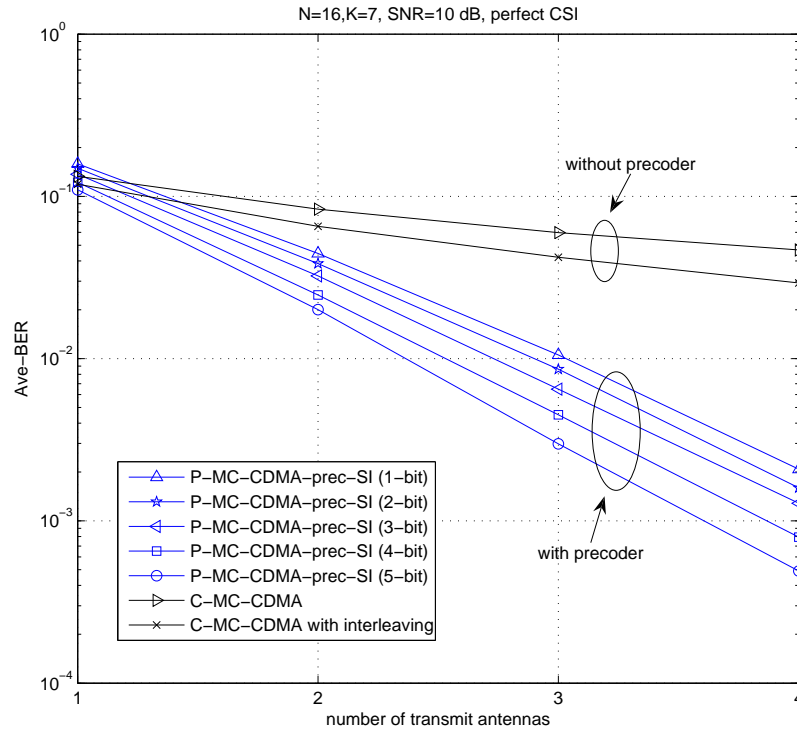


Figure 6.4: Average BER performance versus number of transmit antennas for the proposed downlink schemes with precoders and the conventional MC-CDMA schemes without precoders.

Fig. 6.4 shows the average BER performance of the proposed downlink switched interleaving schemes combined with precoders and the conventional MC-CDMA schemes without precoders. In this experiment, we consider the scenario with a SNR of $10dB$, 7 users, and the knowledge of the CSI is given for the precoders at the transmitter, the interleaving codebook is designed by using the random interleaving method. The schemes with precoders are much better than the conventional MC-CDMA MMSE receivers. As we increase the number of transmit antennas, the average BER decreases and the gap between them becomes larger. Furthermore, the precoders with the proposed switched interleaving scheme outperform the precoder without switched interleaving, the performance improves as the number of the interleaving patterns increases.

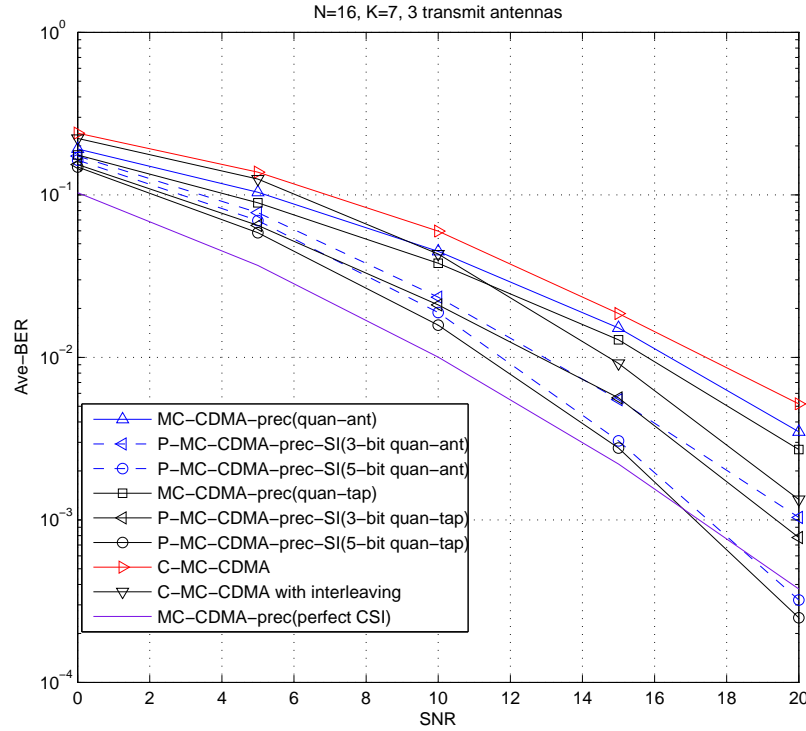


Figure 6.5: Average BER performance versus SNR for the proposed downlink algorithms with different CSI quantization schemes and the conventional MC-CDMA systems.

The second experiment, shown in Fig. 6.5 and Fig. 6.6, considers the comparison in terms of average BER of the CSI quantization scheme across the channel paths for each transmit antenna and that across the transmit antennas for each channel path with the proposed downlink schemes. The interleaving codebook is designed by using the random interleaving method. We use $\delta_1 = 10$ bits to feed back the channel direction and $\delta_2 = 6$ bits to feed back the channel norm. The Lloyd algorithm is used by these two CSI quantization methods. Note that when we quantize the vector across the channel paths, a different codebook which is subject to the constraint of the normalized channel profile is designed. In particular, we show the average BER performance curves versus SNR and number of users (K) for the analyzed schemes. The results in Fig. 6.5 indicate that due to the large quantization error, the performance of the general precoding technique decreases significantly. The quantization scheme across the transmit antennas per tap is slightly better than the one across the taps per transmit antenna. In this case of 3 transmit antennas, the two quantization schemes both require 48 feedback bits for each user. The proposed downlink schemes outperform the general precoding algorithm without switched interleaving and the conventional MC-CDMA MMSE receiver with interleaving and without interleaving. Specifically, the proposed downlink transmission scheme with 5 bits can save up to 5dB in comparison with the general precoding algorithm without switched in-

interleaving, and can save up to over $3dB$ in comparison with the conventional MC-CDMA MMSE receiver with interleaving, at the average BER level of 10^{-2} . Fig 6.6 indicates that the proposed scheme with 5 bits can support up to 4 more users at the average BER level of 10^{-2} , in comparison with the conventional MC-CDMA MMSE receiver. As we increase the number of interleaving patterns, it achieves the performance of the general precoder with perfect CSI.

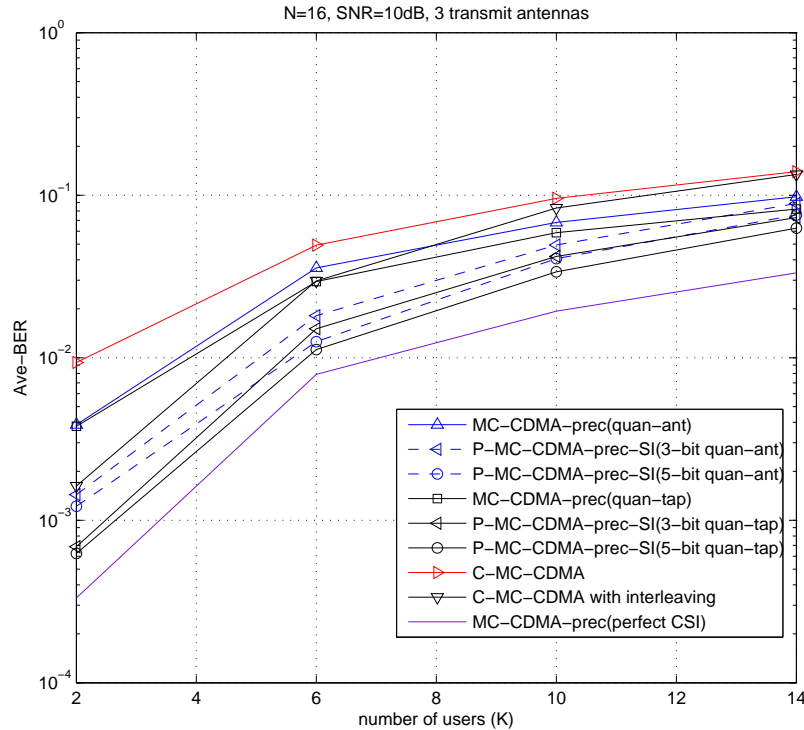


Figure 6.6: Average BER performance versus number of users for the proposed downlink algorithms with different CSI quantization schemes and the conventional MC-CDMA systems.

In the next experiment, we compare the codebooks of the interleavers which are created by the three methods outlined in section V, namely the random interleaving, the block interleaving and the MASS algorithms. In particular, we show the average BER performance curves versus number of feedback bits for the uplink scenario. In this case, we consider $K = 5$, $SNR = 8dB$ and 2 receive antennas at the BS. Note that the codebooks are designed offline. For the MASS algorithm we set the number of simulations $N_e = 1000$ and the number of candidates $\beta = 100$ and 1000 , and one block of symbols is transmitted per simulation. The results for an uplink system with $N = 16$ in the scenario of multipath fading channels are illustrated in Fig. 6.7. We can see that the best performance is achieved with the MASS algorithm, followed by the random interleaving method and the block interleaving method. In particular, as we increase the number of

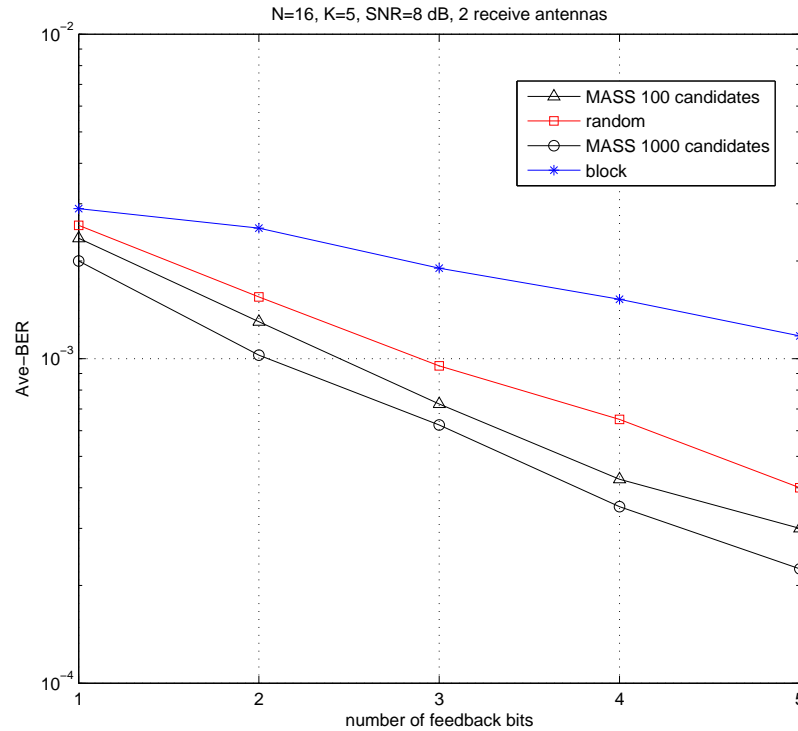


Figure 6.7: Average BER performance versus number of feedback bits for different interleaving codebook.

candidates, the performance is improved for the MASS algorithm.

Now, let us consider the experiments of our proposed uplink preprocessing structure equipped with different number of feedback bits configurations. We compare the performance in terms of average BER of the proposed limited feedback structures with MMSE receivers, namely 1-bit, 2-bit, 3-bit, 4-bit and 5-bit feedback, respectively, and the conventional MC-CDMA system with MMSE receiver. In particular, we show the average BER performance curves versus the SNR and the number of users (K) for the analyzed schemes. In this simulation, the interleaving codebook is designed by the MASS algorithm. At the receiver, the BS is equipped with 2 antennas. The results depicted in Fig. 6.8 and Fig. 6.9, which are based on $K = 12$ and $SNR = 10dB$, respectively, indicate that the best performance is achieved with the novel switched interleaving preprocessing scheme with 5 feedback bits, and we can see the higher number of feedback bits we use the better the performance. Specifically, the proposed scheme with 5 bits can save up to $3dB$, and support up to 8 more users, near the average BER level of 10^{-3} , in comparison with the conventional MC-CDMA MMSE receiver.

Finally, Fig. 6.10 illustrates the average BER performance versus the percentage of

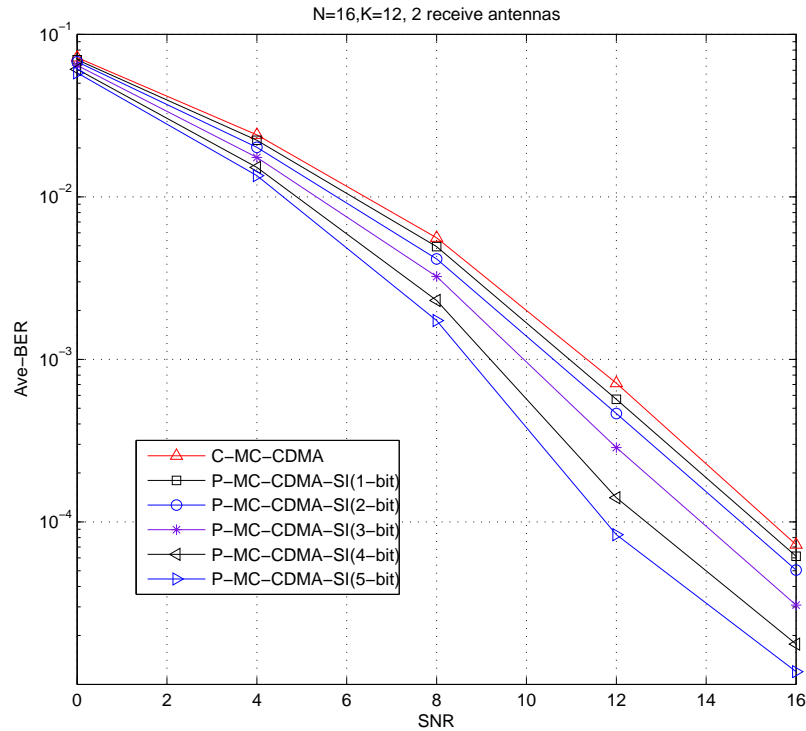


Figure 6.8: Average BER performance versus SNR for the proposed uplink switched interleaving preprocessing schemes and the conventional MC-CDMA MMSE receiver.

each user's feedback errors for both uplink and downlink scenarios. Here, we use 5 bits for the proposed switched interleaving schemes. The interleaving codebooks are based on the random interleaving method. In particular, the downlink scheme quantizes the CSI across the transmit antennas per channel path. We use a structure based on a frame format where the indices are converted to 0s and 1s. This frame of 1s and 0s with the feedback information is transmitted over a binary symmetric channel with probability of error P_e associated. The burst errors scenario in the limited feedback channel can be easily transferred to the case of binary symmetric channel by employing a conventional bit interleaver. As we increase the feedback errors for each user, the performance of the proposed limited feedback schemes decreases. In the case of the downlink, the performance decreases fast after 1%, and compared with the conventional MC-CDMA it starts to lose at 20%. The performance of the uplink decays faster than the one of the downlink, because the interleaver is not in accordance with the deinterleaver due to the feedback errors for the uplink scenario, which creates a significant detection error for a fading block. To ensure the errors are controlled, channel coding techniques should be employed for the feedback channels with errors.

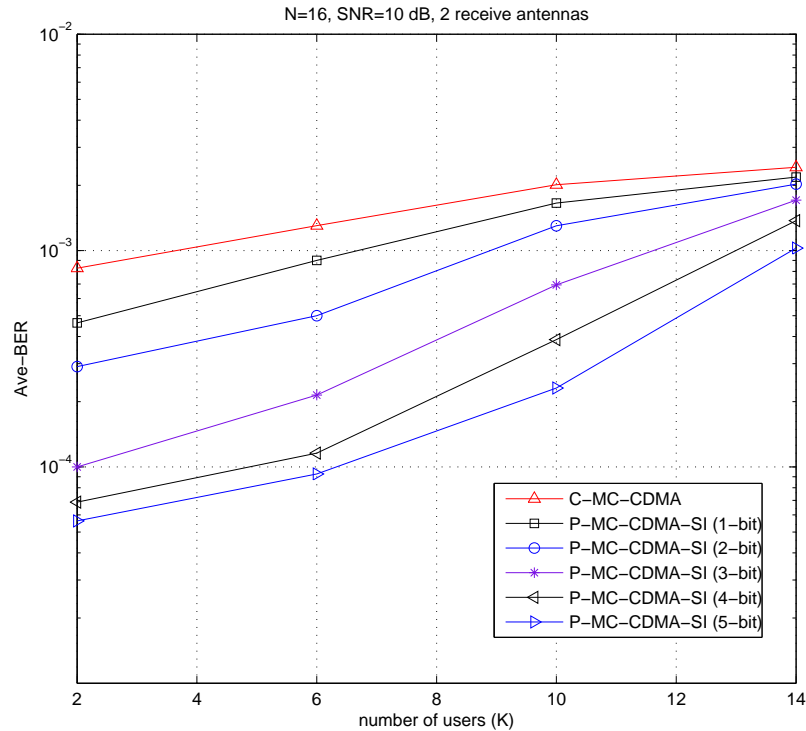


Figure 6.9: Average BER performance versus number of users for the proposed uplink switched interleaving preprocessing schemes and the conventional MC-CDMA MMSE receiver.

6.7 Conclusions

In this chapter, we proposed linear preprocessing schemes based on switched interleaving techniques with limited feedback for both downlink and uplink MC-CDMA systems. The chip-wise linear precoder and the relevant MMSE receivers were introduced, and the selection functions were also proposed to choose the optimum interleaver from the codebook. The CSI quantization scheme based on the Lloyd algorithm and three methods for interleaving codebook design were described. The results show that the proposed interleaving and detection schemes significantly outperform existing algorithms and support systems with higher loads.

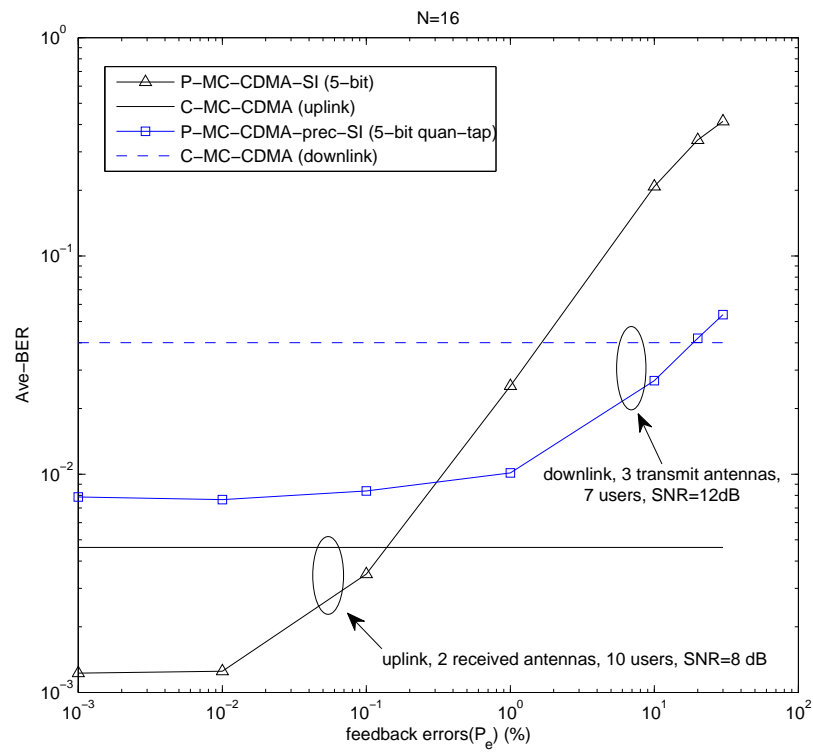


Figure 6.10: Average BER performance versus the percentage of each user's feedback errors for the proposed downlink and uplink schemes.

Chapter 7

Multistage MIMO Receivers Based on Multi-Branch Interference Cancellation for MIMO-CDMA Systems

Contents

7.1	Introduction	123
7.2	System Model	124
7.3	Detectors for MIMO-CDMA Systems	126
7.4	Multistage Multi-Branch SIC Detection	129
7.5	Simulation Results	132
7.6	Conclusion	134

7.1 Introduction

Recently, wireless communication research has focused on MIMO systems in order to exploit the enormous capacity and improve quality and reliability [159]. In MIMO systems, two configurations can be employed, namely transmit diversity and spatial multiplexing, which exploit spatial diversity to combat fading and increase the data rates by transmitting independent data streams, respectively. In particular, spatial multiplexing can be used to transmit multiple data streams that can be separated using signal processing techniques at the receiver. CDMA has been considered in conjunction with MIMO techniques, which is

widely believed to play an important role in future communication systems. These detectors [10–12] have limitations with respect to MUI mitigation and there is relatively little work on MIMO-CDMA receivers with more sophisticated interference cancellation.

In this chapter, we focus on a uplink MIMO-CDMA system affected by multipath fading channels, and propose a novel interference cancellation scheme based on multi-branch processing. Due to a large number of transmit antennas, we face the high complexity of detectors for MIMO-CDMA systems, making it impractical to employ highly complex detectors such as the sphere decoder [160], [161] for the ML detector. We propose a novel multistage receiver based on the MB-SIC. Firstly, the receiver employs the ordered SIC algorithm to detect all the antenna data streams, and the estimated symbols enter a grouping detection scheme, which subtracts the MUI from the received data and retains the antenna data streams corresponding to the desired user. At last, the proposed MB-SIC detector deals with the refined estimated vector by using a group of SICs based on different cancellation orders, and yields different candidates. According to a selection rule we can then select the best estimate for the final output. The simulations show that our proposed algorithm achieves significantly better performance than the conventional spatial multiplexing techniques and approaches the single user bound.

This chapter is structured as follows. Section 7.2 briefly describes the uplink MIMO-CDMA system with multipath channels. The conventional MMSE, the PIC and the SIC receivers are introduced in Section 7.3, the proposed receiver and selection rules are described in Section 7.4. The simulation results are presented in Section 7.5. Section 7.6 draws the conclusions.

7.2 System Model

In this section we describe a multipath channel model for the multiuser MIMO-CDMA system. The uplink synchronous system model with K users is depicted in Fig. 7.1. Multiple antennas are employed for each user, and the k th user's bit stream is split into t_k transmit antenna data streams, where t_k is the number of antenna elements for the user k , $k = 1 \cdots K$. The receiver is equipped with multiple antennas.

Assume that the uplink is an uncoded BPSK system, and the transmit signal has unit power, the $t_k \times 1$ vector $\mathbf{b}_k = [b_{1,k}, \dots, b_{t_k,k}]^T$, $k = 1, \dots, K$, where $b_{i,k}$ denotes the transmit symbol of the k th user at the i th antenna, where $i = 1, \dots, t_k$. It has zero mean and energy $E_b = \mathbf{E}[|b_{i,k}|^2]$, where the total number of transmit antennas is de-

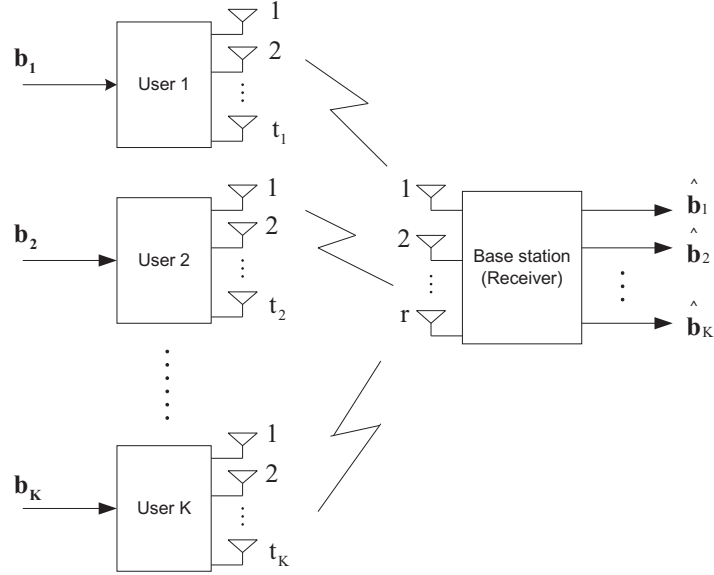


Figure 7.1: MIMO-CDMA uplink model

noted as $T \triangleq \sum_{k=1}^K t_k$. The receiver employs r antennas. To allow multiple access, DS-CDMA is used, and all transmit antennas are assigned different spreading sequences of length N . The spreading sequence of the k th user and the i th antenna is a $N \times 1$ vector $\mathbf{s}_{i,k} = [s_{i_1,k}, \dots, s_{i_N,k}]^T$. Then, if the k th user transmits the symbol $b_{i,k}$ from antenna $i = 1, \dots, t_k$, the transmitted signal is $b_{i,k}\mathbf{s}_{i,k}$. We note that other types of CDMA systems such as MC-CDMA and MC-DS-CDMA are possible with small modifications of the model presented here.

We assume that the link from each transmit antenna to each receive antenna has multipath with L_p taps, and the communication channel between the i th transmit antenna of the k th user and the j th receive antenna for the u th symbol is described by the $L_p \times 1$ channel vector $\mathbf{v}_{j,i}^{(k)}(u) = [v_{j,i,0}^{(k)}(u), \dots, v_{j,i,L_p-1}^{(k)}(u)]^T$ with $v_{j,k,l}(u) = v_{j,k,l}(uT_c)$ for $l = 0, \dots, L_p - 1$, which corresponds to the $M \times 1$ effective spreading code $\bar{\mathbf{s}}_{j,i}^{(k)} = \mathbf{C}_i^{(k)} \mathbf{v}_{j,i}^{(k)}$, where $M = N + L_p - 1$ and the $M \times L_p$ convolution matrix $\mathbf{C}_i^{(k)}$ contains one-chip shifted versions of $\mathbf{s}_{i,k}$. We assume that the channel order is not greater than N , i.e. $L_p - 1 \leq N$ and the spacing is one-chip. We will drop the index u for notation simplicity in what follows.

The received vector of the j th antenna over one symbol interval is

$$\mathbf{r}_j = \sum_{k=1}^K \sum_{i=1}^{t_k} \bar{\mathbf{s}}_{j,i}^{(k)} b_{i,k} + \boldsymbol{\eta}_j + \mathbf{n}_j \quad (7.1)$$

where \mathbf{r}_j is an $M \times 1$ received vector corresponding to antenna j , $j = 1, \dots, r$, and $\boldsymbol{\eta}_j$ is the $M \times 1$ vector of ISI caused by the delay of neighbouring symbols, \mathbf{n}_j is an $M \times 1$

noise vector, we stack all the received vectors in an $Mr \times 1$ vector, and find a system model that is described by the following matrix equation:

$$\mathbf{r} = \mathbf{H}\mathbf{b} + \boldsymbol{\eta} + \mathbf{n}. \quad (7.2)$$

Here \mathbf{r} is the $Mr \times 1$ received column-vector $[\mathbf{r}_1^T, \dots, \mathbf{r}_r^T]^T$, where $\mathbf{b} = [\mathbf{b}_1^T, \mathbf{b}_2^T, \dots, \mathbf{b}_K^T]^T$ is the $T \times 1$ transmitted vector, and $\boldsymbol{\eta} = [\boldsymbol{\eta}_1^T, \boldsymbol{\eta}_2^T, \dots, \boldsymbol{\eta}_r^T]^T$ is the $Mr \times 1$ vector of ISI. The receiver is affected by additive Gaussian noise represented by the $Mr \times 1$ vector $\mathbf{n} = [\mathbf{n}_1^T, \dots, \mathbf{n}_r^T]^T$, the structure of the $Mr \times T$ matrix \mathbf{H} is

$$\mathbf{H} = [\mathbf{h}_1^{(1)}, \mathbf{h}_2^{(1)}, \dots, \mathbf{h}_{t_1}^{(1)}, \dots, \mathbf{h}_1^{(K)}, \mathbf{h}_2^{(K)}, \dots, \mathbf{h}_{t_K}^{(K)}], \quad (7.3)$$

where $\mathbf{h}_i^{(k)} = [\bar{\mathbf{s}}_{1,i}^{(k)T}, \bar{\mathbf{s}}_{2,i}^{(k)T}, \dots, \bar{\mathbf{s}}_{r,i}^{(k)T}]^T$ is an $Mr \times 1$ vector corresponding to the components of the i th transmit antenna stream of the k th user, $i = 1, \dots, t_k$, $k = 1, \dots, K$. We rewrite the matrix \mathbf{H} in another way

$$\mathbf{H} = [\tilde{\mathbf{h}}_1, \tilde{\mathbf{h}}_2, \dots, \tilde{\mathbf{h}}_T], \quad (7.4)$$

where $\tilde{\mathbf{h}}_\beta$ is an $Mr \times 1$ vector corresponding to the β th antenna data stream, where $\beta = 1, \dots, T$. In the following, we assume that the channel gains are independent and identically distributed (i.i.d.) complex Gaussian random variables with zero-mean, and the spreading sequences are randomly generated with i.i.d. real entries.

7.3 Detectors for MIMO-CDMA Systems

In this section, we introduce a linear MMSE receiver which mitigates the multiuser and spatial interference jointly. Subsequently, some existing nonlinear detection schemes based on spatial multiplexing techniques, such as the PIC, and the SIC or V-BLAST algorithms are reviewed.

7.3.1 Linear MMSE Receiver

Let us briefly describe in this part the design of the linear MMSE receiver for MIMO-CDMA systems. We consider a MSE cost function for the total transmitted antenna data streams

$$J_{MSE} = \mathbf{E}[|\mathbf{b} - \mathbf{W}^H \mathbf{r}|^2] \quad (7.5)$$

where \mathbf{W} is the $Mr \times T$ MMSE filter matrix. In order to obtain the matrix, we minimize the cost function by taking the gradient with respect to the filter \mathbf{W}^* and setting it equal

to a zero matrix which yields

$$\mathbf{W} = \arg \min_{\mathbf{W}} J_{MSE} = (\mathbf{H}\mathbf{H}^H + \sigma^2\mathbf{I})^{-1}\mathbf{H}, \quad (7.6)$$

where \mathbf{I} denotes a $Mr \times Mr$ identity matrix. The receiver provide a $Mr \times 1$ estimate vector for all the antenna streams, which is given by

$$\hat{\mathbf{b}} = \text{sgn}(\Re(\mathbf{W}^H \mathbf{r})) \quad (7.7)$$

The receiver is based on the assumption that both the transmitted signal and the noise can be generated as independent Gaussian variables. The complexity of the MMSE receiver per transmit antenna data stream is $O((Mr)^3)$. We note that the linear MMSE receiver also can be designed as a $Mr \times 1$ filter vector corresponding to each transmit antenna stream.

7.3.2 Parallel Interference Cancellation (PIC) Detection Schemes

The PIC algorithm [162] is combined with the linear MMSE detector in our work. Let us assume the output vector of the linear MMSE receiver is $\hat{\mathbf{b}} = \text{sgn}(\Re(\mathbf{W}^H \mathbf{r})) = [\hat{b}_1, \dots, \hat{b}_T]^T$. Assume that we want to detect the data of antenna β_0 , and define the matrix $\bar{\mathbf{H}}_{\beta_0} = [\tilde{\mathbf{h}}_1, \tilde{\mathbf{h}}_2, \dots, \tilde{\mathbf{h}}_{\beta_0-1}, \tilde{\mathbf{h}}_{\beta_0+1}, \dots, \tilde{\mathbf{h}}_T]$, which excludes the vector $\tilde{\mathbf{h}}_{\beta_0}$ from \mathbf{H} , where $\beta_0 = 1, \dots, T$. The output of the PIC receiver is given by

$$\hat{b}_{\beta_0}^{(f)} = \text{sgn}\{\Re(\mathbf{w}_{\beta_0}^H (\mathbf{r} - \bar{\mathbf{H}}_{\beta_0} \bar{\mathbf{b}}_{\beta_0}))\} \quad (7.8)$$

where the column-vector $\bar{\mathbf{b}}_{\beta_0} = [\hat{b}_1, \dots, \hat{b}_{\beta_0-1}, \hat{b}_{\beta_0+1}, \dots, \hat{b}_T]^T$, and the interference part is $\bar{\mathbf{H}}_{\beta_0} \bar{\mathbf{b}}_{\beta_0} = \sum_{\beta \neq \beta_0} \tilde{\mathbf{h}}_{\beta} \hat{b}_{\beta}$. By following the same approach the MMSE receiver \mathbf{w}_{β_0} for the antenna stream β_0 is given by

$$\mathbf{w}_{\beta_0} = (\tilde{\mathbf{h}}_{\beta_0} \tilde{\mathbf{h}}_{\beta_0}^H + \sigma^2\mathbf{I})^{-1} \tilde{\mathbf{h}}_{\beta_0}. \quad (7.9)$$

By using the binomial inverse theorem, we have

$$\mathbf{w}_{\beta_0} = (\mathbf{I} - \frac{\tilde{\mathbf{h}}_{\beta_0} \tilde{\mathbf{h}}_{\beta_0}^H}{\sigma^2 + \tilde{\mathbf{h}}_{\beta_0}^H \tilde{\mathbf{h}}_{\beta_0}}) \frac{\tilde{\mathbf{h}}_{\beta_0}}{\sigma^2} \quad (7.10)$$

The PIC receiver achieves better performance than the linear MMSE detector with the complexity of $O((Mr)^2)$ per transmit antenna data stream.

7.3.3 Successive Interference Cancellation (SIC) Detection Schemes

The SIC algorithm is based on the linear MMSE receiver to form the V-BLAST algorithms [10], which are very popular approaches and have been widely employed in MIMO

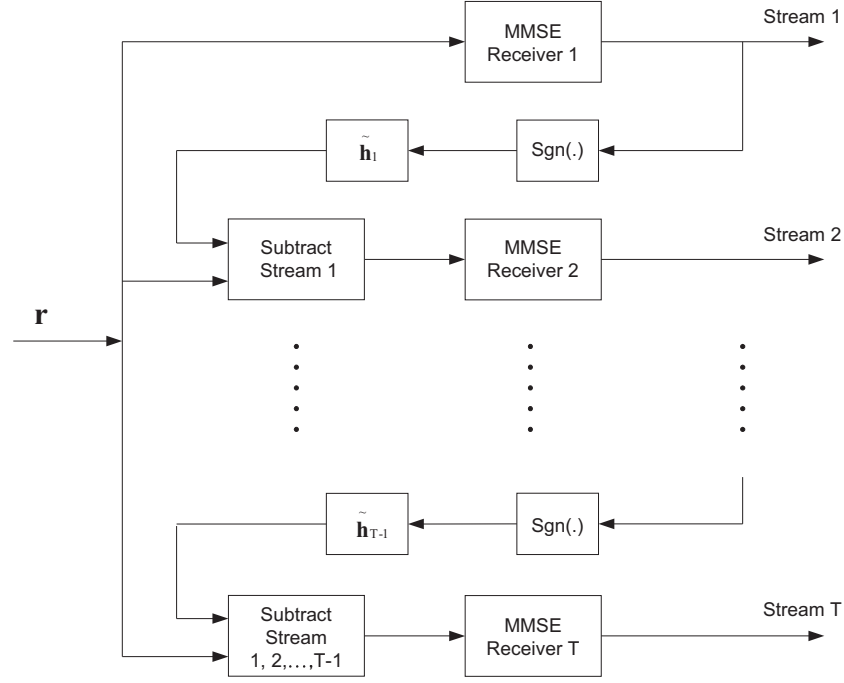


Figure 7.2: The SIC structure based on the MMSE receiver

systems [159]. In this algorithm, rather than cancelling all the undesired signals together, the SIC computes the estimated symbols successively. The structure of the SIC algorithm based on the MMSE receiver is shown in Fig. 7.2. The algorithm corresponding to the γ th antenna stream is mathematically described as follows. When $\gamma = 1$ we have

$$\begin{aligned}\hat{b}_\gamma^{(f)} &= \text{sgn}(\Re(\mathbf{w}_\gamma^H \mathbf{r})), \\ \mathbf{w}_\gamma &= (\mathbf{H}\mathbf{H}^H + \sigma^2\mathbf{I})^{-1}\tilde{\mathbf{h}}_\gamma.\end{aligned}\quad (7.11)$$

For the remaining streams $\gamma = 2, \dots, T$ we obtain

$$\begin{aligned}\mathbf{r}^{(\gamma)} &= \mathbf{r}^{(\gamma-1)} - \tilde{\mathbf{h}}_{\gamma-1}\hat{b}_{\gamma-1}^{(f)}, \quad \mathbf{r}^{(1)} = \mathbf{r}, \\ \hat{b}_\gamma^{(f)} &= \text{sgn}\{\Re(\mathbf{w}_\gamma^H \mathbf{r}^{(\gamma)})\}, \\ \mathbf{w}_\gamma &= (\tilde{\mathbf{H}}_\gamma \tilde{\mathbf{H}}_\gamma^H + \sigma^2\mathbf{I})^{-1}\tilde{\mathbf{h}}_\gamma,\end{aligned}\quad (7.12)$$

where the value $\hat{b}_\gamma^{(f)}$ is the final output corresponding to the antenna stream γ , and we design the matrix $\tilde{\mathbf{H}}_\gamma = [\tilde{\mathbf{h}}_\gamma, \tilde{\mathbf{h}}_{\gamma+1}, \dots, \tilde{\mathbf{h}}_T]$, which excludes the previous detected vectors, $\tilde{\mathbf{h}}_1, \tilde{\mathbf{h}}_2, \dots, \tilde{\mathbf{h}}_{\gamma-1}$, from the matrix \mathbf{H} , where the vector $\tilde{\mathbf{h}}_{\gamma-1}\hat{b}_{\gamma-1}^{(f)}$ is the estimated interference to be cancelled at iteration γ .

The scheme schedules a cancellation order, and the algorithm proceeds accordingly. Normally, MIMO systems obtain the order by arranging the received signals' powers and start to detect from the antenna stream with the strongest power. In the MIMO-CDMA system, we produce the cancellation order by arranging a group of values, namely,

$\{\|\tilde{\mathbf{h}}_1\|, \|\tilde{\mathbf{h}}_2\|, \dots, \|\tilde{\mathbf{h}}_T\|\}$, which corresponds to the columns of the matrix \mathbf{H} . The complexity of the SIC detector based on MMSE receivers is $O((Mr)^3)$ per transmit antenna data stream.

7.4 Multistage Multi-Branch SIC Detection

In this section, we describe the proposed multistage receiver with MB-SIC, and then two selection criteria are introduced.

7.4.1 Proposed MB-SIC Scheme

The structure of the proposed multistage multi-branch SIC (MSMB-SIC) receiver is depicted in Fig. 7.3 (a). In the first stage, the SIC detector processes the received vector and produces the first stage estimation vector, which is $\hat{\mathbf{b}}^{(1)} = [\hat{b}_{1,1}^{(1)}, \dots, \hat{b}_{t_1,1}^{(1)}, \dots, \hat{b}_{1,K}^{(1)}, \dots, \hat{b}_{t_K,K}^{(1)}]^T$, where the quantity $\hat{b}_{i,k}^{(1)}$ corresponds to the symbol of the k th user at the i th antenna, $k = 1, \dots, K$, $i = 1 \dots t_k$. Then, the grouping detection strategy is employed to suppress the MUI by subtracting other users from the received vector \mathbf{r} , and generating the estimated vector $\mathbf{r}_{k_0}^{(1)}$ for desired user k_0 :

$$\mathbf{r}_{k_0}^{(1)} = \mathbf{r} - \check{\mathbf{H}}_{k_0} \check{\mathbf{b}}_{k_0}, \quad (7.13)$$

where $k_0 = 1 \dots K$. Let us recall the way to present the matrix \mathbf{H} in (7.3), where we define

$$\check{\mathbf{H}}_{k_0} = [\mathbf{h}_1^{(1)} \dots \mathbf{h}_1^{(k_0-1)} \dots \mathbf{h}_{t_{k_0-1}}^{(k_0-1)} \mathbf{h}_1^{(k_0+1)} \dots \mathbf{h}_{t_{k_0+1}}^{(k_0+1)} \dots \mathbf{h}_{t_K}^{(K)}], \quad (7.14)$$

which excludes the vectors corresponding to the antenna streams of the k_0 th user, and $\check{\mathbf{b}}_{k_0} = [\hat{b}_{1,1}^{(1)} \dots \hat{b}_{t_{k_0-1},k_0-1}^{(1)}, \hat{b}_{1,k_0+1}^{(1)} \dots \hat{b}_{t_K,K}^{(1)}]^T$, $\check{\mathbf{H}}_{k_0} \check{\mathbf{b}}_{k_0} = \sum_{k \neq k_0} (\sum_{i=1}^{t_k} \hat{b}_{i,k}^{(1)})$ is the MUI. For the sake of simplicity, we assume that the first user is the desired user and we can drop the index k_0 . For the last stage, we focus on the spatial interference cancellation using our proposed MB-SIC shown in Fig. 7.3 (b). Rather than only considering one cancellation order, we use a group of SICs with different cancellation orders and produce a group of different detection vectors $\hat{\mathbf{b}}'_\mu$, where $\mu = 1, \dots, B$ and B is the number of cancellation orders. Based on the MMSE and ML selection rules we can obtain the final output vectors with best performance, where the final decision vector $\hat{\mathbf{b}}^{(f)} = [\hat{b}_{1,1}^{(f)}, \dots, \hat{b}_{t_1,1}^{(f)}]^T$ for the desired user.

The μ th branch of the MB-SIC algorithm corresponding to the φ th antenna of the

desired user is described as follows. For the first stream $\varphi = 1$ we have

$$\begin{aligned} z_{\varphi,\mu} &= \mathbf{w}_{\varphi,\mu}^H \mathbf{r}^{(1)}, \\ \hat{b}_{\varphi,\mu}^{(2)} &= \text{sgn}(\Re(z_{\varphi,\mu})), \\ \mathbf{w}_{\varphi,\mu} &= (\hat{\mathbf{H}}_{\mu} \hat{\mathbf{H}}_{\mu}^H + \sigma^2 \mathbf{I})^{-1} \hat{\mathbf{h}}_{\varphi,\mu}. \end{aligned} \quad (7.15)$$

For the remaining streams $\varphi = 2, \dots, t_1$, we obtain

$$\begin{aligned} \mathbf{r}_{\mu}^{(\varphi)} &= \mathbf{r}_{\mu}^{(\varphi-1)} - \hat{\mathbf{h}}_{\varphi-1,\mu} \hat{b}_{\varphi-1,\mu}^{(2)}, \quad \mathbf{r}_{\mu}^{(1)} = \mathbf{r}^{(1)}, \\ z_{\varphi,\mu} &= \mathbf{w}_{\varphi,\mu}^H \mathbf{r}_{\mu}^{(\varphi)}, \\ \hat{b}_{\varphi,\mu}^{(2)} &= \text{sgn}(\Re(z_{\varphi,\mu})), \\ \mathbf{w}_{\varphi,\mu} &= (\hat{\mathbf{H}}_{\varphi,\mu} \hat{\mathbf{H}}_{\varphi,\mu}^H + \sigma^2 \mathbf{I})^{-1} \hat{\mathbf{h}}_{\varphi,\mu}, \\ &\mu = 1, \dots, B \end{aligned} \quad (7.16)$$

which produces the hard decision vector $\hat{\mathbf{b}}_{\mu}^{(2)} = [\hat{b}_{1,\mu}^{(2)}, \dots, \hat{b}_{t_1,\mu}^{(2)}]^T$ and the soft decision vector $\mathbf{z}_{\mu} = [z_{1,\mu}, \dots, z_{t_1,\mu}]^T$, the matrix $\hat{\mathbf{H}}_{\mu} = \hat{\mathbf{H}} \mathbf{P}_{\mu} = [\hat{\mathbf{h}}_{1,\mu}, \dots, \hat{\mathbf{h}}_{t_1,\mu}]^T$, where $\hat{\mathbf{H}} = [\mathbf{h}_1^{(1)}, \dots, \mathbf{h}_{t_1}^{(1)}]^T$. The quantity \mathbf{P}_{μ} is the permutation matrix corresponding to the cancellation order μ . The matrix $\hat{\mathbf{H}}_{\varphi,\mu} = [\hat{\mathbf{h}}_{\varphi,\mu}, \hat{\mathbf{h}}_{\varphi+1,\mu}, \dots, \hat{\mathbf{h}}_{t_1,\mu}]^T$ which removes the previous detected vectors, $\hat{\mathbf{h}}_{1,\mu}, \dots, \hat{\mathbf{h}}_{\varphi-1,\mu}$, from $\hat{\mathbf{H}}_{\mu}$. The μ th branch output candidate for the desired user is given by:

$$\hat{\mathbf{b}}_{\mu}' = \hat{\mathbf{b}}_{\mu}^{(2)} \mathbf{P}_{\mu}^T \quad (7.17)$$

$$\mathbf{z}_{\mu}' = \mathbf{z}_{\mu} \mathbf{P}_{\mu}^T \quad (7.18)$$

where the matrix \mathbf{P}_{μ}^T is used to transform the vectors $\hat{\mathbf{b}}_{\mu}^{(2)}$ and \mathbf{z}_{μ} to $\hat{\mathbf{b}}_{\mu}'$ and \mathbf{z}_{μ}' . The complexity of the proposed receiver is $O((Mr)^3 B)$ per transmit antenna data stream.

7.4.2 Selection Criteria

The final output vector $\hat{\mathbf{b}}^{(f)}$ for each symbol interval is described by

$$\hat{\mathbf{b}}^{(f)} = \text{sgn}(\Re(\mathbf{z}_{\mu_{opt}}')) \quad (7.19)$$

where μ_{opt} corresponds to the optimum branch. Based on different criteria, such as the ML and the MMSE, the detector can select the branch with the best performance.

Maximum Likelihood

The cost function for ML criterion, which is equivalent to the minimum Euclidean distance criterion, and the optimum branch are written as

$$\mu_{opt} = \arg \min_{1 \leq u \leq B} \xi_{ML} \quad (7.20)$$

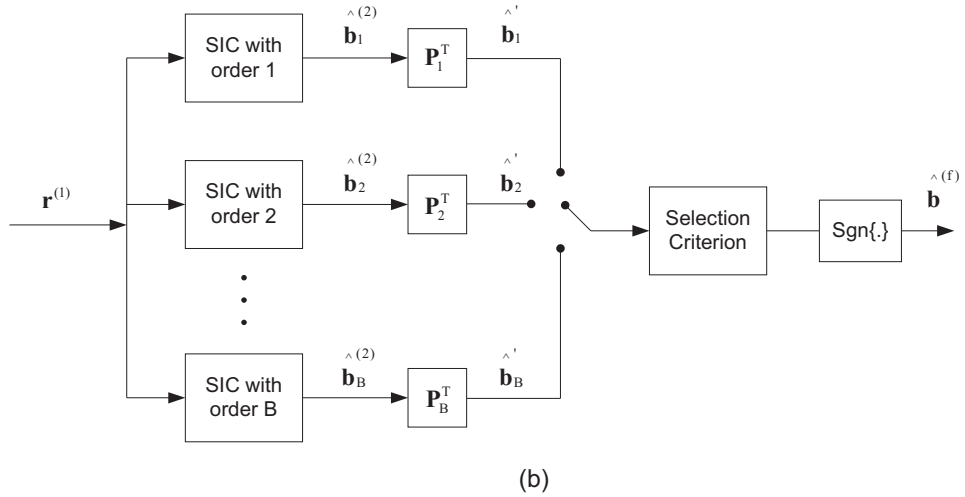
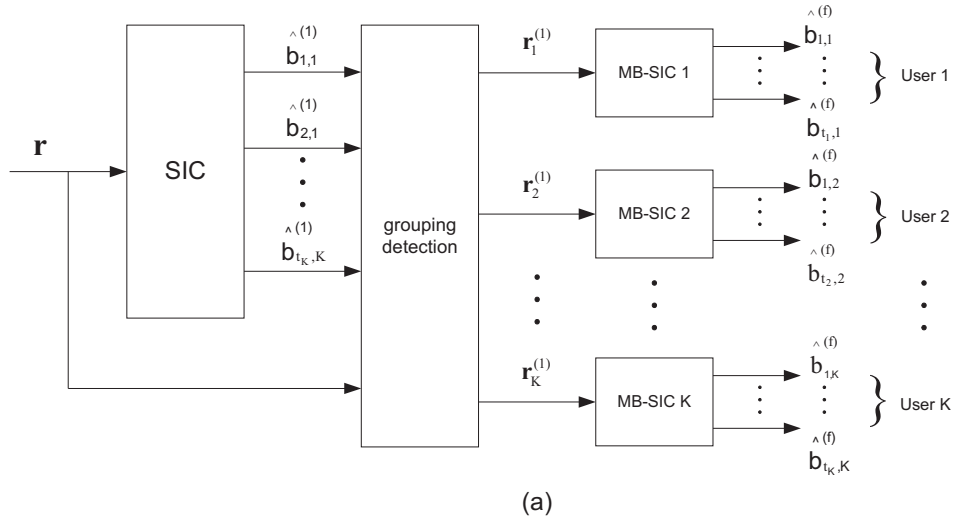


Figure 7.3: (a) The proposed MSMB-SIC receiver and (b) The MB-SIC structure for the desired user.

where

$$\xi_{ML} = \|\mathbf{r}^{(1)} - \hat{\mathbf{H}}\hat{\mathbf{b}}_{\mu}'\|^2 \quad (7.21)$$

Minimum Mean-Squared Error Criterion

The MMSE criterion can be used to select the branch which minimizes the mean square error of transmitted symbols. The optimum branch is given by

$$\mu_{opt} = \arg \min_{1 \leq u \leq B} \xi_{MMSE} \quad (7.22)$$

where

$$\xi_{MMSE} = \|\mathbf{b}_1 - \mathbf{z}'_\mu\|^2 \quad (7.23)$$

The number of parallel branches B that yield detection candidates is a parameter that must be chosen by the designer. In this context, the optimal ordering algorithm conducts an exhaustive search, where the number of candidates is $B = t_1!$. It is indeed practical for uplink MIMO multiuser systems, since each mobile user is equipped with a small number of antenna elements with $t_1 = 2, 3, 4$.

7.5 Simulation Results

In this section, we evaluate the performance of the novel MSMB-SIC receiver and compare it to other existing detection algorithms, namely, the linear [12], the SIC [11] and the PIC [162]. We adopt a simulation approach and conduct several experiments in order to verify the effectiveness of the proposed techniques. We carried out simulations to assess the BER performance of the detection algorithms for different SNR and loads. Our simulation results are based on an uncoded system with perfect channel information at the receiver. All channels have a profile with 3 paths whose powers are $p_0 = 0$ dB, $p_1 = -7$ dB and $p_2 = -10$ dB, which are normalized, and the spacing is 1 chip. The sequence of channel coefficients $h_l(i) = \sqrt{p_l}\alpha_l(i)$ ($l = 0, 1, 2$), where $\alpha_l(i)$ are zero-mean circularly symmetric complex Gaussian random variables with unit variance. The channel coefficients are varying per symbol. We equip each user with 4 antennas and the base station receiver with 4 antennas.

In the first experiment, we study the BER of the proposed receiver and the conventional detection schemes. Here we use random sequences with $N = 16$ as spreading codes. The novel scheme with ML and MMSE selection rules are considered. The results in Fig. 7.4 show BER performance curves versus SNR and indicate that the best performance is achieved with the novel MSMB-SIC receiver with the MMSE selection criterion, followed by the novel receiver with the ML criterion, the SIC detection scheme, the PIC detection scheme, the linear MMSE receiver. Specifically, the proposed MSMB-SIC receiver with the MMSE selection criterion can save up to almost 1.5 (dB) in comparison with the SIC algorithm at the BER level of 10^{-3} .

The next scenario, depicted in Fig. 7.5, shows the BER performance curves versus number of users (K) for the analyzed receivers, where we also use random sequences with $N = 16$ as spreading codes. In particular, the novel MSMB-SIC receiver with the

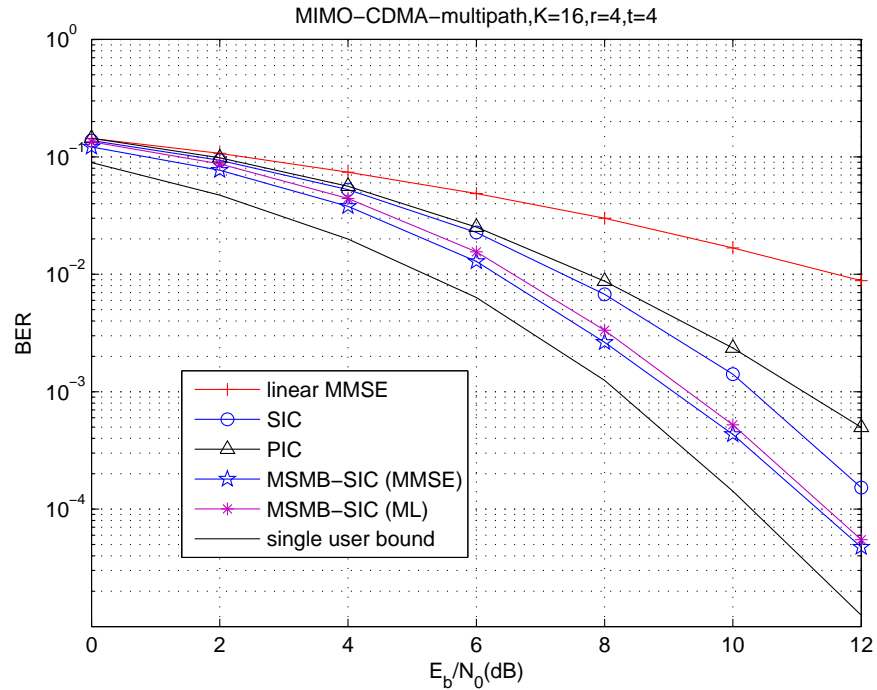


Figure 7.4: BER performance versus SNR. $N = 16$.

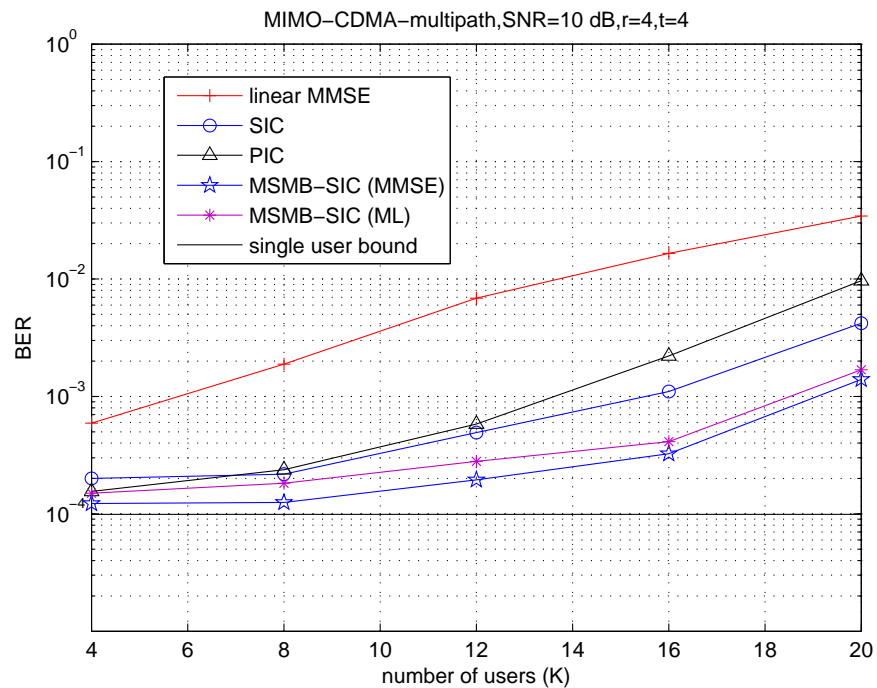


Figure 7.5: BER performance versus number of users (K). $N = 16$.

MMSE criterion can support up to 3 additional users in comparison with the SIC at the BER level of 10^{-3} . It can substantially increase the system capacity. For a low-loaded case the proposed receiver gets close to the single user bound and offers a significant

advantage over the linear detector.

7.6 Conclusion

In this chapter, we proposed multistage MIMO receivers based on multi-branch interference cancellation and introduced two selection rules. The results show that the proposed MSMB-SIC schemes significantly outperform the existing detection algorithms and support systems with higher loads in MIMO-CDMA systems. We remark that our proposed algorithms also can be extended to take into account coded systems, MIMO MC-CDMA systems and other types of communications systems.

Chapter 8

Conclusions and Future Work

Contents

8.1 Summary of the Work	135
8.2 Future Work	136

8.1 Summary of the Work

In this thesis, we have investigated various interference suppression architectures and algorithms, namely, low-complexity adaptive blind variable step-size schemes, novel space-time decision feedback detectors, preprocessing techniques based on switched interleaving and limited feedback and multistage multibranch interference cancellation techniques for different CDMA systems, such as DS-CDMA, MC-CDMA, and multiantenna CDMA systems.

In Chapter 3, we investigated the blind CCM adaptive receivers for DS-CDMA systems that employ SG algorithms with variable step-size mechanisms and proposed a low-complexity variable step-size mechanism for blind CCM CDMA receivers. Moreover, the characteristics of the new mechanism was investigated via derived analytical expressions using the energy-preserving approach to predict the EMSE for convergence and tracking analyses. Simulation showed that the new blind algorithm significantly outperforms the existing variable step-size mechanism for blind CCM receivers.

In Chapter 4, a novel space-time MMSE DF detection scheme for DS-CDMA systems with multiple receive antennas was proposed, which employs MPF for interference can-

cellation. To further mitigate the effects of error propagation, the cascaded DF stages are employed. The multiantenna configurations based on beamforming and diversity techniques were considered. We also presented modified adaptive SG and RLS algorithms that automatically switch to the best available interference cancellation feedback branch and jointly estimate the feedforward and feedback filters.

In Chapter 5, a novel switched interleaving scheme based on limited feedback was developed for both uplink and downlink DS-CDMA systems. The block-based and symbol by symbol receivers with selection functions were proposed. We designed three methods to generate interleaving codebooks, which are random interleaving, block interleaving and FSP methods. Based on the simulation results, we can see the performance of the proposed schemes is significantly better than the conventional CDMA, existing chip-interleaving, linear precoding, and adaptive spreading schemes.

In Chapter 6, we proposed novel transmit processing techniques based on the switched interleaving and limited feedback for both downlink and uplink multiple antenna MC-CDMA systems. For the downlink, a new hybrid preprocessing technique based on switched interleaving and chip-wise precoding was proposed to suppress the MUI. The selection function at the BS picks the optimum interleaver from the interleaving codebook based on all users' quantized CSI. Moreover, a transmit processing technique for the uplink requiring very low rate of feedback information was also proposed. The simulations showed that the performance of the proposed techniques is much better than prior art.

In Chapter 7, we proposed a novel MB-SIC detection scheme for MIMO-CDMA systems, which are equipped with different cancellation orders. Then, the MB-SIC structure was employed in the multistage interference cancellation scheme. It utilizes a conventional ordered SIC for the first stage, followed by a grouping detection strategy and the novel MB-SIC scheme. Thus, at the final stage the branches produce a group of estimated vectors for the desired user, according to a selection rule the MB-SIC selects the refined estimated vector with the best performance for the desired user's antenna streams.

8.2 Future Work

Some other systems can take advantage of the contributions of this thesis to improve the performance. In particular, the novel variable step-size mechanism proposed for DS-CDMA systems in chapter 3 can also be employed for adaptive beamforming, active noise cancellation and echo cancellation systems. The proposed DF receivers in chapter 4 can

be used for MIMO systems with spatial multiplexing techniques which are expected to be exploited for the next generation wireless systems. The ideas of the switched interleaving techniques in chapter 5 and chapter 6 can be extended to CDMA-based multi-hop ad hoc and sensor networks with feedback.

Some suggestions on the possible future work based on this thesis are given below:

Firstly, the bit error probability performance analysis for the multistage MB-SIC receiver proposed in Chapter 7 can be carried out. And the proposed receivers based on adaptive implementation can be developed. The results in Chapter 7 are based on perfect CSI, thus, the proposed receiver employing channel estimation algorithms can be tested. Another possibility is to use the proposed MB-SIC structure for the iterative detection techniques with Turbo and LDPC codes.

Secondly, it is possible to consider to combine the reduced-rank techniques with transmitter and receiver optimization techniques in MIMO MC-CDMA systems, different reduced-rank approaches can be tested. Joint optimization of precoder, receiver, and projection matrix can be investigated.

Thirdly, the switched interleaving algorithms based on limited feedback in Chapter 5 and Chapter 6 can be extended into MIMO-CDMA uplink systems where both BS and users are equipped with multiple antennas. In this case, the technique in [14] may be considered to jointly optimize the beamformer and the receiver. In conjunction with the proposed switched interleaving algorithm, the performance is expected to be improved with reduced feedback bits.

Bibliography

- [1] S. Verdu, *Multuser Detection*, Cambridge, 1998.
- [2] M. L. Honig and H. V. Poor, *Wireless communications: Signal Processing Perspectives*, chapter “Adaptive interference suppression”, pp. 64–128, Englewood Cliffs, NJ: Prentice-Hall, 1998.
- [3] H. Liu, *Signal Processing Applications in CDMA Communications*, Artech House, 2000.
- [4] S. Haykin, *Adaptive Filter Theory*, Englewood Cliffs, NJ: Prentice-Hall, 4th edition, 2002.
- [5] M. Honig, U. Madhow, and S. Verdu, “Blind adaptive multiuser detection”, *IEEE Trans. Inf. Theory*, vol. 41, no. 4, pp. 944–960, Jul. 1995.
- [6] Y. Na, M. Saquib, and M. Z. Win, “Pilot-Aided Chip-Interleaved DS-CDMA Transmission Over Time-Varying Channels”, *IEEE J. Sel. Areas Commun.*, vol. 24, no. 1, pp. 151–160, Jan. 2006.
- [7] S. Zhou, G. B. Giannakis, and C. Martret, “Chip-Interleaved Block-Spread Code Division Multiple Access”, *IEEE Trans. Commun.*, vol. 50, no. 2, pp. 235–248, Feb. 2002.
- [8] B. R. Vojcic, “Transmitter precoding in multiuser communications”, in *Proc. 1995 IEEE IT Workshop on Information Theory, Multiple Access and Queueing Theory*, St. Louis, MO, Apr. 1995.
- [9] P. Rapajic and B. Vucetic, “Linear adaptive transmitter-receiver structures for asynchronous cdma systems”, *Eur. Trans. Telecommun.*, vol. 6, pp. 21–28, Jan.-Feb. 1995.
- [10] G. J. Foschini, “Layered Space-Time Architecture for Wireless Communication in a Fading Environment When Using Multiple Antennas”, *Bell Laboratories Technical Journal.*, vol. 1, no. 2, pp. 41–59, Autumn 1996.

- [11] G. D. Golden, C. J. Foschini, R. A. Valenzuela, and P. W. Wolniansky, "Detection algorithm and initial laboratory results using V-BLAST space-time communication architecture", *Elect. Lett.*, vol. 35, no. 1, Jan. 1999.
- [12] A. Nardio and G. Taricco, "Linear Receivers for the Multiple-Input Multiple-Output Multiple-Access Channel", *IEEE Tran. Commun.*, vol. 54, no. 8, pp. 1446–1456, Aug. 2006.
- [13] T. Dharma, A. S. Madhukumar, and A. B. Premkumar, "MIMO Block Spread CDMA Systems for Broadband Wireless Communications", *IEEE Tran. Wireless Commun.*, vol. 7, no. 6, pp. 1987–1992, Jun. 2008.
- [14] S. Serbetli and A. Yener, "MIMO-CDMA Systems: Signature and Beamformer Design With Various Levels of Feedback", *IEEE Tran. Signal Process.*, vol. 54, no. 7, pp. 2758–2772, Jul. 2006.
- [15] S. Hara and R. Prasad, "Overview of multicarrier CDMA", *IEEE Commun. Mag.*, vol. 35, no. 12, pp. 126–133, Dec. 1997.
- [16] K. Fazel and S. Kaiser, *Multi-carrier and spread spectrum systems*, England, 2003.
- [17] Yu. V. Zakharov and V. P. Kodanov, "Experimental Study of an Underwater Acoustic Communication System with Pseudonoise Signals", *Acoustical Physics*, vol. 40, no. 5, pp. 707–715, 1994.
- [18] L. Vandendorpe, "Multitone Direct Sequence CDMA System in an Indoor Wireless Environment", *Proc. of IEEE First Symposium of Communications and Vehicular Technology*, pp. 4.1.1–4.1.8, Oct. 1993.
- [19] D. J. Love, Jr. R. W. Heath, W. Santipach, and M. L. Honig, "What Is the Value of Limited Feedback for MIMO Channels?", *IEEE Comm. Mag.*, vol. 42, no. 10, pp. 54–59, Oct. 2004.
- [20] P. Ding, D. J. Love, and M. D. Zoltowski, "Multiple Antenna Broadcast Channels With Shape Feedback and Limited Feedback", *IEEE Trans. Signal Process.*, vol. 55, no. 4, pp. 3417–3428, Jul. 2007.
- [21] R. A. Scholtz M. K. Simon, J. K. Omura and B. K. Levitt, *Spread Spectrum Communications Handbook*, NY: McGraw-Hill, 1994.
- [22] Harry L. Van Trees, *Detection, Estimation, and Modulation Theory*, Wiley-Interscience, 2001.

- [23] P. B. Rapajic, M. L. Honig, and G. K. Woodward, "Multiuser decision-feedback detection: Performance bounds and adaptive algorithms", *IEEE Int. Symp. on Inform. Theory*, p. 34, Boston, MA., Aug. 1998.
- [24] J. Miguez and L. Castedo, "A linearly constrained constant modulus approach to blind adaptive multiuser interference suppression", *IEEE Commun. Lett.*, vol. 2, no. 8, pp. 217–219, Aug. 1998.
- [25] C. Xu and G. Feng, "Comments on 'A linearly constrained constant modulus approach to blind adaptive multiuser interference suppression,'" *IEEE Commun. Lett.*, vol. 4, no. 9, pp. 280–282, Sep. 2000.
- [26] G. Feng C. Xu and K. S. Kwak, "A modified constrained constant modulus approach to blind adaptive multiuser detection", *IEEE Trans. Commun.*, vol. 49, no. 9, pp. 1642–1648, Sep. 2001.
- [27] Z. Xu and P. Liu, "Code-constrained blind detection of CDMA signals in multipath channels", *IEEE Signal Processing Lett.*, vol. 9, no. 12, pp. 389–392, Dec. 2002.
- [28] Jr. G. D. Forney, "Burst-correcting codes for the classic bursty channel", *IEEE Trans. Commun.*, vol. 19, no. 5, pp. 772–781, Oct. 1971.
- [29] Y. N. Lin and D. W. Lin, "Multiple access over fading multipath channels employing chip-interleaving code-division direct-sequence spread spectrum", *IEICE Trans. Commun.*, vol. E86-B, no. 1, pp. 114–121, Jan. 2003.
- [30] Y. Na and M. Saquib, "Effects of Time-Variations in Wireless Channels on the Two Different Fade-Resistant CDMA systems", *IEEE Trans. Wireless Commun.*, vol. 7, no. 8, pp. 2923–2929, Aug. 2008.
- [31] C. Schlegel, "CDMA with Partitioned Spreading", *IEEE Commun. letters*, vol. 11, no. 12, pp. 913–915, Dec. 2007.
- [32] M. Costa, "Writing on Dirty Paper", *IEEE Trans. Inf. Theory*, vol. 29, no. 3, pp. 439–441, May 1983.
- [33] E. Sourour R. Esmailzadeh and M. Nakagawa, "Pre-rake diversity combining in time-division duplex CDMA mobile communications", *IEEE Trans. on Vehicular Technology*, vol. 48, no. 3, pp. 795–801, May 1999.
- [34] A. N. Barreto and G. Fettweis, "On the downlink capacity of TDD CDMA systems using a pre-Rake", in *Proc. Global Telecommunications Conf. (GLOBECOM)*, Rio de Janeiro, Brazil, Dec. 1999.

- [35] B. R. Vojcic, "Transmitter precoding in synchronous multiuser communications", in *Symp. on Mobility Management*, George Mason Univ., Fairfax, VA 1994.
- [36] Z. Tang and S. Cheng, "Interference cancellation for DS-CDMA systems over flat fading channels through pre-decorrelating", in *PIMRC' 94*, The Hague, The Netherlands 1994.
- [37] B. R. Vojcic W. Jang and R. L. Pickholtz, "Joint Transmitter-Receiver Optimization in Synchronous Multiuser Communications over Multipath Channels", *IEEE Trans. Commu.*, vol. 46, no. 2, pp. 269–278, Feb. 1998.
- [38] A. K. Khandani E. S. Hons and W. Tong, "An optimized Transmitter Precoding Scheme for Synchronous DS-CDMA", *IEEE Trans. Commu.*, vol. 54, no. 1, pp. 32–36, Jan. 2006.
- [39] C. Rose, S. Ulukus, and R. Yates, "Wireless systems and interference avoidance", *IEEE Trans. Wireless Commun.*, vol. 1, no. 3, pp. 415–428, Jul. 2002.
- [40] D. C. Popescu and C. Rose, "Interference avoidance and dispersive channels: A new look at multicarrier modulation", *Allerton Conf. Comm., Control, and Computing*, Monticello, IL. 1999.
- [41] S. Ulukus and R. D. Yates, "Iterative signature adaptation for capacity maximization of CDMA systems", *Allerton Conf.*, Monticello, IL. Sep. 1998.
- [42] M. K. Varanasi and T. Guess, "Bandwidth efficient multiple access (bema): A new strategy based on signal design with quality-of-service constraints for successive-decoding-type multiuser receivers", *IEEE Trans. commun.*, vol. 49, pp. 844–854, May 2001.
- [43] S. Ulukus and R. Yates, "Iterative Construction of Optimum Signature Sequence Sets in Synchronous CDMA Systems", *IEEE Trans. Inf. Theory*, vol. 47, no. 5, pp. 1989–1998, Jul. 2001.
- [44] C. Rose, "CDMA codeword optimization: Interference avoidance and convergence via class warfare", *IEEE Trans. Inf. Theory*, vol. 47, no. 6, pp. 2368–2382, Sep. 2001.
- [45] G. S. Rajappan and M. L. Honig, "Signature Sequence Adaptation for DS-CDMA With Multipath", *IEEE J. Sel. Areas Commun.*, vol. 20, no. 2, pp. 384–395, Feb. 2002.
- [46] R. Prasad, *CDMA for Wireless Personal Communications*, Artech House, Boston: London 1996.

- [47] Charlotte Dumard and Thomas Zemen, “Low-Complexity MIMO Multiuser Receiver: A Joint Antenna Detection Scheme for Time-Varying Channels”, *IEEE Trans. Signal Process.*, vol. 56, no. 7, pp. 2931–2940, July 2008.
- [48] J-P. Linnartz N. Yee and G. Fettweis, “Multicarrier cdma in wireless radio networks”, *Proc. of IEEE PIMRC’ 93*, pp. 109–113, Yokohama, Japan, Sep. 1993.
- [49] H. Liu and H. Yin, “Receiver Design in Multicarrier Direct-Sequence CDMA Communications”, *IEEE Trans. Commu.*, vol. 49, no. 8, pp. 1479–1487, Aug. 2001.
- [50] T. M. Lok and T. F. Wong, “Transmitter and Receiver Optimization in Multicarrier CDMA Systems”, *IEEE Trans. Commu.*, vol. 48, no. 7, pp. 1197–1207, July 2000.
- [51] E. Telatar, “Capacity of multi-antenna Gaussian channels”, *Eur. Trans. Telecommun.*, vol. 10, no. 6, pp. 585–595, Nov./Dec. 1999.
- [52] G. J. Foschini and M. J. Gans, “On limits of wireless communications in a fading environment when using multiple antennas”, *Wireless Personal Commu.*, vol. 6, no. 3, pp. 311–335, Mar. 1998.
- [53] N. Seshadri V. Tarokh and R. Calderbank, “Space-time codes for high data rate wireless communication: Performance criterion and code construction”, *IEEE Trans. Inf. Theory*, vol. 44, pp. 744–765, Mar. 1998.
- [54] R. D. Yates A. Yener and S. Ulukus, “Interference management for CDMA systems through power control, multiuser detection, and beamforming”, *IEEE Trans. Commun.*, vol. 49, no. 7, pp. 1227–1239, Jul. 2001.
- [55] R. D. Yates A. Yener and S. Ulukus, “Space-time multiuser detection in multipath CDMA channels”, *IEEE Trans. Signal Process.*, vol. 47, no. 9, pp. 2356–2374, Sep. 1999.
- [56] C. Dumard and T. Zemen, “Low-Complexity MIMO Multiuser Receiver: A Joint Antenna Detection Scheme for Time-Varying Channels”, *IEEE Tran. Signal Process.*, vol. 56, no. 7, pp. 2931–2940, Jul. 2008.
- [57] D. J. Love, R. W. Heath, V. K. N. Lau Jr., D. Gesbert, B. D. Rao, and M. Andrews, “An Overview of Limited Feedback in Wireless Communication Systems”, *IEEE J. Sel. Areas Commun.*, vol. 26, no. 8, pp. 1341–1365, Oct. 2008.
- [58] K. K. Mukkavilli et al., “On Beamforming with Finite Rate Feedback in Multiple-Antenna Systems”, *IEEE Trans. Inf. Theory*, vol. 49, no. 10, pp. 2562–79, Oct. 2003.

- [59] D. J. Love and Jr. R. W. Heath, "Grassmannian Precoding for Spatial Multiplexing Systems", *Proc. Allerton Conf. Commun., Control, and Comp.*, Monticello, IL., Oct. 2003.
- [60] G. Caire and S. Shamai, "On the capacity of some channels with channel state information", *IEEE Trans. Inf. Theory*, vol. 45, no. 6, pp. 2007–2019, Sep. 1999.
- [61] Y. Liu V. Lau and T. A. Chen, "Capacity of memoryless channels and block-fading channels with designable cardinality-constrained channel state feedback", *IEEE Trans. Inf. Theory*, vol. 50, no. 9, pp. 2038–2049, Sep. 2004.
- [62] T. T. Kim and M. Skoglund, "On the expected rate of slowly fading channels with quantized side information", *IEEE Trans. Commun.*, vol. 55, no. 4, pp. 820–829, Apr. 2007.
- [63] N. Jindal A. Goldsmith, S. A. Jafar and S. Vishwanath, "Capacity limits of MIMO channels", *IEEE J. Sel. Areas Commun.*, vol. 21, no. 5, pp. 684–702, Jun. 2003.
- [64] Y. Liu V. Lau and T. A. Chen, "On the design of MIMO block-fading channels with feedback-link capacity constraint", *IEEE Trans. Commun.*, vol. 52, no. 1, pp. 62–70, Jan. 2004.
- [65] N. R. Sollenberger, "Diversity and automatic link transfer for a TDMA wireless access link", in *Proc. IEEE Glob. Telecom. Conf.*, vol. 1, pp. 532–536, Nov.-Dec. 1993.
- [66] B. Gyselinckx S. Thoen, L. Van der Perre and M. Engels, "Performance analysis of combined transmit-SC/receive-MRC", *IEEE Trans. Commun.*, vol. 49, no. Jan., pp. 5–8, Jan. 2001.
- [67] D. J. Love and Jr. R. W. Heath, "Limited Feedback Unitary Precoding for Orthogonal Space-Time Block Codes", *IEEE Trans. Signal Process.*, vol. 53, no. 1, pp. 64–73, Jan. 2005.
- [68] J. Choi and Jr. R. W. Heath, "Interpolation Based Transmit Beamforming for MIMO-OFDM With Limited Feedback", *IEEE Trans. on Signal Process.*, vol. 53, no. 11, pp. 4125–4135, Nov. 2005.
- [69] T. Pande, D. J. Love, and J. V. Krogmeier, "A weighted least squares approach to precoding with pilots for MIMO-OFDM", *IEEE Trans. on Signal Process.*, vol. 54, no. 10, pp. 4067–4073, Oct. 2006.
- [70] M. Borgmann and H. Bolcskei, "Interpolation-based efficient matrix inversion for MIMO-OFDM receivers", in *Proc. IEEE Asilomar Conf. on Signals, Systems, and Comp.*, vol. 2, pp. 1941–1947, Nov. 2004.

- [71] B. Mondal W. Choi and Jr. R. W. Heath, "Interpolation based unitary precoding for spatial multiplexing MIMO-OFDM with limited feedback", *IEEE Trans. on Signal Process.*, vol. 54, no. 12, pp. 4730–4740, Dec. 2006.
- [72] T. Pande, D. J. Love, and J. V. Krogmeier, "Reduced feedback MIMO-OFDM precoding and antenna selection", *IEEE Trans. on Signal Process.*, vol. 55, no. 5, pp. 2284–2293, May. 2007.
- [73] B. Mondal and Jr. R. W. Heath, "Algorithms for quantized precoded MIMO-OFDM systems", in *Proc. IEEE Asilomar Conf. on Signals, Systems, and Comp.*, pp. 381–385, Oct.-Nov. 2005.
- [74] R. A. Berry J. Chen and M. L. Honig, "Large system performance of downlink OFDMA with limited feedback", in *Proc. IEEE Int. Symp. Info. Th.*, pp. 1399–1403, Jul. 2006.
- [75] X. Wang A. G. Marques and G. B. Giannakis, "Optimizing energy efficiency of TDMA with finite rate feedback", in *Proc. IEEE Int. Conf. Acoust., Speech and Sig. Proc.*, vol. 3, Apr. 2007.
- [76] W. Santipach and M. L. Honig, "Signature Optimization for CDMA With Limited Feedback", *IEEE Trans. Inf. Theory*, vol. 51, no. 10, pp. 3475–3492, Oct. 2005.
- [77] W. Santipach, "Asymptotic performance of DS-CDMA with linear MMSE receiver and limited feedback", in *Proc. IEEE Int. Conf. on Commun.*, pp. 1393–1397, May 2008.
- [78] Y. Sun and M. L. Honig, "Reduced-rank space-time signature and receiver adaptation", in *Proc. IEEE Mil. Comm. Conf.*, vol. 2, pp. 948–954, Oct.-Nov. 2004.
- [79] Y. Liu W. Dai and B. Rider, "Performance analysis of CDMA signature optimization with finite rate feedback", in *Proc. Conf. Info. Sciences and Systems.*, pp. 426–431, Mar. 2006.
- [80] I. B. Collings M. Peacock and M. L. Honig, "Analysis of multiuser peer-to-peer MC-CDMA with limited feedback", in *Proc. IEEE Int. Conf. on Commun.*, vol. 2, pp. 968–972, Jun. 2004.
- [81] S. Koduri D. C. Popescu and D. B. Rawat, "Interference avoidance with limited feedback", in *Proc. IEEE Asilomar Conf. on Signals, Systems, and Comp.*, pp. 1046–1049, Nov. 2007.
- [82] C. Swannack, G. W. Wornell, and E. Uysal-Biyikoglu, "Efficient quantization for feedback in MIMO broadcasting systems", in *Proc. IEEE Asilomar Conf. on Signals, Systems, and Comp.*, pp. 784–788, Oct.-Nov. 2006.

- [83] G. W. Wornell C. Swannack and E. Uysal-Biyikoglu, "MIMO broadcast scheduling with quantized channel state information", in *Proc. IEEE Int. Symp. Info. Th.*, pp. 1788–1792, Jul. 2006.
- [84] M. Airy R. W. Heath, Jr. and A. J. Paulraj, "Multiuser diversity for MIMO wireless systems with linear receivers", in *Proc. IEEE Asilomar Conf. on Signals, Systems, and Comp.*, vol. 2, pp. 1194–1199, Nov. 2001.
- [85] N. Jindal, "Antenna combining for the MIMO downlink channel", *IEEE Trans. Wireless Commun.*, vol. 7, no. 10, pp. 3834–3844, Oct. 2008.
- [86] N. Ravindran and N. Jindal, "Limited feedback-based block diagonalization for the MIMO broadcast channel", *IEEE J. Select. Areas Commun.*, vol. 26, no. 8, pp. 1473–1482, Oct. 2008.
- [87] F. Roemer B. Song and M. Haardt, "Efficient channel quantization scheme for multi-user MIMO broadcast channels with RBD precoding", in *Proc. IEEE Int. Conf. Acoust., Speech and Sig. Proc.*, pp. 2389–2392, Mar.-Apr. 2008.
- [88] M. Rupi, P. Tsakalides, E. D. Re, and C. L. Nikias, "Constant modulus blind equalization based on fractional lower-order statistics", *Signal Processing*, vol. 84, no. 5, pp. 881–894, 2004.
- [89] D. Godard, "Self-Recovering Equalization and Carrier Tracking in Two-Dimensional Data Communication Systems", *IEEE Trans. on Commun.*, vol. 28, no. 11, pp. 1860–1875, Nov. 1980.
- [90] J. Treichler and B. Agee, "A new approach to multipath correction of constant modulus signals", *IEEE Trans. on Acoustics Speech and Signal Processing*, vol. 31, no. 2, pp. 459–472, Apr. 1983.
- [91] L. Li and H. Fan, "Blind CDMA detection and equalization using linearly constrained CMA", *Proc. ICASSP*, vol. V, pp. 2905–2908, June 2000.
- [92] J. Tugnait and T. Li, "Blind asynchronous multiuser CDMA receivers for ISI channels using code-aided CMA", *J. Select. Areas Commun.*, vol. 19, no. 8, pp. 1520–1530, Aug. 2001.
- [93] R. C. de Lamare and R. Sampaio-Neto, "Blind Adaptive Code-Constrained Constant Modulus Algorithms for CDMA Interference Suppression in Multipath Channels", *IEEE Commun. Letters*, vol. 9, no. 4, Apr. 2005.
- [94] S. Verdú, "Minimum Probability of Error for Asynchronous Gaussian Multiple-Access Channels", *IEEE Trans. on Inf. Theory*, vol. IT-32, no. 1, Jan. 1986.

- [95] Lie-Liang Yang, *Multicarrier Communications*, John Wiley Sons, 2009.
- [96] R. C. de Lamare and R. Sampaio-Neto, “Low-Complexity Variable Step-Size Mechanisms for Stochastic Gradient Algorithms in Minimum Variance CDMA Receivers”, *IEEE Trans. Signal Process.*, vol. 54, no. 6, Jun. 2006.
- [97] V. Krishnamurthy, “Averaged stochastic gradient algorithms for adaptive blind multiuser detection in DS/CDMA systems”, *IEEE Trans. Commun.*, vol. 48, no. 1, Jan. 2000.
- [98] D. Das and M. K. Varanasi, “Blind adaptive multiuser detection for cellular systems using stochastic approximation with averaging”, *IEEE J. Sel. Areas Commun.*, vol. 20, no. 2, pp. 310–319, Feb. 2002.
- [99] P. Yuvapoositanon and J. Chambers, “An adaptive step-size code constrained minimum output energy receiver for nonstationary CDMA channels”, *IEEE Proc. Int. Conf. Acoust. Speech, Signal Process.*, 2003.
- [100] P. Yuvapoositanon and J. Chambers, “Adaptive step-size constant modulus algorithm for DS-CDMA receivers in nonstationary environments”, *Signal Processing*, vol. 82, no. 2, pp. 311–315, Feb. 2002.
- [101] B. T. Polyak and A. B. Juditsky, “Acceleration of stochastic approximation by averaging”, *SIAM J. Contr. Optim.*, vol. 30, no. 4, pp. 838–855, Jul. 1992.
- [102] J. M. Brossier, “Egalization adaptive et estimation de phase: application aux communications sous-marines”, *Ph.D. dissertation*, vol. Inst. Nat. Polytech. Grenoble, Grenoble, France, 1992.
- [103] V. J. Mathews and Z. Xie, “A stochastic gradient adaptive filter with gradient adaptive step size”, *IEEE Trans. Signal Processing.*, vol. 41, no. 6, pp. 2075–2087, Jun. 1993.
- [104] H. J. Kushner and J. Yang, “Analysis of adaptive step-size sa algorithms for parameter tracking”, *IEEE Trans. Autom. Control*, vol. 40, no. 8, pp. 1403–1410, Aug. 1995.
- [105] X. G. Doukopoulos and G. V. Moustakides, “Adaptive Power Techniques for Blind Channel Estimation in CDMA Systems”, *IEEE Trans. Signal Processing*, vol. 53, no. 3, pp. 1110–1120, Mar. 2005.
- [106] Z. Xu and M. K. Tsatsanis, “Blind Adaptive Algorithms for Minimum Variance CDMA Receivers”, *IEEE Trans. Commun.*, vol. 49, no. 1, pp. 532–539, Jan. 2001.

- [107] R. Kwong and E. Johnston, "A Variable Step Size LMS Algorithm", *IEEE Trans. Signal Processing*, vol. 40, no. 7, pp. 1633–1642, Jul. 1992.
- [108] H. H. Zeng, L. Tong, and C. R. Johnson, "Relationships between the constant modulus and wiener receivers", *IEEE Trans. Inf. Theory*, vol. 44, no. 4, pp. 1523–1538, Jul. 1998.
- [109] A. H. Sayed and M. Rupp, "A time-domain feedback analysis of filtered-error adaptive gradient algorithms", *IEEE Trans. Signal Processing*, vol. 44, no. 6, pp. 1428–1439, Jun. 1996.
- [110] A. H. Sayed and M. Rupp, "An l_2 -stable feedback structure for nonlinear adaptive filtering and identification", *Automatica*, vol. 33, no. 1, pp. 13–30, Jan. 1997.
- [111] J. Mai and A. H. Sayed, "A Feedback Approach to the Steady-State Performance of Fractionally Spaced Blind Adaptive Equalizers", *IEEE Trans. Signal Processing*, vol. 48, no. 1, pp. 80–91, Jan. 2000.
- [112] N. R. Yousef and A. H. Sayed, "A Unified Approach to the Steady-State and Tracking Analyses of Adaptive Filters", *IEEE Trans. Signal Processing*, vol. 49, no. 2, pp. 314–324, Feb. 2001.
- [113] J. Whitehead and F. Takawira, "Performance Analysis of the Linearly Constrained Constant Modulus Algorithm-Based Multiuser Detector", *IEEE Trans. Signal Processing*, vol. 53, no. 2, pp. 643–653, Feb. 2005.
- [114] T. Y. Al-Naffouri and A.H. Sayed, "Transient analysis of adaptive filters with error nonlinearities", *IEEE Trans. Signal Process.*, vol. 51, no. 3, pp. 653–663, Mar. 2003.
- [115] B. Widrow and S. D. Stearns, *Adaptive Signal Processing*, Englewood Cliffs, NJ: Prentice-Hall, 1985.
- [116] E. Eweda, "Comparison of RLS, LMS, and sign algorithms for tracking randomly time-varying channels", *IEEE Trans. Signal Process.*, vol. 42, no. 11, pp. 2937–2944, Nov. 1994.
- [117] A. H. Sayed, *Fundamentals of Adaptive Filtering*, John Wiley and Sons, NJ, 2003.
- [118] J. F. Galdino, E. L. Pinto, and M. S. de Alencar, "Analytical Performance of the LMS Algorithm on the Estimation of Wide Sense Stationary Channels", *IEEE Trans. Commun.*, vol. 52, no. 6, pp. 982–991, Jun. 2004.

- [119] R. Lupas and S. Verdu, "Linear multiuser detectors for synchronous code-division multiple-access channels", *IEEE Trans. Inf. Theory*, vol. 35, no. 1, pp. 123–136, Jan. 1989.
- [120] M. Abdulrahman, A. Sheikh, and D. D. Falconer, "Decision Feedback Equalization for CDMA in Indoor Wireless Communications", *IEEE J. Sel. Areas Commun.*, vol. 12, no. 4, pp. 698–706, May 1994.
- [121] P. Patel and J. Holtzman, "Analysis of a Simple Successive Interference Cancellation Scheme in a DS/CDMA Systems", *IEEE J. Sel. Areas Commun.*, vol. 12, no. 5, pp. 796–807, Jun. 1994.
- [122] M. K. Varanasi and B. Aazhang, "Multistage detection in asynchronous CDMA communications", *IEEE Trans. Commun.*, pp. 509–519, Apr. 1990.
- [123] A. Duel-Hallen, "A family of multiuser decision-feedback detectors for asynchronous code-division multiple-access channels", *IEEE Trans. Commun.*, vol. 43, no. 2-4, pp. 421–434, Feb.-Apr. 1995.
- [124] G. Woodward, R. Ratasuk, M. L. Honig, and P. B. Rapajic, "Minimum Mean-Square Error Multiuser Decision-Feedback Detectors for DS-CDMA", *IEEE Trans. Commun.*, vol. 50, no. 12, pp. 2104–2112, Dec. 2002.
- [125] M. L. Honig, G. K. Woodward, and Y. Sun, "Adaptive Iterative Multiuser Decision Feedback Detection", *IEEE Trans. Wireless Comm.*, vol. 3, no. 2, pp. 477–485, Mar. 2004.
- [126] J. E. Smee and S. C. Schwartz, "Adaptive Space-time Feedforward/Feedback Detection for High Data Rate CDMA in Frequency-Selective Fading", *IEEE Trans. Commun.*, vol. 49, no. 2, pp. 317–328, Feb. 2001.
- [127] M. K. Varanasi and T. Guess, "Optimum decision feedback multiuser equalization with successive decoding achieves the total capacity of the Gaussian multiple-access channel", *Proc. 31st Asilomar Conf. Signals, Systems and Computers*, pp. 1405–1409, Monterey, CA., Nov. 1997.
- [128] R. C. de Lamare and R. Sampaio-Neto, "Minimum Mean-Squared Error Iterative Successive Parallel Arbitrated Decision Feedback Detectors for DS-CDMA Systems", *IEEE Trans. Commun.*, vol. 56, no. 5, pp. 778–789, May 2008.
- [129] R. Sampaio-Neto R. C. de Lamare and A. Hjoungnes, "Joint Iterative Interference Cancellation and Parameter Estimation for CDMA Systems", *IEEE Commun. Letters*, vol. 11, no. 12, pp. 916–918, Dec. 2007.

- [130] P. V. Rooyen, M. Lotter, and D. V. Wyk, *Space-time Processing for CDMA Mobile Communications*, Kluwer Academic Publishers, Norwell, Massachusetts, 2001.
- [131] A. Yener, R. D. Yates, and S. Ulukus, “Combined multiuser detection and beamforming for cdma systems: Filter structures”, *IEEE Trans. on Vehicular Technology*, vol. 51, no. 5, pp. 1087–1095, Sep. 2002.
- [132] A. Narula, M. J. Lopez, M. D. Trott, and G. W. Wornell, “Efficient Use of Side Information in Multiple-Antenna Data Transmission over Fading Channels”, *IEEE J. Sel. Areas Commun.*, vol. 16, no. 8, pp. 1423–1436, Oct. 1998.
- [133] B. C. Banister and J. R. Zeidler, “Feedback Assisted Transmission Subspace Tracking for MIMO Systems”, *IEEE J. Sel. Areas Commun.*, vol. 21, no. 3, pp. 452–463, Apr. 2003.
- [134] J. C. Roh and B. D. Rao, “Multiple Antenna Channels With Partial Channel State Information at the Transmitter”, *IEEE Trans on Wireless Commun.*, vol. 3, no. 2, pp. 677–688, Mar. 2004.
- [135] M. Sharif and B. Hassibi, “On the Capacity of MIMO Broadcast Channels With Partial Side Information”, *IEEE Trans. Inf. Theory*, vol. 51, no. 2, pp. 506–522, Feb. 2005.
- [136] D. J. Love, Jr. R. W. Heath, and T. Strohmer, “Grassmannian Beamforming for Multiple-Input Multiple-Output Wireless Systems”, *IEEE Trans. Inf. Theory*, vol. 49, no. 10, pp. 2735–45, Oct. 2003.
- [137] A. D. Dabbagh and D. J. Love, “Multiple Antenna MMSE Based Downlink Precoding with Quantized Feedback or Channel Mismatch”, *IEEE Trans. Commun.*, vol. 56, no. 11, pp. 1859–1868, Nov. 2008.
- [138] R. S. Blum, “MIMO with Limited Feedback of Channel State Information”, *Proc. ICASSP*, vol. 4, pp. 89–92, Hong Kong, China, Apr. 2003.
- [139] A. Duel-Hallen, S. Hu, and H. Hallen, “Long-range prediction of fading signals”, *IEEE Signal Processing Mag.*, vol. 15, no. 3, pp. 62–75, May 2000.
- [140] J. Heo, Y. Wang, and K. Chang, “A Novel Two-Step Channel-Prediction Technique for Supporting Adaptive Transmission in OFDM/FDD System”, *IEEE Trans. on Vehicular Technology*, vol. 57, no. 1, pp. 188–193, Jan. 2008.
- [141] S. Moshavi, D. Yellin, J. S. Sadowsky, Y. Perets, and K. Pick, “Pilot Interference Cancellation Technology for CDMA Cellular Networks”, *IEEE Trans. Vehicular Technology*, vol. 54, no. 5, pp. 1781–1792, Sep. 2005.

- [142] E. Karami, "Tracking Performance of Least Square MIMO Channel Estimation Algorithm", *IEEE Trans. Commun.*, vol. 55, no. 11, pp. 2201–2209, Nov. 2007.
- [143] A. Duel-Hallen, "Fading channel prediction for mobile radio adaptive transmission systems", *Proceedings of the IEEE*, vol. 95, no. 12, pp. 2299–2313, Dec. 2007.
- [144] B. R. Vojcic and W. M. Jang, "Transmitter Precoding in Synchronous Multiuser Communications", *IEEE Trans. Commun.*, vol. 46, no. 10, pp. 1346–1355, Oct. 1998.
- [145] A. Goldsmith, *Wireless Communications*, Cambridge, 2005.
- [146] L. Hanzo et al., *Single and Multi-carrier DS-CDMA: Multi-User Detection, Space-Time Spreading, Synchronisation, Networking and Standards*, IEEE Press-Wiley, Jun. 2003.
- [147] G. B. Giannakis, P. A. Anghel, and Z. Wang, "Generalized Multicarrier CDMA: Unification and Linear Equalization", *EURASIP Journal on Applied Signal Processing*, vol. 2005, no. 5, pp. 743–756.
- [148] R. L. Choi and R. D. Murch, "New transmit schemes and simplified receivers for MIMO wireless communication systems", *IEEE Trans. on Wireless Commu.*, vol. 2, no. 6, pp. 1217–1230, Nov. 2003.
- [149] L. Choi and R. D. Murch, "Transmit-preprocessing techniques with simplified receivers for the downlink of MISO TDD-CDMA systems", *IEEE Trans. on Wireless Commu.*, vol. 53, no. 2, pp. 285–295, Mar. 2004.
- [150] J. Lopez Vicario, R. Bosisio, U. Spagnolini, and C. Anton-Haro, "A throughput analysis for opportunistic beamforming with quantized feedback", in *Proc. IEEE Int. Symp. Personal, Indoor, and Mobile Radio Commun.*, Sep. 2006.
- [151] N. Jindal, "MIMO broadcast channels with finite-rate feedback", *IEEE Trans. Inform. Theory*, vol. 52, no. 11, pp. 5045–5060, Nov. 2006.
- [152] M. Trivellato, F. Boccardi, and F. Tosato, "User selection schemes for MIMO broadcast channels with limited feedback", in *Proc. IEEE Veh. Technol. Conf.*, pp. 2089–2093, Apr. 2007.
- [153] T. Yoo, N. Jindal, and A. Goldsmith, "Multi-antenna downlink channels with limited feedback and user selection", *IEEE J. Sel. Areas Commun.*, vol. 35, no. 7, pp. 1478–1491, Sep. 2007.

- [154] J. Diaz, O. Simeone, and Y. Bar-Ness, "Asymptotic analysis of reduced-feedback strategies for MIMO Gaussian broadcast channels", *IEEE Trans. Inf. Theory*, vol. 54, no. 3, pp. 1308–1316, Mar. 2008.
- [155] R. T. Derryberry, S. D. Gray, D. M. Ionescu, G. Mandyam, and B. Raghothaman, "Transmit diversity in 3G CDMA systems", *IEEE Comm. Mag.*, vol. 40, no. 4, pp. 68–75, Apr. 2002.
- [156] H. Holma and A. Toskala, *WCDMA for UMTS: Radio Access for Third Generation Mobile Communications*, West Sussex, England: John Wiley, 2002.
- [157] C. R. Murthy, J. Zheng, and B. D. Rao, "Performance of quantized methods for equal gain transmission with noisy feedback channels", *IEEE Trans. Sig. Proc.*, vol. 56, no. 6, pp. 2451–2460, Jun. 2008.
- [158] Z. Wang and G. B. Giannakis, "Wireless Multicarrier Communications", *IEEE Signal Process. Mag.*, vol. 17, no. 3, pp. 29–48, May 2000.
- [159] M. Jankiraman, *Space-time codes and MIMO systems*, Artech House, 2004.
- [160] B. Hassibi and H. Vikalo, "On the sphere decoding algorithm: Part I, the expected complexity", *IEEE Tran. Signal Process.*, vol. 53, no. 8, pp. 2806–2818, Aug. 2005.
- [161] E. Viterbo and J. Boutros, "A universal lattice code decoder for fading channels", *IEEE Trans. Inf. Theory*, vol. 45, no. 5, pp. 1639–1642, Jul. 1999.
- [162] M. K. Varanasi and B. Aazhang, "Multistage detection in asynchronous CDMA communications", *IEEE Trans. Commun.*, vol. 38, no. 4, pp. 509–19, Apr. 1990.
- .

List of Figures

2.1	General DF receiver structure	14
2.2	Pilot-aided chip-interleaving scheme	18
2.3	MUI-free transceiver for a single user.	19
2.4	Discrete-time baseband model for joint signature-receiver adaptation	22
2.5	MC-CDMA scheme: transmitter and receiver	23
2.6	MC-DS-CDMA scheme: transmitter and receiver	24
2.7	A block diagram of a limited feedback linear beamforming MIMO system	28
3.1	Block diagram of the blind adaptive CCM receiver with variable step-size mechanisms.	35
3.2	(a) MSE performance in a non-stationary environment with an AWGN channel, where the system starts with 4 users including a 5dB high power level interferer. After 1000 received symbols 4 new users including a 5dB high power level interferer enter the system. (b) Step-size variation in the same non-stationary environment.	48
3.3	(a) SINR performance in non-stationary environment of multipath time-varying channel, (b) Step-size values for the variable step-size mechanisms in the non-stationary environment, SNR=15dB, $f_d T = 5 \times 10^{-6}$, FSS is 10^{-4}	50

3.4	(a) BER versus the SNR with multipath channels and (b) BER versus number of users with multipath channels. $f_d T = 1 \times 10^{-3}$, FSS is 10^{-4}	51
3.5	MSE analytical versus simulated performance for the proposed TASS mechanism convergence analysis. (a) Number of users is 4, the SNR is 16 dB. (b) Number of users is 4.	52
3.6	MSE analytical versus simulated performance for the proposed TASS mechanism tracking analysis. Number of users is 6, the SNR is 15 dB, $f_d T = 5 \times 10^{-5}$	53
4.1	Proposed multi-antenna MPF-DF receiver structure	59
4.2	The two-stage DF receiver with space-time MPF-DF scheme in the first stage	62
4.3	Four adaptive schemes for MPF-DF structure	71
4.4	BER performance versus number of symbols, normalized SG algorithms, $N = 15$, $K=6$ users, $f_d T = 5 \times 10^{-5}$, 1-antenna configuration.	72
4.5	BER performance versus number of antennas, normalized SG algorithms, $N = 15$, $K=6$ users, $f_d T = 1 \times 10^{-3}$	73
4.6	BER performance versus channel fading rate, normalized SG algorithms, $N = 15$, $K=8$ users, 2-antenna for both diversity and beamforming configurations.	74
4.7	BER performance versus (a) Averaged-SNR and (b) number of users (K). Normalized SG algorithms, $N = 15$, $f_d T = 5 \times 10^{-5}$, 2-antenna for beamforming configurations.	75
4.8	BER performance versus (a) Averaged-SNR and (b) number of users (K). RLS algorithms, $N = 16$, $f_d T = 5 \times 10^{-5}$, 2-antenna ($N_{ant} = 2$) for beamforming configurations.	76
4.9	BER performance versus (a) Averaged-SNR and (b) number of users (K). RLS algorithms, $N = 32$, $f_d T = 5 \times 10^{-5}$, 2-antenna ($N_{ant} = 2$) for diversity and beamforming configurations.	77

5.1	Proposed uplink limited feedback-based SIDS-CDMA model and transceiver structure	80
5.2	BER performance versus number of feedback bits. $N = 16$. Downlink system and independent multipath fading channels. $N_e = 10000$. $\beta = 1000$.	94
5.3	BER performance versus (a) SNR and (b) K/N for the proposed SIDS-CDMA schemes, existing chip-interleaving algorithms and the conventional CDMA with MMSE receiver. Downlink block fading channels, Walsh codes and the codebook of block interleavers.	95
5.4	BER performance versus SNR for the proposed SIDS-CDMA schemes and the conventional DS-CDMA precoders with channel quantization. Downlink block fading channels. Walsh codes and the codebook of block interleavers.	96
5.5	Averaged BER performance versus (a) SNR and (b) K/N for the proposed SIDS-CDMA schemes, the block-based MMSE receiver and the conventional DS-CDMA with MMSE receiver. Random spreading sequence and the codebook designed by the FSP algorithm are employed. Uplink multipath fading channels with $f_d T = 0.05$	97
5.6	Averaged BER performance versus SNR for the proposed SIDS-CDMA schemes and the adaptive spreading schemes.	98
5.7	BER performance versus the percentage of feedback errors for the proposed uplink and downlink schemes. The block-based MMSE receivers, random spreading sequence and the codebook designed by the FSP algorithm are employed.	99
6.1	Proposed downlink limited feedback-based multiple antenna MC-CDMA model and transceiver structure	103
6.2	Proposed uplink limited feedback-based multiple antenna MC-CDMA model and transceiver structure	104
6.3	The frame structure of the proposed downlink feedback scheme	111

6.4	Average BER performance versus number of transmit antennas for the proposed downlink schemes with precoders and the conventional MC-CDMA schemes without precoders.	116
6.5	Average BER performance versus SNR for the proposed downlink algorithms with different CSI quantization schemes and the conventional MC-CDMA systems.	117
6.6	Average BER performance versus number of users for the proposed downlink algorithms with different CSI quantization schemes and the conventional MC-CDMA systems.	118
6.7	Average BER performance versus number of feedback bits for different interleaving codebook.	119
6.8	Average BER performance versus SNR for the proposed uplink switched interleaving preprocessing schemes and the conventional MC-CDMA MMSE receiver.	120
6.9	Average BER performance versus number of users for the proposed uplink switched interleaving preprocessing schemes and the conventional MC-CDMA MMSE receiver.	121
6.10	Average BER performance versus the percentage of each user's feedback errors for the proposed downlink and uplink schemes.	122
7.1	MIMO-CDMA uplink model	125
7.2	The SIC structure based on the MMSE receiver	128
7.3	(a) The proposed MSMB-SIC receiver and (b) The MB-SIC structure for the desired user.	131
7.4	BER performance versus SNR. $N = 16$	133
7.5	BER performance versus number of users (K). $N = 16$	133

List of Tables

3.1	Additional computational complexity in multipath channels.	40
4.1	Proposed adaptive estimation algorithm: SG.	67
4.2	Proposed adaptive estimation algorithm: RLS.	69
5.1	Computational complexity	86
5.2	Frequently Selected Patterns (FSP) Scheme	92